2010-09-08

Regulation of Early T Cell Activation by TNF Superfamily Members TNF and FASL: A Dissertation

Bhavana Priyadharshini
University of Massachusetts Medical School

REGULATION OF EARLY T CELL ACTIVATION BY TNF SUPERFAMILY MEMBERS TNF AND FASL

A dissertation presented

By

BHAVANA PRIYADHARSHINI

Submitted to the faculty of the

University of Massachusetts Graduate School of Biomedical Sciences, Worcester

in partial fulfillment of the requirements for the degree of

DOCTOR OF PHILOSOPHY

September 8th, 2010

PROGRAM IN IMMUNOLOGY AND VIROLOGY

COPYRIGHT INFORMATION

REGULATION OF EARLY T CELL ACTIVATION BY TNF SUPERFAMILY MEMBERS

TNF AND FASL

A Dissertation Presented

By

BHAVANA PRIYADHARSHINI

The signatures of the Dissertation Defense Committee signifies completion and approval as to style and content of the Dissertation

Dr. Michael A. Brehm, Ph.D. , Thesis Advisor

Dr. Raymond M. Welsh. Ph.D. , Member of Committee

Dr.Egil Lien, Ph.D. , Member of Committee

Dr.Eva Szomolanyi-Tsuda, M.D. , Member of Committee

Dr. Nancy H. Ruddle, Ph.D. , External Member of Committee

The signature of the Chair of the Committee signifies that the written dissertation meets the requirements of the Dissertation Committee

Dr. Francis Chan, Ph.D. , Chair of Committee

The signature of the Dean of the Graduate School of Biomedical Sciences signifies that the student has met all graduation requirements of the school

Dr. Anthony Carruthers, Ph.D.

Dean of the Graduate School of Biomedical Sciences

Program in Immunology and Virology

September 8th, 2010

ACKNOWLEDGEMENTS

I would first like to thank my teacher, my guru Dr. Michael Brehm for guiding me every step of the way during my thesis research. He has been a constant source of inspiration and motivation in my life and I thank him for always encouraging and believing in me. I would also like to thank my co-mentors Dr. Raymond Welsh and Dr. Dale Greiner for being such exemplary mentors. Along with Dr. Michael Brehm, Dr. Raymond Welsh and Dr. Dale Greiner have always challenged me to do better every step of the way. All three of my mentors have taught me the true meaning of science and I thank them for everything they have taught me. I would also like to thank the rest of my committee members Dr. Francis Chan and Dr. Egil Lien for giving me helpful suggestions during the course of my projects. I would like to especially thank Dr, Eva-Szomolanyi-Tsuda and Dr. Nancy Ruddle for kindly agreeing to be a part of my dissertation committee.

I would like to thank all the lab members of the Welsh and the Greiner group, for all their technical assistance and many scientific discussions. Apart from science, I thank them for all the joy and fun times and more importantly the friendship they have offered me. I would also like to extend my gratitude to all the wonderful lab colleagues from the Selin and the Tsuda group.

I would like to thank my best buddies, Swarna and Chandana for being my pillars of support who have stood by me through thick and thin. Finally, I am forever indebted to my family, my father, my mother, my sister, my bro-in-law and my little nephew for their unconditional love and support. But for my parents' prayers, blessings and the countless sacrifices, this Ph.D dream would have remained a mere wish. I dedicate this thesis to my parents who have taught and encouraged me to give my best in whatever I do and never to give up.

ABSTRACT

The instructive signals received by T cells during the programming stages of activation will determine the fate of effector and memory populations generated during an immune response. Members of the tumor necrosis factor (TNF) superfamily play an essential role in influencing numerous aspects of T cell adaptive immune responses including cell activation, differentiation, proliferation, survival, and apoptosis. My thesis dissertation describes the involvement of two such members of the TNF superfamily, TNF and FasL, and their influence on the fate of T cells early during responses to viral infections and to the induction of transplantation tolerance.

TNF is a pleiotropic pro-inflammatory cytokine that has an immunoregulatory role in limiting the magnitude of T cell responses during a viral infection. Our laboratory discovered that one hallmark of naïve T cells in secondary lymphoid organs is their unique ability to rapidly produce TNF after activation and prior to acquiring other effector functions. I hypothesized that T cell-derived TNF will limit the magnitude of T cell responses. The co-adoptive transfer of wild type (WT) P14 and TNF-deficient P14 TCR transgenic $CD8^+$ T cells, that recognize the GP33 peptide of lymphocytic choriomeningitis virus (LCMV), into either WT or TNF-deficient hosts demonstrated that the donor TNF-deficient P14 TCR transgenic $CD8^+$ T cells accumulate to higher frequencies after LCMV infection. Moreover, these co-adoptive transfer experiments suggested that the effect of T cell-derived TNF is localized in the microenvironment, since the TNF produced by WT P14 TCR transgenic $CD8^+$ T cells did not prevent the

accumulation of TNF-deficient P14 TCR transgenic $CD8^+$ T cells. To determine if T cell-produced TNF is acting on professional APC to suppress the generation of virus-specific T cell responses, I performed co-adoptive transfer experiments with WT P14 TCR transgenic $CD8^+$ and TNF-deficient P14 TCR transgenic $CD8^+$ T cells into TNFR1/2 (1 and 2) deficient mice. These experiments demonstrated that the absence of TNFR1/2 signaling pathway in the host cells resulted in a greater accumulation of WT P14 TCR transgenic $CD8^+$ T cells, thereby considerably diminishing the differences between donor WT P14 TCR transgenic $CD8^+$ and donor TNF-deficient P14 TCR transgenic $CD8^+$ T cells. The increased frequency and absolute numbers of WT P14 TCR transgenic $CD8^+$ T cells in TNFR1/R2 deficient recipients suggests that one mechanism for the suppressive effect of T cell-derived TNF on antigen-specific T cells occurs as a result of TNFR signaling in the host cells. However, the donor TNF-deficient P14 TCR transgenic $CD8^+$ T cells still accumulated to higher frequency and numbers compared to their donor WT transgenic counterparts. Together, these findings indicate that T cell-produced TNF can function both in an autocrine and a paracrine fashion to limit the magnitude of anti-viral T cell responses.

Given the immunoregulatory role of TNF and the ability of peripheral naïve T cells to produce this cytokine, I questioned at what stage of development do T cells become licensed to produce this cytokine. The peripheral naïve T cell pool is comprised of a heterogeneous population of cells at various stages of development, a process that begins in the thymus and is completed after a post-thymic maturation phase in the periphery. I hypothesized that naïve T cells emigrating from the thymus will be

competent to produce TNF only after undergoing a maturation process in the periphery. To test this hypothesis, I compared cytokine profiles of $CD4^+$ and $CD8^+$ single positive (SP) thymocytes, recent thymic emigrants (RTEs) and mature-naïve (MN) T cells during TCR activation. SP thymocytes exhibited a poor ability to produce TNF when compared to splenic T cells despite expressing similar TCR levels and possessing comparable activation kinetics with respect to the upregulation of CD25 and CD69 following stimulation. The reduced ability of SP thymocytes to produce TNF correlated with a decreased level of detectable TNF message following stimulation when compared to splenic counterparts. Stimulation of SP thymocytes in the context of a splenic environment did not fully enable TNF production, suggesting an intrinsic defect in their ability to produce TNF as opposed to a defect in antigen presentation. Using a thymocyte adoptive transfer model, I demonstrate that the ability of T cells to produce TNF increases progressively with time in the periphery as a function of their maturation state. RTEs identified by the expression of green fluorescent protein (GFP) (NG-BAC transgenic mice), showed a significantly enhanced ability to express TNF relative to SP thymocytes, but not to the extent of MN T cells. Together, these findings suggest that TNF expression by naïve T cells is regulated via a gradual licensing process that requires functional maturation in peripheral lymphoid organs. This highlights the functional heterogeneity of the naïve T cell pool (with respect to varying degrees of TNF production) during early T cell activation that can contribute to the many subsequent events that shape the course of an immune response.

The productive activation of naïve T cells requires at least initial two signals; the first being through the TCR and the second is the engagement of co-stimulatory molecules on the surface of the T cells. T cells activated in the absence of co-stimulation become anergic or undergo cell death. Agents that block co-stimulation of antigen-specific T cells are emerging as an alternative to immunosuppressive drugs to prolong allograft survival in transplant recipients. Targeted blockade of CD154-CD40 interactions using a αCD154 monoclonal antibody (MR1) with a simultaneous transfusion of allogeneic splenocytes (donor specific transfusion or DST) efficiently induces tolerance to allografts. This co-stimulation blockade-induced tolerance is characterized by the deletion of host alloreactive T cells within 24 hours of treatment. Toll-like receptor (TLR) agonists abrogate tolerance induced by co-stimulation blockade by impairing the deletion of host alloreactive T cells and resulting in allograft rejection. The goal of my study was to determine the underlying molecular mechanisms that protect host alloreactive T cells from early deletion after exposure to TLR agonists. I hypothesized that TLR ligands administered during co-stimulation blockade regimen differentially regulate the expression of pro- and anti-apoptotic molecules in alloreactive T cells, during the initial stages of activation thereby preventing deletion.

To test this hypothesis, I used syngeneic bone marrow chimeric mice containing a trace population of alloreactive KB5 TCR transgenic $CD8^+$ T cells (KB5 Tg $CD8^+$ T cells) that recognize H-$2K^b$ as an alloantigen. I show here that KB5-$CD8^+$ T cells downregulate CD127 (IL-7Rα) and become apoptotic as early as 12 hrs after co-stimulation blockade. In contrast, KB5 Tg $CD8^+$ T cells from mice treated with bacterial

lipopolysaccaride (LPS) during co-stimulation blockade failed to become apoptotic, although CD127 was downregulated. Examination of the mRNA expression profiles of several apoptotic genes in purified KB5 $CD8^+$ T cells from mice treated with DST+anti-CD154 for 12 hrs revealed a significant upregulation of FasL mRNA expression compared to the untreated counterparts. However, *in vitro* FasL blockade or *in vivo* cytotoxicity experiments with mice deficient in Fas or FasL indicated that the Fas-FasL pathway might not be crucial for tolerance induction. Another pro-apoptotic molecule BIM was upregulated in alloreactive T cells during co-stimulation blockade. This suggests that both the Fas pathway and BIM may be playing complementary roles in inducing deletional tolerance. Although FasL expression was diminished in alloreactive T cells in the presence of LPS, BIM expression was not diminished, suggesting that alloreactive T cells may still be vulnerable to undergo apoptosis. Concomitantly, I also found that LPS treatment during co-stimulation blockade resulted in non-specific upregulation of Fas expression in alloreactive T cells and non-transgenic T cells ($CD4^+$ and $CD8^+$). I demonstrate here that treatment with Fas agonistic antibody in vitro for 4 hours can selectively induce apoptosis of alloreactive T cells that were believed to be refractory to apoptosis during LPS treatment. I speculate that under these conditions, deletion may be occurring due to the involvement of both Fas and BIM. Further, the mRNA expression profile revealed interleukin-10 (IL-10) as a molecule induced in alloreactive T cells during LPS treatment. Analysis of serum confirmed the systemic expression of IL-10 protein in mice treated with LPS during co-stimulation blockade. I hypothesized that LPS-induced IL-10 can have an anti-apoptotic role in preventing the

deletion of alloreactive T cells and mediating allograft rejection. Contrary to my hypothesis, I found that IL-10 KO mice rejected allogeneic target cells similar to their WT counterparts, suggesting that IL-10 may not be required for LPS-mediated abrogation of tolerance induction. In addition to the systemic induction of IL-10, LPS also induced cytokines such as interleukin-6 (IL-6), TNF and interferon-γ (IFN-γ).

These findings suggest that both Fas-FasL and BIM mediated apoptotic pathways may play complementary roles in inducing the early deletion of activated alloreactive T cells during tolerance induction. On the other hand, the mechanism of LPS mediated abrogation of tolerance induction can not be attributed to IL-10 alone as it may be playing a synergistic role along with other proinflammatory cytokines that may in turn result in the prevention of alloreactive T cell death during this process. Most importantly, these findings indicate that despite emerging from a pro-inflammatory cytokine milieu, alloreactive T cells are still susceptible to undergo Fas-mediated apoptosis during the first 24 hours after co-stimulation blockade and LPS treatment. Therefore, targeting the Fas-FasL pathway to induce deletion of alloreactive T cells during the peri-transplant period may still be a potential strategy to improve the efficacy of co-stimulation blockade induced transplantation tolerance during an environmental perturbation such as inflammation or infection.

TABLE OF CONTENTS

Page Number

LIST OF TABLES

LIST OF FIGURES

LIST OF ABBREVIATIONS

7-AAD	7-amino actinomycin D
AICD	Activation-induced cell death
AIRE	Autoimmune regulator
ALPS	Autoimmune lymphoproliferative syndrome
AP-1	Activator protein-1
APC	Antigen presenting cell
BAD	Bcl-2 associated death protein
BAK	Bcl-2 homologous antagonist killer
BAX	Bcl-2 associated X protein
Bcl-2	B cell lymphoma-2
Bcl-xL	B cell lymphoma extra-large
BfA	Brefeldin A
BID	BH3 (Bcl-2 homology domain3) interacting domain death agonist
BIM	Bcl-2 interacting molecule (Bcl-2 like protein 11)
BrDU	Bromodeoxyuridine
Ca^{2+}	Calcium $^{2+}$ ion
CARD	Caspase recruiting domain
CCR/L	(Cysteine-Cysteine) C-C Chemokine Receptor / Ligand
cGy	centriGray
cIAP	Cellular inhibitor of apoptosis
CRAC	Ca^{2+} release-activated Ca^{2+} channel
CTL	Cytotoxic T lymphocyte
CTLA-4	Cytotoxic T-lymphocyte antigen-4
DAG	Diacylglycerol

DAMPS	Danger associated molecular patterns
DC	Dendritic cell
DD	Death domain
DN	Double negative
DP	Double positive
DS	Down syndrome
DST	Donor-specific transfusion
EBV	Epstein Barr Virus
E.coli	Escherichia coli
EDTA	Ethylenediaminetetraacetic acid
ERK	Extracellular Signal activated kinase
FACS	Fluorescence activated cell sorting
FADD	Fas-associated protein with death domain
FBS	Fetal bovine serum
FDC	Follicular dendritic cell
FITC	Fluorescein iso-thiocyanate
FLIP	FLICE like inhibitory protein
FLICE	Fas associated death domain-like interleukin1β converting enzyme (Caspase 8)
FOXP3	Forkhead Box P3
GAD	Glutamic acid decarboxylase
GFP	Green fluorescent protein
Gld	Generalized lymphoproliferative disease
GVHD	Graft versus Host disease
GEF	Guanine exchange factor
GTP	Guanosine triphosphate

HIV	Human immunodeficiency virus
HMGB1	High-motility group protein B1
HSA	Heat-stable antigen
Hsp	Heat-shock protein
HTLV-1	Human T lymphotropic virus
HVEM	Herpes virus entry mediator
ICAM-1	Inter-cellular adhesion molecule-1
ICOS	Inducible co-stimulator
IDO	Indolamine,2,3, dehydrogenase
IFN	Interferon
IKK	IκB kinase
IκB	Inhibitor of NFκB
IL	Interleukin
i.p.	Intra peritoneal
IP3	Inositol triphosphate
IPEX	Immunodysregulated-polyendocrinopathy enteropathy X-linked syndrome
IRF	Interferon regulatory factor
ITAM	Immunoreceptor tyrosine-based activation motif
ITK	IL-2 inducible T cell kinase
i.v.	Intravenous
JNK	c-Jun NH(2)-terminal kinase
KLRG1	Killer cell lectin like –receptor subfamily G member 1
LAT	Linker of activation of T cells
LCK	Leukocyte specific protein tyrosine kinase
LCMV	Lymphocytic choriomeningitis virus

LFA-1	Lymphocyte-function associated antigen-1
LIGHT	Lymphotoxin like inducible protein that competes with glycoprotein D for HVEM on T cells
Lpr	Lymphoproliferation
LPS	Lipopolysaccaride
LT	Lymphotoxin
MACS	Magnetic cell sorting
MAPK	Mitogen activated protein kinase
MAVS	Mitochondrial antiviral signaling protein
MCMV	Murine cytomegalovirus
MCP-1	Monocyte-chemotactic protein-1
MDA-5	Melanoma differentiation-associated gene-5
MFI	Mean fluorescence intensity
MHC	Major histocompatibility complex
MN	Mature-naive
MPECs	Memory precursor effector cells
mTEC	Medullary thymic epithelial cell
MyD88	Myeloid differentiation marker 88
NFAT	Nuclear factor of activated T cells
NFκB	Nuclear factor κ light chain enhancer of activated B cells
NIK	NFκB inducing kinase
NK	Natural Killer
NLR	NOD (Nucleotide-binding domain, leucine rich repeat containing protein) like receptor
PAMPS	Pattern associated molecular patterns
PBS	Phosphate buffer saline

PCD	Passive cell death
PD-1	Programmed Death-1
Pfu	Plaque forming unit
PI3K	Phosphoinositidyl Kinase -3
PIP_2	Phosphotidyl inositol biphosphate
PKB	Protein kinase B (AKT)
PKCθ	Protein kinase C θ
PLAD	Pre-ligand assembly domain
PLC-γ	Phospholipase C
PMA	Phorbol myristate acetate
Poly I:C	Polyinosinic : polycytidylic acid
PV	Pichinde virus
Rag	Recombination activating gene
RANK	Receptor activator of NFκB
Ras	Rat sarcoma (GTPase)
RBC	Red blood cell
RIG-1	Retinoic acid inducible gene-1
RIP1	Receptor-interacting protein
RLR	RIG-1 like receptor
RSV	Respiratory syncytial virus
RTE	Recent thymic emigrant
RTPCR	Reverse transcription polymerase chain reaction
SH-2	Sarcoma (Src)-homology domain
SLECs	Short-lived effector cells
SLO	Secondary lymphoid organs
SLP-76	SH-2 domain containing leukocyte protein

SMAC	Supramolecular activation cluster
S1P	Sphinogosine 1 phosphate
SP	single positive
STAT	Signal transducer activator of transcription
TAK	Transforming growth factor β-activated kinase-1
TBI	Total body irradiation
TCR	T cell receptor
Tc	T-cytotoxic
Tg	Transgenic
Th	T- helper
TNF	Tumor necrosis factor
TLR	Toll-like receptor
TEC	Thymic epithelial cell
TNFR	Tumor necrosis factor receptor
TIR	Toll/interleukin-1 receptor domain
TIRAP	TIR domain containing adaptor protein
TRADD	TNFR associated death domain
TRAM	Translocating-chain associating membrane protein
TRAIL	TNF-related apoptosis-inducing ligand
TREC	TCR rearrangement excision circles
TRIF	TIR domain containing adaptor inducing IFN-β
Treg	T regulatory cell
TSA	Tissue specific antigen
V(D)J	Variable (diversity) joining
VEGI	Vascular- endothelial cell growth inhibitor
VSV	Vesicular stomatitis virus

VV	Vaccinia virus
ZAP70	Zeta chain associated protein kinase-70
Z-VAD	Carbobenzoxy-valyl-alanyl-aspartyl –[o-methyl]-Fluoromethylketone

Chapter 1: Introduction

A. Rationale and thesis outline

Recent studies have highlighted the combined nature of signal 1 (T cell receptor - TCR), signal 2 (co-stimulation) and signal 3 (cytokines) in influencing the early programming of naïve T cells to adopt various fates, whether productive or abortive. The members of the TNF superfamily have been shown to control and orchestrate various aspects of an immune response depending on the context of T cell activation. My thesis involves the study of two prototypic members of the TNF superfamily, TNF and FasL and their respective roles in influencing some of the earliest events of T cell activation during a viral infection and during the induction of peripheral transplantation tolerance.

Several years ago, our lab discovered that TNF is one the earliest pro-inflammatory cytokines that is produced by recently activated naïve T cells (1). However, the importance of T cell-derived TNF and the developmental stage when T cells become licensed to produce this cytokine were not known. TNF was recently shown to limit the magnitude of $CD8^+$ effector T cell responses during acute LCMV infection (2). However, the cellular source of TNF causing this suppressive effect was not determined in these studies. I first hypothesized that T cell-derived TNF can suppress T cell responses during the course of an immune response. Recent studies have shown that developing T cells require emigration into the periphery and contact with secondary lymphoid organs to undergo functional maturation (3). Secondly, I hypothesized that developing T cells will acquire the ability to produce TNF as a consequence of

undergoing functional maturation in the periphery. I used the P14 TCR transgenic $CD8^+$ T cell system, that consist of T cells that recognize the GP33 peptide of LCMV, to address the above two questions in chapter 3 of my thesis. To study the immunoregulatory role of T cell-derived TNF, I used an *in vivo* experimental model where I co-adoptively transferred WT P14 and TNF-deficient P14 TCR transgenic $CD8^+$ T cells into WT, TNF-deficient and TNFR (1 and 2)-deficient hosts and analyzed the accumulation of donor T cells at day 8 post LCMV infection. To study the developmental stage when T cells become licensed to produce TNF efficiently, I studied the TNF producing ability of T cells (both transgenic and polyclonal) before and after thymic emigration into the periphery.

Previous studies by Thornely et. al demonstrated that there is abortive activation and early deletion of T cells responding to alloantigens in the absence of TNF family co-stimulatory signals (CD154-CD40 blockade) (4). This deletion has been shown to be important for the prolonged allograft survival in mice. Exposure to TLR agonists at the time of co-stimulation blockade [DST+ αCD154 (MR1)] prevented the deletion of alloreactive T cells leading to abrogation of tolerance a Type-1 IFN mediated pathway (5). I hypothesized that activation of TLRs (TLR4 agonist - LPS) prevent the abortive activation and the early deletion of alloreactive T cells, that occurs in the presence of CD154-CD40L blockade, by differentially regulating the expression of several pro- and anti-apoptotic genes. In chapter 4 of my thesis, I addressed this hypothesis with the use of a KB5 synchimeric mouse model, that consist of a trace population of KB5 Tg $CD8^+$ T cells (that recognize H-$2K^b$ as an alloantigen), and studied their apoptotic molecular

signature by examining the expression of focused set of apoptotic genes using real-time PCR array, during co-stimulation blockade-induced tolerance and during TLR4 mediated abrogation of co-stimulation blockade-induced tolerance.

B. T cell development: Conventional and unconventional lineages

Of the many cells that constitute the immune system, T lymphocytes (T cells) form an important component of the adaptive immune system. T cell development begins when undifferentiated T cell precursors migrating from the bone marrow enter the thymus. T cell progenitors undergo sequential steps of development and education to become mature naïve T cells before they enter the circulation. In the context of murine T cell development, the early T cell progenitors migrating into the thymic cortex do not express the CD4 and CD8 coreceptors and are referred to as double negative (DN) thymocytes. The classical model of T cell development, consists of immature thymocytes progressing through 4 stages, that are distinguished by the surface expression of CD44 and CD25: DN1 ($CD25^{-}CD44^{+}$) ; DN2 ($CD25^{+}CD44^{+}$) ; DN3 ($CD25^{+}CD44^{-/lo}$) ; DN4 ($CD25^{-}CD44^{-}$) (6-8). The precursors differentiate and rearrange their antigen receptor loci through a process referred to as V(D)J recombination. It is a site-specific recombination process directed by the lymphoid specific recombinases (recombination activating gene or Rag1 and Rag2) and DNA repair proteins (9, 10). The recombination signal sequences flanking the TCR variable (V), diversity (D) and joining (J) gene segments are the target sites for the Rag proteins, which create double stranded DNA breaks and subsequently result in non-homologous end joining of the gene segments (11).

Recombination of TCR δ, TCRγ, TCRβ occur between the DN2 and DN3 stages of T cell development, following which thymocytes commit to either γδ or αβ TCR lineages (11). Thymocytes possessing in frame TCR-γ and TCR-δ rearrangements and expressing mature γδ TCR commit to the γδ T cell lineage while remaining DN (12, 13). In contrast, thymocytes undergoing TCRβ gene rearrangements are required to pass though a subsequent series of biological checkpoints in order to survive.

The first checkpoint for αβ TCR T cell development referred to as "β selection" ensures the selection of a functional TCRβ chain (14, 15). The TCRβ chain is created by a well-ordered recombination event with Dβ-to-Jβ preceding Vβ to DβJβ rearrangement (11). During "β selection", the TCRβ chain associates with a surrogate α chain to form the pre-TCR complex, which drives thymocyte differentiation in a ligand independent manner (15). The assembly of a successful pre-TCR complex prevents cells from undergoing apoptosis and inhibits further rearrangement at the TCRβ gene locus through a phenomenon known as "allelic exclusion" (15). Thereafter, cells transit from DN4 stage and undergo 6 to 8 cell divisions before entering into the $CD4^+CD8^+$ double positive (DP) stage, at which point the rearrangement of the TCRα chain is initiated (16). The TCRα chain continues to rearrange until a αβ heterodimer is produced with sufficient avidity to bind self peptide-MHC complexes (9, 17). During this stage, DP cells expressing the successfully rearranged αβ TCR undergo a process of selection where ~90% of DP cells that develop are eliminated through "death by neglect" due to poor interactions of expressed TCRs with the available self-peptide MHC (major

histocompatibility) complexes (MHC-I in the context of $CD8^+$ and MHC-II for $CD4^+$) that fail to generate viable intracellular signals (18). Those thymocytes expressing TCRs that are able to bind self-peptide/MHC complexes adequately are selected to survive in a process know as “positive selection” (18). DP thymocytes expressing TCRs that bind self-peptide MHC complexes with strong affinity and potentially self-reactive are eliminated by a process of apoptosis referred to as “negative selection” (18, 19). Once thymocytes are successfully selected, they undergo lineage differentiation to become $CD4^+$ or $CD8^+$ single positive (SP) thymocytes (18). The CD4-CD8 lineage commitment is controlled by both TCR signal strength and temporally. Stronger and longer signals through the TCR and CD4-coreceptor lead to the development of $CD4^+$ lineage whereas weaker and shorter signals through the TCR and CD8-coreceptor lead to the development of $CD8^+$ lineage (20, 21). More recently, it was proposed that $CD4^+$/$CD8^+$ lineage commitment is in part regulated by the balance of two tyrosine kinases that act downstream of the TCR namely, Lck (Leukocyte specific protein tyrosine kinase) and ZAP70 (Zeta-chain associated protein kinase-70) (22). This model proposes that during positive selection, if DP cells recognize MHC-II by CD4 coreceptor, they receive a strong Lck-dependent signal and differentiate into SP $CD4^+$ T cells. On the other hand, if DP cells recognize MHC-I by CD8 co-receptor, absence of strong Lck dependent signal prevents their differentiation into SP $CD4^+$ T cells (22). Instead these DP cells increase the expression of ZAP70 and differentiate into SP $CD8^+$ T cells (22).

Along with the development of conventional αβ TCR lymphocytes, unconventional lymphocytes also differentiate in the thymus. Commitment to the γδ

lineage occurs between the DN2 and DN4 stages and prior to the β checkpoint (16, 23). Recent studies show that αβ/γδ T cell lineage decisions do not depend on the nature of TCR complex, but rather the signal strength of the TCR (9). This model predicts that stronger and sustained signals lead to the generation of γδ T cells and that weaker and transient signals generate the αβ T cell lineage (24, 25). In addition to γδ T cells, other unconventional lineages develop from the DP cells in the thymus, including the forkhead box P3 $(Foxp3)^+$ $CD4^+$ $CD25^+$ T regulatory (Treg) cells and the innate -like $CD4^+$ and $CD8^+$ CD1d-specific natural killer T (NKT) cells (26, 27). Other cell lineages that develop from DP precursors include lymphocytes that express CD8αα homodimers instead of the conventional CD8αβ heterodimers; these home to the gut tissue and are known as intraepithelial lymphocytes. The unconventional $CD8^+$ cells and the NKT cells are referred to as "innate-like lymphocytes", as they acquire effector functions during their maturation in the thymus rather than in the periphery after activation (28). Unlike the selection of conventional αβ TCR T cells that occurs by the recognition of classical MHC class-I and class-II molecules expressed on cortical thymic epithelial cells, the selection of innate-like lymphocytes occurs through interactions with molecules expressed on hematopoietic cells (29-34). Therefore, the thymus serves as a central site for the maturation of a variety of lymphocytes that eventually migrate into the peripheral organs.

C. T cell maturation and emigration

It was initially believed that, after positive selection, SP thymocytes reside in the thymic medulla for 2 weeks before they emigrate out of the thymus (35, 36). This lengthy residency period was suggested to serve as an additional checkpoint for the induction of tolerance where selected thymocytes survey tissue specific antigens (TSAs) presented by the medullary thymic epithelial cells (mTEC) (37). During this period, immature SP thymocytes undergo sequential phenotypic and functional maturation that results in remarkable heterogeneity of the SP thymocytes at different stages of maturation (38, 39). Expression of CD69 and CD24 on early immature SP thymocytes (heat stable antigen; HSA), is gradually downregulated in a sequential manner and the expression of CD62L, β_7 integrin and Qa2 (non-classical MHC class I) is upregulated (40). Consequently, the most mature cells ($CD69^-$ $CD24^-$ $Qa2^{hi}$) possess the maximum proliferative capacity and have been shown to produce cytokines, such as IFN-γ, TNF and IL-2 ($CD8^+$ SP thymocytes) upon phorbol myristate acetate (PMA) and ionomycin stimulation when compared to the least mature cells ($CD69^+$ $CD24^{hi}$ $Qa2^-$)(38).

Early studies on thymic emigration tracked thymocytes using techniques such as intra-thymic injection of fluorescein isothiocyanate (FITC), bromodeoxyuridine (BrdU) labeling or detection of non-replicative TCR rearrangement excision circles (TRECs) that are formed as byproduct of TCR gene rearrangements (41). These studies proposed that SP thymocytes required 2 weeks of residency before they emigrate. Recently, the Rag2 (green fluorescent protein) GFP mouse model has been developed to allow the study of

thymic emigration in an unmanipulated setting (41). In the Rag2 GFP mouse model, GFP is expressed under the control of the Rag2 promoter such that the SP thymocytes are GFP-positive. The emigration process was thought to occur via a stochastic mechanism whereby some medullary SP thymocytes leave early and others leave late by a "lucky dip" process (42, 43). Through the use of the Rag2 GFP mouse model, it was revealed that naïve thymocytes emigrate from the thymus 4-5 days after becoming SP thymocytes via a strict "conveyor belt" mechanism where the most mature thymocytes leave first (43). After the final stages of differentiation, SP thymocytes enter the lymphatics and the blood vessels and are exported into the periphery at a rate of 1 to 2% of thymocytes per day (44).

It was proposed during the 1970s that the maturation of SP thymocytes is not completed within the thymus and that cells are required to migrate into the periphery to become fully mature (45). Studies done with the Rag2 GFP mouse model has confirmed that SP thymocytes continue to undergo post-thymic maturation (41). Rag2 is expressed by thymocytes, but this expression is shut down after successful recombination of the TCR. However, GFP expressed by thymocytes in Rag2 GFP mice is stable and can be used to detect recent thymic emigrants. The level of GFP decays gradually in the peripheral T cells, allowing the GFP intensity to identify T cells at different stages of post-thymic maturation. The GFP^{hi} T cells indicate cells that have resided in the periphery for 0-7 days, GFP^{lo} T cells indicate cells that have resided in the periphery for 7-14 days and GFP^{neg} T cells have joined the MN T cell pool (> 14 days in the periphery) (41). These and other studies have revealed that post-thymic maturation of emigrating

thymocytes, both phenotypically and functionally, occurs in secondary lymphoid organs (3, 41). Additionally, CD8αβ^{+} TCRαβ recent thymic emigrants can also home directly to the epithelium of the small intestine, where they have been shown to undergo differentiation and proliferation. The gut environment serves as another environment where RTEs can undergo further education and maturation (46). Collectively these findings show that thymic maturation and emigration of lymphocytes is a tightly regulated process that ensures a homeostatic maintenance of the peripheral T cell pool (47).

D. T cell activation and signaling

Activation of T cells begins when a T cell receptor engages its cognate peptide-MHC complex on an antigen-presenting cell. This is a universal first signal that T cells respond to, whether it is during positive selection, negative selection in the thymus or when naïve T cells in the periphery respond to cognate antigenic ligands during the initiation of an immune response. Depending on the strength of TCR engagement and the stage of development, distinct downstream signaling cascade events are initiated that determine the biological outcome of the response. In addition to signal 1, T cells also require an augmenting second signal or co-stimulation that is mediated by accessory surface molecules. Thirdly, the presence of pro-inflammatory cytokines in the milieu also influences the programming of the responding T cells. In this section, the importance of the three-signal model for T cell activation is discussed.

Signal 1: TCR-peptide MHC interaction

The TCR recognizes proteolytically processed peptides (8-15 amino acids) presented in the context of self-MHC complexes on the surface of antigen-presenting cells (48). The enigma of TCR recognition of antigen in a self-MHC restricted manner was analyzed at the atomic level in 1996 when Garboczi and colleagues showed the crystal structure of a human αβTCR in complex with a histocompatibility antigen (HLA-A2) molecule presenting a peptide derived from the HTLV-1 Tax peptide (49). This was the same year when Rolf Zinkernagel and Peter Doherty were awarded the Nobel prize in Medicine for their ground breaking discovery in 1974, demonstrating that cytotoxic T cells lysed virus-infected target cells in a self-MHC restricted manner (50, 51). At this point in time however, the mechanism of TCR recognition was not clear, although they proposed the term “altered self” recognition by the TCR. In the following years several significant discoveries were made, such as the resolution of TCR complex as a heterodimer composed of α and β chains, as discovered by Mark Davis and other labs (52), studies that ruled out intact viral antigen expressed on the cell surface as a part of the ligand recognized by the TCR (53, 54) and work by Townsend and colleagues that showed that exposure to short peptide sequences can sensitize cells to be lysed by CTLs (55, 56), and studies that showed the crystal structure of human HLA class-I with a cleft that could accept peptides of 8 to 10 amino acids. Together, these pioneering studies paved the way to the final resolution of the TCR-peptide-MHC complex in 1996 (57-59).

The TCR complex is comprised of two subunits, namely the antigen binding subunit consisting of the α and the β chains and the signal transduction subunit consisting of the CD3ε, γ, δ and ζ chains that offers the primary intracellular signal (48, 60). The signal from the TCR is emanated downstream through phosphorylation of CD3ε, γ, δ and ζ chains by Src kinases proximal to the TCR, namely, Lck and Fyn (48, 61). Once activated, the Src kinases recruit ZAP70 to the immunoreceptor tyrosine-based activation motif (ITAM) (48). Following its attachment to the ITAM motif, ZAP70 is phosphorylated by Lck and is activated (62). Additionally, ZAP70 and Lck also interact with each other, resulting in sustained ITAM phosphorylation that leads to the recruitment of additional ZAP70 molecules and kinases such as IL-2 inducible T cell kinase (ITK) (63). The stoichiometry of ITAM phosphorylation has been shown to be directly proportional to the affinity of the TCR for it peptide ligand (64, 65). This may be particularly instrumental in the discrimination of signals emanating downstream of the TCR binding to ligands with different affinities during selection in the thymus or while responding to pathogens in the periphery (66). The activity of Lck is believed to be controlled by CD45, a tyrosine phosphatase that associates with CD4 co-receptor that is attached to Lck (61). CD45 dephosphorylates Lck leading to changes in the conformation and activation of Lck (61).

Kinases such as Lck, ZAP70 and tyrosine protein kinases such as Tec kinases are involved in the phosphorylation of two adaptor proteins, namely linker of activation of T cells (LAT) and SH-2 domain containing leukocyte protein of 76kDa (SLP-76) (61, 67). LAT is a type-III transmembrane protein that serves as a docking site for several sarcoma

(Src)-homology domain (SH2) proteins such as phospholipase C-γ_1 (PLC-γ_1) and phosphoinositidyl kinase-3 (PI-3K). LAT also stabilizes SLP-76 binding to the complex via proteins such as glutamic acid decarboxylase proteins (GADs). SLP-76 recruits a tec kinase that phosphorylates PLC-γ_1 (61). This in turn leads to the activation of PLC-$\gamma_{1,}$ which then cleaves phosphotidyl inositol-4,5 biphosphate (PI-4,5-P_2) into inositol-1,4,5 – trisphosphate (IP_3) and diacylglycerol (DAG). IP_3 signaling leads to the release of $Ca2^+$ from the endoplasmic reticulum storage sites followed by an influx of external Ca^{2+} through Ca^{2+} release-activated Ca^{2+} (CRAC) channels. The increase in $Ca2^+$ leads to the activation of calcineurin, a calcium-calmodulin-dependent serine phosphatase that dephosphorylates nuclear factor of activated T cell (NFAT) transcription factor and leads to its nuclear translocation and the activation of transcription of cytokine genes such as interleukin-2 (IL-2) (68). TCR ligation also results in the activation of rat sarcoma (GTPase) (Ras). The Ras pathway is controlled by guanine exchange factors (GEFs), which activate Ras. Activated Ras complexes with Raf-1, a serine threonine kinase, and this interaction leads to the activation of the extracellular signal activated kinase (ERK) cascade involving several mitogen activated protein kinases (MAPKs). Once ERK is activated it leads to the activation of transcription factors activator protein-1 (AP-1) for the regulation of cytokine genes, such as IL-2 (61). GEFs regulates Ras pathway by activating GTPase–activating proteins that stimulate the intrinsic GTPase activity of Ras and lead guanosine triphosphate (GTP) hydrolysis and Ras inactivation (61). PI-3 kinase is another molecule that is recruited to LAT. It is involved in the phosphorylation of PI-4,5 P_2 and PI-4P to PI-3,4,5-P_3 and PI-3,4 P_2, respectively (61). These molecules further

interact with proteins such as PLC-γ and help retain them at the membrane (61). Additionally, PI-3 kinase is involved in the activation of serine-threonine, protein kinase B (PKB also called Akt) which plays a role in cell survival (69).

Signal 2: Co-stimulation

The second signal that T cells require for activation is a non-specific positive signal that is initiated by the interaction of co-stimulatory molecules between the T cells and antigen-presenting cells. CD28 was one of the first co-stimulatory molecules to be identified (70, 71). TCR engagement in the absence of CD28 signaling results in abortive activation of T cells leading to anergy (70, 71). Binding of CD28 to its ligands (B7-1 and B7-2) on the antigen-presenting cell leads to optimal T cell signaling events that trigger IL-2 production, clonal expansion and generation of effector and memory T cells (71, 72). Following the identification of CD28 mediated co-stimulatory pathway, another structurally related molecule named cytotoxic T lymphocyte antigen-4 (CTLA4) was discovered (73). In contrast to CD28, CTLA-4 binds to B7-1 and B7-2 with much higher affinity and offers an inhibitory signal to the T cells. Recently, other co-stimulatory molecules related to CD28 family have been discovered, including the inducible co-stimulator (ICOS)-ICOSL, and the programmed death (PD)-PD-L1/PD-L2 pathway (72). Similar to CD28, ICOS is a positive co-stimulatory signal induced upon T cell activation and is predominantly dependent upon CD28 co-stimulation (74). ICOS-ICOSL signaling results in the upregulation of CD40L by T cells that in turn stimulates the expression of B7-1 and B7-2 molecules on antigen-presenting cells (APCs) that provide a positive

feedback loop in sustaining CD28 co-stimulation (72). In contrast, the (PD)-PD-L1/PD-L2 pathway is a negative co-stimulatory pathway that has been shown to play a role in self-tolerance. PD-1 is expressed on activated $CD4^+$ T cells, $CD8^+$ T cells, B cells, natural killer (NK) cells and macrophages (75). PD-L1 and PD-L2 are expressed by activated APCs and endothelial cells and constitutively expressed on parenchymal cells of non–lymphoid organs such as heart, kidney and pancreas (76-78). The role of PD-1 in self-tolerance is evident in PD-1 deficient mice, which exhibit an autoimmune phenotype with lupus like-glomerulonephritis and progressive arthritis (79).

Ligation of the CD28 co-stimulatory receptor augments the TCR signal by association with proximal tyrosine kinases such as Lck, Tec and ITK thereby increasing the generalized protein-tyrosine phosphorylation downstream of the TCR (80-82). Additionally, the CD28 signaling activates nuclear factor κ light chain enhancer of activated B cells (NFκB) and c-Jun NH(2)-terminal kinase (JNK) cascades, which stimulate IL-2 production (61). The activation of NFκB downstream of CD28 is believed to occur via the activation and phosphorylation of inhibitor of NFκB (IκB) kinaseβ (IKKβ) by protein kinase Cθ (PKCθ) (83). The activation of the IKK complex (α,β and noncatalytic subunit γ) leads to the subsequent phosphorylation and degradation of IκBα and IκBβ, and the nuclear translocation of NFκB (61). The inhibition of PKCθ results in abrogation of NFκB activation and consequently IL-2 production (61, 83). Another target of activation for the NFκB pathway is the B cell lymphoma extra-large (Bcl-xL)

promoter, which contains a NFκB response element. NFκB activation increases expression of Bcl-xL, which enhances survival of T cells during activation (84, 85).

In addition to the CD28:B7 family of co-stimulatory molecules, members of the TNF-TNFR superfamily members have also been shown to play a vital co-stimulatory role during T cell activation. These include the CD40-CD40L, OX40-40L, 4-1BB-4-1BBL, CD27-CD70, CD30-CD30L and HVEM (herpes-virus entry mediator)-LIGHT (Lymphotoxin like inducible protein that competes with glycoprotein D for HVEM on T cells) members (86). CD40 is constitutively expressed on B cells, DCs, macrophages and thymic epithelium and is induced on endothelial cells and fibroblasts (87). CD40L (CD154) on the other hand, is expressed on activated T cells, NK cells and eosinophils. The binding of CD40L to CD40 initiates signaling in the APCs that in turn augments antigen presentation by the APC and enhances T cell activation (72). CD27 and HVEM are constitutively expressed on naïve T cells and are believed to play a role during early T cell activation (88, 89). Upon activation, CD27 expression is upregulated, reaching peak levels by 24 hours (90). HVEM, on the other hand, is downregulated after activation and is re-expressed when T cells reach the resting memory phase (86, 89). The expression of OX40, 4-1BB and CD30 is induced on activated T cells by the CD28-B7-1/B7-2 (CD80/86) co-stimulatory pathway (86). Similar to the co-stimulatory receptors, expression of the ligands, including OX40L, 4-1BBL, CD70 and CD30L is also induced by 24 hours on activated T cells and lasts for several days after activation, suggesting that these signals function during an ongoing response (86). CD70 is expressed in thymic epithelium and B cells whereas OX-40L, 4-1BBL and CD30L are expressed on activated

dendritic cells (DCs) and B cells (72, 86). In contrast, LIGHT is expressed on immature DCs and its expression is downregulated upon activation.

The downstream signaling via CD40, HVEM, CD27, 4-1BB and CD30 receptors have similar features. These co-stimulatory receptors bind TNFR associated factors (TRAFs), which serve as adaptor proteins. TRAF2 is a crucial adaptor protein that is used by all the TNFR molecules (86). The 3 major signaling cascades that are initiated downstream of TRAF2 involve the JNK and the AP1 (Fos/Jun) transcription factor, NFκB and the PI-3 kinase/PKB (Akt) signaling pathways. Activation of these pathways results in the up-regulation of anti-apoptotic molecules such as Bcl-2 and Bcl-x_L and the induction of cytokines such as IL-2, IL-4 or IFN-γ (86). Therefore both the CD28 and TNFR family co-stimulatory molecules share several of the downstream signaling pathways that are vital for optimal T cell activation.

Signal 3: $CD4^+$ T cell help and cytokines

In addition to signal 1 (TCR) and signal 2 (co-stimulation), naïve $CD8^+$ T cells are now believed to require a third signal for the optimal generation of effector and memory T cells, either as $CD4^+$ T cell help or as the production of inflammatory cytokines (91). $CD4^+$ T cell help is critical early during the activation of $CD8^+$ T cells in order to generate functional memory (92). It was later shown that “helpless” memory $CD8^+$ T cells produce TRAIL (tumor-necrosis factor-related apoptosis inducing ligand) upon restimulation, which mediates AICD of the responding memory population (93). $CD4^+$ T cell help to T cells is thought to occur via two pathways. One pathway is through

interactions of CD40L expressed on the $CD4^+$ T cell and CD40 expressed on the DCs. CD40 engagement on the APC enhances the expression of co-stimulatory molecules that in turn enhance activation of naïve $CD8^+$ T cells (92). The second pathway is by the production of IL-2 by the $CD4^+$ T cells. (91, 94-96). Studies in mice deficient in IL-2 revealed that although the initial division of $CD8^+$ T cells occurred in a IL-2 independent manner, IL-2 was required for sustained expansion of $CD8^+$ T cells (97). Additionally, studies by William and colleagues showed that secondary responses were impaired in CD25-deficient $CD8^+$ T cells, which cannot bind IL-2 with high affinity (98). The defect in memory T cells was rescued when mice were administered IL-2 and IL-2 specific antibody complex at the time of immunization and not during rechallenge (98, 99). These studies suggest that IL-2 signaling is vital for $CD8^+$ T cell activation during the primary phase for optimal memory generation.

The importance of cytokines as a third signal for T cell activation was first demonstrated with in vitro studies where the addition of IL-12 and type-1 IFN along with artificial APCs (class-I MHC/peptide complex on the surface of cell sized microspheres along with B7 ligands) stimulated a strong clonal expansion and cytolytic function of naïve T cells (100-102). The engagement of TLRs (by adjuvants) on antigen presenting cells triggers the production of type1-IFNs or IL-12 that in turn can provide the additional signaling needed for T cell activation (103, 104). Studies have demonstrated that T cells deficient in the cytokine receptors for Type I-IFNs and IL-12 show reduced expansion during infection (105-107). The molecular mechanisms behind the action of these cytokines on T cell responses is thought to be due to increased expression of pro-survival

molecules, such as Bcl-3 (108). In line with this, it is known that Type-1 IFNs induce the production of the γc cytokine IL-15 by DCs that are receptive to IL-15 (109). Additionally naive T cells also express IL-15R (110). Therefore it can be speculated that signaling of IL-15 on DCs and naïve T cells can optimize T cell activation (110).

E. T cell programming for optimal effector and memory generation

T cell responses in secondary lymphoid tissues occur in 4 stages, namely priming of naïve T cells, clonal expansion of effectors followed by a contraction phase and finally memory generation. The nature of the magnitude and quality of T cell responses generated by exposure to antigen are dependent upon various factors including the context in which T cells recognize an antigen (level of co-stimulation and inflammatory cytokines), the abundance of antigen and the duration of antigen exposure (111). $CD4^+$ and $CD8^+$ T cells exhibit varying degrees of dependence on co-stimulation. For example, the absence of CD28, CD154 (CD40L) or OX-40 has shown to impair $CD4^+$ T cell responses but cause only a modest effect on $CD8^+$ T cells (112). On the other hand 4-1BB is required for CTL responses but not for $CD4^+$ T cells (111, 113). The differential requirement for co-stimulatory molecules by $CD4^+$ and $CD8^+$ T cells suggests that $CD4^+$ and $CD8^+$ T cells may have different thresholds of activation that may be influenced by both intrinsic and extrinsic factors (111). The duration of antigenic signal is an additional factor that can influence the generation of T cell responses. Studies have shown that naïve $CD4^+$ T cells require at least 6 hours of antigenic stimulation in the presence of co-stimulation for commitment to proliferation and at least 24 hours in the absence of co-

stimulation (114-116). For $CD8^+$ T cells, 2 to 24 hours of exposure to the antigen can enable them for 7-10 cell divisions (117). During the initial stages of activation, T cells require extended contact with antigen-presenting cells in the secondary lymphoid tissues (118). Two photon microscopy studies have revealed that the priming stage can be broadly classified into 3 successive phases. In phase one, T cells undergo short encounters with DCs for up to 8 hours, during which time they lose their motility and up-regulate activation markers (118). This is followed by long-lasting stable interactions with DCs that can last for 12 hours as T cells begin to secrete cytokines such as IL-2 and IFN-γ (118). Over the next 24 hours, T cells gain the capability to proliferate and exhibit high motility (118). It was determined that an initial short encounter of naïve $CD8^+$ T cells with antigen was sufficient to program the daughter cells to proliferate in the absence of further stimulation (117). Collectively, these studies suggest that once a certain threshold of activation has been attained during the initial period of priming, naïve T cells embark on a proliferative response where they differentiate and clonally expand in a programmed fashion (111).

The next phase of an immune response is the effector phase where activated T cells migrate to various tissues to remove virus-infected cells by producing effector cytokines such as TNF and IFNγ and IL-2 and also exhibit cytolytic functions associated with the production of perforin and granzyme-B (119). With respect to the memory T cell generation, effector T cells are distinguished into two broad populations. One population is referred to as the memory precursor effector cells (MPECs) that is destined to persist into memory, and the other population is referred to as short lived effector cells (SLECs)

that do not survive into long-term memory. Of the many markers used to distinguish these populations, killer cell lectin-like receptor G1 (KLRG1) and IL-7R have become the standards where MPECs are identified as $KLRG1^{lo}$ and $IL7R^{hi}$ and SLECs are identified as $KLRG1^{hi}$ and $IL\text{-}7R^{lo}$ (120-122). However, this distinction between MPECs and SLECs using KLRG1 and IL-7R is not always absolute, as other studies have shown that some $KLRG1^{hi}$ $IL\text{-}7R^{lo}$ do persist into memory and some memory cells express both KLRG1 and IL-7R (120, 121). A recent study demonstrated a role for pro-inflammatory cytokines such as IL-12 in determining whether activated $CD8^{+}$ T cells develop into SLECs or MPECS. The levels of IL-12 produced during the immune response were shown to control the expression of the transcription factor T-bet, with high levels driving the development of SLECs and low levels favoring MPECS (121). These findings suggest that the cytokine milieu can also influence the fate of effector T cells during an immune response.

The effector phase is followed by a contraction phase where 90 to 95% of cells in the spleen undergo programmed cell death leaving a small population of cells that persist into memory. Several studies have suggested that the contraction phase is programmed early after infection and is not influenced by the duration of antigenic stimulation. In experiments with *Listeria monocytogenes,* where infected mice were treated with antibiotics two days after infection to reduce the antigen load, neither the onset or magnitude of T cell contraction was significantly different as compared to control infected animals (123). Additionally, the contraction phase during LCMV infection was independent of the magnitude of expansion, dose and duration of infection or amount of

antigen displayed (123). Several molecular mechanisms have been studied for a role in regulating the contraction phase. Studies using P14 TCR transgenic T cells deficient in TNFR1 and CD95 (both molecules required for activation induced cell death) have shown that both these molecules are dispensable for T cell contraction during a viral infection (124, 125). On the other hand, the absence of BIM (Bcl-2 interacting mediator of cell death) results in defective contraction of activated T cells (126, 127). BIM mediates the apoptosis of IL-7R^{lo} effector T cells during a viral infection (128, 129). While some antigen-specific T cells (GP33 and GP276) do undergo contraction during an LCMV infection of BIM deficient mice, other epitope-specific responses do not contract, such as NP396-specific CD8^{+} T cells, suggesting the existence of other mechanisms controlling contraction phase (130). Supporting this idea, recent studies on Fas and BIM double-deficient mice revealed there was 100-fold more accumulation of antigen-specific memory CD8^{+} T cells in Fas-BIM double-deficient mice compared to their WT counterparts after LCMV infection, suggesting a combined effect of these molecules during the contraction phase of an immune response (131).

The cells that survive the contraction phase enter the memory pool. Memory T cells are a heterogeneous population of cells that require IL-7 and IL-15 for their survival and maintenance (110). Memory T cells are classified into two types of cells, namely CD62L^{lo} (Cysteine-Cysteine) C-C Chemokine Receptor-7 ^{lo} (CCR7^{lo}) effector memory and CD62L^{hi} CCR7^{hi} central memory T cells, and these 2 subsets have distinct homing properties (91). On one hand, central memory T cells primarily localize to secondary lymphoid tissues, and have low cytolytic function and migratory potential. In contrast,

effector memory T cells reside in non-lymphoid tissues, are cytolytic and exhibit circulatory potential (132). Studies in IL-12- deficient and T bet-deficient mice show that effector cells rapidly acquire memory characteristics, suggesting that the early production of inflammatory cytokines can influence the rate at which memory is generated (133, 134).

Several models for differentiation of effector and memory cells have been proposed that are not mutually exclusive. One of the simplest of the models is the uniform potential model, which proposes that all effector cells are homogenous with equal memory potential. Extrinsic factors such as growth factor withdrawal will determine the number of cells that enter memory (135, 136). The second model is the decreasing potential model that predicts that a shorter duration of antigenic stimulation leads to the formation of MPECs that give rise to central memory T cells whereas longer stimulation leads to terminal differentiation of effector T cells that lose memory potential (136). The prediction for this model is that the process will create heterogeneity in the effector T cell pool. The third model is the fixed lineage model, which predicts that T cells commit to either effector or memory phenotype early during activation. In this model, memory T cells are mature and can bypass the need to become effectors by directly entering the memory T cell pool (136). Supporting this model, it was shown that asymmetric first division of daughter T cells could determine the fate of the responding T cell with the proximal T cells becoming effector cells and the distal ones becoming the memory T cells (137). The fourth model is the fate commitment and progressive differentiation model, which suggests that the strength of signal determines the fate of T

cells during early activation. The MPECs acquire effector functions but also retain the ability to become SLECs and those that survive become central memory T cells (136). The SLECs undergo apoptosis and a few that survive become end-stage T effector memory T cells (136). More recently two studies used *in vivo* transfer of single naïve $CD8^+$ T cells and of naïve T cells with distinct genetic tags (barcodes generated by transduction of OT-1 thymocytes with retroviral library with nearly 3500 unique genetic tags and GFP) methods to decipher the developmental potential of naïve T cells (138, 139). These studies support a model that one naïve T cell has multiple fates and that it can differentiate into both effector and memory T cells and is not determined by the nature of priming antigen presenting cell or the duration of the priming (138, 139).

F. Role of TNF superfamily members in T cell immune regulation and homeostasis

Historical landmarks in the discovery of TNF/TNFR superfamily members

The tumor necrosis factor (TNF)/TNF receptor superfamily is a collection of ligands and receptors that are key mediators in the regulation of immune responses (140, 141). The action of TNF was first described by P.Bruns, a German physician who observed the regression of tumors in humans after a bacterial infection (141). Later, W.Coley used bacterial toxins for the treatment of human cancers (142). In 1944, LPS isolated from bacterial extracts was shown to be sufficient to mediate tumor regression (141, 143), Following this, in 1962, the role of LPS in the regression of the tumors was shown to be indirect and mediated by the induction of a serum factor named “tumor necrotizing factor”(144). Subsequently, in 1975, activated macrophages were also

described to be a source of this cytotoxic factor and the group renamed it as “tumor necrosis factor”(145). In 1983, it was found that even B lymphoblastoid cell lines were capable of producing TNF (146).

In 1968, both Granger and Ruddle discovered that lymphotoxins (LTs) were produced by lymphocytes and could kill tumors (147-150). In 1985, the amino acid sequences of TNF and LT were described to be homologous by Aggarwal et al (151, 152). Later, it was found that TNF and LT also share functional homology (153) in their ability to bind common receptors (TNFR1 and TNFR1) which led to renaming TNF as TNFα and LT as TNFβ (141). It was discovered that LPS induced cachexia (wasting) was mediated by murine TNFα (154). Subsequently, Takeda and coworkers discovered that the TNF was the myeloid differentiation factor as well (155). Since then numerous molecules belonging to the family of TNF and LT (ligands for the TNFRs) have been discovered, and they have both unique and redundant roles in the immune system.

TNF-TNFR family and signaling

The TNF superfamily is comprised of at least 19 different ligands, including FasL, TRAIL, CD70, CD30L, CD40L, 4-1BBL,OX40L and LIGHT (141). With the exception of LTα and vascular endothelial cell-growth inhibitor (VEGI), all of the TNF ligands are type II transmembrane proteins with the carboxy terminus localized in the extracellular domain, the amino-terminus in the intracellular domain and containing a single transmembrane domain (141). The extracellular domain is referred to as the TNF homology domain and has 20 to 30% homology among the superfamily members.

TRAIL and FasL have the highest homology to TNF among all the TNF members and like TNF can induce apoptosis (141). All TNF family members form either soluble or membrane-bound homotrimers or trimerize with other members of the TNF family ($LT\alpha_1\beta_2$ for example)(156).

There are 29 receptors that belong to the TNF receptor superfamily (141), including TNFR1/2, Fas, TNF –related apoptosis-inducing ligand receptor (TRAIL-R), LTβR, receptor activator of NFκB (RANK), CD27, CD30, CD40, 4-1BB and OX40. The receptors in this family are all type-1 transmembrane proteins with the carboxy-terminus localized to the intracellular domain and the amino-terminus in the extracellular domain. One of the hallmark features of the TNFR superfamily is the presence of cysteine rich domains (CRDs) in the extracellular domains (157). The most common structure of the TNFR family consists of 3 CRD repeats (TNFR1 and TNFR2) but structures up to 6 repeats (CD30) can also be found(157). The TNFR superfamily members preassemble on the surface of the cell prior to ligand binding, and this process requires the presence of the N-terminal domain called PLAD (preligand assembly domain) that is distinct from the domain required for ligand binding (141, 158). Some of the receptors such as Fas, TNFR1, TRAILR1, TRAILR2 and TRAILR4 contain the “death domains (DD)” in the cytoplasmic domain, while the other receptors such as TNFR2 do not (157). As described earlier, almost all the TNFRs including TNFR1, TNFR2, and CD40 bind to TRAFs, which can stimulate the activation of NFκB and JNK pathways (described above)(141). In the next section, I shall discuss the down stream signaling of TNFR1, TNFR2 and Fas.

TNFR1 is a 60 kDa protein that is expressed on most cell types and binds its ligand TNF (26 kDa transmembrane protein that can also be cleaved into a 12 kDa soluble TNF by metalloproteases) (159, 160). When TNF binds TNFR1, it triggers the association of complex I, which includes a death domain containing protein, TNFR-associated death domain (TRADD) that recruits kinase receptor interacting protein 1 (RIP1), cellular inhibitor of apoptosis (cIAP1) and TNF receptor associated factor 2 (TRAF2) (161). TRAF2 stabilizes the cIAP proteins and prevents their autoubiquitination (161). The formation of complex-I leads to the activation of NFκB and MAPK pathways. RIP1 is K63 polyubiquitinated by cIAP proteins, resulting in the assembly of protein complex consisting of transforming growth factorβ- activated kinase 1 (TAK1) and TAK1 binding protein 2/3 (TAB2/3) (161). This leads to the activation of the inhibitor κB kinase (IKK complex) that promotes NFκB activation. NFκB then translocates into the nucleus and induces the expression of genes required for cell survival and also initiates a negative feedback loop by up-regulating deubiquitinases of RIP1 (A20 and CYLD)(161).

Under certain conditions, for example when RIP1 is deubiquitinated, complex I dissociates from TNFR1 to form a cytosolic complex, or complex II (DISC, death inducing signaling complex) that involves RIP1 and RIP3, TRADD, Fas associated death domain protein (FADD) and caspase-8 (recruited by FADD)(161). This results in cleavage of RIP1 and RIP3 and initiates an apoptotic death pathway. Alternatively, during reduced caspase activity (treatment with pan-caspase inhibitors carbobenzoxy-valyl-alanyl-aspartyl-[o-methyl]-fluromethylketone (Z-VAD) or in the presence of

SMAC mimetics that degrade cIAPs and prevent RIP1 ubiquitination) the cleavage of RIP1 and RIP3 is prevented that results in the sensitization of cells to TNF induced necrosis (161).

Along with TNFR1, TNF also binds TNFR2, a 80 kDa protein that is expressed predominantly on lymphoid and blood endothelial cells and does not contain a death domain in its cytoplasmic tail (159). TNFR2 directly interacts with TRAF2 that in turn interacts with NFκB-inducing kinase (NIK), which is a member of the serine-threonine mitogen-activated protein kinase kinase kinase (MEKK) family. NIK phosphorylates IKK and activates the NFκB pathway (160). Additionally, the TRAF proteins are involved in the activation of JNK, p38, extracellular signal related kinase (ERK) and the PI3K pathways that lead to the induction of genes involved in the cell survival and proliferation in activated T cells (162). Recent work has suggested that there is a degree of cross talk between the signaling pathways triggered from TNFR1 and TNFR2 (163). For example, during cell stress, TNFR2 signaling can lead to the induction of apoptosis via RIP1-mediated recruitment of FADD (163). Another study showed that TNFR2 induced cIAP-mediated ubiquitination of TRAF2 (164). These studies suggest that both TNFR1 and 2 can participate in both cell survival and apoptosis depending on the context of activation.

Fas (CD95) is 45 kDa type I cell surface protein that binds FasL (CD95L) a 40 kDa type II surface protein (165). Activation of Fas causes the rapid assembly of the death-inducing complex (DISC). During the formation of this complex, Fas recruits

FADD (Fas associated death domain) via homotypic death domain interactions (165, 166). FADD in turn recruits capsase-8 via the DED (death effector domains) interactions. This causes a conformational change in caspase-8 in the DISC that allows the caspase to attain full enzymatic function (166). Activated caspase-8 undergoes an auto-proteolytic cleavage and leads to formation of a heterotetrameric form of the caspase-8 that results in the cleavage of caspase-3 and -7 (166). These executioner caspases lead to proteolysis of several cellular proteins, such as lamins and ICAD (inhibitor of caspase activated DNAse), which inhibits CAD (caspase-activated DNAse) that causes DNA fragmentation (166). Caspase-8 can also cleave BID, another pro-apoptotic member of the Bcl-2 family that is involved in the mitochondrial death pathway (discussed later), ultimately leading to cell death.

Biological Role of TNF during immune responses

TNF, LTα, LTβ belong to a subfamily of a larger family of the TNF ligands members, with their genes linked within a compact 12-kb cluster inside the MHC complex locus (167). TNF is initially synthesized as membrane-bound trimer that is later cleaved by various metalloproteases into a soluble form. Both the soluble and membrane bound forms of TNF are bioactive and mediate their effect via interacting with TNFR1 (p55) and TNFR2 (p75) (141, 168-170). TNFR1 is expressed by most cell-types, but TNFR2 is expressed by cells of haematopoitic origin and binds to membrane bound form of TNF more efficiently than the soluble form. TNF is produced by both lymphoid and non-lymphoid cells (171). LTα and LTβ are produced by activated lymphocytes, NK

cells and a population of $CD4^+$ $CD3^-$ cells and play a role in lymph node organogenesis and peyer's patches (172, 173). LTα3 and TNF share the TNFR1 and 2 while LTα1β2 signals via the LTβR (174).

TNF has been shown to have very unique functions during an immune response, depending on the cellular source (175). Targeted knockout of TNF revealed that TNF produced by monocytes and neutrophils is pro-inflammatory and pre-dominantly provides resistance to intracellular pathogens such as Listeria, at low, moderate and high bacterial doses, while T cell-produced TNF was important for bacterial resistence at higher bacterial loads (175). TNF is also important for formation of B cell germinal centers and follicular dendritic cells (FDCs) and for effective B cell responses to Listeria infection (176). LTα and LTβ are also shown to play a role in the development of lymph nodes and peyers patches and the organization of white pulp in the spleen (177-181). Mice with triple LTβ/TNF/LTα gene deficiency show a more profound alteration in splenic architecture than their single deficient counterparts, suggesting the involvement of these cytokines in the development and maintenance of lymphoid organs (167).

In addition to being a major inducer of inflammation during innate immune responses, TNF signaling also mediates immunomodulatory effects in adaptive immune responses (175). For example, TNF signaling plays a vital role in the generation of functional T cell responses to tumor antigens, DNA vaccines and recombinant adenoviruses (182-185). More specifically, signaling through TNFR2 but not TNFR1 has a synergistic role with CD28 co-stimulation, reducing the threshold of activation for

optimal IL-2 expression during the initial stages of T cell activation (182, 186-188). In contrast, a recent study showed that TNF signaling via TNFR1 has a positive co-stimulatory role after early TCR engagement as TNFR1-deficient T cells showed delayed kinetics of proliferation at 72 hours and delayed upregulation of IL-2 and CD25 expression (189). However, by 96 hours TNFR1-deficient T cells showed enhanced levels of cytokines such as TNF, IFN-γ and IL-2, suggesting a suppressive role at later time points in activation. Other studies have suggested a suppressive role for TNF in the generation of T cell responses after infection of mice with LCMV. For example, higher frequencies of LCMV-specific $CD4^+$ and $CD8^+$ memory T cells are detectable in mice with defective TNF signaling pathways (190-192). These studies together indicate that effects of TNF signaling on the induction of adaptive immune responses are dependent on the nature of the antigenic challenge.

Deregulation of TNF signaling pathways has been implicated in the pathogenesis of several diseases, including rheumatoid arthritis (RA), Crohn's disease (CD), inflammatory bowel disease (IBD) and multiple sclerosis (MS), and hence therapeutic agents that target and block the activity of TNF have been developed for clinical use (170, 182, 193-197). Agents that block TNF activity such as the anti-TNF antibody (infliximab), and the human TNFR2-Ig fusion protein ENBREL (etanercept), are being used for the treatment of Crohn's disease and Rheumatoid arthritis (141). In addition to TNF blockade therapies, TNF therapeutics for the treatment of sarcomas and melanomas have been approved (198, 199). Short-term strategies using TNFR2 agonists have shown promise in their ability to kill autoreactive T cells in the blood samples of patients with

Type-I diabetes (163). These studies suggest that the dual role of TNF in regulating immune responses.

Role of Fas and FasL in immune responses

Fas is predominantly known to be a death receptor that binds FasL and induces apoptosis. Recent studies have demonstrated that the membrane-bound FasL is essential for Fas-induced apoptosis (200). In the early 1990s, two Fas mutations (lpr and lpr^{cg}) and a FasL (gld) mutation were discovered, with the mutant mouse strains developing lymphoadenopathy and systemic lupus erythematosus (SLE) (201) that result in the accumulation of CD4-CD8- T cells (202, 203). It was later found that human patients with autoimmune lymphoproliferative syndrome (ALPS) have heterozygous mutations in the *fas* gene (204, 205). These studies suggested that Fas-FasL pathways played a vital role in maintaining immune homeostasis. Recently it was demonstrated that Fas receptor expression on germinal center B cells is required for maintaining T and B cell homeostasis, and B cells have been shown to be crucial for the development of ALPS (206-208). The *fas* gene in the lpr mutant mice has an early transposable element (consisting of poly A tail sequences) inserted within intron 2 that leads to early truncation of Fas transcript and therefore is prematurely spliced (209). However, the lpr mutation is leaky, and full length Fas mRNA has been detected in the thymus and livers of lpr mice (209). The lpr^{cg} mutation, on the other hand, results in the expression of the full length Fas mRNA with a mutation (T to A) in the cytoplasmic tail region that in turn results in an amino acid change, from isoleucine to asparagine. This mutation abrogates the ability

of Fas to mediate death signals to the cells (209). The gld mutation is also a point mutation (T to C) near the C-terminus of the coding region of FasL. This results in the change of phenylalanine to leucine that abrogates the ability of FasL to bind to Fas (209). The Fas-FasL pathway has an important role at immune privileged sites such as eye, testis, placenta, brain, ovary and pregnant uterus by inducing apoptosis in Fas+ T cells that infiltrate these sites (201). Although the Fas-FasL pathway is vital for apoptosis, a process vital for T cell development, lpr and gld mice show normal thymic development, suggesting that other apoptotic pathways exist during thymic selection (209, 210). In the periphery, the Fas-FasL pathway has been shown to play a role in AICD and also in CTL-mediated cytotoxicity (209). In addition to a role in apoptosis, other studies have shown positive roles for Fas-FasL during T cell activation and proliferation. For example, OT-1 transgenic $FasL^{neg}$ $CD8^{+}$ T cells have a diminished antigen-driven expansion compared to the WT counterparts in response to OVA peptide immunization, suggesting a co-stimulatory role for FasL (211). However, recent studies with human T cells stimulated with αCD3 and αCD28 antibodies along with plate bound FasL inhibited the activation of naïve T cells (212). The discrepancy between the studies may reflect differences for activation in vitro and *in vivo*. Together, these studies indicate the important contribution of the Fas-FasL pathway in controlling immune homeostasis and potentially in regulating immune responses.

G. Programmed cell death

Programmed cell death occurs under normal circumstances during various stages of development and aging to maintain overall homeostasis (213). Specifically with regard to T cell homeostasis, there are two main events during the lifetime of T cells that represent the quintessential examples of programmed cell death. The first is during T cell development when T cells that fail to undergo productive rearrangements of their TCRs or cells that have a strong affinity to their self-ligands are removed by apoptosis (214). A second instance is during the contraction phase of an immune response where the majority of effector cells die by apoptosis, leaving a small population of cells that survive into memory (125, 214).

Programmed cell death can be broadly classified into three forms, namely, apoptosis, necrosis and autophagy (161). The characteristic morphological features of apoptosis are cell shrinkage, dense cytoplasm, dense packing of intact organelles, chromatin condensation, membrane blebbing and formation of apoptotic bodies and DNA fragmentation (213). This process of death is non-inflammatory, as the apoptotic bodies are quickly engulfed by macrophages (213). The second form of cell death is called necrosis and is characterized by the swelling of the organelles such as endoplasmic reticulum and mitochondria and the eventual rupture of cell membrane (161). The third form is autophagy, characterized by the sequestration of the cytoplasm and organelles into double or multi-membrane vesicles and delivery to the lysosomes for degradation (213). The hallmark of apoptosis is that it is caspase-dependent, whereas necrosis is

caspase-independent (161). TNF–TNFR family members play an important role in the induction of apoptosis as well necrosis (213). In the next section, I will discuss the two pathways involved in apoptosis.

Apoptosis can occur via two pathways, the extrinsic pathway and intrinsic pathway. The extrinsic pathway requires the activation of a death receptor such as Fas, which triggers the formation of the DISC and the activation of caspase-8 and cleavage of downstream caspases such as caspases 3 and 7 (214). On the other hand, factors such as extracellular stress, growth factor deprivation, cytotoxic drugs or irradiation can trigger the intrinsic or the mitochondrial pathway of apoptosis (214). This process is regulated by the members of the Bcl-2 family that consists of prosurvival proteins such as Bcl-2, Bcl-x_L (bcl-2l1), Bcl-w (bcl-2l2), Mcl1 and pro-apoptotic members such BAX, BAK, BAD, BIM (214). Upon activation, BIM can directly activate pro-apoptotic proteins BAX (bcl-2 associated X protein) and BAK (bcl2 antagonist/ killer) that lead to the loss of membrane potential of mitochondria and the release of cytochrome c. The anti-apoptotic proteins Bcl-2 and Bcl-xL prevent the loss of mitochondrial membrane permeability by inhibiting BAX and BAK. BIM can also interact with Bcl-2 and mediate the activation of BAX and BAK. Cytochrome-c binds apoptotic protease-activating factor-1 (Apaf-1) and pro-caspase-9, forming an apoptosome in the cytoplasm. Formation of the apoptosome activates casapse-9 that cleaves caspase 3, 6 and 7. The executioner caspases then cleave cellular substrates such as Poly ADP-ribose polymerase (PARP), cytosketal proteins, NUMA (nuclear protein), lamins, gelsolin and ICAD (inhibitor of caspase activated DNase) and cause cell death (213). The extrinsic and the intrinsic pathways are not

mutually exclusive, and there is cross talk between both the pathways. For example, activated caspase-8 can also cleave BID that is involved in the mitochondrial death pathway (214).

Of the several members involved in the extrinsic and the intrinsic pathways, Fas and BIM are recognized as two major regulators of apoptosis (214). As with Fas (lpr) mice, BIM deficient mice (129-B6 genetic background) develop autoimmunity due to accumulation of lymphocytes (215). Studies with HY transgenic thymocytes (at the DP stage) from male mice showed that absence of BIM abrogated their deletion, suggesting the role of BIM during negative selection (216). However, recent studies have indicated that although BIM expression is essential for the apoptosis of DP thymocytes, it was not required for negative selection (217). In the periphery, BIM but not Fas has been shown to be important for the contraction phase of an immune response during herpes simplex virus (HSV) infection (127). As mentioned earlier BIM and Fas can also play complimentary roles in inducing programmed cell death of T cells during the contraction phase after LCMV infection (131).

H. Principles of self-tolerance: The default response

"*Immunological tolerance*" is defined as a state of unresponsiveness to a particular antigen (67) . The function of immunological self-tolerance is to prevent an individual's immune system from attacking and destroying self-tissues. Self-tolerance is established by two distinct phenomena, namely central and peripheral tolerance. "*Central tolerance*" occurs in the thymus. During T cell development, maturing T cells whose TCRs exhibit

strong affinity towards self-peptide MHC complexes pose a threat of becoming auto-reactive and therefore are centrally eliminated by the process of negative selection (218). Thymic epithelial cells (TECs) and dendritic cells (DCs) mediate negative selection by presenting endogenous and exogenous self-antigens (218). Importantly, the expression of autoimmune regulator *(AIRE)* gene expressed in TECs enables the constitutive presentation of several tissue-specific antigens that would be otherwise absent in the thymus, thereby mediating self-tolerance (219, 220).

Although, negative selection provides stringent scrutiny of T cells in the thymus, some self-reactive T cells do escape selection and reach the periphery. Therefore, the immune system has developed several T cell intrinsic and extrinsic mechanisms to maintain "*peripheral tolerance*" (67, 218, 221). Anergy and clonal deletion are two examples of intrinsic mechanisms of tolerance induction. Anergy is a state of non-functionality induced by exposure to very high doses of chronic antigen, whereas exposure to low doses results in clonal deletion (218, 222). An additional intrinsic mechanism is the expression of negative co-stimulatory molecules such as CTLA-4 and PD1 by T cells that attenuate responses and aid in T cell homeostasis in the periphery. CTLA-4 deficiency in mice leads to massive lymphoproliferation and lethality (223, 224). This may be due to the lack of CTLA-4 expression on normal T cells as well as due to an impaired Treg population (225, 226). As mentioned earlier, PD1 deficiency on C57BL/6 background leads to development of lupus like arthritis and glomerulonephritis (67, 227-229). Thus, there are multiple intrinsic mechanisms to maintain peripheral T cell tolerance that prevents the activation of auto-aggressive T cells.

One of the primary extrinsic mechanisms in the maintenance of peripheral tolerance involves $CD4^{+}CD25^{+}$ T regulatory cells (Treg) that suppress the activity of T cells. Treg cells are generated in the thymus and express the Foxp3 transcription factor that is crucial for their function and development (230). The absence of Tregs leads to the induction of numerous autoimmune conditions. Mutations in Foxp3 cause an autoimmune disease in humans called Immunodysregulation, Polyendocrinopathy Enteropathy, X-linked (IPEX) syndrome and is homologous to scurfy mutation in mice that develop severe lymphoproliferative disorders and exhibit inflammatory pathologies (231). The suppressive effects of Treg cells are not only mediated by cell contact but also by secretion of anti-inflammatory cytokines such as IL-10 (232). Additionally, absence of inflammation and exposure to dying cells leads to generation of tolerogenic immature antigen presenting cells (iDCs) that are also shown to suppress and anergize T cells (233). These findings indicate the existence of multiple and robust self-regulatory mechanisms that protect against autoimmune disease.

I. Transplantation tolerance: An acquired response

The “Holy Grail” of transplantation immunology has been to efficiently exploit the mechanisms of self-tolerance and to extend this tolerance to transplanted non-self tissues. There are several features of transplantation tolerance that are synonymous with self-tolerance. For instance, both phenomena require tolerization to a diverse array of antigens (234). In the case of self-recognition, there are a plethora of self-peptides generated from self-proteins that are recognized by T cells in the context of self-MHC

complexes. During allo-recognition, alloreactive T cells recognize a variety of donor antigens presented to them by both donor and host antigen presenting cells. There are central and peripheral mechanisms that induce transplantation tolerance, in a manner similar to self-tolerance. Central mechanisms of tolerance include the deletion of alloreactive T cells when allogeneic cells are injected into the thymus or during bone marrow transplantation. Peripheral mechanisms include anergy, deletion, induction of Tregs and iDCs. I shall discuss some these mechanisms in detail in this section.

Mechanisms of acquired transplantation tolerance.

As described above, phenomena that operate during transplantation tolerance harness the mechanisms of central and peripheral self-tolerance that maintain immune homeostasis. Our initial understanding of the mechanisms involved in the central tolerance to alloantigens came from the studies by Ildstad and Sachs in animals receiving bone marrow transplantation with T cell-depleted donor and recipient bone marrow cells after lethal irradiation (235). These bone marrow chimeric mice received solid organ transplants and showed prolonged graft survival. This observation highlighted the concept of central tolerance in mixed allogeneic chimeras where the presence of donor cells in the thymus leads to the deletion of donor-reactive T cells and the continued presence of donor cells within the thymus ensures permanent tolerance to donor antigens (236). Direct evidence of central deletion of alloreactive T cells was shown by intrathymic injection of allogeneic cells in combination with peripheral T cell depletion, which led to prolonged allograft survival (237-239). These studies incorporated the

treatment of the recipients with anti-lymphocyte serum to deplete the pre-existing mature alloreactive T cells in the periphery (240). Both of these studies emphasize the importance of strategies that induce tolerance to alloantigens in the recipient thymus. Strategies to induce peripheral tolerance include preconditioning of recipients with donor cells and blocking co-stimulatory molecules (such as CD40L or CD28) and the use of drugs such as cyclosporine and rapamycin that block mature T cell activation. The induction of peripheral donor tolerance includes three basic mechanisms, peripheral T cell deletion, inactivation and the induction of Treg cells.

a) Ignorance

Ignorance is a mechanism that occurs when alloreactive T cells fail to be primed when they encounter donor antigens outside secondary lymphoid tissues (241). This situation arises in mice that do not contain lymph nodes (LT-deficient) and that have been splenectomized, resulting in extended cardiac graft survival (242). This is, however, not one of the dominant mechanisms of tolerance, as alloreactive T cells have been shown to be activated in the allograft, and memory T cells, that do not require secondary lymphoid tissues, can be reactivated and mediate graft rejection (243, 244).

b) Immune deviation

Another less dominant mechanism revolves around the Th1 and Th2 paradigm. In animals as well in humans, rejection is correlated with Th1 cytokines such as IFNγ and tolerance with Th2 cytokines such as IL-4 and IL-10 (245). However, recent data suggest otherwise. For example IFNγ–deficient mice rejected cardiac transplants, and IL4-

deficient mice accepted allogeneic islets and hearts (246-248). It was shown that IFNγ conditioning of naïve $CD4^+$ T cells ex vivo prevents their diversion to Th2 and results in the up-regulation of Foxp3 and CD62L and converts them into T regulatory cells that resulted in skin and islet graft acceptance (249). In another study using a cardiac allograft model, IFNγ induced both the survival of Foxp3+ Tregs and also induced graft endothelial cells to make indoleamine 2,3-dioxygenase (IDO), which has a role in T cell apoptosis and anergy (250). These studies highlight an unexpected role for IFNγ in the induction of Treg cells that is being considered as another potential therapeutic target.

Some studies however, still show the importance of a Th2 cytokine environment for prolongation of allograft survival (245). For example, neutralization of IL-4 and IL-10 resulted in the rejection of allografts in mice receiving anti-LFA1 and anti-ICAM-1 blockade (251). Additionally, there was increased expression of IL-4 and IL-10 in surviving heart allografts of mice receiving anti-CD4 antibody treatment (252). In contrast, absence of IFNγR expression can shift the response of alloreactive $CD4^+$ T cells into a Th2 pathway that can result in eosinophilic inflammation, which can cause tissue damage (253). Overall these studies suggest that the effects of Th1 and Th2 cytokines on transplantation tolerance will be determined by the specific environment, the timing and the nature of the transplanted tissue.

c) Anergy

Alloreactive cells that escape deletion during tolerance induction are in many instances anergic or unresponsive. The critical downstream signaling events of the TCR

vital for productive T cell activation do not occur in anergic cells. There is no activation of kinases such as Lck and ZAP-70 or phosphorylation of the CD3 ε and ζ chains (67). Concomitantly, there is no activation of Ras, ERK, and JNK MAP kinases, although phosphorylation of Fyn, increases in Ca^{2+} levels, phosphorylation of PLC-γ and increased levels of phosphotidylinositol 1,4,5 triphosphate are reported to be normal (67). During anergy, Rap1 (another GTP binding-protein of the Ras family) is activated that is shown to inhibit IL-2 gene transcription (254). Anergic cells are also functionally unresponsive to IL-2 signaling and produce reduced levels of IL-2 (241, 255, 256). In addition, anergic $CD4^+$ T cells can inhibit the maturation of DCs, thereby leading to tolerance (257). T cell anergy can be prevented in the presence of γc cytokines such as IL-2 (258). These studies indicate the role of cytokines in the reversal of a T cell from a state of unresponsiveness.

d) Passive and active deletion

The T cell pool size hypothesis predicts that during tolerance induction, the balance of the alloreactive T cells to Tregs determines if immunity or tolerance is the outcome. The precursor frequency of alloreactive T cells may be as high as 1 in 20 peripheral T cells (259). Hence the deletion of activated alloreactive T cells by apoptosis is considered to be an important event for the induction of tolerance. There are 2 forms of apoptosis that I have previously described. The passive cell death (PCD) process is also referred to as the intrinsic apoptotic pathway, while the activation-induced cell death (AICD) process is mediated by death receptors of the extrinsic pathway such as Fas. AICD is triggered in the presence of strong antigenic stimulation and is enhanced by IL-

2. IL-2-deficient mice given co-stimulation blockade have defects in AICD and hence reject grafts (240, 260, 261). The effect of IL-2 on activated T cells is believed to occur via the up-regulation of FasL and suppression of the caspase-8 inhibitory protein (FLIP), an inhibitor of Fas signaling pathway (262). Reagents such as Rapamycin have been shown to block the proliferative component of IL-2 signaling while keeping the IL-2 mediated priming of AICD, thereby leading to prolonged islet graft survival (260).

Growth factor deprival leads to the induction of PCD that is regulated by the anti- and pro-apoptotic members of the Bcl-2 family of proteins such as Bcl-2 and BIM. Two of the known mouse models used to study PCD include the human Bcl-2 expressing transgenic mice and BIM deficient mice that are both defective in PCD (215, 263). However, both Bcl-2 transgenic mice and BIM deficient mice given CTLA-4 Ig and anti-CD154 (MR1) accept islet allografts, suggesting that blocking PCD alone does not prevent tolerance induction in certain situations (264). Bcl-xL is another pro-survival protein that is sustained by CD28-mediated co-stimulatory signals during T cell activation (265). Over-expression of Bcl-xL in T cells also prevents PCD. Administration of CD28 and CD154 blocking antibodies in Bcl-xL transgenic mice results in chronic rejection of cardiac allografts, indicating an important role for PCD in inducing cardiac allograft tolerance (260). Recent studies have highlighted the importance of both AICD and PCD in inducing tolerance. For example, studies in Fas-deficient or Bcl-xL transgenic mice receiving bone marrow transplants and αCD154 + CTLA-4 Ig therapy showed impaired alloreactive $CD4^+$ T cell death in both mouse models (266). As

previously mentioned, these studies indicate that there may be involvement of both the pathways in inducing tolerance.

e) Treg cells

One of the major mechanisms operating in transplantation tolerance is $CD4^+$ $CD25^+$ Tregs, and their relevance in transplantation was first demonstrated with their ability to reduce mouse graft versus host disease (GVHD), a condition where the T cells in the graft mount an immune response against host cells (240, 267, 268). There are two phenomena that are linked to the role of Treg cells, namely " Linked suppression" and "Infectious tolerance". In linked suppression, induction of tolerance to a particular antigen "A" can induce tolerance to a third party antigen "B" if it is processed and presented by the same APC. Exposure to a single oral alloantigen (K^b) was sufficient to induce tolerance to fully allogeneic cardiac allografts ($H2^b$: K^b +D^b + L^b +IA^b) through indirect antigen presentation (240, 269, 270). Studies have also demonstrated a phenomenon mediated by Tregs in a contact dependent manner termed "infectious tolerance" that is partly controlled by TGFβ produced by the tolerant cells (271, 272). This is a mechanism of suppression where tolerance can be transferred into naive mice carrying donor allografts from mice that have been tolerized with the donor antigen (240).

One of the limitations of Tregs is that they alone cannot induce tolerance across MHC-mismatched barriers. This may be attributed to the existence of high frequency of the number of alloreactive T cells that needs to be brought below a particular threshold

for tolerance to occur (234, 240). Deletion of alloreactive T cells and induction of Treg cells are both important mechanisms to establish productive tolerance.

J. Historical overview to the field of transplantation tolerance

There have been numerous attempts in the field of transplantation immunology, to breach the immunological barrier and attain successful allograft acceptance and donor specific tolerance with certain success stories and with concomitant failures. Despite obstacles, transplantation immunology as a discipline has made significant breakthrough discoveries in understanding the mechanisms of tolerance (described above) and devising ways to give life saving solutions to many patients with terminal end-stage organ diseases. From renal transplantation in the 1950s to cranio facial transplantation to day, the field of transplantation has indeed come a long way.

In 1954, Dr. J.E Murray received the Nobel Prize for the first successful transplantation in identical twins. Mrs. Edith Helm received the first kidney transplant from her twin sister Mrs. Wanda Foster and they are the longest surviving examples of a successful transplantation (273). Before this, there had been many significant studies that culminated to this point of time in history. In 1937, Dr. J. Brown observed permanent skin graft survival between monozygotic twins. In 1943, Gibson and Medawar demonstrated the “second set phenomenon” where the second allograft from the same donor was rejected more rapidly than the first, proving that rejection occurred via an immunological reaction (273-275). In 1946, Dr Owen discovered the coexistence of different blood types in twin freemartin cattle (free martin refers to the females of the

male-female twin pair), an observation that was previously demonstrated by F.R Lillie in 1917.

In 1948 came the breakthrough discovery by Gorer and Snell who identified the major-histocompatabiltiy complex that forms the basis of the complexity of alloantigens (275). In 1951, Anderson and his coworkers showed successful skin allograft survival between freemartin cattle (273). In 1951, French surgeons described surgical procedures of renal transplantation into pelvic location that is performed to this day unmodified (274). The concept of neonatal tolerance was established by Burnet and Fenner, who won the Nobel prize in medicine for their discovery showing that mice infected with LCMV during development will recognize it as self antigen and fail to mount an immune response resulting in a persistent infection (276). In 1953 Billingham, Brent and Medawar showed the presence of neonatal tolerance in mice that were tolerized to donor antigens from a genetically different mouse strain and tolerance was extended to donor skin grafts (273). Together all these discoveries in tolerance laid the foundation for the Nobel prize winning operation performed by Murray in 1954.

Several other discoveries followed. In 1955 and 1956, attempts to reproduce tolerance in adult mice were being pursued with total body irradiation (TBI). In 1957, Billingham, Brent and Medawar discovered graft versus host disease (GVHD) in mice and chickens. In 1958, Dauseet and Van Rood discovered the human MHC antigens – human leukocyte antigen (HLA). In 1959 came the advent of immunosuppressive drug use by Schwartz and Dameshek, who used 6-mercaptopurine, an antimetabolite, to prevent rabbit antibody

production to human serum albumin. Modifications to mercaptopurine created more effective drugs, such as the imadozole derivatives Azathiopurine (Imarun). Despite having toxic side effects, this drug was widely marketed until other suitable alternatives were discovered. The late 1960s saw the advent of anti-lymphocyte antibodies raised in horse, rabbit and sheep for use in the clinic.

The success of kidney transplants encouraged the transplantation of other organs. Liver transplantation was successfully performed in 1967, followed by the first heart transplantation by Dr. Christian Barnard in South Africa, although the patient did not survive long. Single and double lung transplants soon followed. Skin remained one of the most difficult organs to transplant. Work on the mechanisms of non-reactivity began in late 1960s, although it was only during the 1990's that the basis of organ tolerance was established to involve microchimerism in bone marrow transplantation.

K. Revolution of immunosuppressive drugs in transplantation tolerance

The use of immunosuppressive drugs revolutionized the field of organ transplantation. The discovery of cyclosporine and tacrolimus by Borel and Goto, respectively, allowed the transplant of allogeneic tissues and are still used in the field at present. More efficient drugs, such as rapamycin, are continuing to be developed.

Immunosuppressive drugs can be classified into various categories based on the primary site of action. These classifications include inhibitors of T cell activation, transcription, growth factor signal transduction, nucleotide synthesis and differentiation (277). Cyclosporine (fungal peptide) and tacrolimus (FK506) have similar mechanisms of

action in blocking T cell activation(277). Both drugs block Ca2+ dependent activation of calcineurin and thereby inhibit the translocation of NFAT into the nucleus and subsequent gene expression. Rapamycin (Sirolimus) blocks CD28-mediated signaling and IL-2-dependent signaling. Azothioprine, mizoribine and mycophenolate mofetil inhibit purine synthesis, inosine monophosphate dehydrogenase and prevents de novo guanosine and deoxyguanosine synthesis in lymphocytes. Corticosteroids inhibit cytokine synthesis. A recent development in the field is the use of FTY720 (an immunosuppressive fungal metabolite that binds and blocks sphinogosine 1 phosphate ($S1P_1$) signaling) along with cyclosporine to induce tolerance to skin allografts as it results in the sequestration of alloreactive T cells to secondary lymphoid organs.

L. Advent of alternative approaches in transplantation tolerance

Although immunosuppressive drugs have advanced the field of transplantation, there are a number of side effects. The primary problem is the generalized immunosuppression and susceptibility of the patients to cancer and infections. Life long use of immunosuppressive drugs can also result in organ toxicity. Cyclosporine increases cholesterol levels, resulting in secondary complications. Rapamycin binds TOR (Target of Rapamycin) protein kinases and blocks T cell activation and proliferation, causing deletion of reactive T cells and the induction of Tregs. However, Phase III clinical trials with Rapamycin have shown side effects such as hypercholesterolemia, hypertriglyceridemia and hypertension.

Advancements in understanding the mechanisms of T cell activation have led to the development of many alternative approaches to extend allograft survival in transplant recipients. For example IL-2Rα blocking antibody targets activated T cells, thereby blocking high affinity IL-2 binding. One of the concerns regarding the use of this approach is the expression of CD25 on Treg cells. Recent studies have shown that IL-2Rα blocking antibody does not affect Treg maintenance though concerns regarding its effect of Treg function remain to be investigated (278). OKT3 is a CD3-specific antibody that is given along with diptheria-derived immunotoxin to mediate profound T cell depletion (241). OKT3 was later administered along with deoxyspergualin, a polyamine antibiotic that inhibits APC function. Another antibody is CAMPATH-1H, which is a humanized antibody directed at CD52 that is present on T and B cells. This causes the depletion in primary as well as secondary lymphoid organs. It has been clinically tested in conjunction with rapamycin and sequestering anti-TNF antibody (236).

M. Co-stimulation blockade to induce transplantation tolerance

Co-stimulation blockade protocols in regulating allo-specific immune responses are alternative approaches that have gained recent interest in the field of transplantation tolerance. As described earlier, there are broadly two classes of co-stimulatory molecules belonging to the CD28-B7 family and TNF-TNFR family respectively that can serve as potential targets for inhibiting T cell activation. Blockade of the CD28 pathway using CTLA-4-Ig that binds B7 molecules with high affinity prevents allograft rejection in cardiac allograft models (279, 280). Combination of CTLA4Ig along with donor-specific

transfusion (DST) results in promotion of allograft tolerance in comparison to CLTLA4 monotherapy (281, 282). Studies in CD28 deficient mice that reject allografts suggest that in addition to this classical co-stimulatory molecule, other independent pathways may also serve as targets for tolerance induction (72, 283). Blocking of CD40 using αCD154 (MR1) has been shown to prolong allograft survival (284, 285). In line with this finding, CD154-deficient mice do not reject cardiac allografts, although they do develop complications of vasculopathy (286). Additionally, αCD154 has been shown to prolong allograft (islet and renal) survival in some non-human primate models (287-290).

In addition to these classic models other novel pathways are being studied for their effect on transplantation tolerance. ICOS has emerged as an alternative target for tolerance (72). Blocking ICOS along with anti-CD154 and CTLA-4Ig induces donor specific tolerance without the development of chronic vasculopathy (291). Additionally, ICOS blockade along with DST induces apoptosis of donor-reactive $CD4^+$ T cells and promotes tolerance (292). PD1 is a negative co-stimulatory molecule that plays a role in self-tolerance (76, 78, 79). Administration of anti-PDL1 antibody results in acceleration of the rejection cardiac allografts (293). Other molecules which have shown promise for tolerance induction included CD134, 4-1BB and CD27 that synergize with CD28 blockade to promote allograft survival (72). Therefore, blocking of co-stimulatory pathways is an attractive target for inducing tolerance.

N. Immunological challenges in transplantation tolerance

Despite the development and successful implementation of many immunological strategies to induce donor specific tolerance in rodent models and in humans, transplant immunologists are still faced with many challenges to attain successful allograft acceptance. There are a number of immunological barriers that impede successful transplantation of organs. Below are some of the known barriers to transplantation tolerance.

a) Context of antigen recognition (direct vs indirect)

In the context of allo-recognition, T cells recognize many donor antigens. This recognition occurs when they interact with either an intact donor MHC antigen on the transplanted tissue via the direct pathway or when T cells recognize the donor-antigens that are processed and presented in a self-restricted manner on host APC via the indirect pathway (240). There are currently two models for direct allo-recognition. One is the high-density determinant model, where an alloreactive T cell directly recognizes the donor MHC antigen irrespective of the peptide that is bound. Alternatively, the other model is the multiple-binary complex model, where an alloreactive T cell recognizes both the bound-peptide and the allo MHC complex. It is proposed that in reality, these models represent two extremes of a spectrum as allogeneic MHC, and the peptide ligand may contribute to varying degrees to the strength of ligand binding to the TCR (240). The source of antigens in the indirect allorecognition pathway comes from either dying donor APCs in the draining secondary lymphoid tissues or when recipient APCs that are

migrating through the graft and take up donor antigens. The antigens are then processed and presented by recipient APCs in a classical MHC-II restricted fashion (240).

$CD8^+$ T cells are predominantly implicated in the direct pathway of allo-recognition and are involved in acute rejection of allografts. $CD4^+$ T cells, on the other hand are involved in the indirect allo-recognition that has been shown to provide continuous antigens and result in chronic rejection (294). Additionally, cross presentation of exogenous alloantigenic peptides via MHC-I to $CD8^+$ T cells via the indirect pathway can also occur (240). The role of $CD4^+$ T cells in the indirect allo-recognition is dual, as it can also result in the induction of Treg cells (295). It was found that indirect alloantigen persists in the recipient's lymph nodes and is suggested to be an important mechanism of tolerance induction (296). Alternatively, effector $CD4^+$ T cells are also involved in the rejection of cardiac allografts via the direct allo-recognition (alloantigens presented by donor MHC-II molecules) (297, 298).

The effects described so far for direct and indirect allo-recognition are instances of solid organ transplantation and graft rejection. Another phenomenon by which the donor immune system and the host interact is during allogeneic hematopoietic transplantation. Bone marrow transplantation has been used as a treatment for leukemia and lymphomas. However, a side effect of this procedure is the immune response mounted by the donor T cells to host antigens via the direct or the indirect pathway. This process is referred to as graft versus the host disease (GVHD) (299). Together these findings indicate that the

context of interactions between alloreactive T cells with donor antigens is an important mechanism that is involved in tolerance induction.

b) Role of innate immunity in transplantation tolerance

The relevance of innate immunity in organ transplantation came to light in 1994 with the use of superoxide dismutase (SOD), as a free radical scavenger in patients receiving kidney transplants. These patients had reduced incidence of acute and chronic rejection events and increased long-term survival outcomes (300). This highlighted the "injury hypothesis" and the "danger associated molecular patterns" (DAMPS) during reperfusion injury to the organs that activated the innate immunity. Since then, there has been accumulating evidence showing the role of the innate immune system in allograft rejection and tolerance. For example, It was shown by He and colleagues that in the absence of adaptive immune cells in Rag-/- mice, there was pro-inflammatory cytokine and chemokine receptor expression and infiltrating cells in the graft as with WT control mice suggesting a role for antigen independent inflammation in the transplanted tissues (253, 301, 302). In this section I will first provide a brief overview of the signaling components in the innate pathway and the role of these pathways in immunity and tolerance and then discuss in further detail the implications of TLR signaling in transplantation immunology.

c) Innate Pattern recognition receptors (PRRs)

The innate immune system recognizes pathogens or danger signals via three germline encoded receptors namely, Toll like receptors (TLRs), Nod (nucleotide binding and oligomerization domain) like receptors (NLRs) and RIG-I (retinoic acid-inducible gene – I) like receptors, RLRs. TLRs recognize a wide variety of pathogen associated molecular patterns (PAMPs) and DAMPS from pathogenic or endogenous danger ligands through receptors that are either membrane bound or in the endosomal compartment. The NLRs and RLRs recognize ligands in the cytoplasm of the cells.

TLR signaling

Several cell types such as pDCs, monocytes, B cells, T cells, endothelial and parenchymal cells express TLRs on their surface (253, 303, 304). There are 11-12 TLRs that have been identified in mice and in humans. TLR1, 2, 4, 5, 6 and 11 are membrane bound that recognize microbial membrane ligands whereas the intracellular endosomal receptors, TLR3, 7, 8 and 9 recognize the microbial nucleic acids. The TLR1 and TLR2 heterodimer and TLR2 and TLR6 heterodimer recognize tri-acylated and di-acylated lipopeptides from gram-positive bacteria, respectively (304). TLR2 has been shown to recognize the lipoprotein Pam3CSK4 from *E coli*. TLR2 ligation can also induce Type–I IFN upon vaccinia virus (VV) infection of monocytes. TLR5 and TLR11 recognize bacterial flagellin and uropathogenic bacteria respectively (304) and TLR4, recognizes bacterial LPS and respiratory syncytial virus (RSV) (304).

The intracellular TLR3 recognizes dsRNA of viruses such as RSV, encephalomyelitis virus and West Nile virus that is mimicked by polyinosinic:polycytidylic acid (Poly I:C) that induces Type-I IFN (304). TLR7 recognizes ssRNA of viruses such as Vesicular stomatitis virus (VSV) and Human immunodeficiency virus (HIV), Poly U containing RNA and small RNAs. It also recognizes RNA of streptococcus. It was originally shown to recognize imidazoquinoline derivatives or guanosine analogs. TLR8 recognition is similar to TLR7. TLR9 recognizes unmethylated CpG DNA motifs of bacteria and viruses. TLR9 ligation can activate DCs, B cells and drive Th1 responses. It serves as a sensor for Herpes simplex viruses 1 and 2 (HSV1 and HSV2) and recognizes hemozoin, a byproduct of hemoglobin digestion by Plasmodium falciparum.

There are many adaptor proteins downstream of the TLRs. MyD88 (Myeloid differentiation primary response gene-88) is an adaptor protein that is required for signaling by IL-1/IL-18 and all the TLRs except for TLR3, which uses the adaptor molecule Toll/IL-1R domain containing adaptor-inducing IFNβ (TRIF). Additionally, TLR4 also signals through the TRIF-mediated pathway. The MyD88-dependent pathway primarily stimulates the production of inflammatory cytokines, while the TRIF-dependent pathway induces the production of Type-1 IFN. MyD88 gets recruited to the TLR by the adaptor protein called Toll/IL-1R domain containing adaptor (TIRAP). MyD88 then recruits and activates IRAK4 (IL-1 receptor associated kinase-4), leading to sequential activation of IRAK1 and IRAK2. This activation recruits TRAF6 (TNF receptor associated factor), leading to its K63 (Lysine-63) linked polyubiquitination. The polyubiquitination chains bind regulatory proteins TAB2 and TAB3 to activate TAK1.

The K63 polyubiquitination chains also bind to NEMO (IKK). TAK1 forms a complex within the IKK and then phosphorylates IKKβ that leads to subsequent phosphorylation of IκB and its degradation and NFκB activation. TAK1 can also activate the MAPK ERK1, ERK2 and JNK, leading to the activation of the transcription factor AP1. NFκB activation leads to the activation of many cytokine genes such as IL-6, IL-12p40 and TNF and other genes related to NFκB pathway (304).

In the TRIF- mediated pathway, another adaptor protein TRAM (translocating-chain associating membrane protein) recruits TRIF to either TLR4 or TLR3. TRIF then recruits TRAF6 and results in TAK1 and NFκB activation. TRIF also recruits RIP1 through homotypic binding. RIP1 undergoes K63 polyubiquitination and forms a complex with TRADD, leading to the activation of TAK1 and NFκB activation. Additionally, TRIF also results in the activation of IRF3 (Interferon-regulatory factor) that is important for synthesis of Type-I IFN. TRIF recruits TRAF3 followed by the activation of TBK and IKKi (non-canonical IKKs), leading to the phosphorylation of IRF3 and its nuclear translocation. During intracellular TLR7 and TLR9 signaling, both TLRs require MyD88 for Type-I IFN production. There is a multi-complex formation with IRAK4, TRAF6, IRAK1, TRAF3 and IKKα that leads to the activation of IRF7 and its nuclear translocation for Type-I IFN induction (304). The induction of Type-I IFNs and other pro-inflammatory cytokines initiate and influence the adaptive immune responses.

Innate alloimmunity to endogenous ligands

The innate arm of the immune response can be activated by either the presence of pathogens or by the presence of endogenous ligands. This is the basis of the danger hypothesis proposed by Matzinger as an extension of Janeway's theory on the importance of the innate immune system for adaptive responses (305, 306). In the context of transplantation, not only are viral and bacterial infections a major threat to the abrogation of tolerance but the injury to the allograft during its procurement or during reperfusion can also result in the release of endogenous danger signals. Studies have shown that TLR2 and TLR4 are major TLRs that are activated in response to a variety of endogenous danger ligands such as hyaluronan, heparan sulfate, high motility group protein B1 (HMGB1), fibronectin extra domain A, β-glycan, heat shock proteins 60 and 70 (Hsp 60 and 70) and gp96 (253, 307) that are present during organ reperfusion injury. Although there is skepticism with regard to these ligands due to possible contamination with LPS in the reagent preparation (308), there have been other studies showing the effect of these ligands in rejection (309, 310).

Innate alloimmunity to pathogenic ligands

Several studies have used mice deficient in the expression of TLRs or the downstream adaptors such as MyD88 and TRIF to show the effect of TLR ligation pathways in transplantation tolerance models. Studies by Goldstein et al showed that skin grafts from MyD88-deficient male mice were not rejected by the MyD88-deficient female mice (311). In contrast, grafts from TLR-2-deficient, TLR4 -deficient and

caspase-1-deficient male mice were rejected by the corresponding female mice. This study showed the importance of MyD88 adaptor molecule in graft rejection across a minor mismatch model. However, studies across fully mismatched skin and heart allografts showed that rejection occurred independent of MyD88 signaling, suggesting that other pathways may be involved in graft rejection (312). On the other hand, studies using skin graft models and co-stimulation blockade with MyD88-deficient mice resulted in prolonged allograft survival (313, 314). This was attributed to the inability of DCs to produce IL-6 in the absence of MyD88 and hence better suppressive ability of Tregs (315). Administration of TLR-4 and TLR-3 agonists at the time of co-stimulation blockade prevents the deletion of alloreactive T cells and abrogates tolerance and requires signaling via MyD88 (4, 5). Further, it was shown that LPS did not shorten allograft survival in Type-I IFNR–deficient mice given co-stimulation blockade, suggesting that TLR agonists abrogate tolerance induction in a Type-I IFN-dependent manner (5). Exposure to TLR-9 agonist (CpG) has also been shown to abrogate tolerance induction to cardiac allografts grafts (316). Therefore, these studies suggest an important role of innate immunity in transplantation tolerance.

e) Homeostatic proliferation of alloreactive T cells

A major concern with lymphocyte depletion strategies is the problem of homeostatic proliferation of T cells. This is a property of T cells to expand and attain memory phenotype during conditions of lymphopenia. Homeostatic proliferation of alloreactive T

cells is considered a major obstacle in tolerance induction (317) as these expanded memory phenotype cells become resistant to co-stimulation blockade regimens.

f) Heterologous immunity

Memory T cells exhibit properties that are hard to circumvent for tolerance induction. For example, memory T cells have a lower threshold of activation, are less dependent on co-stimulatory molecules and do not require secondary lymphoid organs for priming, as they can home to and undergo activation in peripheral tissues (318). Also, memory T cells are not subject to the suppressive effects of Treg cells and the reason is still unclear (319). Whether the effect of Tregs on memory T cells may be quantitative or qualitative remains to be further investigated.

Alloreactive memory T cells have been indentified in individuals who have never been exposed to alloantigens (320). Studies with infection models with viruses such as LCMV, Pichinde virus (PV), VV and murine cytomegalovirus (MCMV) and Epstein-Barr virus (EBV) in humans have revealed the presence of allo-specific $CD8^+$ T cells (320). T cells generated during viral infections that can react with alloantigens are termed cross-reactive. Recently, our group showed that cross-reactive LCMV-specific memory T cells proliferate *in vivo* in response to allogeneic skin grafts and potentially mediate graft rejection (321) . T cells generated in an individual in response to a virus consist of the usage of different TCR repertoires that is unique to that individual, a phenomenon that is referred to as “private specificity” (322). Our group also showed that the magnitude and hierarchy of epitope-specific responses of cross-reactive LCMV-specific memory T cells

responding to alloantigens vary with the private specificities of individual memory T cell repertoire (321).

Another kind of cross-reactive T cells are alloreactive T cells that can also recognize viral antigens. Studies by our group and other labs have shown that acute and persistent viral infections result in the abrogation of co-stimulation blockade-induced tolerance that result in the rapid rejection of allografts (323-327). One of the mechanisms by which co-stimulation blockade facilitates allograft acceptance is by the deletion of alloreactive T cells within 24 hours of treatment (4, 328). Viral infections at the time of co-stimulation blockade abrogate tolerance induction, by rescuing alloreactive T cells from deletion that then become activated and proliferate and eventually mediate graft rejection (4, 328). Interestingly, acute viral infections of mice at later time points after co-stimulation blockade treatment, for example 1 or 15 days post transplantation abrogated co-stimulation blockade induced-tolerance despite the early deletion of alloreactive T cells (324, 326). However, administration of TLR3 ligand (polyI:C) that mimicks viral inflammation at 1 day post transplant did not abrogate co-stimulation blockade-induced tolerance suggesting that activation of innate immune responses after the loss of alloreactive T cells is not sufficient to abrogate tolerance (320, 324). These studies therefore suggested that viral infections at later time points may activate residual alloreactive T cells that fail to undergo deletion during co-stimulation blockade, that may cross-reactive with viral antigens and cause graft rejection. Together these studies indicate the heterologous immunity poses a difficult barrier to tolerance induction.

Chapter 2: Materials and Methods

A. Mice

Male and female Ly5.2 (CD45.2$^+$) C57BL/6J (*H-2^b*) mice were purchased from The Jackson Laboratory (Bar Harbor, ME) and used at 6-12 weeks of age. Male Ly5.1 (CD45.1$^+$) B6.SJL-ptprc<a> model#004007 mice were purchased from Taconic Farms and used at 6-12 weeks of age. Male BALB/CJ (*H-2^d*) mice were purchased from the Jackson Laboratory and used at 6- 12 weeks of age. Male SCID and αβγδ TCR KO and μMT (B cell) KO mice were bred at the University of Massachusetts Medical School (UMMS) Department of Animal Medicine and were used between 6-12 weeks of age. CD45.1$^+$ P14 CD8$^+$ TCR-transgenic mice, with T cells that recognize the D^b-restricted, LCMV epitope GP $_{33\text{-}41}$ (329), CD45.1$^+$ SMARTA CD4$^+$ TCR-transgenic mice, with T cells that recognize the IA^b-restricted, LCMV epitope GP $_{61\text{-}80}$ (330) and CD45.2$^+$ HY TCR transgenic male and female mice, with T cells that recognize the D^b – restricted, HY epitope Smcy$_{738\text{-}746}$ (331, 332)were bred at the University of Massachusetts Medical School (UMMS) Department of Animal Medicine. CD45.1$^+$ OT-1 CD8$^+$ TCR-transgenic mice, with T cells that recognize the K^b-restricted, ovalbumin epitope OVA $_{257\text{-}264}$ (333), and CD45.1$^+$ OT-2 CD4$^+$ TCR-transgenic mice, with T cells that recognize the IA^b-restricted, ovalbumin epitope OVA $_{323\text{-}339}$ (334) were provided by Dr. Kenneth Rock (Department of Pathology, UMMS, Worcester, MA). The Ly5.2 (CD45.2$^+$) TNF

deficient and Ly5.2 ($CD45.2^+$) TNFR1/2 (1 and 2) deficient C57BL/6J ($H\text{-}2^b$) mice were bred at the UMMS Department of Animal Medicine. The Ly5.2 ($CD45.2^+$) TNFKO mice were intercrossed with Ly5.1 ($CD45.1^+$) P14 $CD8^+$ TCR transgenic mice to generate Ly5.1 ($CD45.1^+$) Ly5.2 ($CD45.2^+$) double positive TNFKO P14 $CD8^+$ TCR transgenic mice. NOD (Non-obese diabetic) mice and NZB (New Zealand Black) mice and IL-10KO mice were obtained from Rossini/Greiner group (Department of Medicine, UMMS, Worcester, MA). NG-BAC transgenic mice, originally obtained from Dr. Michel Nussenzweig were backcrossed to the $CD45.1^+$ and $CD45.2^+$ background and were used at 6-12 weeks of age (41, 335). Homozygous C57BL/6Ji-D^{btm1} N12 ($H\text{-}2D^b$ KO) mice were purchased from Taconic Farms and used at 6 weeks of age. CBA/J ($H\text{-}2^k$) mice were purchased from the Jackson laboratory and used for the generation of KB5 synchimeric mice at 6-12 weeks of age described later in this section. (CBA/J X KB5.CBA/J) F1 $CD8^+$ T cell transgenic male and female mice that consist of T cells restricted to $H\text{-}2^k$ and recognizing $H\text{-}2^b$ as alloantigen (336-338) were bred at UMMS Department of Animal Medicine and used between 6 and 12 weeks of age. The B6.MRL-Fas lpr mice that were also bred at the UMMS Department of Animal Medicine and B6 Smn.C3-FasL<gld>/J that were purchased from the Jackson Laboratory were age and weight matched and used between 6-7 weeks of age before they developed lymphoproliferative disorders at later time points. All animals were housed and maintained within the Department of Animal Medicine at UMMS. All the experiments were done in compliance with the

institutional guidelines as approved by the Institutional Animal Care and Use Committee of UMMS.

B. Generation of $CD8^+$ KB5 TCR Transgenic Synchimeric CBA/J mice

To study the mechanism of alloreactive T cell deletion during co-stimulation blockade-induced tolerance, I generated KB5 synchimeric mice as described previously (338). Briefly, non-transgenic CBA/J ($H2^k$) mice were sublethally irradiated with 200 cGy. The total body irradiation was performed using ^{137}Cs source (GammaCell 40; Atomic energy of Canada, Ottawa, Ontario, Canada or Mark I-30 series 2000 Ci; JL Shepherd and Associates, San Fernando, CA). After 4 hours of irradiation, mice were injected intravenously (i.v) with 0.5-1 x 10^6 bone marrow cells (isolated from femurs and tibias) from either male or female (CBA/J X KB5.CBA/J) F1 $CD8^+$ T cell transgenic mice. These transgenic mice contain $CD8^+$ T cells that express TCR recognizing the B6 ($H\text{-}2^b$) alloantigen. At the end of 12-18 weeks post treatment, KB5 synchimeric mice are generated that consist of $CD8^+$ KB5 TCR transgenic T cells constituting 5-8% of the circulating lymphocytes. These transgenic $CD8^+$ T cells can be differentiated from their endogenous counterparts with a clonotypic mAb called DES (337).

C. Media and chemical reagents

All the cell preparations unless specified were cultured in RPMI 1640 (Gibco Invitrogen, Carlsbad, CA) that was supplemented with 10% FBS, 100U/ml penicillin, 100μg/ml streptomycin sulfate (Gibco Invitrogen) and 2mM L-glutamine (Gibco

Invitrogen). For 24 hour long-term in vitro experiments, T cell media was prepared with RPMI 1640 containing 10% FBS, 100U/ml penicillin, 100µg/ml streptomycin sulfate and 2mM L-glutamine, 5 ml of (100X) non essential amino acids (Gibco Invitrogen, Carlsbad), 5 ml of 100mM (100X) sodium pyruvate, 5 ml of (1M) HEPES (Gibco invitrogen, Carlsbad, CA) and 2.5 ml of 10^{-2} M β-mercaptoethanol (diluted in RPMI). Adoptive transfer of cells into mice and CFSE labeling of cells were performed in HBSS buffer (Gibco Invitrogen). For surface and intracellular staining, fluorescence activated cell sorting (FACS) buffer containing 1X phosphate buffer saline (PBS), 2% fetal bovine serum (FBS) and 5 ml of 2% sodium azide solution was used. Dead cells were excluded using Live Dead Aqua Dead cell stain (Invitrogen; Molecular probes) using IX PBS. For cell purification and enrichment, magnetic cell sorting (MACS) buffer containing 1X PBS, 2% FBS and 2mM ethylenediaminetetraacetic acid (EDTA) was used. For phospho ERK and BIM staining experiments, incubation buffer containing 0.5% BSA in 1X PBS was made and methanol free formaldehyde was purchased from Thermo Scientific (Rockford, IL). For lysing red blood cells (RBCs) during immunostaining of blood samples, 1X BD lysing solution was used (stock 10X from BD Pharmingen). For bacterial cell transformation LB broth was used. For agarose gel electrophoresis, 1X Tris-acetate EDTA (TAE) buffer was prepared from a stock of 50X (Gibco Invitrogen). Actinomycin D (A9415) and cycloheximide (C7698 and C1988) were purchased from Sigma and used at final concentrations of 20µg/ml and 5µg/ml respectively. CFSE and brefeldin A were purchased from Sigma (suspended with DMSO).

D.Viruses

Stocks of LCMV, strain Armstrong, and a LCMV variant GP1V virus that possesses an amino acid mutation at position 38 (F to L) in the GP33-41 epitope of LCMV Armstrong were used. This mutation results in the escape of the virus from recognition by LCMV specific D^b-restricted CTL (339). Both LCMV stocks were prepared in baby hamster kidney cells (BHK21), as previously described, and mice were infected with 5×10^4 PFU of each virus strain intra peritoneally (i.p.) (1).

E. TLR agonists

Ultra Pure LPS from *Escherichia coli (E.coli)* 0111:B4 strain –TLR4 ligand was purchased from Invivogen (San Diego, CA) and stored at -20°C until use. The lyophilized LPS was suspended at 5mg/ml concentration in sterilized water, and the suspended solutions were stored at 4°C. The working concentration of LPS solution was prepared to 500μg/ml, and each mouse was administered 200 μl of the working solution containing 100μg of LPS i.p along with donor specific transfusion (DST) and αCD154 (MR1).

F. In vitro T cell stimulations

Single cell suspensions of thymocytes and splenocytes were prepared in RPMI 1640 supplemented with 10% FBS, 100U/ml penicillin, 100μg/ml streptomycin sulfate and 2mM L-glutamine and stimulated as indicated. For intracellular cytokine assays, lymphocytes (2×10^6 cells) were stimulated with either 1 μM of the indicated peptide or

with monoclonal antibodies specific for CD3e (0.25 μg/ml, 145-2C11, BD Pharmingen) along with antibodies to CD28 (2.5μg/ml, 37.51, BD Pharmingen) or with PMA (0.5 μg/ml) and ionomycin (0.5μg/ml) in the presence of GolgiPlug^{TM} (0.1 μg/ml) for 4 hours at 37°C in 5% CO_2. In co-culture experiments, thymocytes were co-cultured at 1:1 ratios with either splenocytes from the indicated mouse strains or with the indicated cell populations derived from the spleens of congenic B6 mice and stimulated simultaneously as described. For transwell experiments, 24 mm (diameter) 6 well transwell plates containing the standard transwell inserts with 0.4 μm polyester membranes with a pore density of 4×10^6 pores/ cm^3 (Corning *Life Sciences*, Lowell, MA). 10×10^6 thymocytes were seeded in the upper compartment and 5×10^6 thymocytes and 5×10^6 splenocytes were seeded in the lower compartment. Cells in both the compartments were stimulated as described above for 4 hours. At the end of the stimulation, cells were harvested into a 96 well plate and stained by the standard intracellular cytokine assay.

G. Flow cytometry and intracellular cytokine assays

After the incubation, cells were stained with monoclonal antibodies specific for congenic markers (CD45.1: A20) and (CD45.2: 104), CD4 (RM4-5), CD8α(53-6.7), CD8β (H35-17.2), CD25 (PC61), CD44 (IM7), CD62L (MEL-14), CD69 (H1.2F3), CD24 (M1/69), Qa2 (1-1-2), TCR Vα2 mAb (B20.1) and Vβ8.1 mAb (MR5-2), Fas (Jo2), FasL (MFL3) and IL7R (A7R34) were purchased from BD Pharmingen and CD45RB (C363.16A) from eBioscience. Primary BIM (C34C5) rabbit mAb (Cat #2933 at 22.8μg/ml), the corresponding rabbit (DA1E) mAb IgG XP^{TM} isotype control (Cat

#3900 at 2.5mg/ml) and the secondary Anti-Rabbit IgG (H+L), $F(ab')_2$ Fragment (Alexa Fluor® 647 Conjugate) were purchased from Cell Signaling. Following the surface stain, cells were either fixed using BD Cytofix solution and permeabilized using BD Cytofix/Cytoperm^{TM} solution and then stained for intracellular TNF (MP6-XT22 from BD Pharmingen) and CD4 as described previously (1). For immuno staining blood samples, blood collected in tubes containing 5µl (1000U/ml) heparin were washed with FACS buffer followed by surface staining similar to staining for cells in the culture. Following the surface staining, cells were suspended in 1X BD lysing solution (BD pharmingen) for 5-7 min at 37°C. Cells were finally washed with FACS buffer (2X). For analysis of lymphocytes from NG-BAC transgenic mice, GFP positive cells were determined on the basis of the fluorescence intensity found in SP thymocytes (41). Fixation slightly diminished the GFP signal during intracellular staining but lymphocytes could still be differentiated as GFP^{hi+lo} and GFP^{neg} cells in the thymus and the spleen. For tracking alloreactive KB5 transgenic $CD8^+$ T cells in KB5 synchimeric mice, primary DES clonotypic antibody was used. This antibody identifies the TCR of KB5 transgenic $CD8^+$ T cells that recognize the ($H\text{-}2^b$) alloantigen. Staining with the primary antibody was performed for 20 min followed by staining with a secondary flourochrome conjugated IgG2a antibody (R19-15) purchased from BD biosciences. Samples were analyzed using a Becton Dickinson LSRII Flow Cytometer (BD Biosciences) and FlowJo software (Tree star Inc, Ashland, OR).

H. Cell purification and enrichment

Single cell suspensions of thymocytes and splenocytes from the indicated mouse strains were purified by staining with anti-CD4, anti-CD8 and anti-CD44 antibodies in 1X PBS with 2% FBS, 2mM EDTA and sorted for $CD4^+$ $CD8^-$ and $CD4^-$ $CD8^+$ SP thymocytes and naïve ($CD44^{low}$) splenic T cells to using the MoFlo^{TM} XDP cell sorter (Beckton Coulter). For cell enrichment, subsets of P14-$CD8^+$ T cells were obtained by negative magnetic selection in 1X PBS with 2% FBS, 2mM EDTA. For this, thymocytes were depleted of $CD4^+$ cells and splenocytes were depleted of $CD4^+$ and $CD19^+$ cells by initially staining the cells with biotinylated anti-CD4 (RM4-5; BD Pharmingen) and anti-CD19 (ID3; BD Pharmingen) followed by selection with Streptavidin (SA) microbeads (Miltenyi Biotech, Auburn, CA). The purification of $CD8^+$ cells after negative selection was nearly 70% from both tissues. To isolate cell subsets from the $CD45.2^+$ splenocytes for the co-culture experiments described above, B cells were positively selected using anti-CD19 microbeads and T cells were positively selected by Thy1.2 microbeads (Miltenyi Biotech). The cells remaining in the flow-through were used as a source of splenic APCs (20% $CD11c^+$). To purify transgenic alloreactive T cells from KB5 synchimeric mice, splenocytes were stained with Des clonotypic antibody and CD8β and sorted using the MoFlo^{TM} XDP cell sorter (Beckton Coulter).

I. Analysis of RNA expression by RT PCR*.*

Total RNA was isolated using a RNA isolation kit (Qiagen Valencia, CA). An additional step was incorporated to remove genomic DNA using a RNase-free DNase kit

(Qiagen). The concentration of recovered RNA was determined using either the Beckman Coulter DU® 530 Life Science UV/VIS spectrophotometer or the NanoDrop® ND-1000 spectrophotometer (Thermo Scientific Willmington, DE). An equal amount of RNA was reverse transcribed into cDNA using a superscript^{TM} III first strand synthesis system (Invitrogen Carlsbad, CA) consisting of oligo (dT) primers. Amplification of the equal quantity of cDNA was performed using Platinum® Blue PCR SuperMix (Invitrogen Carlsbad, CA) with Mouse/Rat TNF primer pairs (Cat# RDP-60) and β actin primer pairs (Cat # RDP-105) (R&D systems, Minneapolis, MN). The predicted TNF and β actin cDNA product sizes were 585bp and 302bp respectively. RT PCR for FasL expression was done with FasL specific primers (Cat# RDP-58) purchased from R&D systems, Minneapolis, MN. The predicted size of FasL cDNA product is 239bp.The following program was used to amplify the cDNA by PCR, Cycle 1: (1X) step 1: 94°C for 3:00; Cycle 2: (35X) step 1: 94°C for 00:45; step 2: 55°C for 0:45; step 3: 72°C for 0:45; Cycle 3: (1X) step 1: 72°C for 10:00; Cycle 4: (1X) Step 1: 4°C for ∞. For semiquantitative RT PCR, cDNA was synthesized as described above, and three serial dilutions of cDNA were used during the PCR with cycle 2 having only 30 instead of 35 cycles in order to better visualize the differences in RNA expression among samples.

J. Agarose gel electrophoresis

Agarose gel electrophoresis was performed using 1% agarose gel prepared in 1X Tris-acetate EDTA buffer (TAE) (Gibco invitrogen, Carlsbad, CA). To confirm the size of the bands, (0.1μg-0.5μg) of 100 bp ladder (500μg/ml) was used (New England

BioLabs or Invitrogen) with the loading buffer (Promega). The gels were stained with 1% ethidium bromide and photographed using the Bio Rad Molecular Imager® Gel Doc™ XR+ system.

K. Real-time PCR

T cell subsets purified either by sorting or enrichment were used as indicated. Total RNA was isolated using a RNA isolation kit (Qiagen Valencia, CA). An additional step was incorporated to remove genomic DNA using a RNAse-free DNAse kit (Qiagen). The concentration of recovered RNA was determined using the NanoDrop® ND-1000 spectrophotometer (Thermo Scientific Willmington, DE). RNA (as indicated) was reverse-transcribed into cDNA using Superscript™ III first strand synthesis system (Invitrogen Carlsbad, CA) using oligo (dT) primers. Amplification of the cDNA was then performed by Real time PCR with the SYBR® green mastermix (Applied Biosystems Foster City, CA) using MyiQ™ BioRad icycler. The following TNF primers: FW 5'-CAT CTT CTC AAA ATT CGA GTG ACA A-3', RV 5'- TGG GAG TAG ACA AGG TAC AAC CC-3' primers (annealing temp: 60℃ and 175 bp product) (340); β actin primers: FW 5'-CGA GGC CCA GAG CAA GAG AG-3', RV 5'- CGG TTGGCC TTA GGGTTC AG-3' and (annealing temp: 62℃ and 150 bp product) were used. To confirm the expression FasL in alloreactive T cells during co-stimulation blockade by RTPCR, FasL specific primers (Cat # PPM02926A) from Superarray were purchased. The predicted gene product size is 171bp. The following program was used for the real time PCR reaction, Cycle 1: (1X) step 1: 95℃ for 10:00; Cycle 2: (40X) step 1: 95℃ for

00:15; step 2: 60°C for 1:00; Cycle 3: (1X) step 1: 95°C for 1:00; Cycle 4: (80X) Step 1: 55°C for 00:10. For absolute quantification of the data, standard curves were generated using serial dilution of pCR® 4 –TOPO TA plasmids containing cDNA clones of TNF and β actin.

L. Quantification of TNF mRNA expression levels by real time PCR (preparation of TNF cDNA standards).

Splenocytes (2×10^6) from C57BL/6J mice were stimulated with monoclonal antibodies specific for CD3e (0.25 μg/ml, 145-2C11, BD Pharmingen) for 4 hours. RNA was isolated and cDNA synthesized and amplified using TNF specific primers (R&D systems; predicted TNF product size: 585bp) by RT PCR as described above. The PCR product was cloned into pCR® 4 –TOPO TA cloning vector according to the manufacturer's protocol (Invitrogen, Carlsbad, CA). Briefly TOPO® cloning reaction mixture (6μl) containing the PCR product and the pCR® 4 –TOPO TA cloning vector were incubated for 5 min at room temperature (22-33°C). Following this, 2μl of the cloning mixture was mixed with 100μl of chemically competent DH5α™ –T1^R One shot® *E coli* and incubated at 4°C for 30 min. Subsequently, heat shock was performed on the cells at 42°C for 1 min and the tubes were immediately transferred to 4°C where they were rested for another 2 min. At the end of this step, 1ml of LB broth was added to the mixture and the vial was positioned in the shaker at 37°C for 1 hour. The mixture was pelleted down at 5000 rpm for 5 min and the pellet was resuspended in 100μl of media. The resuspended cells were plated onto an LB plate containing ampicillin (50-100μg/ml)

and incubated overnight at 37°C. To analyze the positive clones, colony PCR was performed on 5 randomly picked colonies using TNF specific primers (585bp from R&D systems). Positive clones were picked and cultured overnight in LB media containing 100μg/ml ampicillin followed by plasmid isolation (Qiagen QIA prep® Miniprep). DNA concentration was measured using the NanoDrop® ND-1000 spectrophotometer (Thermo Scientific Willmington, DE). The plasmid was sequenced at the sequencing facility at UMMS, Worcester, MA using M13 primers provided in the TOPO TA cloning kit from invitrogen. The sequence obtained was screened with VecScreen in Pubmed to identify and differentiate the PCR product sequence from the sequences that may be of vector origin. The sequence was aligned using BLAST search and confirmed with the murine TNF gene sequence. Following this, a stock concentration containing 1×10^{10} copies of the plasmid was determined by the following formula {(Molecular weight of the entire plasmid/6.023×10^{23}) 1×10^{10}}. Serial dilutions of the cDNA plasmid were performed and amplified by real-time PCR as described in the above section using the following real-time PCR TNF primers: FW 5'-CAT CTT CTC AAA ATT CGA GTG ACA A-3', RV 5'- TGG GAG TAG ACA AGG TAC AAC CC-3' primers (annealing temp: 60°C and 175 bp product) that were obtained from IDTechnologies (340).

M. Real time PCR array

Alloreactive $DES^{+}CD8\beta^{+}$ T cells were purified using the MoFlo^{TM} XDP cell sorter (Beckton Coulter) to >98% purity. Total RNA was isolated using a RNA isolation kit (Qiagen Valencia, CA). An additional step was incorporated to remove genomic DNA

using a RNase-free DNase kit (Qiagen). The concentration of recovered RNA was determined using the NanoDrop® ND-1000 spectrophotometer (Thermo Scientific Willmington, DE). Subsequently, RNA was subjected to another clean up step with total RNA mixed with $1/10^{th}$ volume of 3M Sodium acetate (NaoAc) pH-5.2 and 2.5 volume of 100% ethanol and 1µl glycoblue (15mg/ml) and kept at -20°C for ≥ 1 hour. This method is used to precipitate RNA as ethanol (having a lower dielectric constant) allows better interactions of Na+ ions with the PO_3^- ions on nucleic acid backbone thereby making the RNA less hydrophilic. The glycoblue is a blue dye that is covalently linked to glycogen that helps in the sodium/ethanol precipitation of RNA by increasing the size and visibility of the pellet. Following the incubation, the solutions were pelleted at ≥ 12000g for 20min at 4°C. This was followed by 2 washes with 80% ethanol at -20°C for 5-10 min. The pellets were air-dried and the RNA was suspended in DEPC water. It was then reverse-transcribed into cDNA using RT^2 PCR Array First Strand Kit (Superarray cat# C-02). Real time PCR was performed on the synthesized cDNA by mixing it RT^2 Real-Time™ SYBR Green/ ROX PCR master mix according to the manufacturer's protocol (Superarray) and aliquoted across the Apoptotic PCR array. The array consists of primer sets for 84 apoptotic pathway specific genes, 5 housekeeping genes and 3 RNA and PCR quality control (PAMM-012). The following program was used for the real time PCR reaction, Cycle 1: (1X) step 1: 95°C for 10:00; Cycle 2: (40X) step 1: 95°C for 00:15; step 2: 60°C for 1:00; Cycle 3: (1X) step 1: 95°C for 1:00; Cycle 4: (80X) Step 1: 55°C for 00:10 using MyiQ™ BioRad icycler. The Ct values obtained from the real time PCR were uploaded into the Superarray Web-based PCR array analysis software. The

gene expression changes were normalized to the house keeping genes and compared to the untreated group. The fold regulation was calculated by the software using the ΔΔCt method (Super array). The positive fold changes >1 indicated the fold upregulation and fold changes <1 were represented as negative inverse of fold change that indicated fold downregulation.

N. Phospho-flow

SP P14 $CD8^+$ thymocytes and splenic T cells (1×10^6) purified by cell enrichment were activated with 1 μM GP33 peptide in RPMI 1640 supplemented with 10% FBS, 100U/ml penicillin, 100μg/ml streptomycin sulfate and 2mM L-glutamine for the indicated time points at 37°C. Stimulation with PMA (0.5 μg/ml) and ionomycin (0.5 μg/ml) for 30 min was used as a positive control. Cells were stained according to the manufacturer's protocol (Cell Signaling Technology, Danvers, MA). Briefly, cells were fixed immediately after activation with 2% formaldehyde (methanol free) (Thermo Scientific Rockford, IL) for 10 min at 4°C. Cells were then pelleted and suspended slowly in 90% methanol and incubated for 30 min at 4°C or left at -20°C overnight. Following permeabilization, cells were rinsed twice with 2 ml of incubation buffer (0.5% BSA in 1X PBS). Mouse monoclonal antibodies to phosphorylated and total extracellular signal-regulated kinases (pERK and total ERK) conjugated to Alexa-647 (Cell Signaling Technology) were added along with antibodies to CD8, CD4 and CD44 and cells were incubated for 60 min in the dark at room temperature. Cells were rinsed and resuspended in 500μl incubation buffer and analyzed immediately on a LSR2 flow cytometer.

O. In-vivo brefeldin A (BfA) Assay

This assay was modified from a previously published protocol (341) and used to detect TCR-transgenic T cells producing TNF *in vivo*. Briefly, unpurified thymocytes or splenocytes from Ly5.1 ($CD45.1^+$) P14 and Ly5.2 ($CD45.1^+$) SMARTA mice (mixed at a 1:1 ratio) were treated in vitro with 0.5 μg/ml GolgiPlug^{TM} (BD biosciences) for 20 min at 37°C. Following the incubation, the cells were adoptively transferred into $CD45.2^+$ B6 hosts that were infected 2 days previously with 5×10^4 plaque forming units (Pfu) of LCMV Armstrong or GP1V CTL escape variant. Additionally each mouse received 250 μg of BfA (Sigma) i.v. Four hours after transfer, host spleens were harvested and donor T cells were stained directly for TNF using the intracellular cytokine staining protocol as described above.

P. Adoptive transfer of endogenous and transgenic SP thymocytes

30×10^6 Ly5.1 ($CD45.1^+$) B6 thymocytes were labeled with 2μM CFSE (HANKS buffer) were transferred into Ly5.2 ($CD45.1^+$) B6 congenic mice. Host spleens were harvested 6 hours, 12 hours, day1, 2 and 4 and 8 followed by stimulations with αCD3 (0.25μg/ml) and αCD28 (2.5μg/ml) for 4 hours in vitro followed by standard intracellular staining for cytokines. For transgenic cells, 20×10^6 P14 thymocytes and splenocytes were transferred separately into $CD45.2^+$ B6 hosts. Host spleens were harvested 1, 2, 7 and 14 days after transfer and stimulated in vitro with 1 μM GP33 peptide and αCD28 (2.5μg/ml) in the presence of GolgiPlug^{TM} (0.1 μg/ml) for 4 hours at 37°C in 5% CO_2 incubator followed by standard intracellular cytokine staining protocol for TNF by donor

T cells as described above. Dead cells were excluded using Live Dead Aqua Dead cell stain (Invitrogen; Molecular probes Carlsbad, CA) for this experiment. Ly5.1 (CD45.1+) WT and Ly5.1 Ly5.2 ($CD45.1^+$ and $CD45.2^+$) TNF deficient $CD8^+$ P14 TCR transgenic splenic T cells were co-transferred (1:1 ratio with 1×10^4 of each population) into Ly5.2 ($CD45.2^+$) WT, TNF deficient or TNFR1/2 deficient hosts. The mice were infected with 5×10^4 pfu of LCMV Armstrong i.p the following day. On day 8, recipient spleens were harvested and the cells were stained as indicated.

Q. Tolerance induction regimen

Recipient mice (specified strains) were given donor specific transfusion (DST) and anti-CD154 (MR1) antibody as described previously (4). Briefly, mice were given 10×10^6 splenocytes from B6 ($H\text{-}2^b$) or BALB/C ($H\text{-}2^d$) mice as DST in 200µl volume HBSS i.v along with 500µg of anti-CD154 (MR1) antibody in 200µl volume i.p, on day -7 prior to skin grafting or transferring allogeneic and syngeneic target cells for *in vivo* cytotoxicity assay on day 0. On day -4 and day -1, recipient mice also received extra doses of 500µg of anti-CD154 (MR1) antibody. To determine the effect of TLR activation at the time of tolerance induction, mice also received LPS (100µg/mouse) diluted in HBSS in 200µl volume i.p (as described above in TLR agonists section in *Materials and Methods*) along with DST and MR1 injection on day -7. To determine the fate of alloreactive T cells under these treatments in KB5 synchimeric mice, recipient spleens were harvested at 9,11, 12 or 15 hours post treatment (as indicated) followed by

surface staining for DES and CD8β to monitor alloreactive cell number or alloreactive T cells were sorted for Real time PCR array.

R. Annexin-V, Active Capase3 and TUNEL staining

To analyze the apoptotic profile of the T cells, annexin-V staining was performed. One of the features of early apoptosis is that the membrane phosphotidyl serine that is usually expressed in the inner leaflet of the plasma membrane is flipped out to the outer membrane in apoptotic cells. Spleens from the indicated mice were harvested after the indicated time points and the (1×10^6) splenocytes were pre-incubated in 48 well flat bottom plate for 4 hours *in vitro* at either the physiological temperature 37 °C or at 4°C control. Incubation at 37°C slows the scavenging activity of macrophages so that there could be better staining for apoptotic cells. After incubation, cells were transferred into a 96 well plate and stained for surface markers for 20 min. This was followed by 15 min of incubation with 5µl of annexin-V (BD pharmingen) and 1µl of 7AAD (BD pharmingen) in 1X annexin-V buffer at room temperature in the dark. The cells were rinsed and washed with annexin-V buffer and immediately analyzed on a LSR2 flow cytometer.

To corroborate the annexin-V profile in alloreactive T cells, active caspase-3 (Casp GLOW™ Fluorescein Active Caspase-3 staining kit; Cat# K183-25; Biovision) and terminal deoxynucleotidyl (TdT) dUTP nick end labeling (TUNEL) (ApoDIRECT *In situ* DNA fragmentation Assay kit Cat# K402-50; Biovision) staining were performed according to the manufacturer's protocol. For activated caspase 3 staining, splenocytes isolated from KB5 synchimeric mice were pre- incubated for 3 hours at 37°C similar to

the method for annexin-V staining but in the presence or absence of caspase inhibitor ZVAD-FMK (1µl/well) (inhibits caspase 3 activation). At the end of the 3rd hour, cells were stained for surface markers followed by the addition of (1µl/well) FITC DEVD-FMK (that binds activated caspase 3). Samples were then incubated for another 1 hour at 37°C. The cells were finally washed and stained for annexin-V and 7AAD. For TUNEL staining, splenocytes were pre-incubated for 4 hours *in vitro* at 37 °C followed by surface staining and fixation using BD cytofix (100µl/well) solution. Subsequently, cells were resuspended in 70% ethanol and stored at -20°C overnight. The following day, samples were washed and stained according to the Apo-DIRCET assay protocol (Biovision). For counter staining, 7AAD was used instead of propidium iodide (PI). The samples were finally rinsed and analysed on the LSR2.

S. Use of FasL antagonistic and Fas agonistic antibodies during in vitro cultures

Splenocytes (1×10^6) isolated from KB5 synchimeric mice (after the indicated treatments) were pre-incubated in 48 well flat bottom plates for 4 hours *in vitro* at either the physiological temperature 37 °C or at 4°C control for annexin-V, caspase 3 and TUNEL staining. To determine the effect of FasL blockade on the apoptotic profile of alloreactive T cells, splenocytes were incubated with 20 µg/ml of FasL- blocking antibody (MFL-4; BD Biosciences) during the 4 hour culture period at 37 °C (342) followed by annexin-V, activated caspase3 or TUNEL staining. To determine the effect of Fas agonistic antibody on the apoptotic profile of alloreactive T cells, splenocytes were

incubated with 5, 2.5, 1.25 and 0.625 μg/ml of Fas (Jo2) antibody (BD Biosciences) for 4 hours *in vitro* (343) followed by annexin-V staining.

T. FasL and BIM staining

The protocol for FasL surface staining was kindly provided by Mr. Ryan A. Langlois from The University of Iowa. All the steps were performed at 4 °C. Splenocytes (2×10^6) from KB5 synchimeric mice were incubated with Syrian hamster serum (1:100 dilution), rat serum (1:100 dilution) purchased from Jackson Immunoresearch plus (1:400 dilution) free streptavidin (SA) (Molecular probes Cat#S888) for 10 min at 4°C. This blocking step with serum and free SA blocks the Fc receptors that could be bound by FasL antibody and the biotin expressed on the surface of cells respectively. Following the blocking step, cells were washed (2X) before staining with primary clonotypic DES and biotinylated αFasL (MFL-3) antibody for 25 min at 4°C. Subsequently, cells were stained with flourochrome-conjugated reagents or antibodies; for example, SA-PE (1:100 dilution; BD biosciences) in case of FasL and FITC conjugated IgG2a (R19-15) for DES and incubated for 15-25 min at 4°C. Finally, the cells were thoroughly washed in FACS buffer (2X) and the samples were immediately analyzed on the LSR2. To confirm the staining protocol, splenocytes from day 9 LCMV Armstrong infected were stained for FasL.

Staining for BIM was performed according to the manufacturer's protocol (Cell Signaling). Briefly, splenocytes from the treated mice were either stained directly or incubated 4 hours before surface staining for the antibodies. Cells were immediately

fixed using 2-4% formaldehyde solution (methanol free) for 10 min at 37°C. This was followed by methanol permeabilization for 30 min at 4°C as described in manufacturer's protocol. The cells were then washed with 1X incubation buffer (1X PBS with 0.5% BSA) followed by staining with primary BIM (C34C5) rabbit mAb (Cat #2933 at 22.8μg/ml;Cell signaling) and the corresponding rabbit (DA1E) mAb IgG XP^{TM} isotype control (Cat #3900 at 2.5mg/ml; Cell Signaling) for 1 hour at room temperature. The cells were washed at the end of the incubation and cells were re-incubated with secondary Anti-Rabbit IgG (H+L), F(ab')$_2$ Fragment (Alexa Fluor® 647 Conjugate; Cell signaling) for 30 min at room temperature. The cells were finally washed and analysed on the LSR2.

U. In vivo cytotoxicity assay

The *in vivo* cytotoxicity assay was performed as previously described(344). Briefly, the indicated mouse strains (H-2^b) (B6 mice, lpr, gld and IL-10 KO) received 10×10^6 BALB/c (H-2^d) splenocytes in the form of DST i.v along with (500μg/mouse) MR1 on day -7 i.p with respect to day 0 when the mice either received allogeneic target cells instead of skin grafts. With regard to the IL-10 KO (H-2^b) mice also received (100μg/mouse) LPS i.p. All mice received extra injections of MR1 on day-4 and day 0 as per the tolerance induction regimen. To truly estimate the cytolytic ability of alloreactive CD8$^+$ T cells, mice were given NK1.1 depleting antibody from purified ascites (1:20) on day -1, a day prior to receiving the target cells. On day 0, target syngeneic B6 (H-2^b) and allogeneic BALB/c (H-2^d) splenocytes were prepared as

described previously (345). Briefly, syngeneic B6 (H-2^b) and allogeneic BALB/c (H-2^d) splenocytes were incubated with 2.5μM and 0.5μM of CFSE respectively for 15-20 min at 37°C, with shaking every 5 min. The cells were washed with cold HBSS (2X). The syngeneic B6 (H-2^b) and allogeneic BALB/c (H-2^d) splenocytes were recounted and then mixed at equal ratios. A total of 20× 10^6 cells were adoptively transferred into each of recipient mice as indicated. Around 20 hours post injection of the target cells, the recipient mice were sacrificed and their splenocytes were analyzed for allogeneic target cell lysis based on CFSE detection. The percentage lysis was calculated according to the following formula: 100-{[(% allogeneic target population in experimental / % syngeneic target population in experimental) ÷ (% allogeneic target population in NK depleted naïve control / % syngeneic target population in NK depleted naïve control)] × 100} as described previously (345, 346).

V. Serum cytokine analysis using BD™ Cytometric Bead Array (CBA)

Serum from blood of KB5 synchimeric mice that were either untreated or treated with DST, DST+MR1 or DST+MR1+ LPS for 8 hours was isolated. The following were the inflammatory cytokines measured in the serum: IL-6, IL-10, monocyte chemoattractant protein-1 (MCP-1), IFN-γ, TNF, and interleukin-12p70 (IL12p70). The quantity of each of inflammatory cytokines was measured using the BD™ Cytometric Bead Array (CBA). Briefly, the mouse inflammation standards containing the lyophilized mouse recombinant proteins were prepared as per the recommended protocol in the kit. Next, the capture bead mixture for every assay tube was prepared, containing

10 µl of each of the 6 capture beads possessing distinct fluorescence intensities (coated with the capture antibody for each cytokine in the kit). Then, the serum samples were diluted to 1:2 and 1:16 times in the appropriate volume of assay diluent (provided in the kit). Once these reagents were prepared, the capture beads were mixed with standards and the diluted samples. Subsequently, the PE detection reagent was added to the above mixed samples and the tubes were incubated for 2 hours at room temperature in the dark. The samples were washed with the wash buffer before resuspending the bead pellet in the wash buffer again. The samples were then analyzed with appropriate FITC and PE single color controls according to the protocol on the LSR2 in the FACS core facility at UMMS.

X. Statistics

Sample analyses were also done using Graph Pad Prism (Graph Pad Software). Samples were analyzed by unpaired t test wherever specified and P values are indicated. A one-way ANOVA with a Tukey post-test was used to compare multiple samples, with a P value of <0.05 considered significant.

Chapter 3: Maturation-dependent licensing of naïve T cells for rapid TNF production

Chapter 3: Abstract

TNF is a well-documented pro-inflammatory cytokine that has recently been shown to play an immunoregulatory function in limiting the magnitude of virus-specific T cell responses during a viral infection. Naïve T cells in secondary lymphoid organs (SLOs) exhibit a unique ability to produce TNF rapidly after activation and prior to acquiring other effector functions and hence serve as one of the sources of TNF during an immune response. My studies revealed that TNF deficiency in T cells could limit the magnitude of virus-specific T cell responses, suggesting the suppressive role of T cell-derived TNF during a viral infection. Peripheral naive T cells are a heterogeneous population of cells at various stages of post-thymic development. Comparison of TNF cytokine profiles of single positive thymic T cells, splenic RTEs and MN T cells during TCR activation revealed that thymic T cells exhibited a poor ability to produce TNF when compared to splenic T cells, despite possessing a similar potential for activation. Splenic RTEs had a significantly enhanced ability to produce TNF relative to their SP thymic precursors, while MN T cells were the most efficient of TNF producers. Together, these findings suggest that the regulation of TNF expression by naïve T cells is influenced by the post-thymic maturation status of T cells. The hierarchical pattern of TNF production by different naïve T cell subsets in the periphery results in the establishment of functional heterogeneity in the naïve T cell pool that in turn might affect T cell fate decisions during the initiation phase of T cell responses.

Chapter 3: Introduction

T cell development begins within the thymus and is driven to completion after single positive (SP) thymocytes exit the thymus and seed secondary lymphoid organs, where they undergo progressive phenotypic and functional maturation (3). The peripheral naïve T cell pool is therefore comprised of a heterogeneous population of cells at different stages of post-thymic development, encompassing T cell subsets from the fully mature to the most recently emigrated thymic T cells (347). The recent thymic emigrants (RTEs) which are 0-2 weeks old in the periphery have a distinct phenotypic profile ($CD24^{high}$, $Qa2^{low}$, $CD45RB^{low}$) relative to their mature naïve (MN) counterparts, that are resident in the periphery for > 3 weeks ($CD24^{low}$, $Qa2^{high}$, $CD45RB^{high}$) (3, 41). RTEs have been shown to also differ functionally, producing less IL-2, exhibiting a decreased ability to proliferate upon 48 hours of *in vitro* TCR stimulation and producing less IFN-γ after 7 days of infection with ovalbumin-expressing *Listeria monocytogenes (r*LM-OVA) (3, 41). Our laboratory has previously shown that recently activated naïve T cells in secondary lymphoid organs rapidly produce TNF within 4-5 hours of TCR engagement (1). The kinetics of TNF production by naïve T cells suggests that this potent immunomodulatory cytokine is released during the initial encounter between T cells and APCs, a critical phase in the programming of antigen-specific responses (117, 348-354). However, when and how naïve T cells acquire this unique capability to produce TNF during development is not known.

Given the important role of TNF in regulating immune responses and the ability of naïve T cells to produce this cytokine early during activation, I first determined the immunoregulatory role of T cell-derived TNF in shaping the immune response during the acute phase of LCMV infection using a co-adoptive transfer model of WT and TNF deficient P14 TCR transgenic $CD8^+$ T cells into either WT, TNF deficient or TNFR1/2 deficient hosts. These studies demonstrate that T cell-derived TNF plays a suppressive role in limiting the magnitude of CTL responses during the acute phase of an immune response. This suppressive effect of T cell-derived TNF is localized and is partly manifested through its paracrine effect on other surrounding cells.

Subsequently, I determined the developmental stage when naïve T cells become competent to produce TNF by comparing the capability of SP naïve T cells to produce TNF before and after emigration from the thymus. Since, the ability of naïve T cells to produce TNF is primarily mediated by TCR signaling, I performed these studies comparing 2 modes of activation of T cells, namely with anti-CD3 antibody and peptide stimulation of polyclonal T cells and transgenic T cells, respectively. These studies reveal that $CD4^+$ $CD8^-$ and $CD4^-$ $CD8^+$ SP thymocytes possess a poor ability to produce TNF upon stimulation when compared to their counterparts in secondary lymphoid organs. Contact with secondary lymphoid cells (spleen and lymph node) during TCR activation partially enables SP thymocytes to produce TNF *in vitro* by providing optimal antigen-presentation. However, the frequency of TNF producing cells is still significantly lower than in the periphery. RTEs in the spleen on the other hand, display an intermediate TNF response, which is higher than their SP thymic precursors but lower relative to the MN T

cells. Interestingly, the difference in the TNF profile exhibited by these 3 populations of lymphocytes mirrors their distinctive maturation status. Moreover, as developing T cells mature in the periphery, they show a progressive increase in their capability to produce TNF upon TCR activation. Together, these findings suggest that naïve T cells become gradually licensed to efficiently produce TNF in a maturation-dependent manner that requires their localization to secondary lymphoid organs.

Chapter 3: Results

A. T cell-derived TNF limits the magnitude of CD8$^+$ T cell responses during the effector phase of the immune response

TNF has been shown to have an immunoregulatory role during viral and some bacterial infections (191, 192). These studies showed that T cells from TNF-deficient mice exhibited reduced apoptosis during the contraction phase of the immune response suggesting a role for TNF in suppressing CD8$^+$ T cell responses. However, these studies did not show the cellular source of TNF that was responsible for this suppressive effect. To test if T cell-derived TNF can limit effector CD8$^+$ T cell responses, I adoptively transferred WT P14 and TNF-deficient P14 TCR transgenic CD8$^+$ T cells (designated as P14 Tg CD8$^+$ from here on) into mice that were either WT or TNF-deficient and infected them with LCMV the following day (Fig. 3.1 A). The only source of TNF in the TNF-deficient hosts is the TNF that is produced by WT P14 Tg CD8$^+$ T cells. I found that by day 8 of LCMV infection, TNF-deficient P14 Tg CD8$^+$ T cells accumulated to higher levels both in frequency (average 33 ± 1.5 % P14 WT compared to 66 ± 1.5 % TNF-deficient in WT host and average 19.2 ± 0.6 P14 WT compared to 80.8 ± 0.6 P14 TNF-deficient in TNF deficient host) and absolute cell number (11.8 ± 1.9 × 10^6 P14 WT compared to 23.1 ± 2.6 × 10^6 P14 TNF-deficient in WT host and 4.8 ± 1.3× 10^6 P14 WT compared to 19.8 ± 5.3× 10^6 P14-TNF deficient in TNF deficient hosts) than the P14 WT counterparts confirming previous reports that TNF has a suppressive role during LCMV infection (Fig 3.1 B). This was not attributed to the differences in clearance of the viral

antigen, as the viral titers in WT and TNFKO animals observed at day 8 have been shown to be similar(2). The TNF that is produced by the WT P14 Tg $CD8^+$ T cells did not affect the TNF-deficient P14 Tg $CD8^+$ cells, suggesting a localized effect of this cytokine. I also found that the ratio of donor TNF-deficient P14 Tg $CD8^+$ T cells to the WT counterparts in the TNF-deficient host was higher than in the WT host (Fig 3.1D). The more pronounced differences in frequency of TNF-deficient P14 Tg $CD8^+$ T cells to the WT P14 Tg $CD8^+$ T cells in the TNF-deficient hosts suggests that TNF derived from cell types other than antigen-specific $CD8^+$ T cells also contributes to the suppressive effect. Next, I hypothesized that accumulation of TNF-deficient P14 Tg $CD8^+$ T cells could be due to reduced apoptosis. To test this, I performed annexin-V and 7AAD staining on splenocytes isolated from WT or TNF-deficient mice that received a co-transfer of P14 WT and TNF-deficient Tg $CD8^+$ T cells. I incubated the cells for 4 hours *in vitro* before staining for annexin-V and 7AAD. I observed no differences in percentages of annexin-V positive cells or the mean fluorescence intensities (MFI) of annexin-V in WT P14 or TNF-deficient P14 Tg $CD8^+$ T cells that were transferred into either hosts on day 8 post infection. This indicated that TNF-deficient T cells are not resistant to apoptosis during this period (Fig 3.1C). Together these results suggest that the absence of T-cell derived TNF leads to accumulation of antigen-specific T cells to higher frequencies during LCMV infection, and this increase in number is not due to reduced apoptosis of antigen-specific T cells.

Figure 3.1. TNF-deficient P14 TCR transgenic (Tg) CD8+ T cells accumulate to higher frequencies than their WT counterparts after LCMV infection

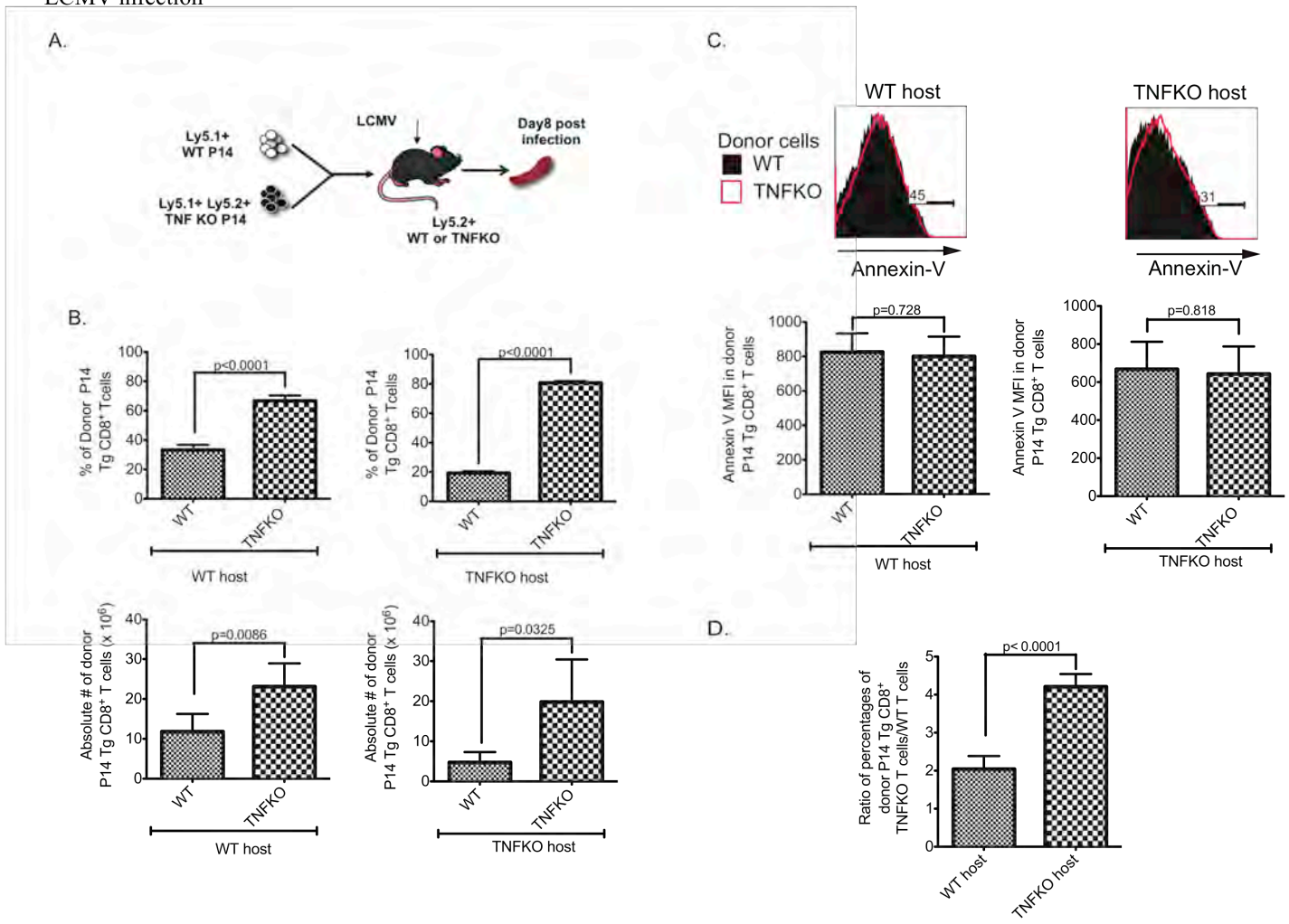

Figure 3.1. TNF-deficient P14 TCR transgenic (Tg) CD8$^+$ T cells accumulate to higher frequencies than their WT counterparts after LCMV.

P14 Ly5.1 (CD45.1$^+$) WT and P14 Ly5.1 Ly5.2 (CD45.1$^+$ and CD45.2$^+$) TNF-deficient Tg CD8$^+$ splenic T cells were co-transferred (1:1 ratio with 1× 10^4 of each population) into either Ly5.2 (CD45.2$^+$) WT or TNF-deficient hosts. The mice were infected with 5×10^4 pfu of LCMV Armstrong i.p.the following day. Panel A shows the experimental design of the co-transfer. Panel B shows the percentages and the absolute cell numbers of donor P14 WT and TNF-deficient Tg CD8$^+$ T cells in either WT (N =5) or TNF-deficient hosts (N =4) respectively. Panel C shows the percentages of donor cells (WT-black histograms and TNF-deficient- red histograms) positive for annexin-V in WT or TNF-deficient hosts and their respective MFI. Panel D shows the comparison of ratio of the percentages of donor P14 TNF-deficient Tg CD8$^+$T cells to donor P14 WT Tg CD8$^+$ T cells in the WT and TNF-deficient hosts. The values in each graph were compared using an unpaired test. P values are indicated in each graph. Error bars indicate SD.

B. The suppressive effect of T cell-derived TNF is in part mediated by its influence on host cells

I next wanted to determine if the mechanism by which the localized effect of T cell-derived TNF occurred is via an autocrine or a paracrine phenomenon. To test this, I co-transferred WT P14 and TNF-deficient P14 Tg $CD8^+$ T cells into either WT or TNF receptor (TNFR 1 and 2 designated as TNFR1/2) -deficient hosts and infected them with LCMV Armstrong (Fig 3.2A). At day 8 post-infection, I observed higher percentages and absolute number of donor TNF-deficient P14 Tg $CD8^+$ T cells compared to donor WT P14 Tg $CD8^+$ T cells in both WT (average frequency 32.6 ± 1.1 % P14 WT compared to 67.1 ± 1.2 % P14 TNF-deficient and average cell number 7.8 ± 0.5 × 10^6 P14 WT compared to 16.5 ± 1.6 × 10^6 P14 TNF-deficient) and TNFR1/2-deficient hosts (average frequency 40.4 ± 0.9 % P14 WT compared to 59.5 ± 0.9% P14 TNF-deficient and average cell number 37.1 ± 4 × 10^6 P14 WT compared to 55.8 ± 7.1 × 10^6 P14 TNF-deficient) (Fig 3.2B). This suggests that the localized effect T cell-derived TNF may be occurring in an autocrine fashion at this stage of infection.

Interestingly, I also observed that the donor WT P14 Tg $CD8^+$ T cells accumulated to slightly higher frequencies in the TNFR1/2-deficient hosts although they were still lower compared to donor TNF-deficient P14 Tg $CD8^+$ T cells (Fig 3.2B in TNFR1/2 deficient hosts right side columns). The average number of WT P14 Tg $CD8^+$ T cells in the WT host 7.8 ± 0.5 × 10^6 compared to 37.1 ± 4 × 10^6 in TNFR hosts. This suggests the donor WT P14 Tg $CD8^+$ T cells were less suppressed in the TNFR1/2

deficient hosts. This could mean that in addition to the autocrine effect of T cell-derived TNF, paracrine signaling via the TNFR1/2 on the surrounding cells may also be playing a role in mediating the suppression on antigen-specific T cells during an immune response. Consequently, I observed that the ratio of percentages of TNF-deficient P14 Tg $CD8^+$ T cells to its WT counterparts was reduced in TNFR1/2 KO host relative to the WT host (Fig 3.2C). This was not attributed to the differences in clearance of the viral antigen, as the viral titers in WT and TNFR1/2 KO animals observed at day 8 have been shown to be similar(191).

Next, I performed annexin-V and 7-AAD staining on splenocytes from either WT or TNFR1/2 deficient mice that were co-transferred with WT P14 Tg or TNF-deficient P14 Tg $CD8^+$ T cells. I observed no differences in percentage of annexin-V positive cells in P14 WT or TNF-deficient Tg $CD8^+$ T cells (Fig 3.2C). Together, these results suggest the effect of T cell-derived TNF is partly mediated by its effect on other cell types.

Figure 3.2. The suppressive effect of T cell-derived TNF occurs due to both autocrine and paracrine signaling

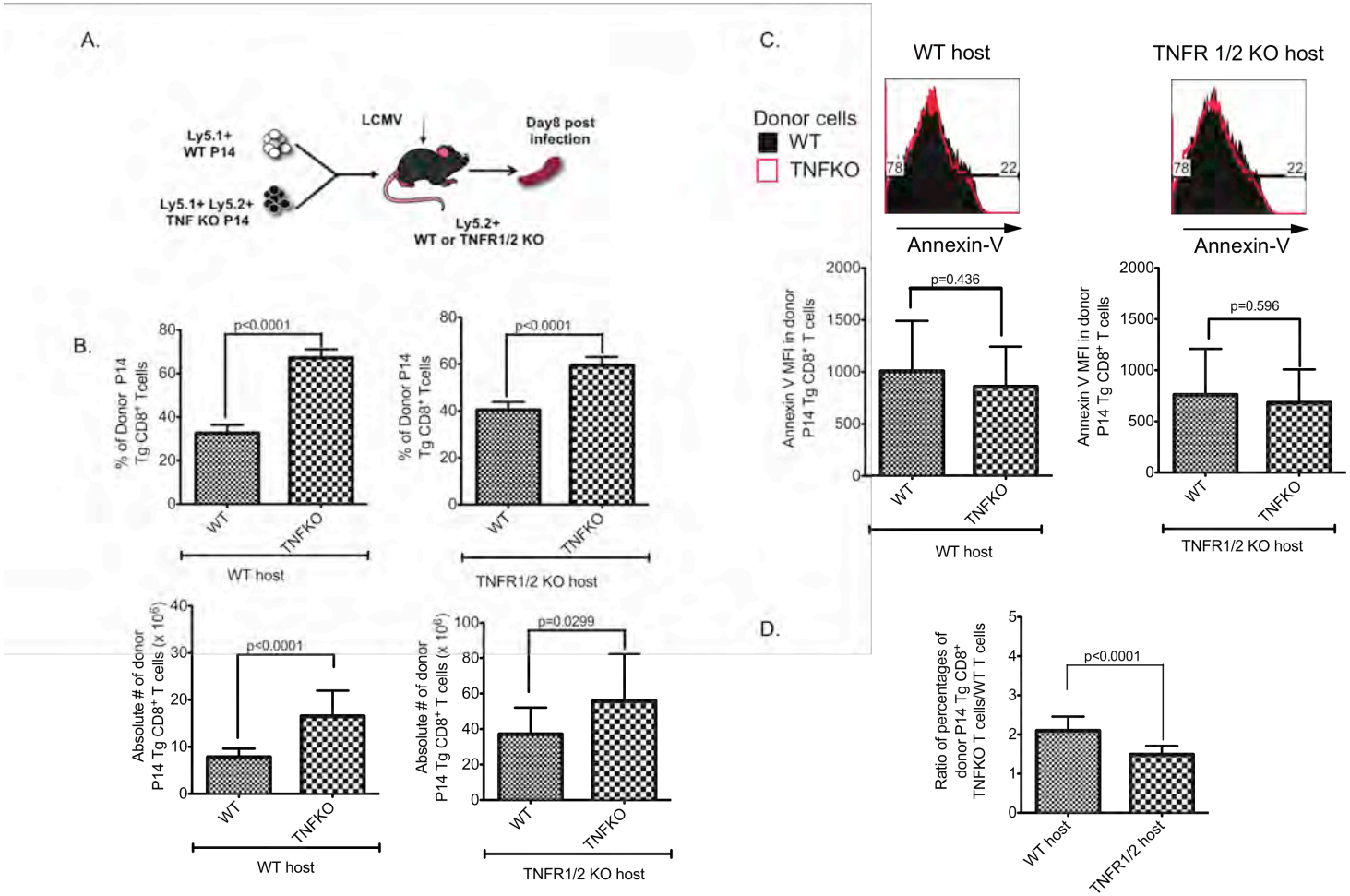

Figure 3.2. The suppressive effect of T cell-derived TNF occurs due to both autocrine and paracrine signaling

Ly5.1 (CD45.1$^+$) WT and Ly5.1$^+$ Ly5.2$^+$ (CD45.1$^+$ and CD45.2$^+$) TNFR1/2-deficient CD8$^+$ P14 TCR transgenic splenic T cells were cotransferred (1:1 ratio with 1× 10^4 of each population) into Ly5.2 (CD45.2) WT (N=11) or TNFR1/2-deficient hosts (N=15). The mice were infected with 5×10^4 pfu of LCMV Armstrong i.p. Panel A shows the experimental design of the cotransfer. Panel B show the percentages and the absolute cell numbers of donor P14 WT and P14 TNF-deficient cells in either WT or TNFR1/2-deficient hosts. Panel C shows the percentages of P14 donor cells (WT and TNF-deficient) positive for annexin-V in WT or TNFR1/2-deficient hosts and their respective MFI. Panel D shows the comparison of ratio of the percentages of P14 TNF-deficient T cells to WT donor T cells in the WT and TNFR1/2 deficient hosts. The values in each graph were compared using an unpaired test. P values are indicated in each graph. Error bars indicate SD.

C. Addition of αCD28 co-stimulation during αCD3 stimulation in vitro augments the TNF producing ability of polyclonal peripheral naïve (CD44^{lo}) T cells.

Previously, it was shown that naïve splenic CD44^{lo} polyclonal CD8^{+} and CD4^{+} T cells rapidly produce TNF upon *in vitro* αCD3 stimulation (1, 345). This indicated that the production of TNF by recently activated naïve T cells is a TCR-dependent phenomenon. Co-stimulation with αCD28 has been shown to augment TCR mediated signals for cytokine production such as IL-2 (61). Therefore, I wanted to determine if provision of αCD28 antibody would augment the production of TNF by naïve CD44^{lo} T cells stimulated with αCD3 antibody. I found that addition of αCD28 along with αCD3 antibody during the 4-hour stimulation period increased the percentages of naïve splenic CD8^{+} and CD4^{+} T cells that produced TNF when compared to cells that were stimulated with αCD3 antibody alone (Fig 3.3A and B). The addition of αCD28 did not enable the CD44^{lo} cells to produce IFNγ, though the CD44^{hi} cells had a higher percentage of cells producing IFNγ. Together, these results suggest that co-stimulation enhances the ability of naïve T cells to produce TNF more efficiently.

Figure 3.3. Enhanced production of TNF by recently activated naive (CD44-lo) polyclonal peripheral T cells stimulated with αCD3 and αCD28 for 4 hours in vitro

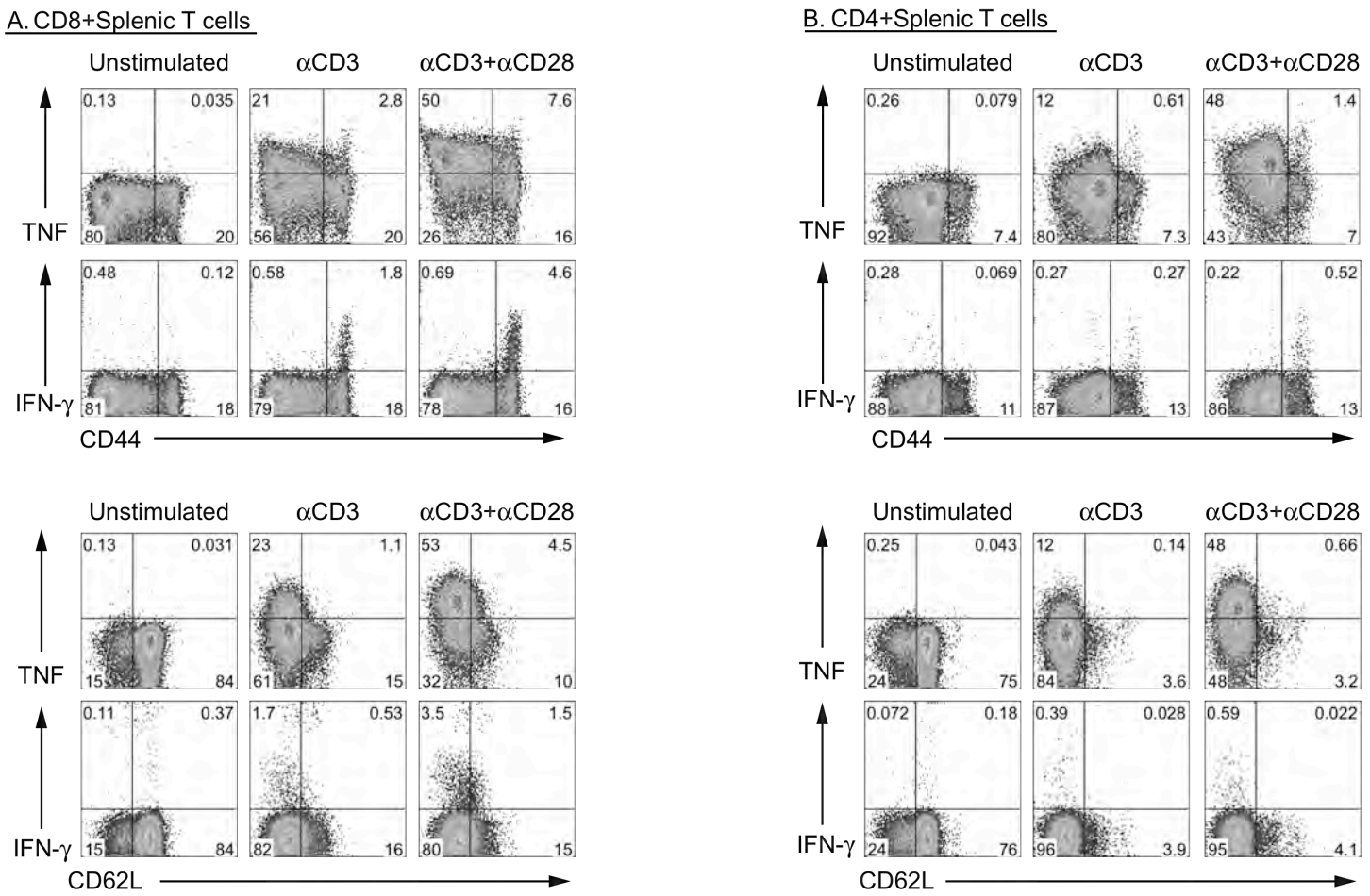

Figure 3.3. Enhanced production of TNF by recently activated naïve ($CD44^{lo}$) polyclonal peripheral T cells stimulated with αCD3 + αCD28 for 4 hours in vitro.

Splenocytes from naïve C57BL6 mice were stimulated as indicated for 4 hours in vitro followed by intracellular staining for TNF and IFNγ by $CD44^{lo}$ $CD62L^{lo}$ $CD8^{+}$ and $CD4^{+}$ T cells. Panel A and B show the percentages of $CD8^{+}$ T cells and $CD4^{+}$ T cells producing TNF and IFNγ with respect to CD44 and CD62L expression.

D. Polyclonal naïve T cells produce TNF rapidly and transiently after αCD3 and αCD28 stimulation

Antigen-specific effector T cells exhibit a transient TNF cytokine profile even in the continuous presence of antigen (355). To determine the kinetics of TNF production by naïve splenic polyclonal T cells, I performed a modified version of the intracellular cytokine assay. Briefly, splenocytes from B6 mice were stimulated with αCD3 and αCD28 co-stimulation in the presence of bfA for the indicated time periods to assess the production of TNF (plots on the left Fig 3.4A). Consistent with the previous findings, the percentage of $CD44^{lo}$ recently activated naïve T cells producing TNF peaked at 4 to 5 hours and reached a plateau by 7- 8 hours (Fig 3.4 Panel 1). This was associated with a similar increase in the TNF MFI observed in these $CD44^{lo}$ recently activated naïve T cells. The addition of bfA throughout the culture period indicates the cumulative frequency of TNF producing cells and the amount of intracellular TNF accumulated on a per cell basis until each indicated time point. In order to determine the production of TNF on an hourly basis, cells were stimulated for the indicated time periods and bfA was added only during the last hour stimulation (plots on the far right Fig 3.4 Panel 3). The addition of bfA during the last hour of stimulation indicates that the percentage of cells producing TNF at that time point and the amount of TNF produced per cell peaked at 4 to 5 hours and was rapidly extinguished by 7- 8 hours. Both $CD8^{+}$ and $CD4^{+}$ T cells follow a similar trend for TNF production (Fig 3.4 B Panels 1 and 3).

Since TNF is found in a membrane-bound form in addition to being secreted, the TNF detected in cultures containing bfA during the last hour of stimulation is a sum of both intracellular and surface bound forms of TNF. Therefore, I wanted to determine the surface expression of TNF in the absence of bfA (Fig 3.4 A and B, Panels 2). When I examined the expression of the membrane-bound TNF, I observed that there was minimal accumulation of TNF at the surface, which mirrored the transient profile of intracellular TNF (Fig 3.4 A and B, Panels 2). The peak of the surface expression of TNF and the percentage of cells producing the cytokine coincided at 4-5 hours and decreased by 7- 8 hours. This confirmed that the TNF detected during the last hour of stimulation for every time point was an indicator of TNF production in that hour and not predominantly due to the accumulation of TNF at the surface. Additionally, these results confirm that co-stimulation enhances the ability of naïve T cells to produce TNF (Fig 3.4 A and B). The controlled production of TNF by naïve T cells reflects its tight regulation that is consistent with the property exhibited by effector T cells at a later stage of an immune response. Together, these results indicate that there is a rapid and transient burst of TNF by activated naïve $CD44^{lo}$ T cells that quickly is extinguished despite the continuous presence of stimulation.

Figure 3.4. Rapid and transient production of TNF by polyclonal naïve ($CD44^{lo}$) $CD8^+$ and $CD4^+$ splenic T cells

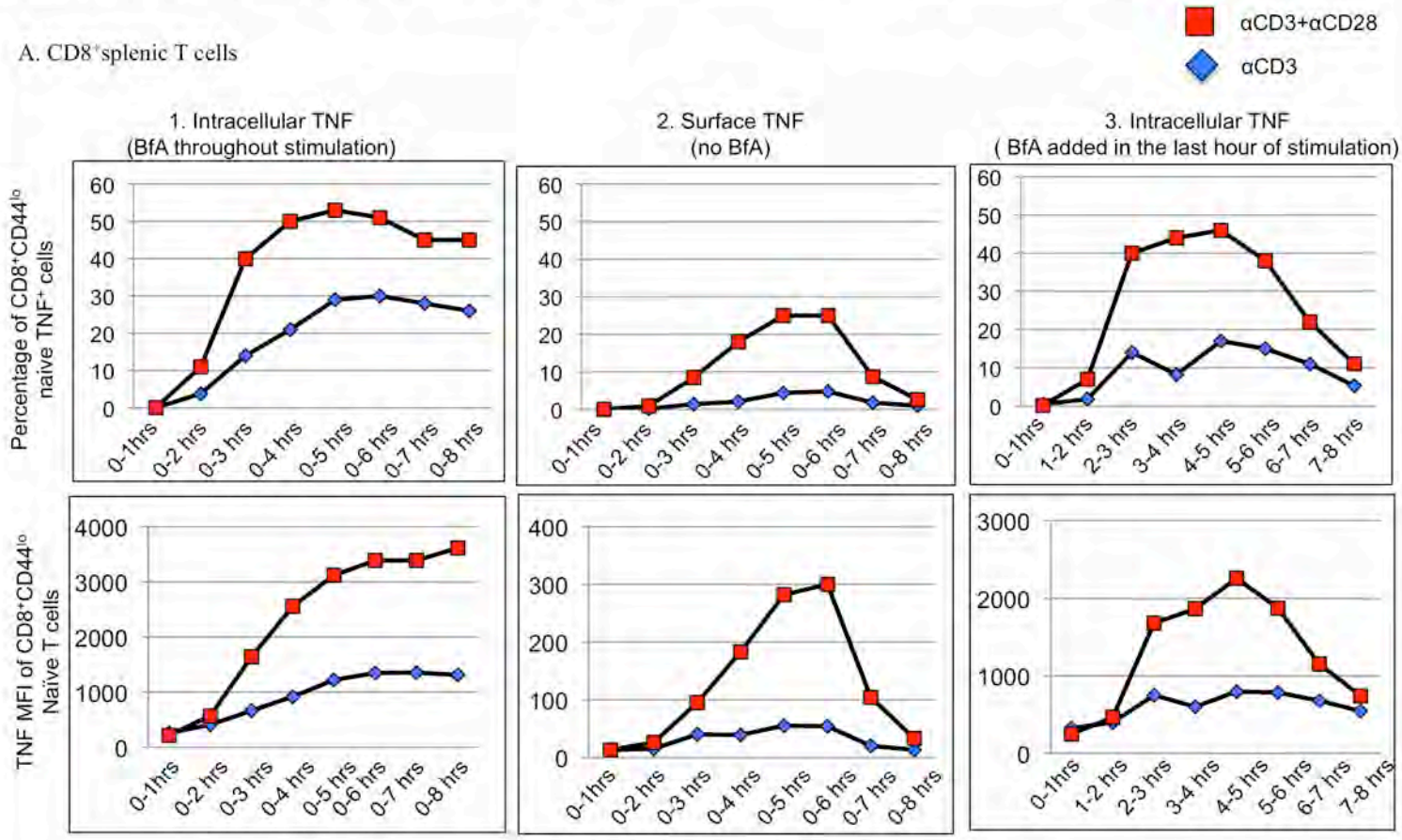

Figure 3.4 (Contd). Rapid and transient production of TNF by polyclonal naïve ($CD44^{lo}$) $CD8^+$ and $CD4^+$ splenic T cells

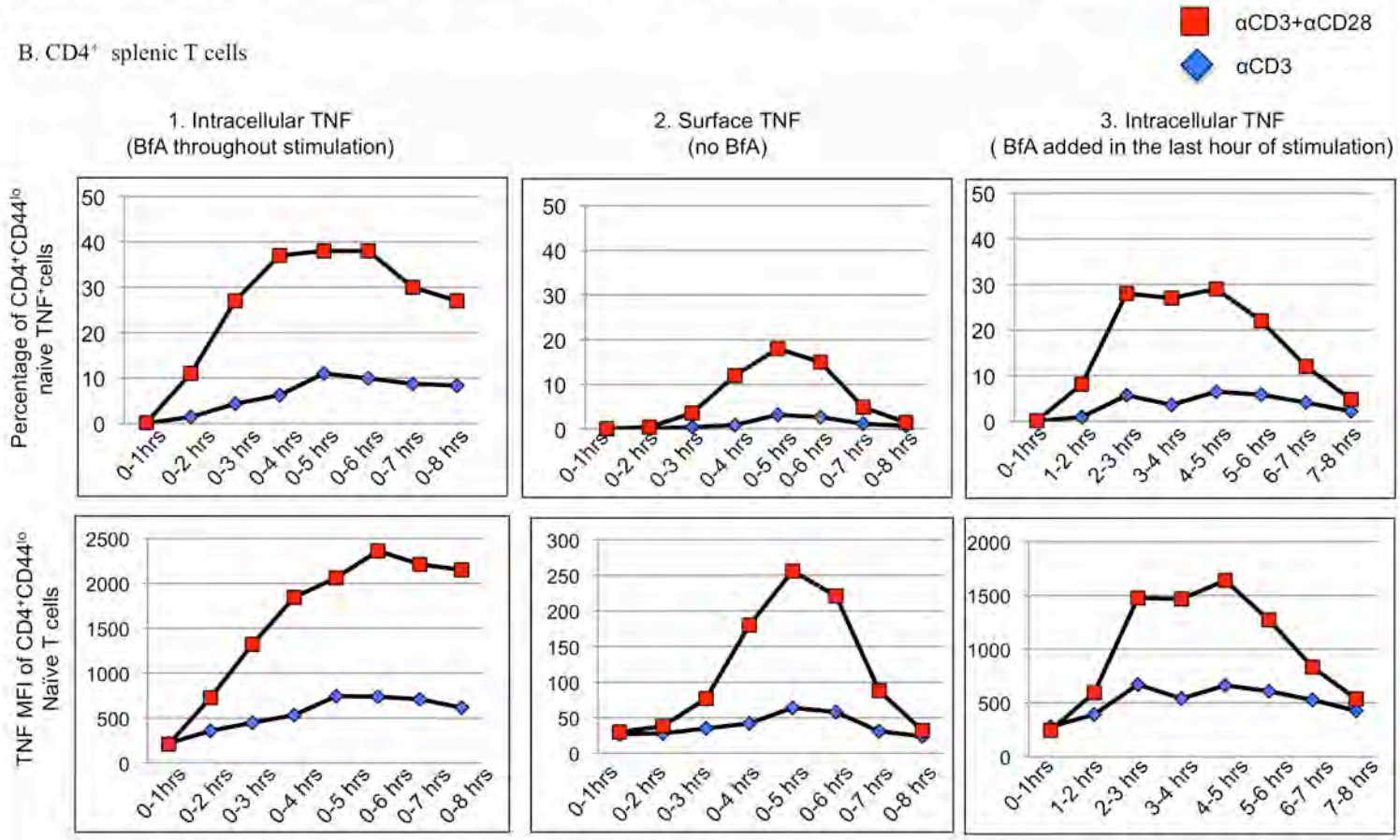

Figure 3.4. Rapid and transient production of TNF by polyclonal naïve ($CD44^{lo}$) $CD8^+$ and $CD4^+$ splenic T cells.

Splenocytes from naïve C57BL6 mice were stimulated in vitro as indicated for 4 hours in the presence or absence of bfA (Golgi Plug™ 0.1μg/ml). To assess the total production of TNF cytokine during 8 hours of stimulation, bfA was included for the entire length of the stimulation (graphs in the first column). To assess the production of TNF on the surface, bfA was not included in the culture period (graphs in the middle column), and finally to assess the kinetics of TNF production on an hourly basis, bfA was added in the last hour of each incubation period (graphs in the far right column). For example, if the cells were stimulated for 4 hours, bfA was added at the end of the 3rd hour so that the production of TNF between 3rd and the 4th hour (last hour of stimulation) could be determined. Panel A and Panel B show the percentages by naïve $CD44^{lo}$ splenic $CD8^+$ and $CD4^+$ T cells producing TNF at different time points and their respective MFI at each of the time point analyzed respectively.

E. Polyclonal CD8$^+$ and CD4$^+$ single positive (SP) thymocytes exhibit a poor ability to produce TNF relative to their secondary lymphoid counterparts

Naïve CD4$^+$ and CD8$^+$ T lymphocytes (CD44^{lo}) from secondary lymphoid organs rapidly and transiently produce TNF after TCR engagement and before gaining other effector functions. However, it is not known at what stage of development T cells acquire the ability to produce TNF. To determine this, thymocytes, and splenocytes from naïve non-transgenic B6 mice were stimulated using monoclonal antibodies to CD3 (αCD3) and antibodies to CD28 (αCD28; co-stimulation) for 4 hrs *in vitro*, respectively. Fig 3.5A and Fig 3.5C show that a significantly lower proportion of CD4$^+$ CD8$^-$ and CD4$^-$ CD8$^+$ single positive (SP) thymocytes produced TNF when compared to naïve (CD44^{lo}) splenic T cells during TCR stimulation. Addition of αCD28 co-stimulation did not further enhance the ability of thymocytes to produce TNF. PMA and ionomycin was used as a positive control for bypassing the effects of TCR activation. CD4$^+$ SP thymocytes appeared more responsive to PMA and ionomycin but there was still a reduced frequency of CD4$^+$ SP thymocytes to produce TNF upon activation. Fig 3.5B and D are summaries of 12 independent experiments showing the differences in the percentages of thymocytes producing TNF when compared to naïve T cells in the spleen.

Figure 3.5. Polyclonal CD8+ and CD4+ single positive (SP) thymocytes exhibit a poor ability to produce TNF relative to their counterparts in secondary lymphoid organs upon αCD3+αCD28 stimulation.

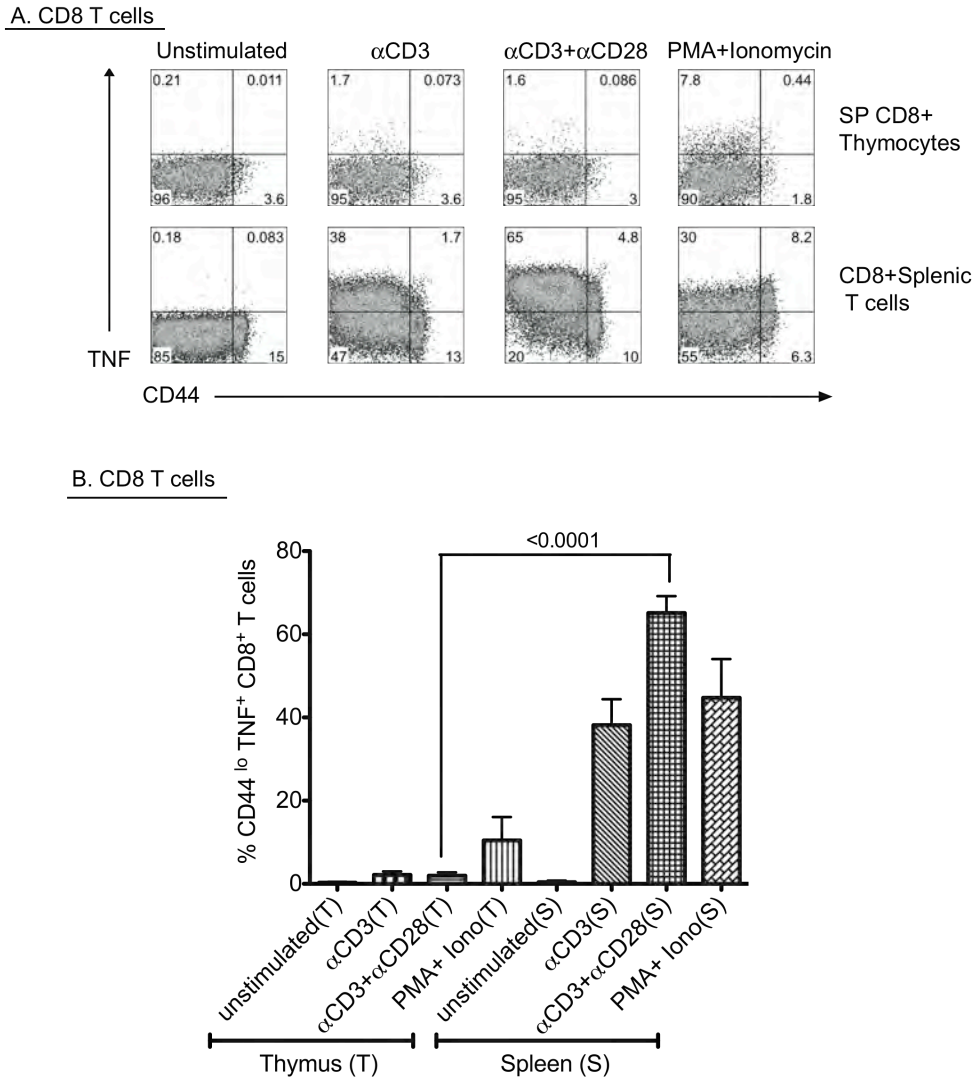

Figure 3.5. (Contd) Polyclonal CD8+ and CD4+ single positive (SP) thymocytes exhibit a poor ability to produce TNF relative to their counterparts in secondary lymphoid organs upon αCD3+αCD28 stimulation.

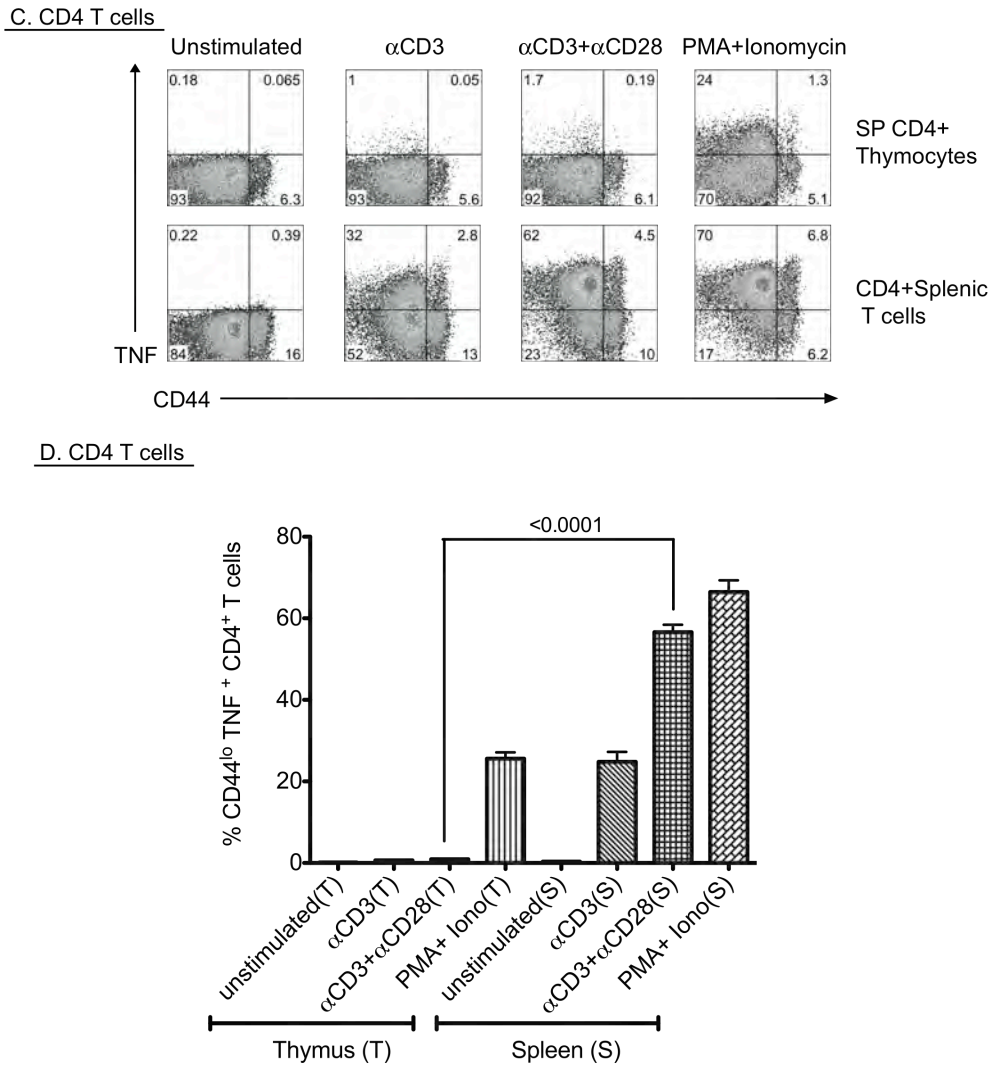

Figure 3.5. Polyclonal $CD8^+$ and $CD4^+$ single positive (SP) thymocytes have a poor ability to produce TNF relative to their secondary lymphoid counterparts upon αCD3 + αCD28 stimulation.

Thymocytes and splenocytes were stimulated with αCD3 (250ng/ml) in the absence or the presence of αCD28 (2.5μg/ml) as indicated. PMA (0.5μg/ml) and Ionomycin (0.5μg/ml) were used as a positive control to bypass a TCR requirement, as described in Materials and Methods. Panel A and C show the percentages of $CD8^+$ SP and $CD4^+$ SP thymocytes producing TNF with respect to their CD44 expression in the 2 subsets. Panel B and D shows comparison of the percentages of naïve ($CD44^{lo}$) $CD8^+$ SP and $CD4^+$ SP thymocytes producing TNF relative to their splenic counterparts from a pool of 12 experiments. The values were analyzed by one-way ANOVA with a Tukey post-test. The p value $<0.0001^{***}$ between the groups compared. The error bars indicate SD.

F. Varying the concentrations of either soluble or plate-bound αCD3 does not enhance the ability of polyclonal SP thymocytes to produce TNF.

I next hypothesized that increasing the concentration of αCD3 or offering a stronger signal to thymocytes with plate-bound αCD3 antibody will enable SP thymocytes to produce TNF. In order to address this question, I stimulated thymocytes with varying concentrations of either soluble αCD3 or plate-bound αCD3 in the presence or absence of αCD28. I found that varying the concentrations of αCD3 (soluble or plate-bound) enabled neither $CD8^+$ SP thymocytes nor $CD4^+$ SP thymocytes to produce TNF (Fig 3.6A and B) respectively. The overall TNF response in T cells from the plate-bound αCD3 was slightly reduced compared to the soluble antibody stimulated T cells. Nonetheless, splenic $CD8^+$ and $CD4^+$ naive T cells still responded, whereas the $CD8^+$ and $CD4^+$ SP thymocytes did not. Together, these results indicate that increasing the TCR signal strength did not overcome the inability of thymocytes to produce TNF.

Figure 3.6: Varying either the concentrations of soluble or plate-bound αCD3 antibody does not promote the ability of $CD8^+$ and $CD4^+$ SP thymocyte for TNF production to the levels of naïve splenic T cells.

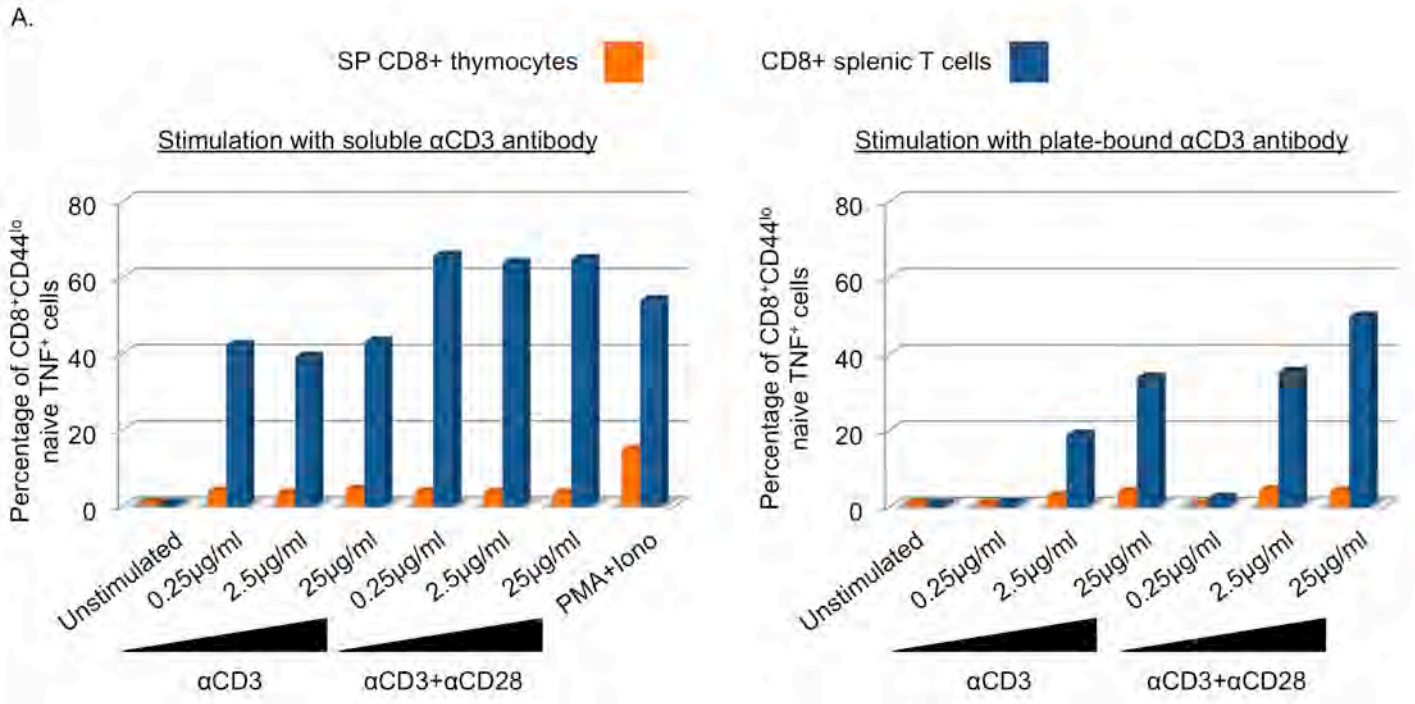

Figure 3.6: (Contd) Varying either the concentrations of soluble or plate-bound αCD3 antibody does not promote the ability of $CD8^+$ and $CD4^+$ SP thymocyte for TNF production to the levels of naïve splenic T cells.

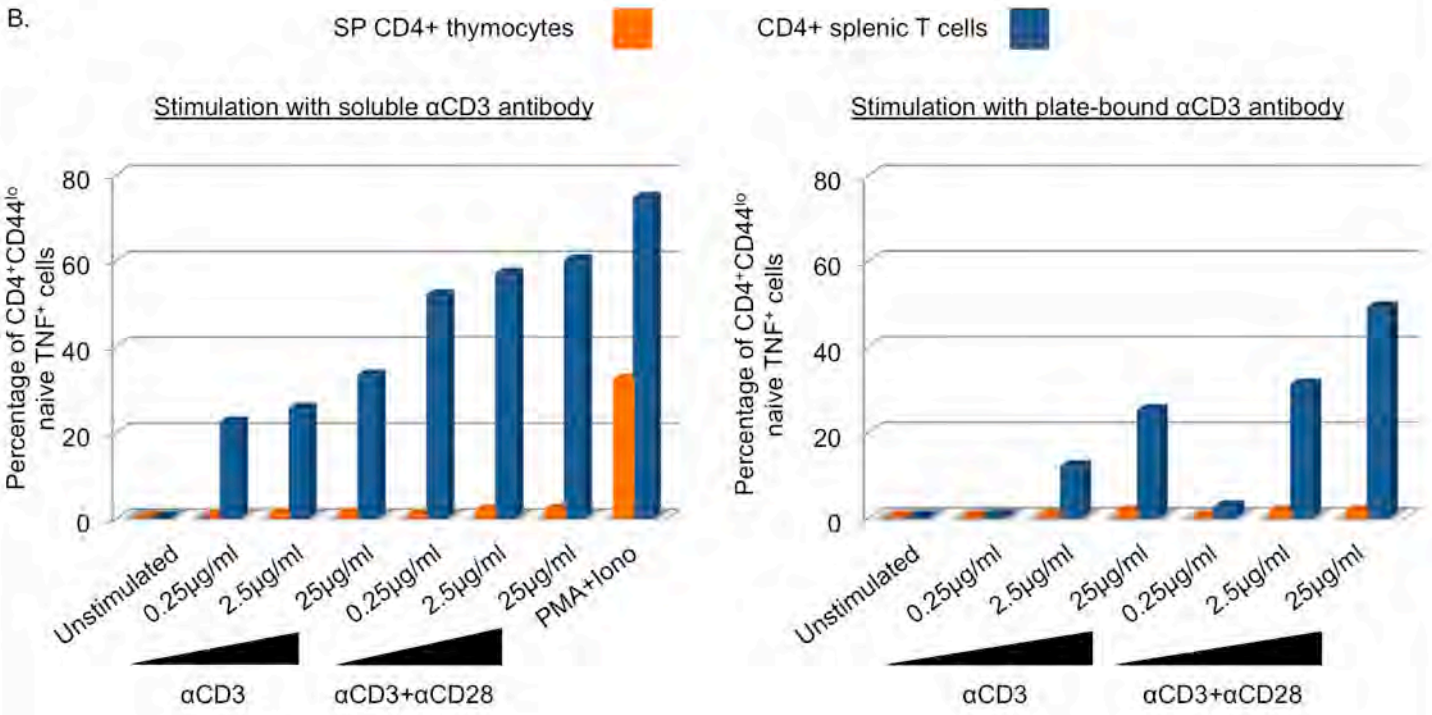

Figure 3.6. Varying either the concentrations of soluble or plate-bound αCD3 antibody does not promote the ability of SP thymocytes to produce TNF to the levels of naïve splenic T cells.

Thymocytes and splenocytes from B6 mice were stimulated with varying concentrations of soluble αCD3 antibody or along with αCD28 as indicated for 4 hours in vitro as described in Materials and Methods. In case of plate-bound αCD3 stimulations, a 96 well plate was coated with varying concentrations of αCD3 suspended in IX PBS overnight at 4 ℃. The following day, the PBS was decanted and soluble αCD28 antibody was added to the required wells before seeding the cells for stimulation. Panel A shows the percentages of $CD8^+$ SP thymocytes (orange bars) producing TNF after stimulation in comparison with $CD8^+$ ($CD44^{lo}$) splenic T cells (blue bars) with either soluble or plate bound antibody stimulation. Panel B shows the percentages of $CD4^+$ SP thymocytes (orange bars) and $CD4^+$($CD44^{lo}$) splenic T cells (blue bars) producing TNF.

G. Polyclonal SP thymocytes exhibit a lower activation profile compared to their splenic counterparts

In order to determine if the poor ability of SP thymocytes to produce TNF may be due to a defect in their activation, I examined the phenotypic changes in their activation profile. While both $CD8^+$ and $CD4^+$ SP thymocytes showed up-regulation of CD25 and CD69 and a down-regulation of CD62L following stimulation, these changes were reduced compared to the splenic T cells (Fig 3.7). Together these results indicate that the defect in the ability of polyclonal thymocytes to produce TNF in response to αCD3 + αCD28 may be partly attributed to the generalized defect in activation of polyclonal thymocytes.

Figure 3.7. Polyclonal SP thymocytes exhibit a lower activation profile relative to their splenic counterparts

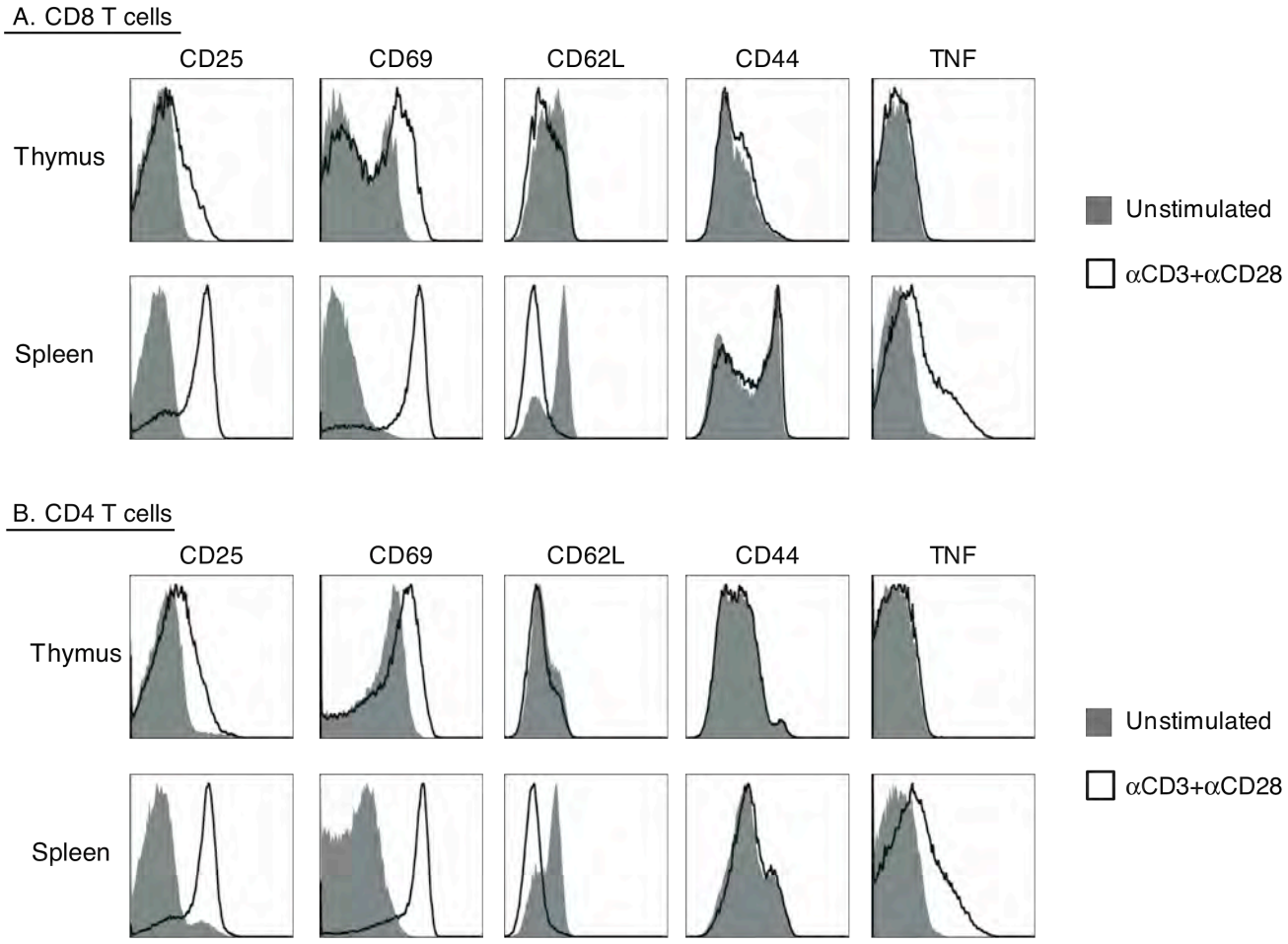

Figure 3.7. Polyclonal SP thymocytes exhibit a lower activation profile relative to their splenic counterparts.

Thymocytes and splenocytes were stimulated with αCD3+αCD28 for 4 hours in vitro. Panel A and Panel B show the differences in the surface expression of markers such as CD25, CD69, CD62L, CD44 and TNF in unstimulated (gray histograms) and stimulated (black line histograms) SP thymocytes and splenic T cells in the $CD8^+$ and $CD4^+$ subsets respectively.

H. The resting steady-state expression of TNF message is similar between polyclonal SP thymocytes and splenic naïve T cells

I next wanted to determine if the differences in TNF production between SP thymocytes and splenic T cells may be correlated with differences in the steady state levels of TNF message in these subsets. To test this, I sorted purified $CD4^+$ and $CD8^+$ SP T cells from thymi and spleens of B6 mice and analyzed the expression of TNF mRNA in unstimulated cells using RT PCR. I found that DP cells in the thymus did not express TNF message, but $CD4^+$ and $CD8^+$ SP thymocytes expressed a similar level of TNF mRNA compared to their splenic counterparts (Fig 3.8A). In order to better quantify the steady state levels of TNF message in naïve T cells, I purified $CD4^+$ and $CD8^+$ SP thymocytes and sorted for naïve $CD44^{lo}$ splenic T cells (to avoid contamination with $CD44^{hi}$ memory phenotype cells in my analysis). I performed real-time PCR to quantify the steady state levels of TNF message under unstimulated conditions. The levels of TNF message were similar between SP thymocytes and splenic naïve T cells in both $CD4^+$ and $CD8^+$ subsets (Fig 3.8B). I found that levels of TNF message were slightly higher in the $CD44^{hi}$ memory phenotype cells though the difference was not significant. Together, these results indicate that inability of polyclonal SP thymocytes to produce TNF is not due to differences in the expression of TNF message under resting steady state (unstimulated conditions).

Figure 3.8.Similar steady-state level of TNF mRNA expression in polyclonal SP thymocytes relative to splenic naive T cells under unstimulated conditions

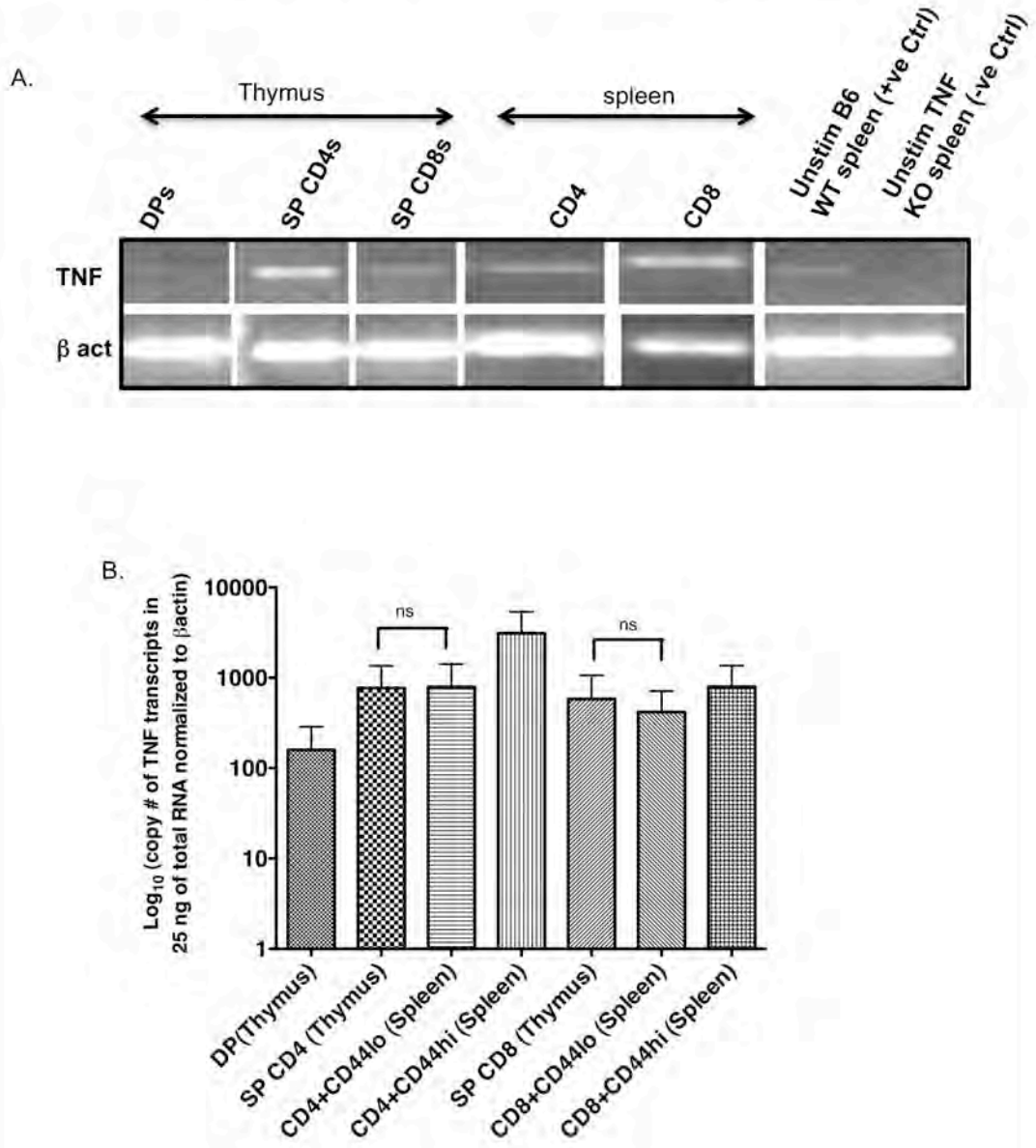

Figure 3.8. Similar steady-state levels of TNF mRNA expression in polyclonal SP thymocytes relative to splenic naive T cells under unstimulated conditions.

Panel A. $CD4^+$ $CD8^+$ DP thymocytes, $CD4^+$ SP and $CD8^+$ SP thymocytes were sorted to >90 % purity by a MoFlo cell sorter. In case of splenic T cells, $CD4^+$ and $CD8^+$ T cells were purified by MACS separation by positively selecting for $CD4^+$ and $CD8^+$ T cells containing both $CD44^{lo}$ and $CD44^{hi}$ populations. RNA was isolated and cDNA was synthesized by RT PCR. cDNA synthesized from RNA isolated from unpurified splenocytes from B6 mice that express TNF message was used as a positive control. Splenocytes from TNF-deficient (indicated as TNF KO) mice were used as a negative control. Panel B. DP thymocytes, $CD4^+$ SP and $CD8^+$SP thymocytes were sorted to >98% purity. Concomitantly, naïve $CD44^{lo}$ splenic $CD4^+$ and $CD8^+$ T cells were sorted from $CD44^{hi}$ memory phenotype cells to > 98% purity. cDNA was synthesized from total RNA isolated from all the purified subsets of cells by real-time PCR. The copy number of TNF transcripts in 25ng of total RNA normalized to β-actin in the indicated populations at steady state is shown. These data are averages of 3 independent experiments that were analyzed using One-way ANOVA with a Tukey post-test. Error bars indicate SD.

I. αCD3+αCD28 antibody mediated cross-linking of polyclonal thymocytes in the presence of secondary lymphoid cells results in a modest increase in the frequency of TNF producing polyclonal SP thymocytes.

Given the differences between SP thymocytes and splenic T cells in the ability to produce TNF, I questioned if this may be due to better stimulation of T cells in the presence of antigen presenting cells that enables T cells in the spleen to produce TNF. I hypothesized that SP thymocytes stimulated in the presence of splenocytes will be better able to produce TNF than when stimulated alone. To test this, I stimulated Ly5.1 ($CD45.1^+$) thymocytes with αCD3 and αCD3+αCD28 for 4 hours in the presence of Ly5.2 ($CD45.2^+$) B6 splenocytes. I found that there was a small increase in the percentage of SP thymocytes ($CD8^+$ and $CD4^+$) producing TNF when stimulated in the presence of splenocytes (Fig 3.9 A and C). Fig 3.9 B and D are a pool of 13 experiments showing SP thymocytes capable of producing TNF in the context of splenocytes. Together, these results suggest that although polyclonal SP thymocytes gain a partial ability to produce TNF, they are still poor producers of TNF compared to naïve splenic T cells.

Figure 3.9. Partial increase in the percentages of polyclonal SP thymocytes producing TNF when stimulated in the presence of splenocytes

A. Gated on Ly5.1 CD8 T cells

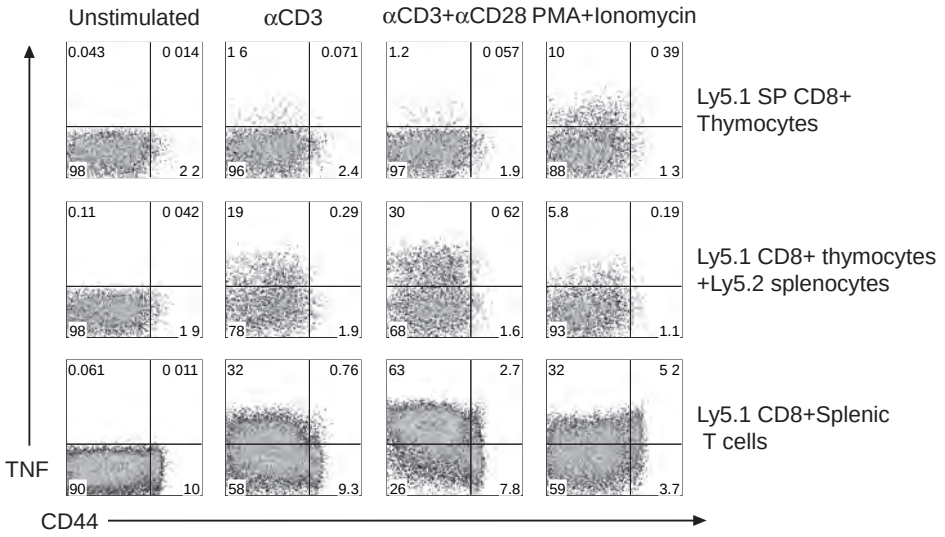

B. Gated on Ly5.1 CD8 T cells

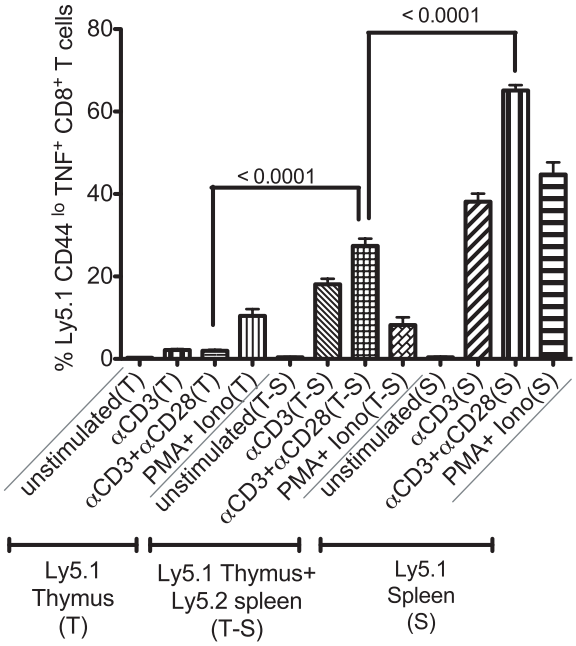

Figure 3.9. (Contd) Partial increase in the percentage of polyclonal SP thymocytes producing TNF when stimulated in the presence of splenocytes

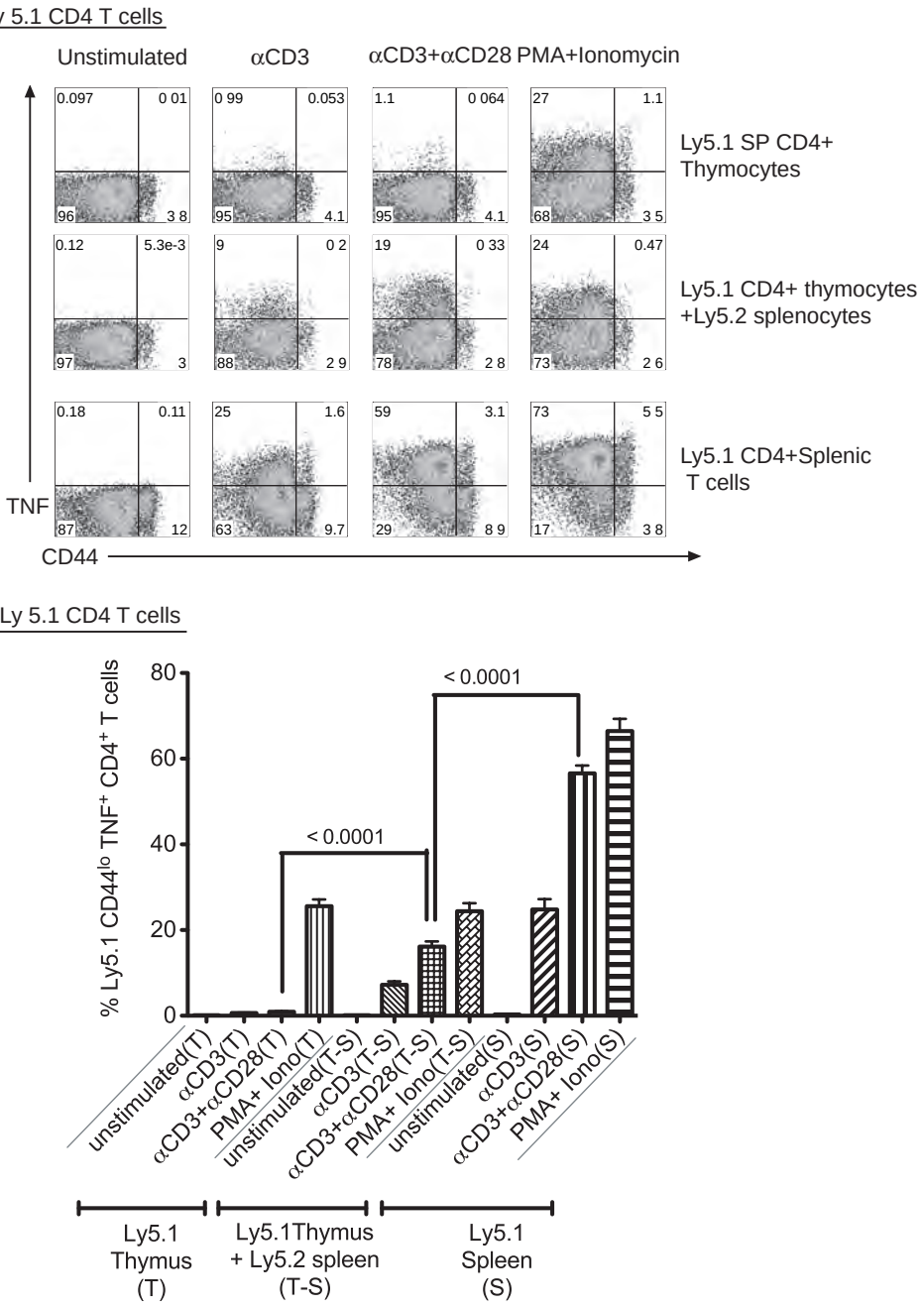

Figure 3.9. Small increase in the percentages of polyclonal SP thymocytes producing TNF stimulated in the presence of splenocytes.

*Ly5.1 ($CD45.1^+$) thymocytes were either stimulated alone or in the presence of Ly5.2 ($CD45.2^+$) splenocytes at (1:1 ratio) with indicated stimulations for 4 hours in vitro. Panel A and Panel C show the percentages of $CD4^+$ and $CD8^+$SP thymocytes (the first 2 rows) or splenic T cells (last row in each panel) producing TNF. Panel B and D shows the average percentages of ($CD4^+$ and $CD8^+$) SP thymocytes producing TNF when stimulated alone or in the presence of splenocytes. These data are a pool of 13 experiments. The values were analyzed by one-way ANOVA analysis with Tukey post-test. P value < 0.0001*** and error bars indicate SD.*

J. The effect of the cells of secondary lymphoid organs on TNF production by polyclonal SP thymocytes is dose dependent and is mediated by splenic B cells and nonB/T cells in a contact-dependent manner.

I next characterized the partial enhancement of TNF-production by thymocytes stimulated in the presence of splenocytes. To determine if the partial enhancement is dependent on cell dose, I stimulated thymocytes with varying numbers of splenocytes with αCD3 and αCD28. I found that the enhancement of TNF production by thymocytes was dependent on the number of splenocytes (Fig 3.10A and B). I further determined which cell types in the splenocyte population enabled thymocytes to produce TNF. I stimulated Ly5.1 ($CD45.1^+$) thymocytes in the presence of purified Ly5.2 ($CD45.2^+$) splenic B cells and T cells and non-lymphocyte populations in the flow-through that contains B220+ and CD11c+ cells. I found that splenic B cells and the cells in the flow-through enabled the modest increase in the percentages of thymocytes producing TNF (Fig 3.11). I next tested if the increase in TNF production by thymocytes enabled by splenic B cells and nonB/T cells in the flow-through was mediated by cell contact or by a soluble factor. To do this, I performed a transwell assay. Briefly, the top-wells were seeded with thymocytes and the bottom wells with thymocytes and splenocytes stimulated with αCD3 and αCD28 (Fig 3.12). I found that thymocytes in the top well did not produce TNF, whereas cells stimulated in the presence of splenocytes in the bottom well produced TNF (Fig 3.12). Together, these results indicate that contact with the cells of secondary lymphoid organs enables SP thymocytes to partially produce TNF.

Figure 3.10. The effect of splenocytes on TNF producing capability of polyclonal SP thymocytes during αCD3+αCD28 stimulation is dose-dependent.

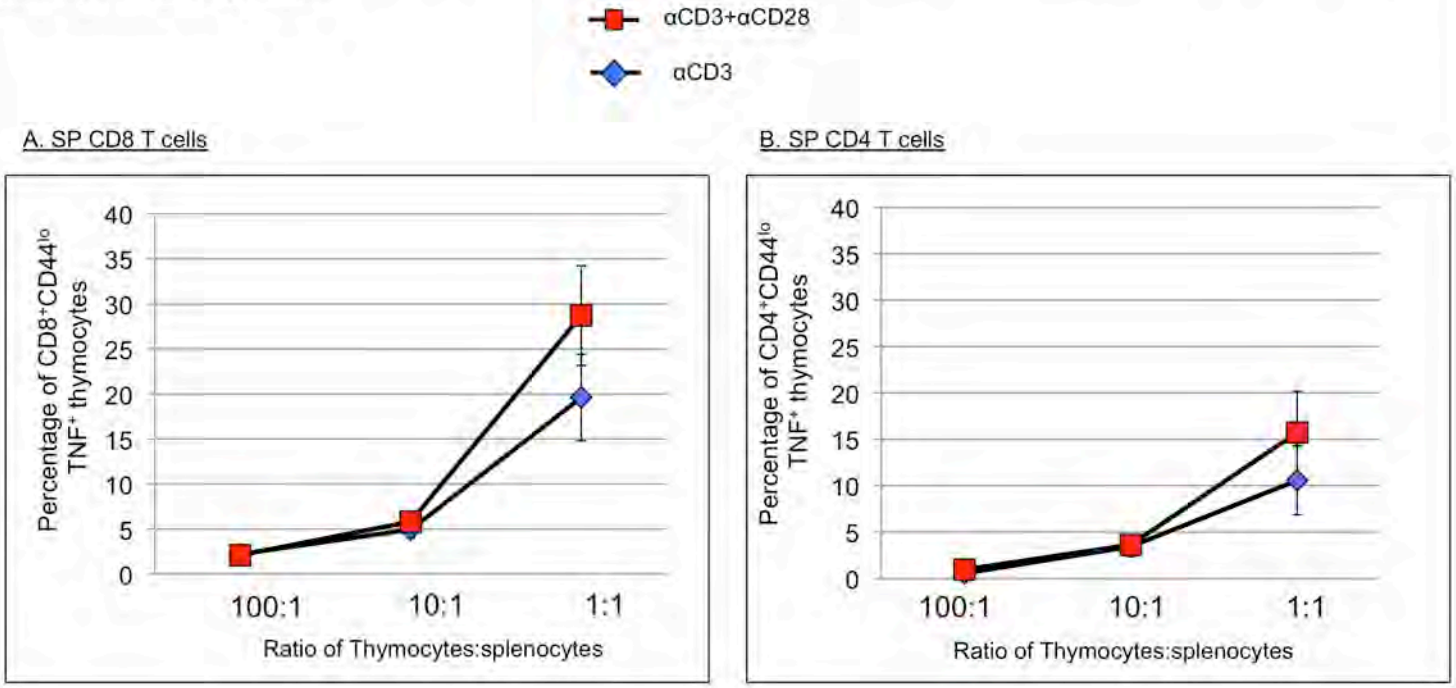

Figure 3.10. The effect of splenocytes on TNF producing ability of polyclonal SP thymocytes during αCD3+αCD28 is dose-dependent.

2×10^6 Ly5.1 (CD45.1) thymocytes were stimulated as indicated in the presence of 2×10^6 Ly5.2 (CD45.2) splenocytes (1:1) and stimulated as indicated. Additionally, thymocytes were also stimulated with decreasing ratios of splenocytes at 2×10^5 (10:1) and 2×10^4 (100:1) cells respectively. Panel A shows the percentages of SP $CD8^+$ thymocytes and Panel B shows the percentages of SP CD4+ thymocytes producing TNF. The values are averages of 3 experiments. Error bars indicate SD.

Figure 3.11. Resting splenic B cells and non B/T cell population of cells containing CD11C+ cells are required for the modest increase in the proportion of polyclonal SP thymocytes producing TNF during αCD3+ αCD28 stimulation.

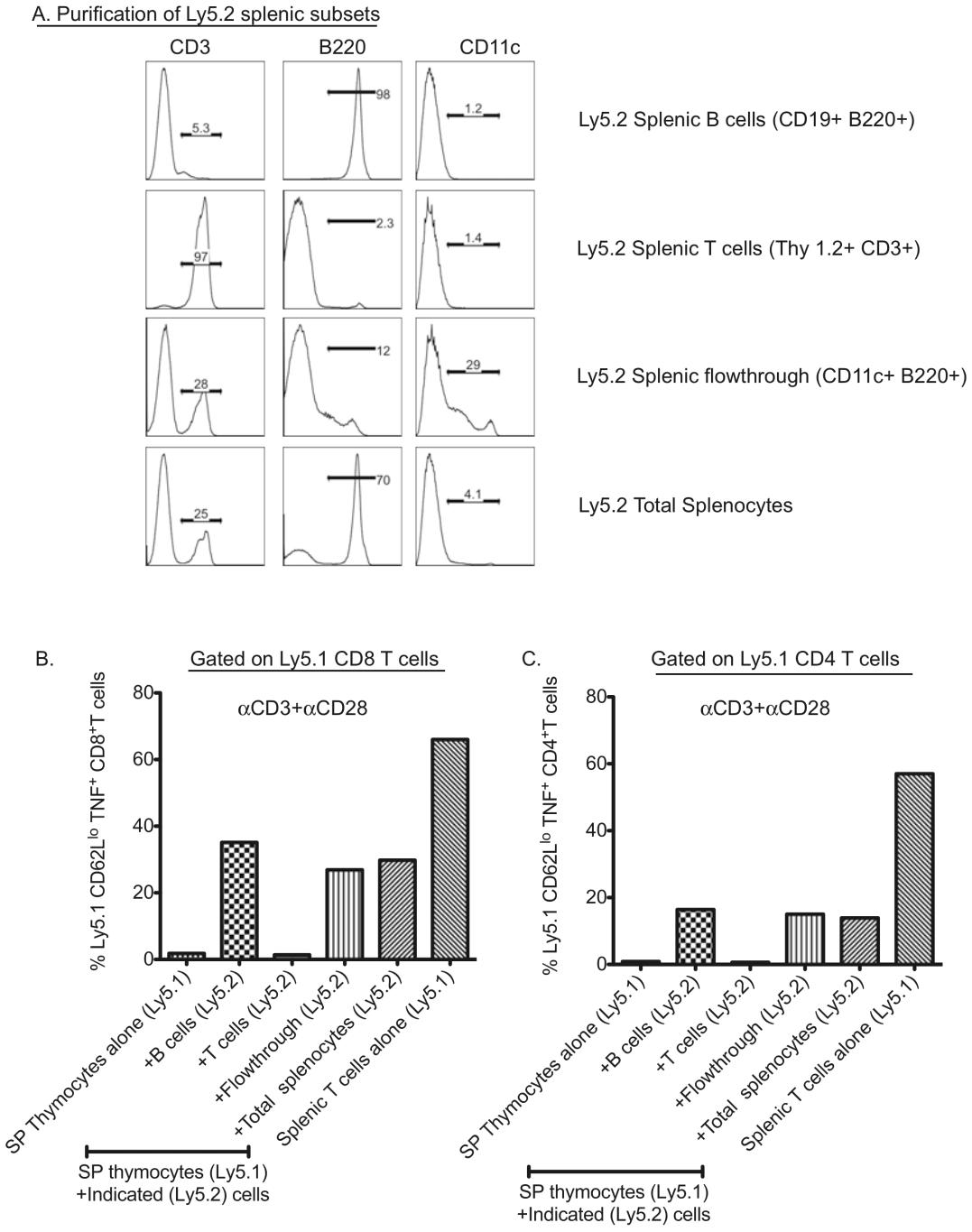

Figure 3.11. Resting splenic B cells and non-B and T cell subsets that contain CD11c+ cells are responsible for the modest increase in TNF production by SP thymocytes.

Panel A, Ly5.2 ($CD45.2^+$) splenocytes were dissected into purified splenic B cells ($CD19^+B220^+$), purified T cells ($Thy1.2^+CD3^+$) and non-B and T cells ($CD11c^+$ cells in the flowthrough during purification). The cells were >96% pure in B and T cell subsets. Ly5.1 ($CD45.1^+$) thymocytes were stimulated alone or with indicated purified populations of splenocytes or with control total splenocytes for 4 hours in vitro. Panel B and C, the percentages of $CD62L^{lo}$ activated SP thymocytes (both $CD8^+$ and $CD4^+$) producing TNF in the context of the indicated cell populations are shown.

Figure 3.12. Polyclonal SP thymocytes (Ly5.1) stimulated in the presence of splenocytes (Ly5.2) acquire a modest ability to produce TNF in a contact-dependent manner

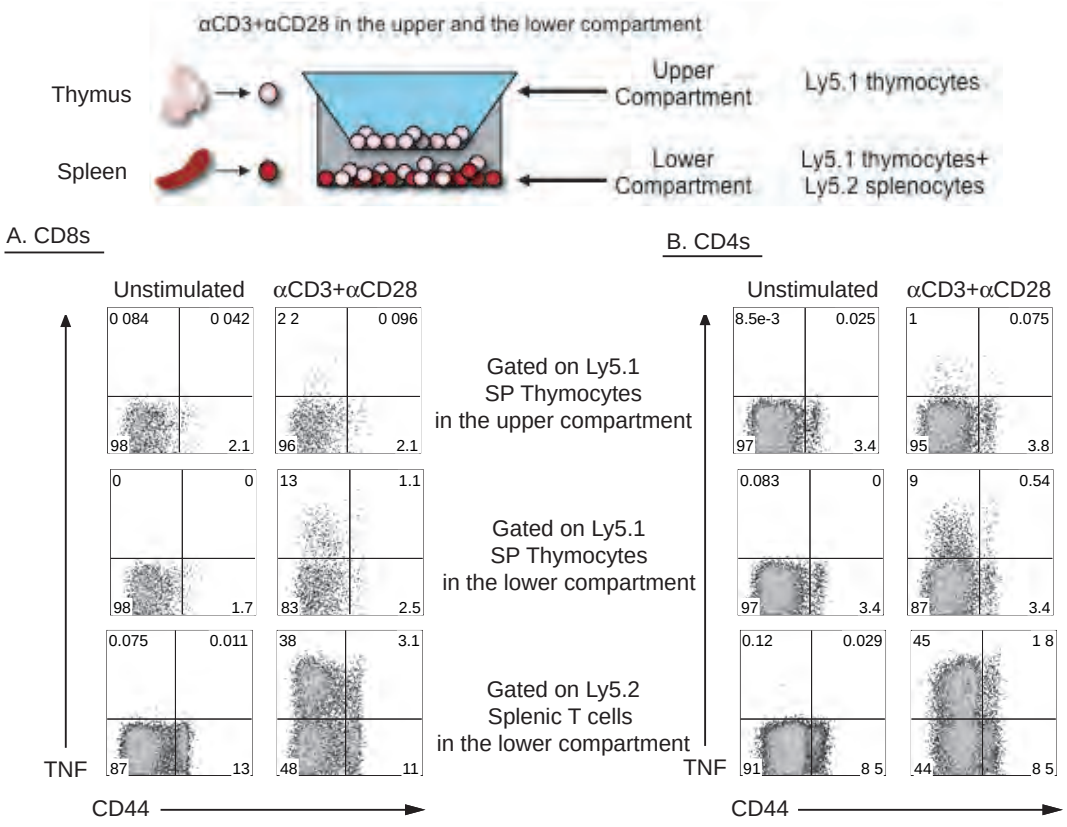

Figure 3.12. Polyclonal SP thymocytes stimulated in the presence of splenocytes acquire a modest ability to produce TNF in a contact-dependent manner.

10×10^6 Ly5.1 ($CD45.1^+$) thymocytes were seeded into the upper compartment of 6 welled transwell plate followed by the lower compartment that was seeded with 5×10^6 Ly5.1 ($CD45.1^+$) thymocytes along with 5×10^6 ($CD45.2^+$) splenocytes. Both the compartments were stimulated as indicated. Following stimulations, cells were aliquoted into smaller 96 well plates for intracellular staining for TNF. Panel A and Panel B show the percentages of TNF producing $CD8^+$ and $CD4^+$ SP thymocytes in the upper and the lower compartment in the transwell (First 2 rows). The bottom row shows the percentages of TNF producing control Ly5.2 ($CD45.2^+$) splenic T cells in Panel A and Panel B.

K. Polyclonal splenic T cells require the presence of accessory cells from the spleen to produce TNF during αCD3+αCD28 stimulation.

To determine if stimulation in the presence of cells of the secondary lymphoid organs for optimal TNF production is an absolute necessity for naïve splenic polyclonal T cells to produce TNF or if it is a requirement solely of SP polyclonal thymocytes, I purified polyclonal splenic naïve T cells ($CD8^+$ and $CD4^+$) and stimulated them either alone or in the presence of cells other the spleen such as the thymus. Additionally, I also stimulated purified splenic T cells with the cells of spleen that were left in the flowthrough. I observed that during αCD3+αCD28 stimulation, the TNF producing ability of purified splenic T cells was reduced in the absence of splenocytes (APCs) [orange bars] or when splenic T cells were stimulated in an environment other than the splenic environment (the presence of thymocytes) [Green bars]. Stimulation of splenocytes containing splenic B cells and APCs restored the TNF producing capability of splenic T cells (Fig 3.13). Purified splenic T cells however still retained the ability to produce TNF during PMA and ionomycin stimulation that bypasses the TCR activation. Together, these results indicated a requirement of splenic environment to enable SP thymocytes as well as naïve splenic T cells to be able to produce TNF during TCR activation.

Figure 3.13. Polyclonal splenic T cells require contact with cells of secondary lymphoid organs for optimal TNF production during αCD3+αCD28 stimulation.

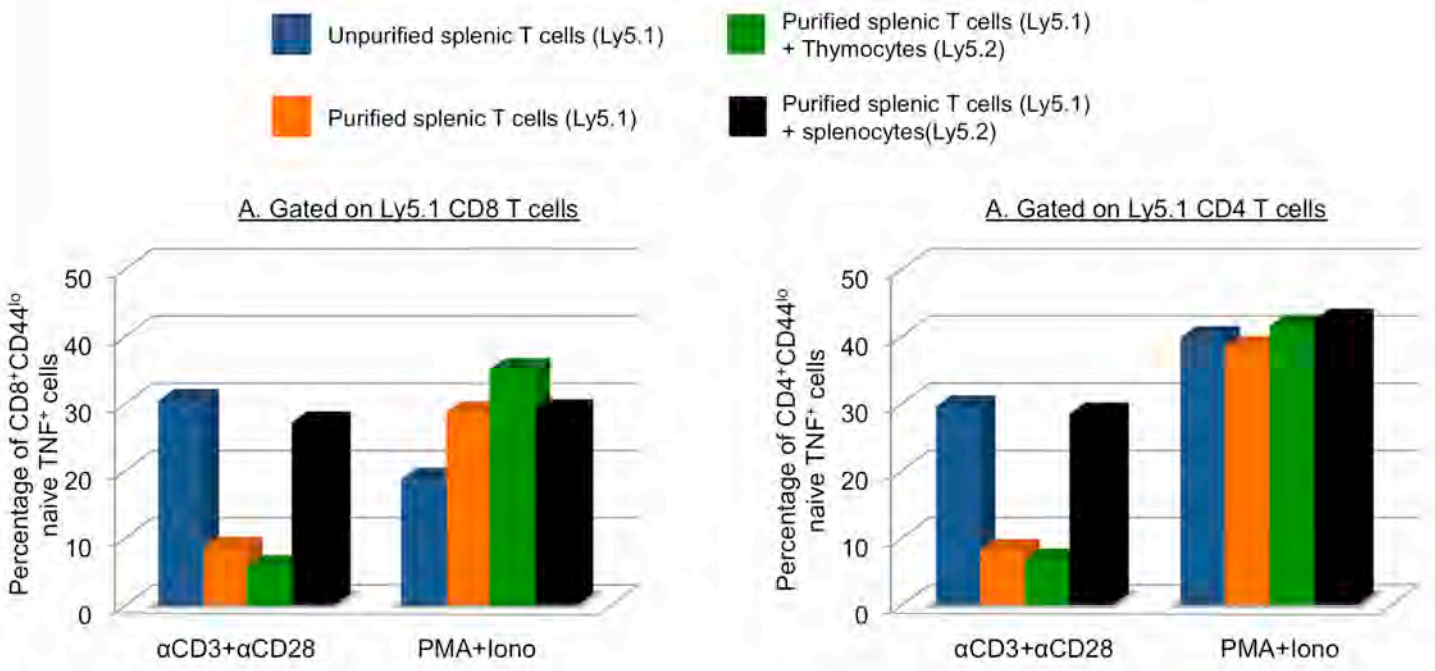

Figure 3.13. Polyclonal splenic T cells require contact with cells of secondary lymphoid organs for optimal TNF production during αCD3+αCD28 stimulation .

Ly5.1 (CD45.1$^+$) unpurified splenocytes (blue bars) and Ly5.1 (CD45.1$^+$) splenic T cells (orange bars) that were purified using Thy1.2 miltenyi microbeads (93% purity) were stimulated with αCD3+αCD28 or with PMA and ionomycin as described in Materials and Methods. Additionally purified splenic T cells were stimulated either in the presence of Ly5.2 (CD45.2$^+$) thymocytes (green bars) or Ly5.2 (CD45.2$^+$) total splenocytes (black bars). Panel A and panel B show the percentages of Ly5.1 (CD45.1$^+$) naïve (CD44^{lo}) CD8$^+$ and CD4$^+$ splenic T cells producing TNF after 4 hours of stimulation in vitro.

L. Blockade of Fc receptors on splenocytes abrogates the TNF producing ability of polyclonal SP thymocytes during TCR stimulation.

Given that thymocytes require cell contact with splenocytes to produce TNF upon αCD3+αCD28 stimulation, I wanted to determine the nature of the signal (constitutive or induced during activation) that is required to augment TCR activation. I used two approaches to address this question. Thymocytes were stimulated in the presence of splenocytes treated with either actinomycin D (that blocks new transcription) or paraformaldehyde (cytofix). I found that the ability of the thymocytes stimulated with actinomycin D-treated splenocytes to produce TNF was diminished slightly (Fig 3.14A), suggesting that there is not an absolute requirement for the induction of surface molecules on splenocytes to augment TNF production by SP thymocytes. Next, I questioned if any cell-surface molecule on splenocytes could be involved in the enhancement of TNF production by thymocytes. To test this, I treated splenocytes with cytofix solution containing 4% paraformaldehye that crosslinks proteins on the surface of splenocytes. I then stimulated thymocytes with αCD3+αCD28 antibodies along with cytofix-treated splenocytes. Thymocytes showed a marked reduction in TNF production when stimulated with cytofix treated splenocytes, suggesting a potential role for a surface molecule which may be affected by paraformaldehye treatment, in the enhancing the ability of thymocytes to produce TNF stimulated in the context of splenocytes (Fig 3.14 B).

Given the above observation, I hypothesized that surface Fc receptors expressed on splenic B cells and APCs may be responsible for better cross-linking of the αCD3 and αCD28 antibodies, thereby providing a stronger TCR signal to the thymocytes. To determine this, I first pretreated splenocytes with a Fc-blocking antibody for 10 min at various dilutions (Fig 3.14 C and D) and then stimulated thymocytes with αCD3 and αCD28 antibodies in the presence of the Fc-blocked splenocytes. I found that use of Fc receptor-blocked splenocytes completely abrogated the production of TNF by SP thymocytes ($CD8^+$ and $CD4^+$) (Fig 3.15C). This suggests two possible mechanisms for the splenocyte-mediated stimulation of SP polyclonal thymocytes for TNF production. One is that the presence of Fc receptors resulted in better cross-linking of αCD3 and αCD28 antibodies. The second is that the interaction of the αCD3 and αCD28 antibodies with the Fc receptors may bring cells in close proximity, thus resulting in optimal clustering of accessory molecules that may enhance TNF production by thymocytes.

Figure 3.14. Evaluation of various parameters involved in the splenocyte-mediated enhancement of TNF production by polyclonal SP thymocytes during αCD3+αCD28 stimulation

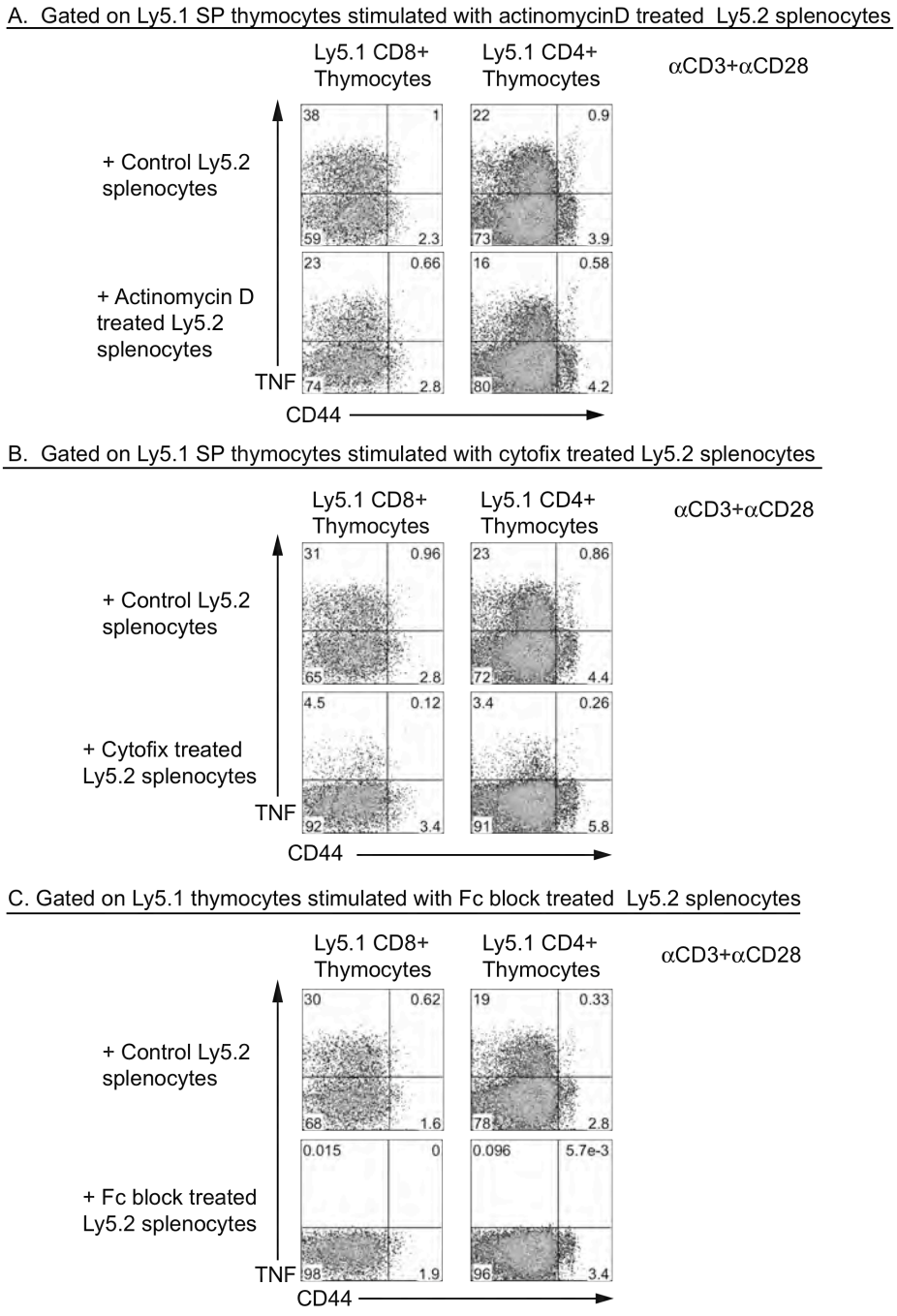

D.

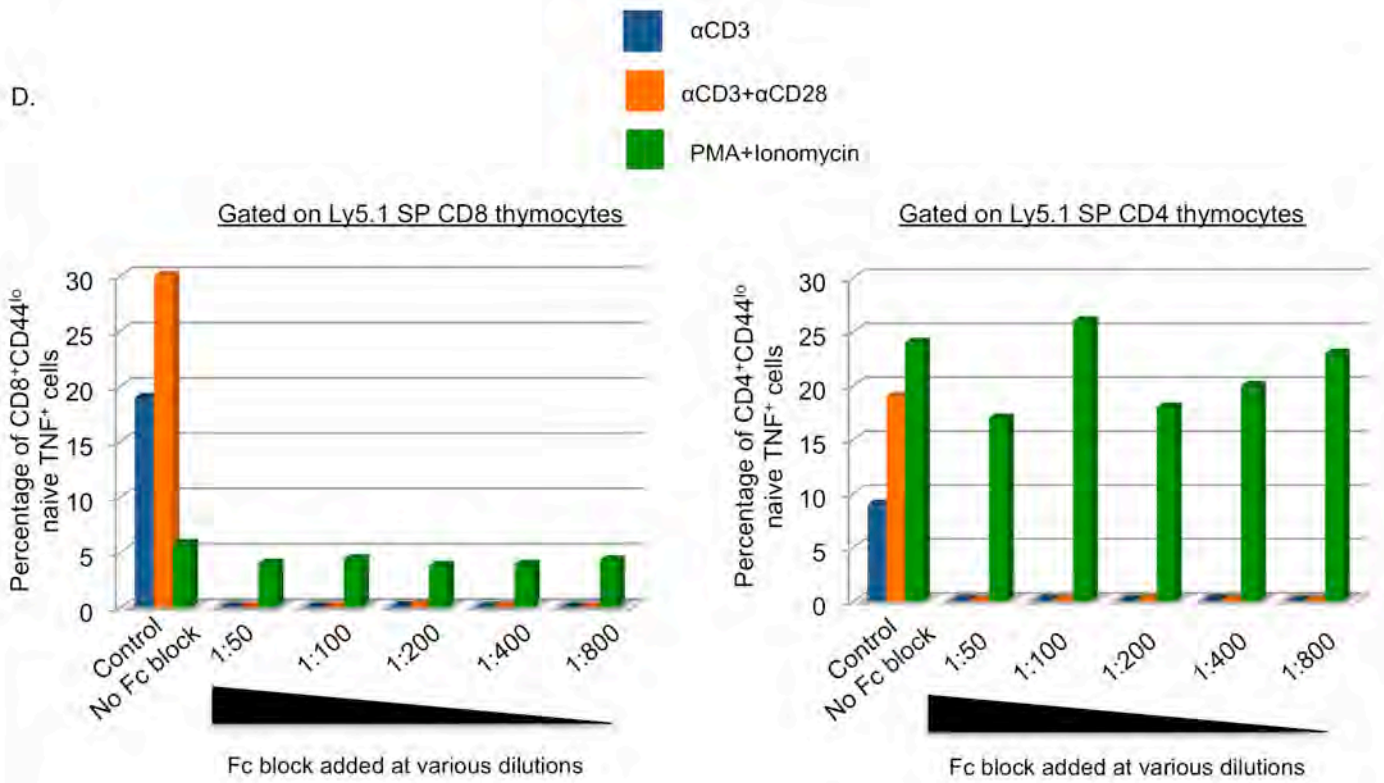
αCD3
αCD3+αCD28
PMA+Ionomycin
Gated on Ly5.1 SP CD8 thymocytes
Percentage of CD8+CD44lo naive TNF+ cells
30
25
20
15
10
5
0
Control
No Fc block
1:50
1:100
1:200
1:400
1:800
Fc block added at various dilutions
Gated on Ly5.1 SP CD4 thymocytes
Percentage of CD4+CD44lo naive TNF+ cells
30
25
20
15
10
5
0
Control
No Fc block
1:50
1:100
1:200
1:400
1:800
Fc block added at various dilutions

Figure 3.14. Evaluation of various parameters involved in splenocytes mediated enhancement of TNF production by polyclonal SP thymocytes during αCD3+αCD28 stimulation.

Panel A, Ly5.1 ($CD45.1^+$) thymocytes were stimulated along with either control Ly5.2 ($CD45.2^+$) splenocytes or splenocytes that were pretreated with actinomycinD (20μg/ml) for 1 hour at 37℃. Panel B, Ly5.1 ($CD45.1^+$) thymocytes were stimulated along with either control Ly5.2 (CD45.2) splenocytes or splenocytes that were pretreated with cytofix (1 ml) for 5-10 min at 4℃. Panel C, Ly5.1 ($CD45.1^+$) thymocytes were stimulated along with either control Ly5.2 ($CD45.2^+$) splenocytes or splenocytes that were pretreated with Fc block (2.5μg/ml) for 20 min at 37℃. The percentages of naïve $CD44^{lo}$ ($CD8^+$ and $CD4^+$) SP thymocytes producing TNF when stimulated with splenocytes from all the treatment are shown. Panel D. shows the percentages of TNF producing thymocytes stimulated with splenocytes that were pretreated with Fc block at varying dilutions as indicated.

M. Preconditioning of polyclonal thymocytes with splenic APCs prior to activation does not enhance their ability to produce TNF.

Naïve T cells in the periphery are known to require a low level of TCR-self MHC interactions to respond optimally upon antigen encounter (356). I hypothesized that pre-conditioning of polyclonal thymocytes with splenocytes may enhance their ability to produce TNF upon stimulation with αCD3+αCD28 stimulation. Ly5.1 ($CD45.1^+$) thymocytes were incubated with Ly5.2 ($CD45.2^+$) B6 splenocytes for 3 and 6 hours before stimulating them with αCD3 and αCD28. Pre-incubation did not enhance the ability of thymocytes to produce TNF when compared to thymocytes stimulated with splenocytes without any pre-conditioning (Fig 3.16). This suggests that prior interactions with splenic cells, is not sufficient for thymocytes to increase their ability to produce TNF during stimulation.

Figure 3.15. Preincubation of polyclonal SP thymocytes with splenocytes for 6 hours prior to stimulation does not enhance their ability for optimal TNF production.

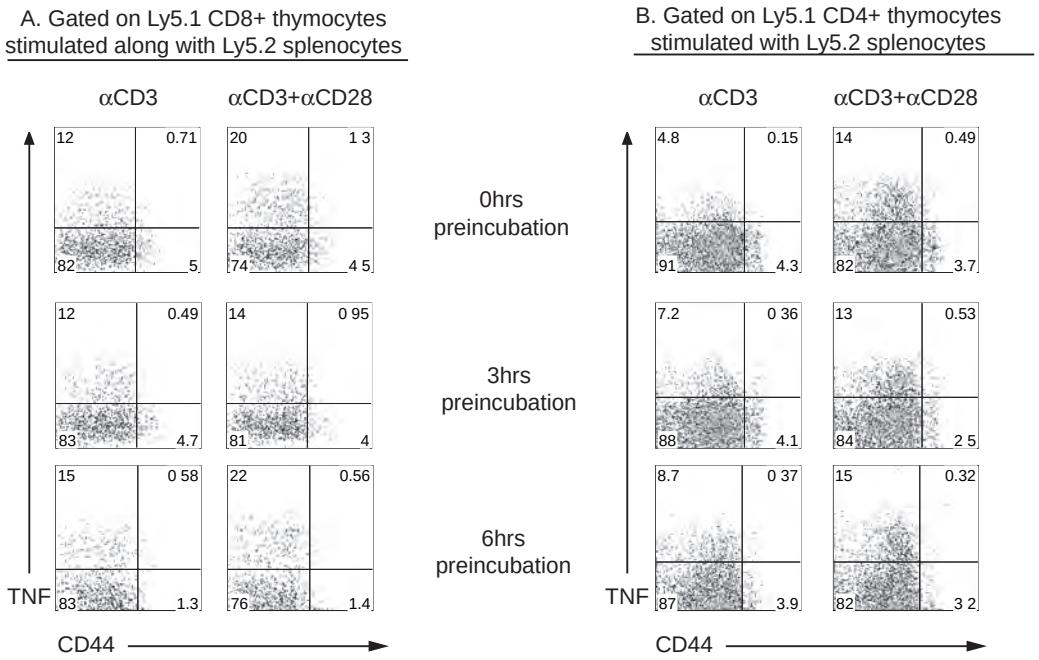

Figure 3.15. Pre-conditioning of polyclonal SP thymocytes with splenocytes does not enhance their TNF producing capability in vitro.

Ly5.1 ($CD45.1^+$) thymocytes were pre-incubated with Ly5.2 ($CD45.2^+$) splenocytes for 3 hours or 6 hours before they were stimulated with $\alpha CD3+\alpha CD28$ for another 4 hours. Cells that were immediately stimulated for 4 hours were used as a control (0 hours pre-incubation). Panel A and Panel B show the percentages of SP thymocytes ($CD8^+$ and $CD4^+$) producing TNF.

Interim Summary

In sections A and B, I studied the immunoregulatory role of T cell-derived TNF in limiting the magnitude of antigen-specific T cell responses during a viral infection. Given this and the ability of naïve T cells to produce TNF early during activation, I speculate the effect of T cell-derived TNF on T cells may be occurring early during activation, such that in the absence of TNF, there may be altered T cell programming resulting in higher accumulation at the peak of the immune response. I next sought to determine at what stage of development naïve T cells become competent to produce TNF.

In sections C-M in this chapter, I studied the differential ability of TNF production by polyclonal SP thymocytes relative to their splenic counterparts in response to a general αCD3+αCD28 antibody mediated TCR stimulation. One disadvantage of polyclonal SP thymocytes is that they express a diverse array of TCR with varying affinities and many respond differently to TCR activation (section G; Fig 3.7). In addition, polyclonal thymocytes and splenic T cells require splenic APCs for providing optimal crosslinking of the αCD3+αCD28 antibodies during activation. Therefore it is difficult to deduce the T cell-intrinsic and extrinsic mechanisms that may result in the differential ability of TNF production between thymocytes and splenic T cells.

To better determine the differences in TNF production between SP thymocytes and splenic T cells, I wanted to study the TNF producing capabilities of thymic and splenic T cells that have a monoclonal TCR with identical affinity that can be stimulated specifically with their cognate peptide ligands. In the following sections of this chapter, I

have used thymocytes and splenic T cells from P14 TCR transgenic mice whose $CD8^+$ T cells recognize the GP33 peptide of LCMV in the context of $H\text{-}2D^b$. Additionally, this is a good system as I have an *in vivo* infection model to test the differences in the TNF producing capability of SP thymocytes and splenic T cells in the presence of physiologically relevant levels of antigen during LCMV infection.

N. Co-stimulation augments the TNF producing capability of TCR transgenic CD8$^+$ and CD4$^+$ naive T cells.

Given the differences in the TNF producing capability of naïve polyclonal thymocytes and splenic T cells during TCR activation with respect to αCD3+αCD28 mediated cross-linking, I next tested if this profile of TNF production recapitulates with TCR-transgenic (monoclonal) T cells stimulated with cognate peptide ligand. Previously, it was shown that the P14 TCR transgenic (Tg) CD8$^+$ and SMARTA TCR transgenic CD4$^+$ splenic T cells produced TNF when stimulated with their cognate peptide. In order to test if co-stimulation enhances the production of TNF by Tg CD8$^+$ and CD4$^+$ naïve splenic T cells, I used splenic T cells from P14 TCR and SMARTA TCR Tg mice that recognize the GP33 peptide and GP61 peptide derived from LCMV, respectively. I found that the percentages of transgenic T cells producing TNF increased after stimulation with their cognate peptides and co-stimulation (Fig 3.16 A and B). There was, however, no increase in the production of IFNγ.

My data with the polyclonal system suggest that the activation for polyclonal splenic T cells required the presence of splenic B cells and APCs (that offer better Fc receptor mediated cross-linking of antibodies) during activation of T cells (section K; Fig 3.13). To determine if TCR-transgenic splenic T cells are also dependent upon a splenic environment (containing B cells and other APCs), I purified populations of transgenic P14 T cells and stimulated them with GP33 and GP33+αCD28 for 4 hours. I found that, in contrast to the polyclonal T cells stimulated with αCD3+αCD28 antibodies, purified

transgenic P14 Tg T cells stimulated with soluble peptide produced TNF upon stimulation (Fig 3. 17A). This suggested that the peptide-mediated stimulation of purified transgenic T cells is sufficient to activate purified T cells and enables them to produce TNF bypassing the requirement for splenic APCs. This could be potentially occurring due to peptide presentation between T cells as P14 Tg T cells express the MHC-I (H-2D^{b}) on their surface that is required for GP33 presentation. Addition of actinomycin D or cycloheximide completely abrogated the production TNF by purified P14 Tg T cells (Fig 3.17B), suggesting that transcription and protein synthesis is required to occur in naïve T cells during stimulation. Together, these results indicate that P14 Tg naïve splenic T cells are capable of producing TNF *in vitro* without the requirement of splenic APCs, unlike polyclonal T cells.

Figure 3.16. Costimulation (αCD28) enhances the TNF producing capability of TCR transgenic peripheral naive (CD44-lo) T cells.

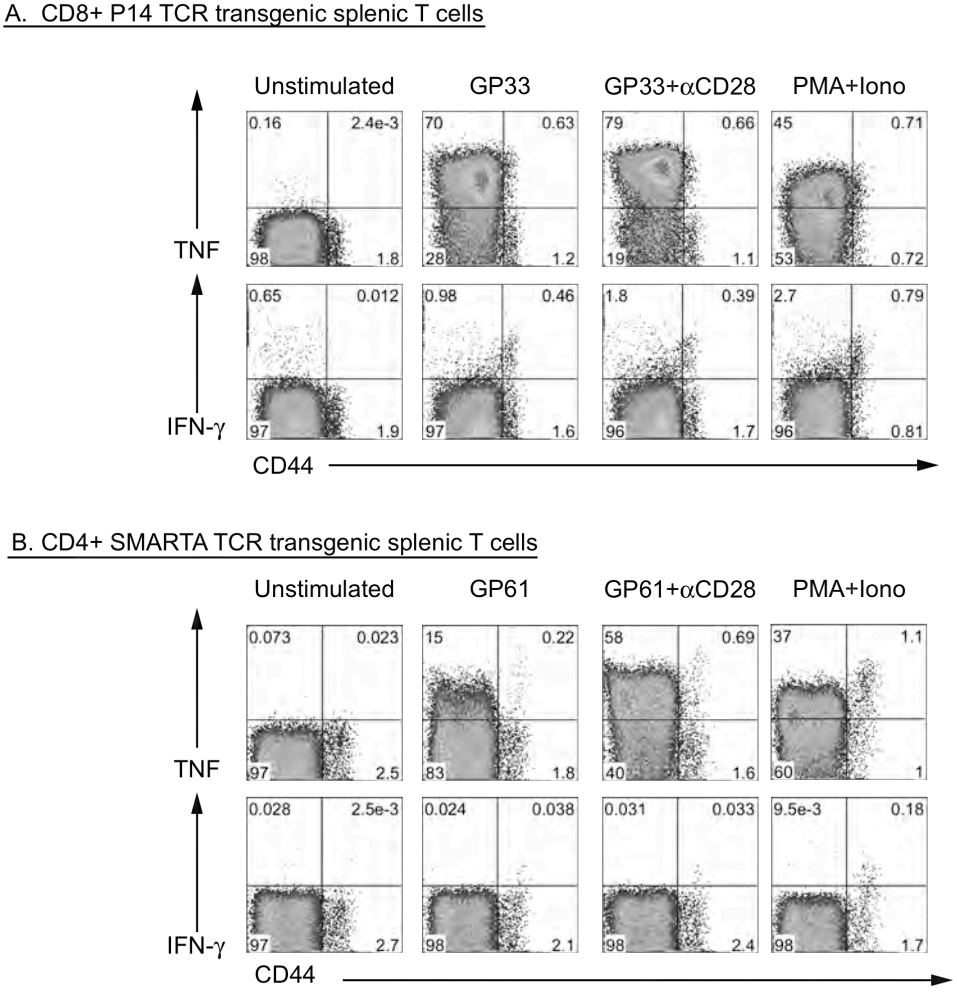

Figure 3.16. Enhanced production of TNF by naïve ($CD44^{lo}$) TCR transgenic peripheral T cells stimulated with cognate peptide + αCD28 for 4 hours in vitro.

$CD8^+$P14 TCR transgenic and $CD4^+$ SMARTA TCR transgenic splenocytes were stimulated with LCMV derived GP33 and GP61 cognate peptides along with or without co-stimulation for 4 hours respectively in vitro followed by intracellular cytokine stain for TNF as described in Materials and Methods. PMA+ Ionomycin was used as positive control for bypassing the TCR mediated activation. Panel A and B shown the percentages of naïve ($CD44^{lo}$) P14 and SMARTA TCR transgenic T cells producing TNF.

Figure 3.17. New transcription and translation is required for TNF production in purified naive CD8+ P14 TCR transgenic T cells during GP33+ αCD28 stimulation.

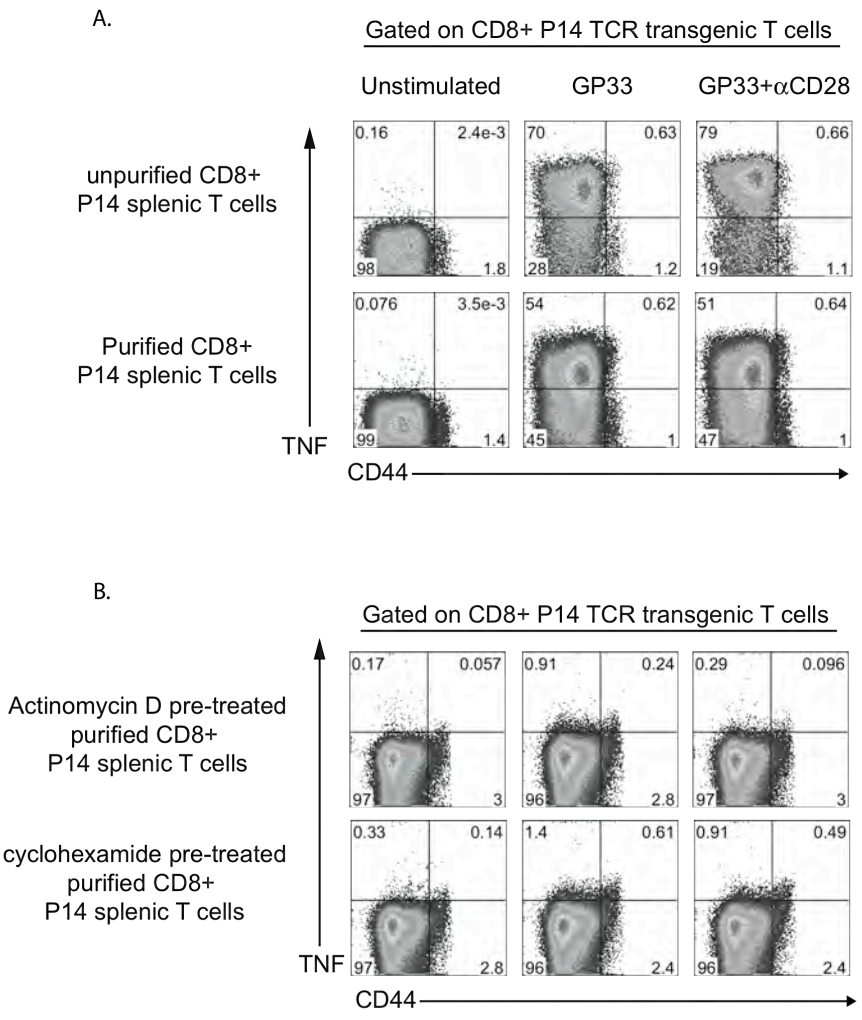

Figure 3.17. New transcription and translation is required for TNF production by purified naïve CD8$^+$ P14-TCR transgenic T cells during GP33+α CD28 stimulation.

CD8$^+$P14 TCR transgenic T cells were MACS sorted by positive selection to 95% purity. Cells were pretreated with either actinomycin D (20μg/ml) or cycloheximide (5μg/ml) for 30 min at 37℃. The cells were then stimulated with 1μM GP33 peptide in absence or presence of co-stimulation αCD28 (2.5μg/ml) and bfA for 4 hours in vitro followed by intracellular staining for TNF. Cells are gated on CD8$^+$ T cells for analysis. Panel A shows the percentages of unpurified and purified T cells producing TNF upon stimulation. Panel B shows percentages of T cells positive for TNF under actinomycin D and cycloheximide treatment.

O. CD8$^+$ P14 TCR-transgenic SP thymocytes exhibit a poor ability to produce TNF after peptide stimulation.

Next, I wanted to determine if CD8$^+$ P14 TCR transgenic thymocytes also lack the ability to produce TNF with respect to CD8$^+$ P14 TCR transgenic T cells in secondary lymphoid organs. CD8$^+$ P14 thymocytes and splenocytes were stimulated with GP33 and GP33+αCD28. PMA and ionomycin was used as a positive control. CD8$^+$ P14 TCR-transgenic SP thymocytes showed a poor ability to produce TNF relative to splenic or lymph node T cells as shown in Fig 3.18 A and B. Varying the concentrations of GP33 peptide did not increase the ability of P14 thymocytes to produce TNF *in vitro*. Addition of αCD28 did not further enhance the ability to produce TNF by thymocytes (Fig 3.19).

To determine if the reduced production of TNF by SP TCR-transgenic thymocytes was due to a lower level of TCR expression(357-359), CD8$^+$ P14 Tg SP thymocytes and CD8$^+$ P14 Tg naïve (CD44^{lo}) splenic T cells were stained with mAbs to TCR Vα2 and TCR Vβ8.1. Fig. 3.20A shows that Vα2 and Vβ8.1 expression in CD8$^+$ P14 Tg SP thymocytes and CD8$^+$ P14 Tg splenic T cells were similar at all dilutions of the antibodies, with the splenic T cells showing a slightly lower expression than their thymic counterparts. To determine if the reduced ability of CD8$^+$ P14 Tg SP thymocytes to produce TNF was due to a generalized defect in their activation, I examined the expression of activation markers CD25, CD69, CD44 and CD62L on the CD8$^+$ P14 Tg SP thymocytes and CD8$^+$ P14 Tg naive (CD44^{lo}) splenic T cells. As shown in Fig. 3.20B, CD8$^+$ P14 Tg SP thymocytes and CD8$^+$ P14 Tg splenic T cells exhibited a comparable

level of activation at 4 hours, with the expression of CD25 and CD69 being up-regulated and the expression of CD62L down-regulated. These results together suggest that SP TCR-transgenic thymocytes are incompetent to produce TNF when compared to splenic T cells upon TCR stimulation despite exhibiting similar phenotypic changes in the expression of activation markers. This observation of a comparable activation profile between $CD8^+$ P14 Tg SP thymocytes with respect to their splenic counterparts upon peptide stimulation is in contrast to the observation made in the polyclonal system. In section G (Fig 3.7), I showed that polyclonal SP thymocytes exhibited lower activation profiles relative to their splenic counterparts during αCD3-mediated crosslinking. These differences between Tg T cells and polyclonal T cells may be attributed to two possibilities. 1) One possibility is that both polyclonal and Tg SP thymocytes may have similar levels of activation thresholds compared to their splenic counterparts, and it is the mode of stimulation (antibody vs peptide) that may dictate their activation response. In other words, the αCD3+αCD28-mediated stimulation may not be optimally activating polyclonal SP thymocytes when compared to peptide stimulation of Tg SP thymocytes 2) The second possibility is that polyclonal and Tg SP thymocytes may have different levels of activation thresholds that are reflected in the differences in their activation status after stimulation. Nonetheless, despite these differences, the common observation is that both polyclonal and Tg SP thymocytes are still poor producers of TNF relative to their splenic counterparts.

Figure 3.18. CD8+ P14 TCR transgenic SP thymocytes exhibit a poor ability to produce TNF relative to their counterparts in secondary lymphoid organs.

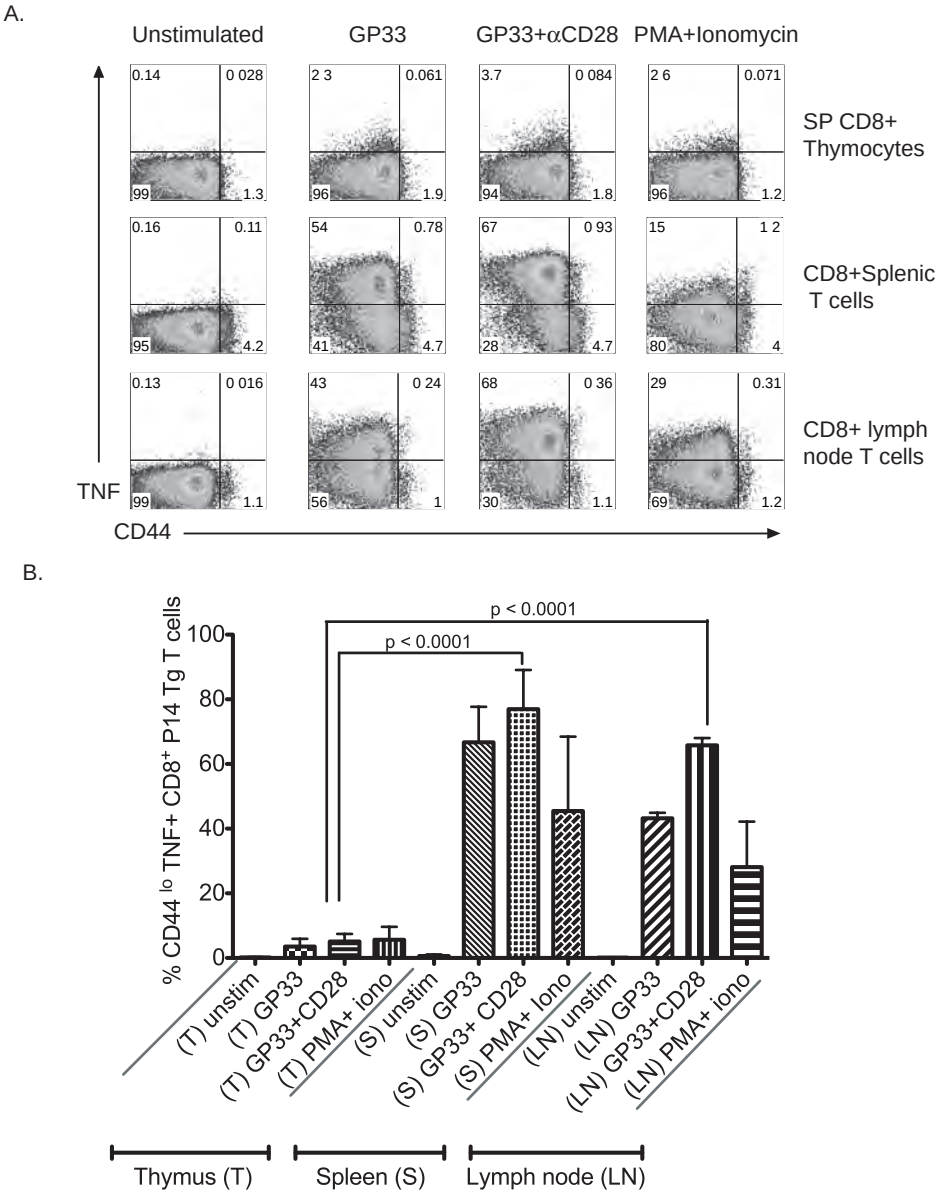

Figure 3.18. $CD8^+$ P14 TCR transgenic SP thymocytes exhibit a poor ability to produce TNF relative to their counterparts in secondary lymphoid organs.

*$CD8^+$ P14 TCR transgenic SP thymocytes, splenocytes and lymph node cells were stimulated with GP33 peptide alone or along with co-stimulation (αCD28) for 4 hours in vitro. PMA+Ionomycin was added as a positive control to bypass the TCR mediated activation. Panel A shows the representative plots of percentages of TNF producing $CD8^+$ SP thymocytes relative to T cells in the spleen and the lymph node with various stimulations. Panel B shows pool of 15 experiments for the thymocytes, 18 experiments for the splenocytes and 3 individual mice for the lymph node cells. The values were analyzed by one-way ANOVA analysis with Tukey post-test. P value <0.0001***. Error bars indicate SD.*

Figure 3.19. Varying the concentrations of GP33 peptide does not promote the ability of CD8$^+$ P14 TCR transgenic SP thymocytes to produce TNF to the levels of their splenic counterparts.

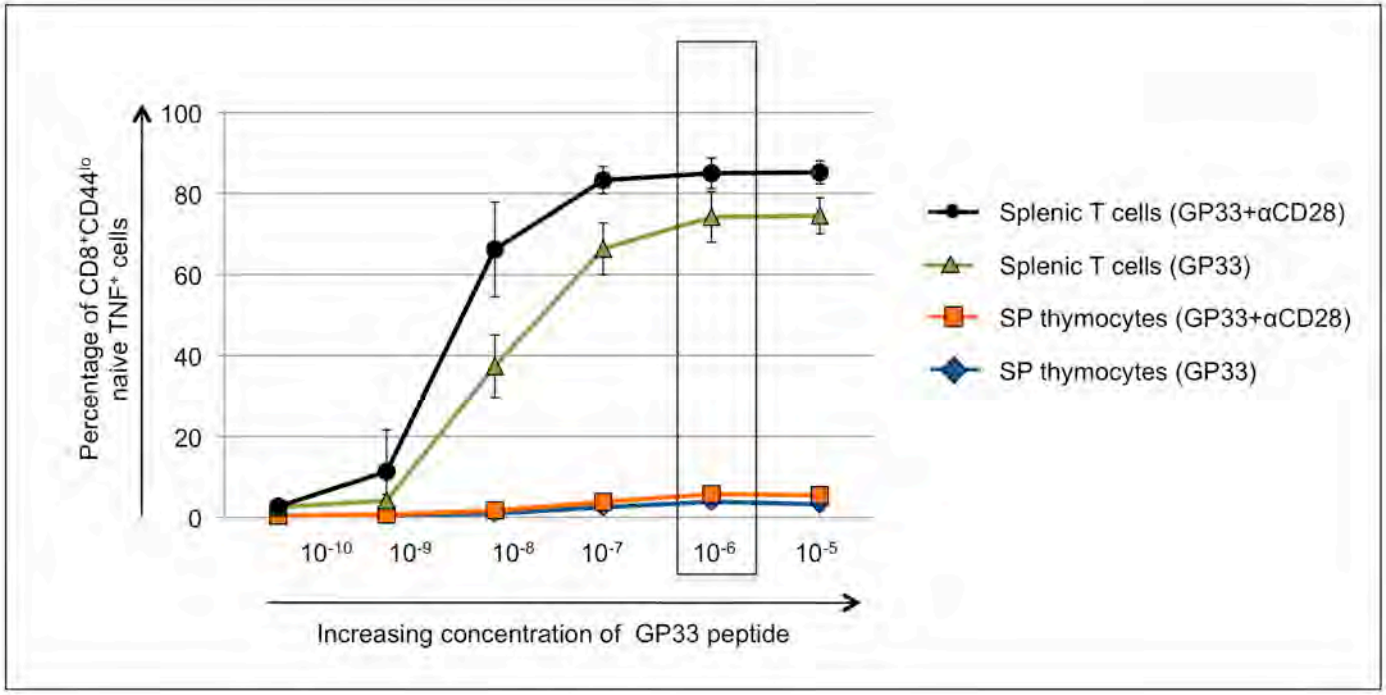

Figure 3.19. Varying the concentrations of the peptide did not promote the ability of transgenic SP thymocytes to produce TNF to the levels of their secondary lymphoid counterparts.

SP $CD8^+$ P14 TCR transgenic thymocytes and splenocytes from 3 individual mice were stimulated with varying concentrations GP33 peptide (10^{-10} to 10^{-5} M) alone or along with constant αCD28 co-stimulation (2.5μg/ml) for 4 hours in vitro followed by intracellular staining for TNF cytokine. The splenic T cells stimulated with peptide alone are indicated by the light green line with green triangles and those stimulated with peptide and αCD28 are indicated by the black line with black circles. Similarly, thymocytes that are stimulated with peptide alone are indicated by the blue line with blue diamonds and those stimulated with peptide and αCD28 are indicated by the orange line with orange squares. The error bars indicate SD. The box indicating 10^{-6} M is the concentration that has been used for all the analysis for comparison between thymocytes and splenic T cells.

Figure 3.20. CD8+ P14 TCR transgenic SP thymocytes and Splenic T cells exhibit similar TCR levels at resting state and comparable phenotypic changes in activation markers upon stimulation.

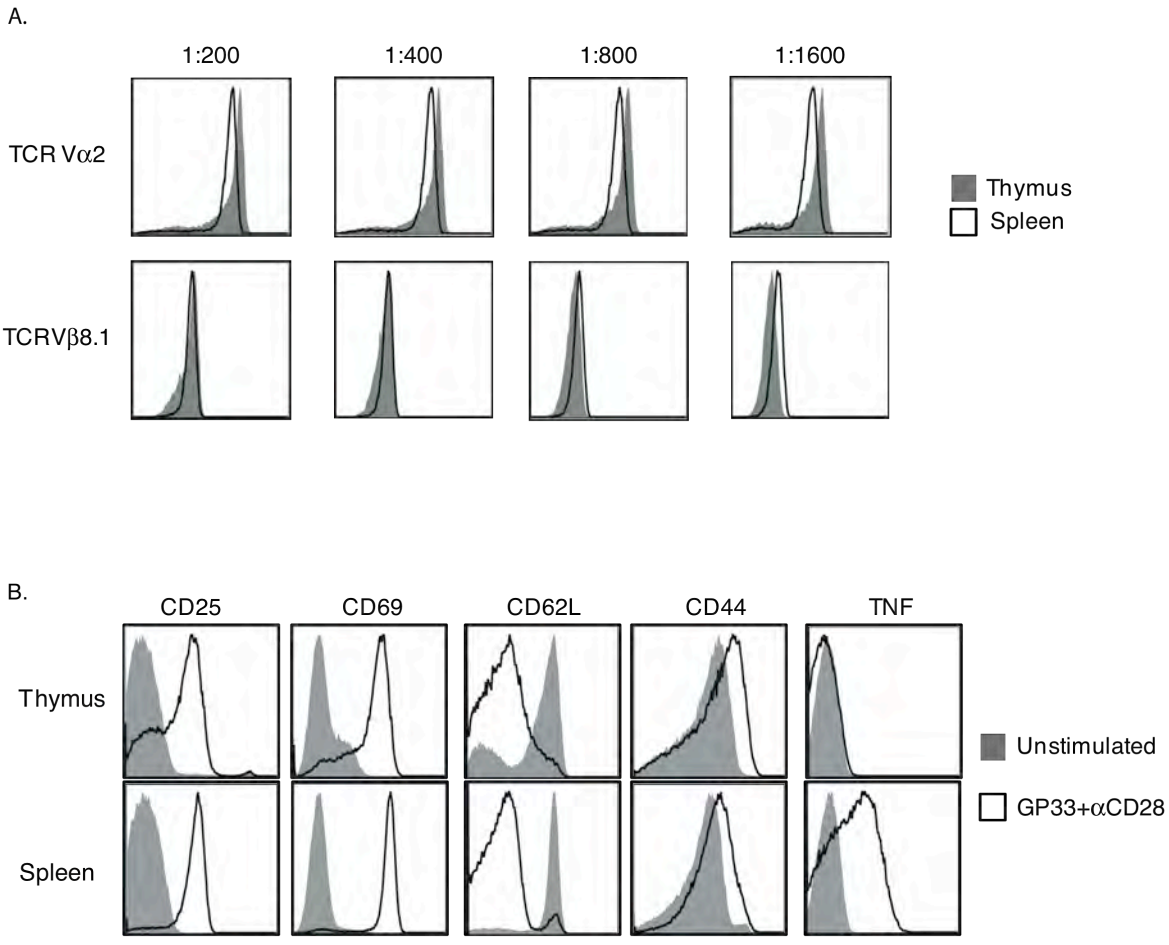

Figure 3.20. $CD8^+$ P14 TCR transgenic SP thymocytes and splenic T cells exhibit similar TCR levels at resting state and comparable phenotypic changes in activation markers upon activation.

Panel A. Resting $CD8^+$ P14 Tg thymocytes and naïve splenocytes were stained with mAbs to Vα2 and Vβ8.1 at various dilutions as indicated. The profile for the SP thymocytes is shown in gray solid histograms and for splenic T cells in black line histograms. Panel B. P14-$CD8^+$ thymocytes and naïve splenocytes were either unstimulated (gray solid histograms) or stimulated (black line histograms) for 4 hours with GP33+αCD28 in vitro and stained with mAbs to the indicated surface molecules.

P. Reduced ERK phosphorylation in SP transgenic thymocytes relative to naïve splenic T cells upon TCR activation.

TNF production induced by TCR engagement requires signaling through the mitogen activated protein kinase (MAPK) pathway (229). To determine if there are differences in the initial proximal signaling events downstream of the TCR between $CD8^+$ P14 Tg SP thymocytes and naïve ($CD44^{lo}$) splenic T cells, I examined phosphorylation of the MAP kinases, ERK during the first hour of activation. Phosphorylated ERK was first detectable at 5 min post-stimulation and continued to increase during the stimulation period in both SP P14-$CD8^+$ thymocytes and naïve splenic T cells. However, the levels of phosphorylated ERK as well as the extent of phosphorylation on a per cell basis were higher in naïve splenic T cells than in $CD8^+$ P14 Tg SP thymocytes between 20 min and 1 hour after stimulation (Fig.3.21 *A* and *B*). Similar levels of total ERK were detected in $CD8^+$ P14 Tg SP thymocytes and $CD8^+$ P14 Tg naïve splenic T cells (data not shown). These results indicate that signaling via the ERK pathway is diminished in $CD8^+$ P14 Tg SP thymocytes when compared to their splenic counterparts, and may account for their reduced production of TNF. However, it is noteworthy to mention that $CD8^+$ P14 Tg SP thymocytes and $CD8^+$ P14 Tg naïve splenic T cells used in this experiment were not purified. Therefore there is a possibility that these differences between SP thymocytes and their splenic counterparts may be attributed to the presence of APCs in the splenic T cell cultures during stimulation.

Figure 3.21. CD8+ P14 TCR transgenic SP thymocytes exhibit slower and lower levels of ERK phosphorylation compared to splenic T cells after GP33 peptide stimulation.

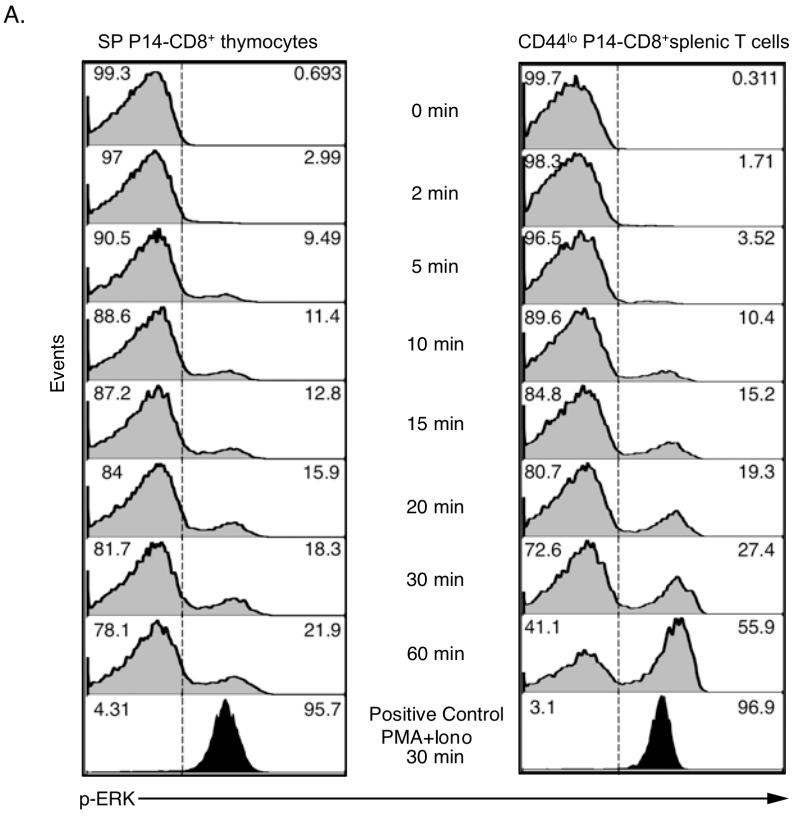

Figure 3.21.CD8$^+$ P14 TCR SP transgenic thymocytes exhibit slower and lower levels of ERK phosphorylation compared to splenic T cells after TCR stimulation.

CD8$^+$ SP thymocytes and CD8$^+$ splenic T cells from P14-CD8$^+$ TCR transgenic mice were purified by cell enrichment and stimulated with 1μM of GP33 peptide for the indicated time points. PMA and ionomycin stimulation for 30 min was used as a positive control (black histograms). Cells were immediately fixed and permeabilized before staining, as described in Materials and Methods. For analysis, cells were gated on CD8$^+$ CD44^{lo} cells. A, The differences in phosphorylation kinetics of ERK in SP P14-CD8$^+$ thymocytes and splenic T cells upon TCR activation from 0 to 60 min respectively are shown. B, The differences in the MFI of phosphorylated ERK between SP P14-CD8$^+$ thymocytes (black squares) and splenic T cells (white squares) are shown. This profile is representative of 4 individual experiments.

Q. Lower level of TNF transcription in CD8$^+$ P14 TCR SP transgenic thymocytes relative to naïve splenic counterparts during TCR activation.

I next hypothesized that the reduced ability of thymocytes to produce TNF may be correlated to the lower levels of mature TNF message levels within these cells. Therefore, I first quantified the resting steady-state levels of mature TNF mRNA in purified SP P14 thymocytes and their respective naïve splenic (CD44^{lo}) counterparts. Fig. 3.22A shows the copy number of TNF transcripts detected in the indicated groups by quantitative real-time PCR. The levels of mature TNF message in CD8$^+$ P14 Tg SP thymocytes and their naïve splenic counterparts were similar and the differences were not significant (Fig. 3.22A). This observation is similar with purified non-transgenic SP thymocytes and naïve (CD44^{lo}) splenic T cells (section H; Fig. 3.8).

To determine if the diminished ability of SP thymocytes to produce TNF protein is due to reduced transcription of the TNF gene upon stimulation, I compared the levels of TNF transcripts in purified CD8$^+$ P14 Tg SP thymocytes and CD8$^+$ P14 Tg naïve (CD44^{lo}) splenic T cells that were either unstimulated or stimulated as indicated. I found that the levels of TNF mRNA were dramatically upregulated in (CD44^{lo}) CD8$^+$ P14 Tg splenic T cells during GP33 and GP33+αCD28 stimulation relative to CD8$^+$ P14 Tg SP thymocytes. The levels of TNF transcripts increased in the thymic subsets as well but not to the extent detected in the splenic subset (Fig. 3.22*B*). Together these results indicate that despite having a basal level of TNF transcription of the TNF gene, SP thymocytes

appear to lack the ability to induce TNF transcription efficiently upon stimulation relative to naïve splenic T cells.

Figure 3.22. Reduced upregulation of TNF message in CD8+P14 TCR transgenic SP thymocytes relative to their naive (CD44-lo) splenic counterparts

A.

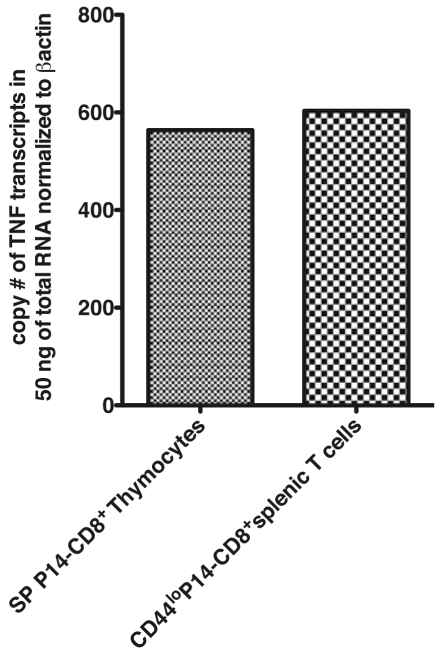

B.

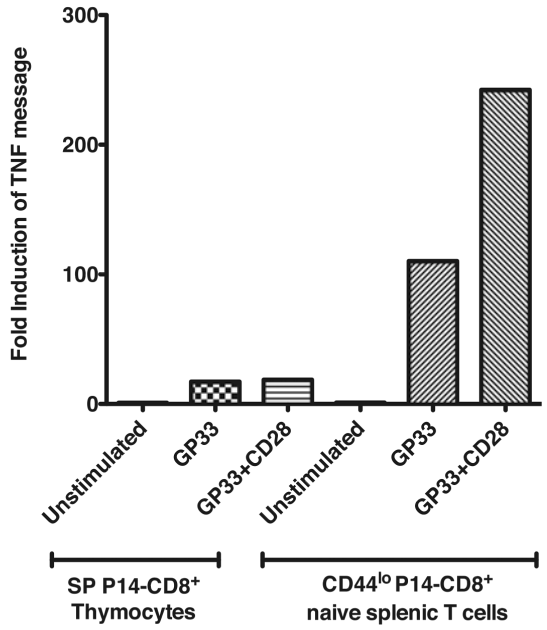

Figure 3.22. Reduced upregulation of TNF message in CD8$^+$ P14 TCR transgenic SP thymocytes relative to naïve splenic counterparts upon TCR stimulation.

Panel A and Panel B. CD8$^+$ P14 Tg SP thymocytes and (CD44^{lo}) CD8$^+$ P14 Tg naïve splenic T cells were purified by cell sorting and stimulated in the presence of GP33 and GP33+αCD28 for 4 hours followed by RNA isolation and cDNA synthesis from 50 ng of RNA and then amplified using TNF specific primers by quantitative real time PCR from the indicated populations as described in Materials and Methods. The basal level of TNF transcripts in 50 ng of total RNA (normalized to a β-actin control) isolated from unstimulated CD8$^+$ P14 Tg SP thymocytes and (CD44^{lo}) CD8$^+$ P14 Tg naïve splenic T cells is shown in Panel A. The increase in TNF message in these subsets upon stimulation with GP33 and GP33+αCD28 is shown in Panel B in terms of fold induction with respect to unstimulated SP thymocytes been (normalized to a β-actin control). This profile is representative of 3 individual experiments.

R. Stimulation in the presence of splenocytes enables a modest increase in the proportion of CD8$^+$ P14 TCR-transgenic SP thymocytes producing TNF.

Similar to polyclonal SP CD8$^+$ thymocytes, CD8$^+$ P14 Tg SP thymocytes were also identified to be poor producers of TNF. To determine if stimulation in the presence of appropriate APCs can enable P14 SP thymocytes to produce TNF upon stimulation, Ly5.1 (CD45.1$^+$) CD8$^+$ P14 Tg SP thymocytes were co-cultured with wild type (WT) Ly5.2 (CD45.2$^+$) B6 splenocytes and simultaneously stimulated with the GP33 for 4 hours *in vitro*. There was a partial increase in the proportion of TNF producing CD8$^+$ P14 Tg SP thymocytes that were stimulated in the presence of splenocytes compared to CD8$^+$ P14 Tg SP thymocytes stimulated alone (Fig. 3.23A). TNF production was enhanced in the presence of αCD28 antibody, indicating the importance of co-stimulation in enhancing TNF production. Fig 3.23B is a pool of 10 experiments showing the intermediate response of thymocytes producing TNF in the context of splenocytes.

I next wanted to determine if the ability of CD8$^+$ P14 Tg SP thymocytes to produce TNF in the context of splenocytes was dependent on the number of antigen presenting cells in the spleen. CD8$^+$ P14 Tg thymocytes were stimulated with varying numbers of splenocytes and the enhancement of TNF-production by the thymocytes was again a dose dependent phenomenon (Fig 3.24A). In order to identify the secondary lymphoid subsets that best stimulate CD8$^+$ P14 Tg SP thymocytes, purified splenic B cells, T cells or APCs (T cell and B cell depleted populations) were co-cultured separately with CD8$^+$ P14 Tg SP thymocytes and simultaneously stimulated with GP33+αCD28. Both purified splenic

B cells and APCs but not T cells enabled $CD8^+$ P14 Tg SP thymocytes to produce TNF (~20% TNF positive, (Fig 3.24B). These results indicate that splenocytes (data not shown) can enable SP thymocytes to gain a partial ability to produce TNF. These data also suggest that the inherent defect of $CD8^+$ P14 Tg SP thymocytes to efficiently produce TNF during TCR activation cannot be completely rescued by optimal antigen-presentation *in vitro*. Together, these results indicate that splenic B cells and APCs in the flowthrough offer better signals and enable more thymocytes to produce TNF.

Figure 3.23. Modest increase in the percentage of CD8+ P14 TCR transgenic single positive thymocytes producing TNF when stimulated in the presence of splenocytes.

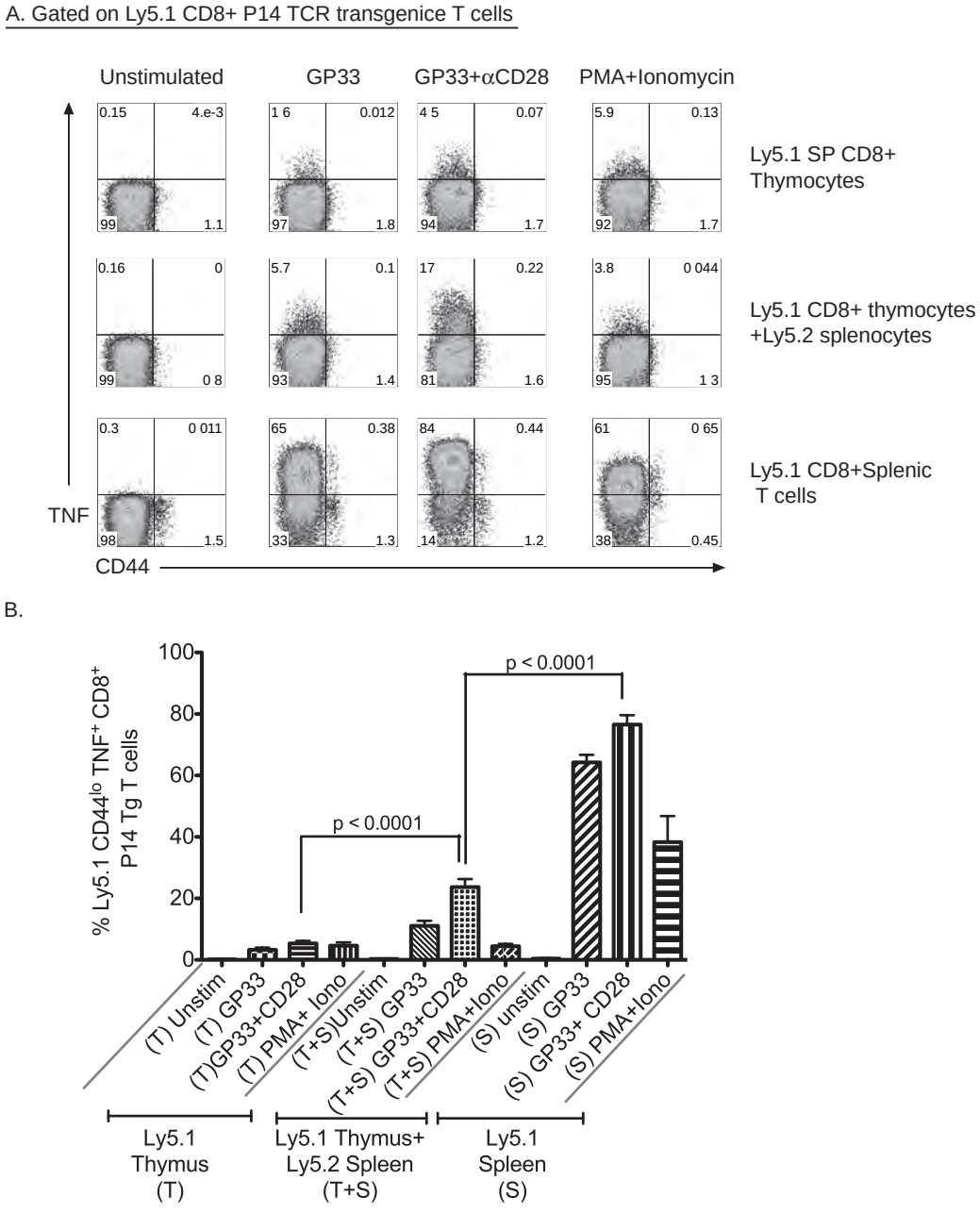

Figure 3.23. Modest increase in the percentages of $CD8^+$ P14 TCR transgenic SP thymocytes producing TNF when stimulated in the presence of cells from secondary lymphoid organs.

*Ly5.1 ($CD45.1^+$) $CD8^+$ P14 Tg SP thymocytes were either stimulated alone or in the presence of Ly5.2 ($CD45.2^+$) splenocytes at a 1:1 (responder:stimulator) ratio with 1μM of GP33 alone or along with αCD28 for 4 hours, followed by surface and standard intracellular staining for TNF cytokine, as described in Materials and Methods. For analysis, the cells were gated on Ly5.1 ($CD45.1^+$) $CD8^+$ cells. Panel A. The percentages of $CD45.1^+CD8^+$ P14 Tg SP thymocytes alone, $CD45.1^+$ $CD8^+$ P14 Tg SP thymocytes in the presence of $CD45.2^+$ splenocytes and splenic $CD45.1^+$ $CD8^+$ P14 Tg T cells (both $CD44^{lo}$ and $CD44^{hi}$) staining positive for TNF after stimulation are shown. Panel B, shows the pool of 9 experiments showing the differences in the percentages of TNF producing $CD8^+$P14 TCR transgenic SP thymocytes that are stimulated under the indicated conditions. P value <0.001*** and error bars indicate SD.*

Figure 3.24. The effect of splenocytes on the TNF producing ability of CD8+ P14 TCR Tg SP thymocytes is dose-dependent and is mediated by splenic B cells and a non B/T population containing CD11c+ cells.

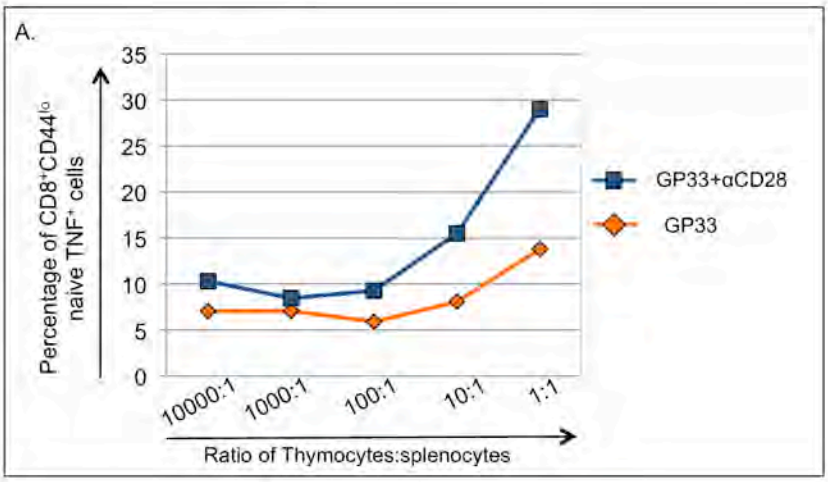

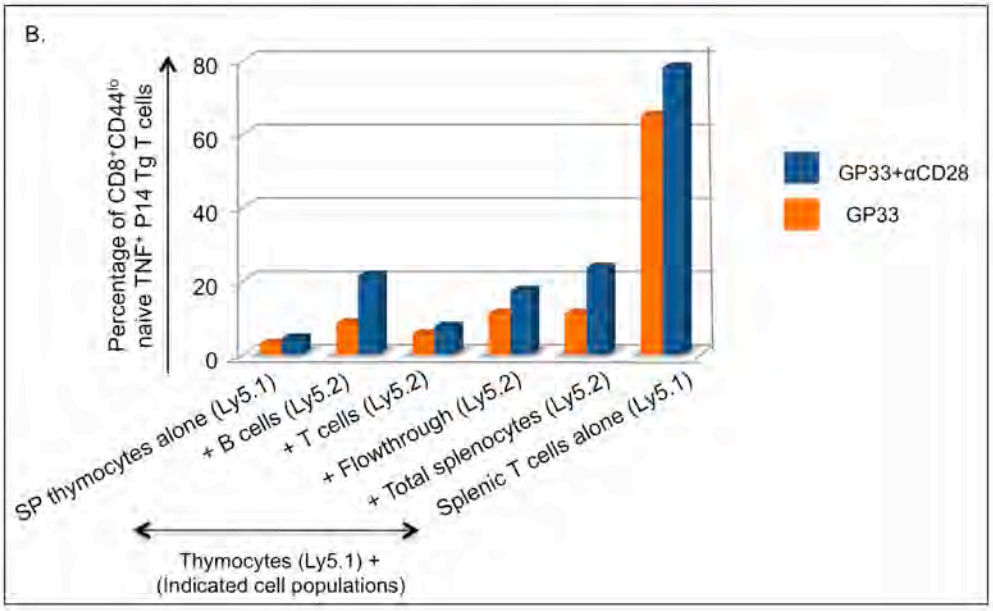

Figure 3.24. The effect of splenocytes on TNF producing ability of $CD8^+$ P14 Tg SP thymocytes is dose-dependent and is mediated by splenic B cells and a NonB/T cell population containing CD11c+ cells.

Panel A. 2×10^6 $CD8^+$P14 TCR transgenic thymocytes are stimulated with varying ratios of splenocytes as indicated. Cells were stimulated in the presence of either 1μM GP33 peptide alone or along with αCD28 antibody followed by standard intra-cellular staining for TNF. Panel B. Ly5.2 ($CD45.2^+$) B6 splenocytes were magnetically separated into purified populations of splenic B cells ($CD19^+B220^+$-97.4%) and T cells ($Thy1.2^+CD3^+$-83.2 %) and into T cell and B cell depleted populations ($CD11c^+$- 30.4%). Ly5.1 ($CD45.1^+$) $CD8^+$ P14 Tg SP thymocytes were stimulated with these subsets at 1:1 ratio with GP33 +αCD28 for 4 hours and then stained for intracellular TNF. The percentages of $CD45.1^+$ $CD8^+$ P14 Tg SP thymocytes ($CD44^{lo}$ and $CD44^{hi}$) staining positive for TNF are shown.

S. The differential ability of TNF production between thymocytes and splenic T cells exists in other TCR-transgenic systems.

In order to determine if the differential ability of SP thymocytes and splenic T cells to produce TNF was also evident in other TCR-transgenic T cells, I stimulated OT-I- $CD8^+$, HY- $CD8^+$, SMARTA- $CD4^+$, and OT-II-$CD4^+$ transgenic thymocytes with their cognate peptides and αCD28. Transgenic SP thymocytes from all these mice showed a poor capacity to produce TNF in contrast to their splenic counterparts (Fig 3.25 A, B, C and D). Stimulation in the presence of splenocytes enabled a small increase in the percentage of thymocytes producing TNF, but they were nevertheless still defective in their ability to produce TNF compared to their splenic counterparts. Together, these results suggest that the poor ability of SP thymocytes to produce TNF is applicable to other TCR-transgenic systems.

Figure 3.25. The differential expression of TNF between thymocytes and splenic T cells is observed in other transgenic T cells (CD8+ and CD4+).

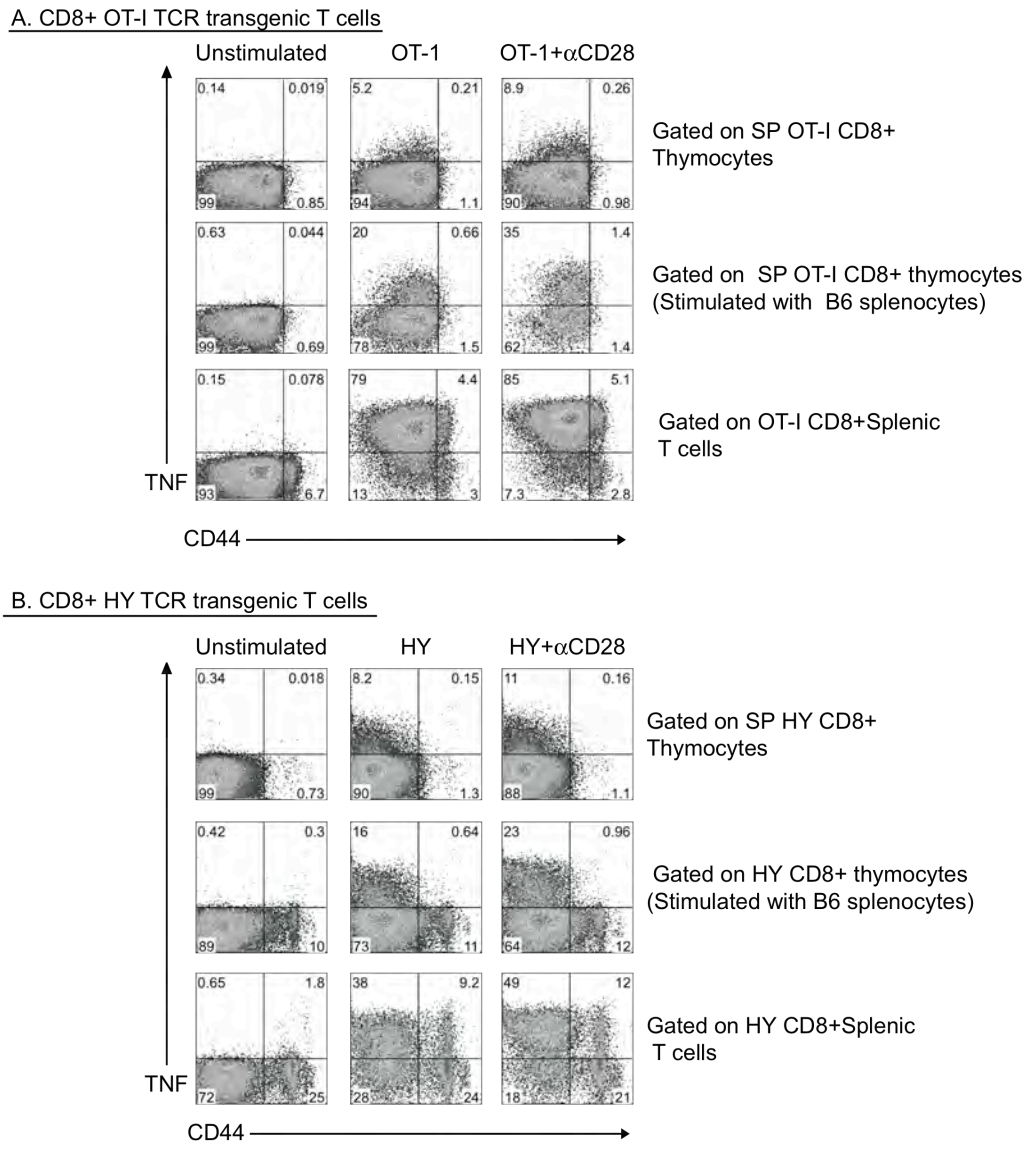

C. SMARTA CD4+ TCR transgenic T cells

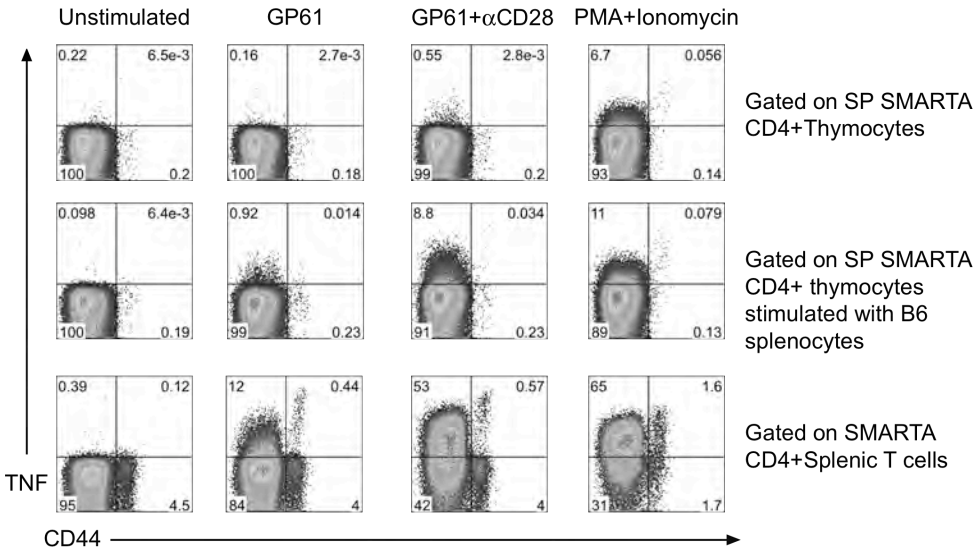

D. OT-II CD4+ TCR transgenic T cells

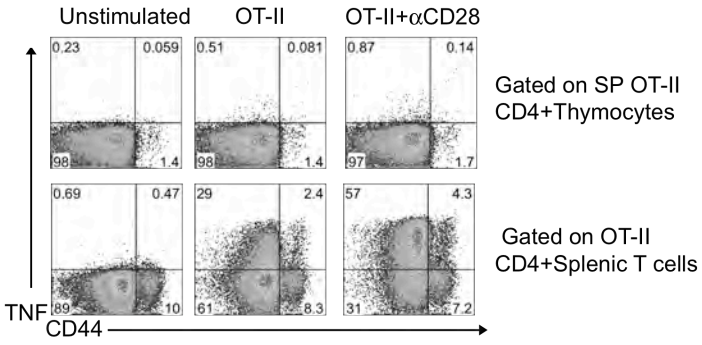

Figure 3.25. The differential expression of TNF production between SP thymocytes and splenic T cells is observed in other TCR-transgenic systems.

Thymocytes and splenocytes from naïve OT-I-CD8$^+$, HY-CD8$^+$ and SMARTA-CD4$^+$ and OT-II-CD4$^+$ TCR transgenic mice were stimulated in vitro as indicated for 4 hours and then stained for intracellular TNF cytokine, as described in Materials and Methods. For analysis, the cells were gated on either SP CD8$^+$ CD4$^-$ or SP CD4$^+$ CD8$^-$ cells. Panel A and Panel B show the percentages of CD8$^+$ (both CD44^{lo} and CD44^{hi}) T cells from thymi and spleens of OT-I-CD8$^+$, HY-CD8$^+$ TCR transgenic mice staining positive for TNF cytokine. Panel C and Panel D show the percentages of SP P14-CD4$^+$ thymocytes and splenic T cells (both CD44^{lo} and CD44^{hi}) from SMARTA-CD4$^+$ and OT-II-CD4$^+$ TCR transgenic mice staining positive for TNF. As indicated the percentages of TNF producing SP thymocytes that were stimulated in the presence of splenocytes are shown in the respective panels.

T. Appropriate TCR-MHC interactions with splenic APCs promote SP thymocytes to produce TNF during activation.

I next hypothesized that enhanced antigen-presentation by the splenocytes in the co-culture enables SP P14-$CD8^+$ thymocytes to produce TNF. To test this I used two approaches. First, purified Ly5.1 ($CD45.1^+$) $CD8^+$ P14 Tg SP thymocytes were stimulated with GP33 peptide in the presence of control Ly5.2 ($CD45.2^+$) $H2^b$-positive B6 splenocytes or in the presence of Ly5.2 ($CD45.2^+$) $H2^d$-positive BALB/c splenocytes. GP33 is presented by $H2D^b$ and will not be presented by $H2^d$ cells. I found that there was partial increase in the percentages of P14 thymocytes producing TNF in the presence of Ly5.2 ($CD45.2^+$) B6 splenocytes. However, there was no increase in the percentage of Ly5.1 ($CD45.1^+$) $CD8^+$ P14 Tg SP thymocytes producing TNF that were stimulated in the presence of Ly5.2 ($CD45.2^+$) BALB/c splenocytes (Fig 3.26 A and B). As expected, Ly5.1 ($CD45.1^+$) $CD8^+$ P14 Tg splenic T cells produced TNF in the presence of both B6 and BALB/c splenocytes, highlighting the ability of mature splenic T cells in the periphery to present peptide to each other during stimulation. These findings suggest that a primary role for the splenocytes in the co-culture is to present antigen to the thymocytes. Although there was a trend for a modest increase in the proportion of $CD8^+$ P14 Tg SP thymocytes producing TNF in the presence of WT B6 splenocytes as opposed to BALB/c splenocytes, it was not statistically significant. This may be attributed to non-specific peptide binding to cells in the BALB/c splenocyte cultures.

To clearly the determine the role of antigen-presentation by splenocytes, I used a cleaner system where purified Ly5.1 ($CD45.1^+$) $CD8^+$ P14 Tg SP thymocytes were stimulated in the presence of either WT Ly5.2 ($CD45.2^+$) $H2D^b$-positive B6 splenocytes or Ly5.2 ($CD45.2^+$) $H2D^b$-deficient B6 splenocytes. Ly5.1 ($CD45.1^+$) $CD8^+$ P14 Tg SP thymocytes were partially enabled to rapidly produce TNF by WT B6 splenocytes (Fig. 3.27 A and B), but this did not occur when they were stimulated with $H2D^b$-deficient splenocytes. This indicated that TCR-MHC interactions provided by secondary lymphoid cells enabled SP thymocytes to produce TNF partially. Stimulation of $CD8^+$ P14 Tg SP thymocytes with irradiated B6 splenocytes did not impair the ability of SP thymocytes to produce TNF (Fig. 3.27C), indicating that viable splenocytes were not necessary for this effect. Together, these results indicated the importance of appropriate antigen presentation via MHC interactions for P14 thymocytes to produce TNF.

Figure 3.26. Antigen stimulation in the presence of appropriate MHC molecule on splenocytes is required for the modest increase in the proportion of CD8+ P14 TCR Tg SP thymocytes producing TNF.

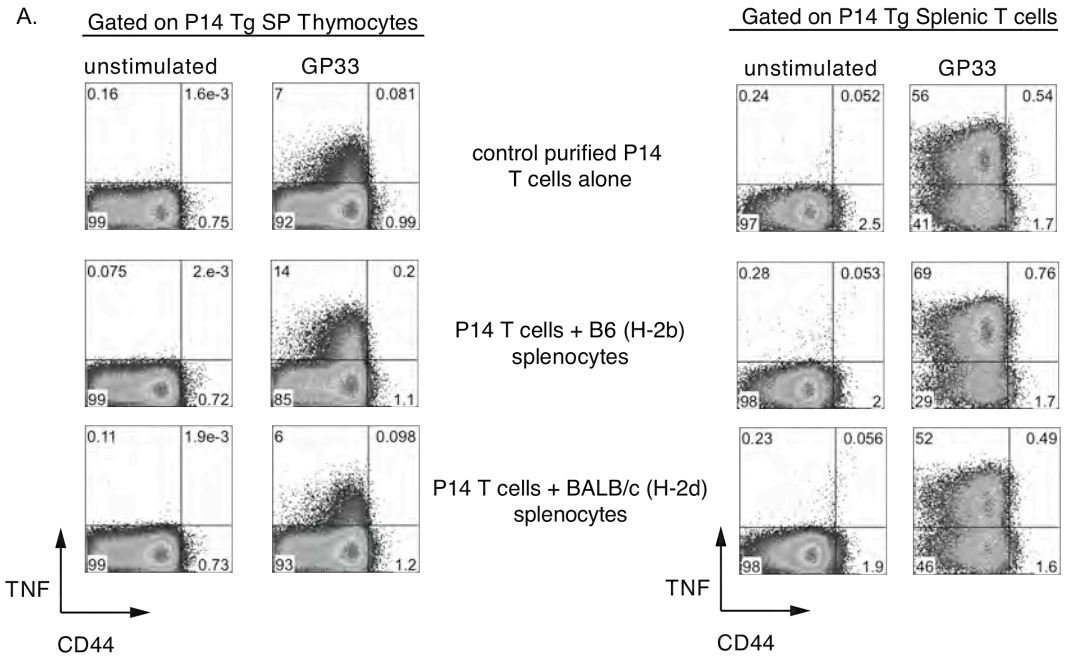

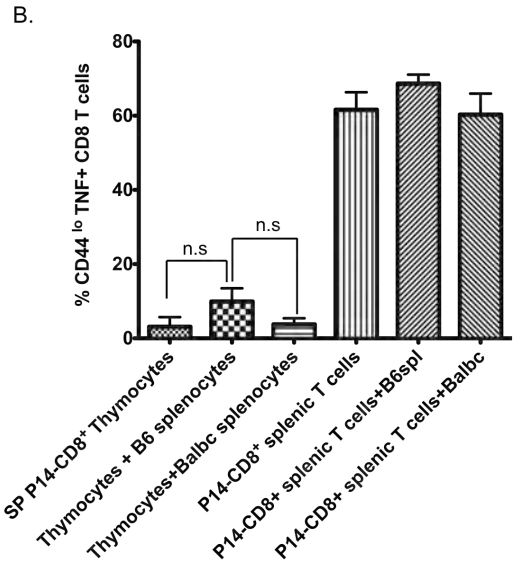

Figure 3.26. Antigenic stimulation in the presence of appropriate MHC molecule on splenocytes is required for modest increase in the percentages of CD8$^+$P14 TCR transgenic SP thymocytes producing TNF.

Panel A. Ly5.1 (CD45.1$^+$) CD8$^+$P14 TCR transgenic SP thymocytes were purified by negative selection and stimulated in the presence of Ly5.2 (CD45.2$^+$) C57BL6 splenocytes (H2^b) splenocytes or Ly5.2 (CD45.2$^+$) BALB/c splenocytes (H2^d) at 1:1 ratio in the presence of 1μM GP33 peptide for 4 hours in vitro followed by intracellular staining for TNF. Panel B shows the average percentages of naïve (CD44^{lo}) TNF producing thymocytes and splenic T cells under the indicated conditions from 4 experiments. The values were analyzed by one-way ANOVA analysis with Tukey post-test. Error bars indicate SD and n.s. indicates not significant.

Figure 3.27. Absence of an appropriate MHC molecule abrogates splenocyte-mediated TNF production by CD8+ P14 TCR Tg SP thymocytes during TCR activation.

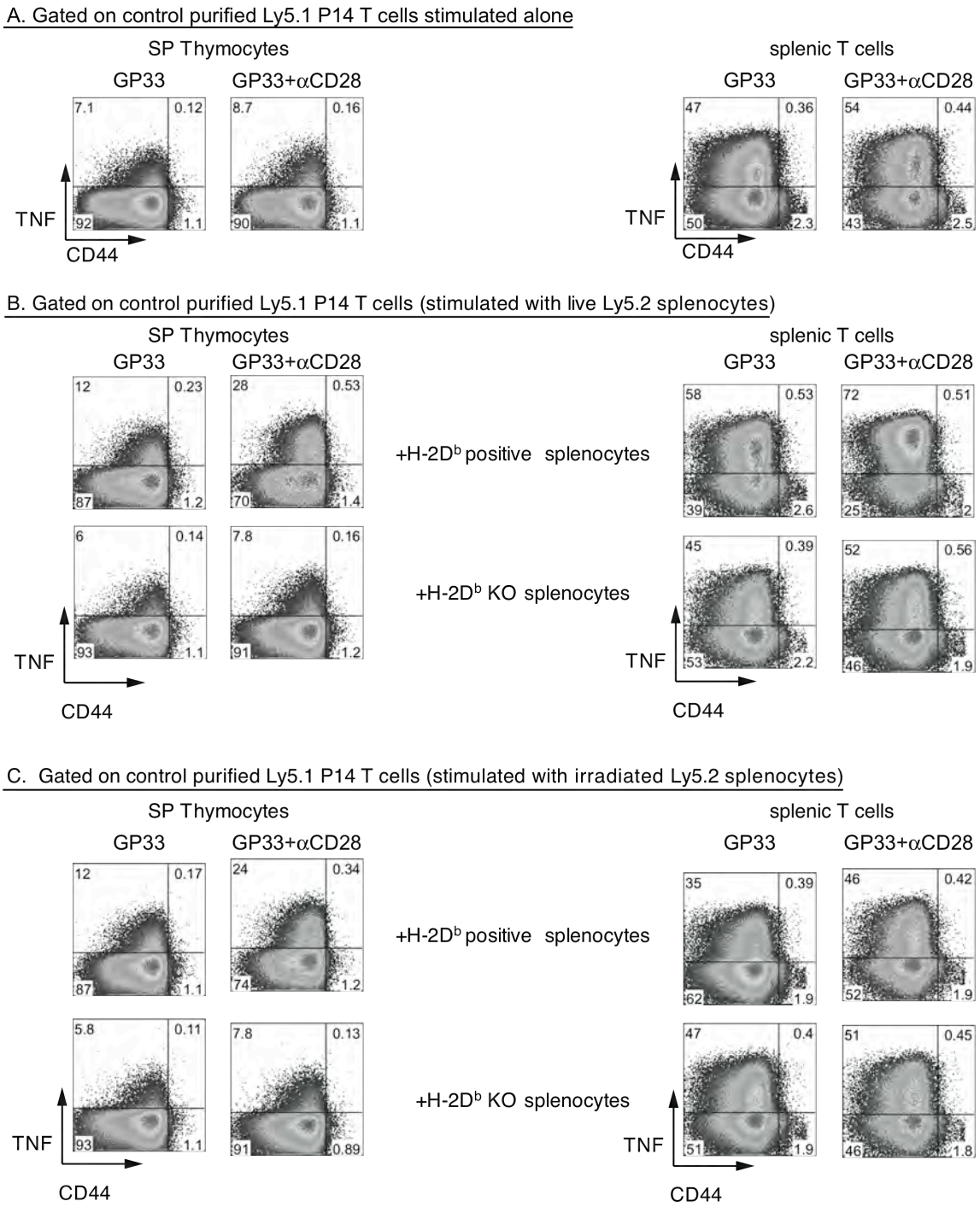

Figure 3.27. Absence of appropriate MHC molecule abrogates splenocyte-mediated TNF production by CD8$^+$ P14 TCR transgenic SP thymocytes during TCR activation.

Panel A. Ly5.1 (CD45.1$^+$) SP P14-CD8$^+$ thymocytes and splenic T cells were enriched by negative selection as described in Materials and Methods. Enriched thymocytes and splenic T cells were stimulated either with GP33 or GP33 +αCD28 for 4 hours. Panel B and C, Enriched cells were stimulated either in the presence of live or irradiated H2D^b WT or H2D^b KO splenocytes respectively in parallel. Cells were gated on SP CD8$^+$ T cells and the plots show the percentages of TNF producing naïve (CD44^{lo}) thymocytes and splenic T cells.

U. Differential ability of SP thymocytes and naïve splenic T cells to produce TNF during TCR activation in vivo.

To first determine if naïve splenic T cells produced TNF in the presence of physiologically relevant levels of antigen, I performed an *in vivo* cytokine assay (341). Briefly, CD45.1$^+$ P14-CD8$^+$ and CD45.1$^+$ SMARTA-CD4$^+$ TCR-transgenic splenic T cells were treated *in vitro* with BfA, a Golgi transport inhibitor that captures cytokines within the producing cell. These cells were then mixed and co-transferred into recipients that were infected with either WT LCMV-Armstrong or a GP33-CTL escape variant of LCMV (GP1V) for 2 days previously. The spleens of recipient mice were recovered 4 hours after transfer and directly stained for intracellular TNF by the donor T cells. Both P14-CD8$^+$ and SMARTA-CD4$^+$ donor T cells produced TNF in mice that were infected with WT LCMV Armstrong (Fig. 3.28A). Only T cells that had down-regulated CD62L, which is consistent with a TCR-mediated activation event, were able to produce TNF. In contrast, P14 -CD8$^+$ donor T cells in mice that were infected with GP1V mutant virus were impaired in their ability to produce TNF (Fig. 3.28A), while SMARTA-CD4$^+$ donor T cells were unaffected. These findings indicate that the *in vivo* production of TNF by naïve CD8$^+$ T cells during LCMV infection was specifically initiated by TCR-mediated signaling and was not due to non-specific effects on naïve T cells by virus-induced inflammation.

I next examined the ability of SP P14-CD8$^+$ thymocytes and SMARTA-CD4$^+$ thymocytes to produce TNF in the same scenario. A small but reproducible proportion of

both donor SP P14-CD8$^+$ and SMARTA-CD4$^+$ thymocytes produced TNF (4 to 6% TNF positive of total T cells) during LCMV infection (Fig. 3.28B). As expected, infection with GP1V mutant impaired the ability of the donor SP P14-CD8$^+$ thymocytes to produce TNF. Fig. 3.28C shows the average percentages of TNF producing SP P14-CD8$^+$ donor thymocytes and splenic T cells that had down-regulated their CD62L expression under the indicated conditions. Together, these results confirm our *in vitro* data indicating that SP thymocytes are impaired in their ability to produce TNF efficiently when compared to naïve splenic T cells during a viral infection.

Figure 3.28. CD8+ and CD4+transgenic SP thymocytes and their respective splenic counterparts exhibit a differential ability to produce TNF during in vivo TCR activation.

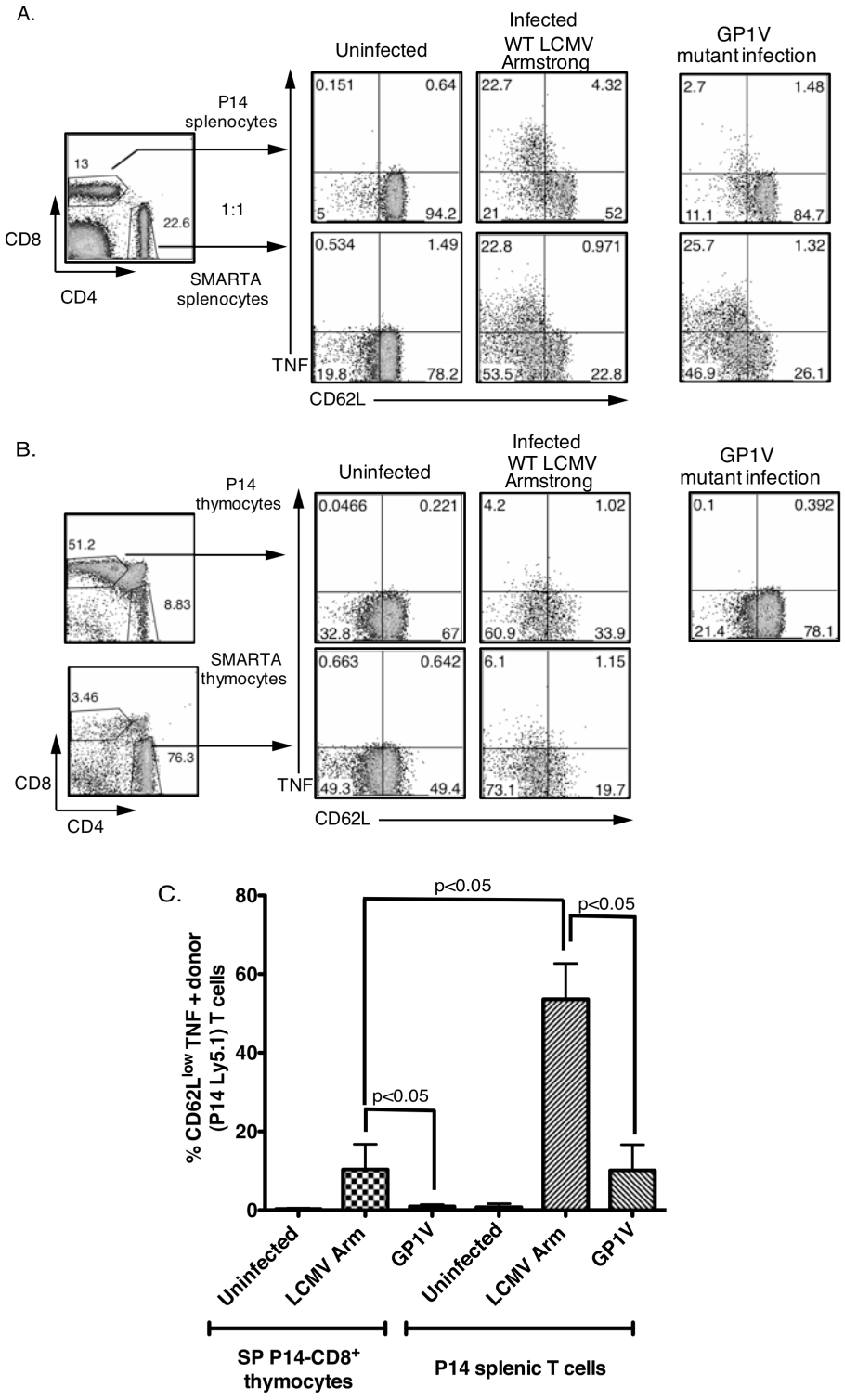

Figure 3.28. $CD8^+$ and $CD4^+$ TCR transgenic SP thymocytes and their respective splenic counterparts exhibit a differential ability to produce TNF during in vivo TCR activation.

Panel A and B, Ly5.1 ($CD45.1^+$) P14-$CD8^+$ and Ly5.1 ($CD45.1^+$) SMARTA-$CD4^+$ splenocytes were mixed at a 1:1 ratio, treated with bfA and transferred into Ly5.2 ($CD45.2^+$) congenic hosts that were uninfected or infected with either WT LCMV Armstrong or the LCMV variant GP1V. Ly5.1 ($CD45.1^+$) P14-$CD8^+$ and Ly5.1 ($CD45.1^+$) SMARTA-$CD4^+$ thymocytes were treated with bfA and transferred separately into Ly5.2 ($CD45.2^+$) congenic hosts that were infected with either WT LCMV Armstrong or the viral variant GP1V. Spleens from all recipient mice were harvested 4 hours later and directly stained for intracellular TNF. The percentages of donor Ly5.1 ($CD45.1^+$) P14-$CD8^+$ and Ly5.1 ($CD45.1^+$) SMARTA-$CD4^+$ splenic T cells and Ly5.1 ($CD45.1^+$) SP thymocytes that are TNF positive and have down-regulated CD62L are shown. Panel C, The average percentages of $CD62L^{lo}TNF^+$ donor T cells detected ex vivo are shown. One-way ANOVA with Tukey post-test was used to compare the mice that received P14 thymocytes or splenocytes and were either uninfected or infected with WT LCMV strain or the viral mutant strain ($p<0.05$). These data are a pool of 6 experiments. Error bars indicate SD.

V. Preconditioning of CD8+ P14 TCR transgenic SP thymocytes with splenocytes providing appropriate TCR-self MHC interactions prior to activation does not enhance their ability to produce TNF during stimulation.

Naïve T cells require low levels of TCR- MHC interactions for their survival in the periphery and to respond optimally to an antigen during activation (356). Preconditioning of polyclonal thymocytes with splenocytes for 6 hours *in vitro* did not enhance their ability to produce TNF. Given that, I hypothesized that conditioning of SP thymocytes with appropriate TCR-peptide/MHC interactions may be important for their ability to produce TNF. In order to test this hypothesis, purified P14 thymocytes were pre-incubated with B6 splenocytes or H-2D^{b} KO splenocytes for 6 hours and then stimulated with GP33-pulsed B6 splenocytes. I found no difference in the ability of thymocytes producing TNF between cells that were stimulated with B6 WT versus H-2D^{b} KO splenocytes (Fig 3.31). These results suggest that conditioning of thymocytes with appropriate TCR-MHC interactions does not enhance the TNF producing ability of SP during stimulation. This is line with the observation made with polyclonal SP thymocytes (section M; Fig 3.15) that did not exhibit an enhancement in TNF production when they were preconditioned with splenocytes prior to stimulation.

Figure 3.29. Pre-conditioning of CD8+P14 TCR transgenic SP thymocytes for 6 hours with appropriate TCR- MHC interactions prior to stimulation does not boost their capability to produce TNF during stimulation.

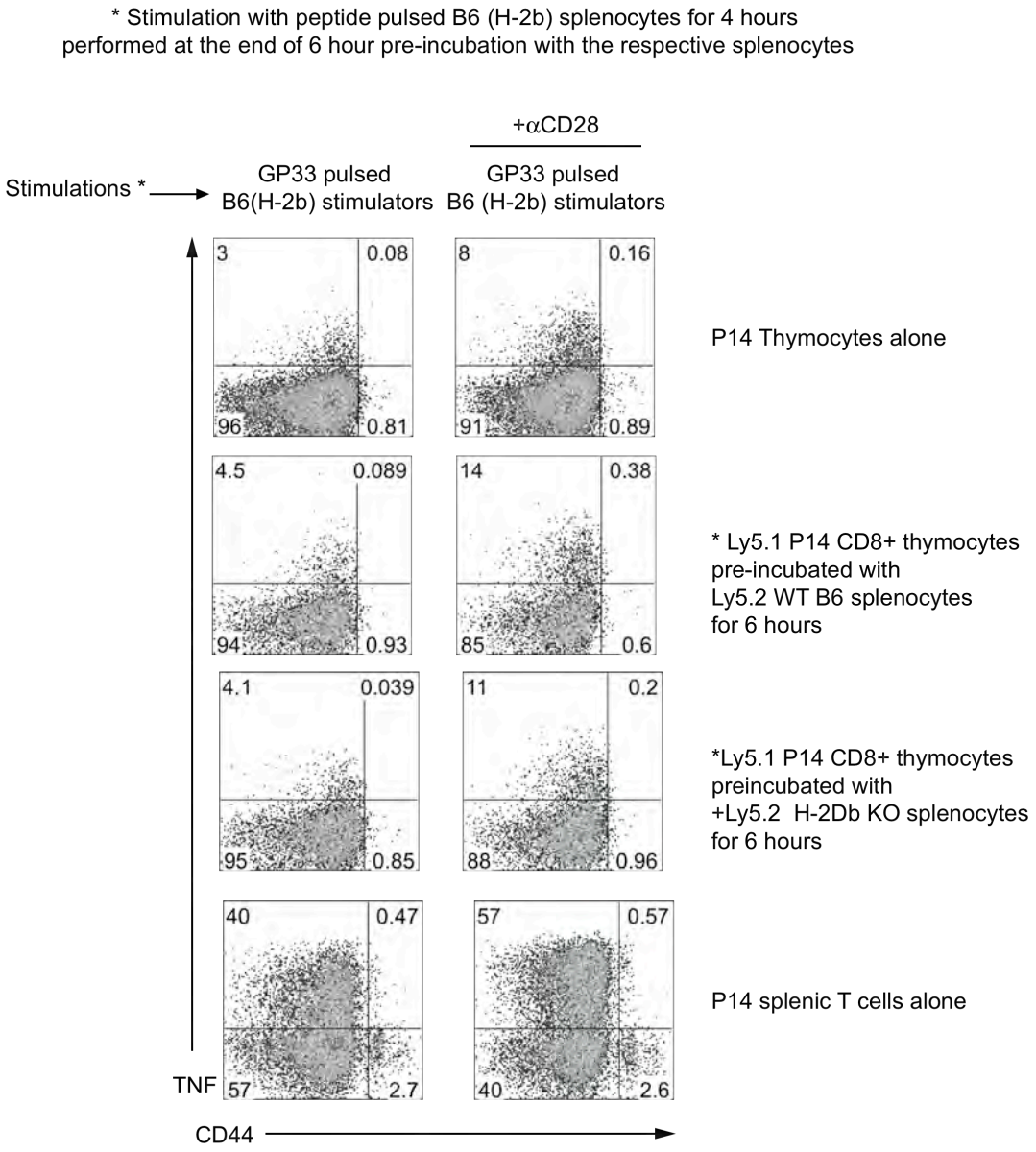

Figure 3.29. Pre-conditioning of CD8+P14 TCR transgenic SP thymocytes for 6 hours with appropriate TCR-MHC interactions prior to stimulation does not boost their capability to produce TNF upon stimulation.

Ly5.1 (CD45.1^{+}) CD8^{+} P14 TCR transgenic thymocytes and splenocytes were stimulated either alone with GP33 peptide-pulsed and irradiated B6 (H-2^{b}) stimulators at 1:1 ratio or in the presence of αCD28 for 4 hours as described in Materials and Methods (1st and 4th row plots). Subsequently, CD8^{+} P14 TCR thymocytes were pre-incubated with either control B6 (H-2^{b} WT) splenocytes or B6 (H-2^{b} KO) splenocytes at 1:1 ratio for 6 hours in vitro at 37 ℃ (2nd and 3rd row plots). The percentages of CD44^{lo} naïve T cells producing TNF under the described conditions are shown.

X. TNF producing capability of CD8$^+$ P14 TCR transgenic SP thymocytes correlates with their maturation state.

SP thymocytes are comprised of a heterogeneous population consisting of cells at different levels of maturity (43). Immature SP thymocytes express high levels of CD24 (HSA), which is down-regulated as cells progress into maturity (360). This is accompanied by down-regulation of CD69 and the up-regulation of other markers such as CD62L, CD45RB and Qa2 (40, 361, 362). I first compared the maturation profile of the total TNF-producing thymocytes with their TNF non-producing counterparts. I broadly classified SP P14-CD8$^+$ thymocytes based on their CD24 and Qa2 expression into 4 subgroups (Fig 3.30A) namely Subgroup 1 (CD24^{hi} Qa2^{lo}) followed by Subgroup 2 (CD24$^{hi\text{-}int}$ Qa2^{lo}), Subgroup 3 (CD24^{lo} Qa2^{lo}) and finally Subgroup 4 (CD24^{lo} Qa2^{hi}) (38). The small population of CD8$^+$ P14 Tg SP thymocytes that produced TNF displayed a more matured phenotypic profile with the majority of the TNF producers falling in subgroups 2 and 3 compared to the TNF non-producers that fell mostly in subgroups 1 and 2. The maturation differences between the TNF-producing SP thymocytes and the non-producers were also seen in the MFI changes in CD24, CD45RB and Qa2 (dotted line histograms and gray histograms in Fig 3.30C). However, the TNF producing CD8$^+$ P14 Tg SP P14-CD8$^+$ thymocytes possessed a less mature phenotype when compared to their splenic counterparts. As described in Fig 3.30A and Fig 3.30B, >60% of the TNF producing thymocytes constituted subgroups 2 and 3 relative to the TNF producing splenic T cells that constituted >80% in subgroups 3 and 4. The differences were also reflected in the MFI of maturation markers (dark line histograms and black histograms in

Fig. 3.30C). I next examined the TNF-producing capability of each of the 4 subgroups in the SP thymic subset individually. The subgroups showed increasing MFI of CD45RB, consistent with their maturation state (Fig 3.32D*)*. There was a progressive increase in TNF production on a per cell basis that correlated with maturation with Subgroup 4 having the highest percentage of TNF^+ cells. Together, these results suggest that though the small population of TNF producing SP P14-$CD8^+$ thymocytes is more mature than the TNF non-producing counterparts, these cells are still phenotypically less mature than P14-$CD8^+$ naïve T cells localized in the spleen.

Figure 3.30.TNF producing CD8+P14 TCR transgenic SP thymocytes exhibit a lower maturation status relative to their splenic counterparts

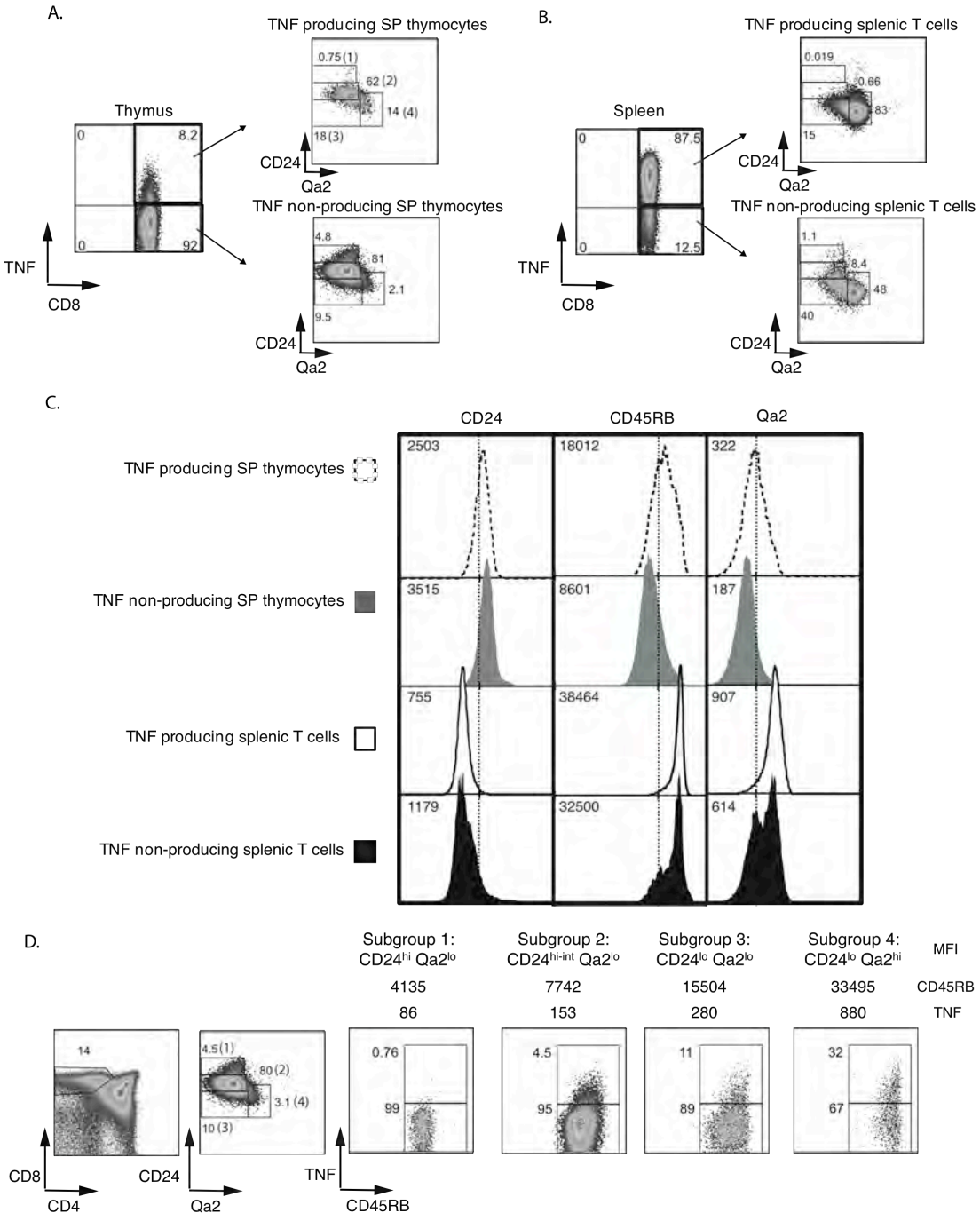

Figure 3.30. TNF producing CD8$^+$ P14 TCR Tg SP thymocytes exhibit a lower maturation profile relative to their splenic counterparts.

Panel A and B, Ly5.1 (CD45.1$^+$) CD8$^+$ P14 Tg SP thymocytes were stimulated with GP33+αCD28 for 4 hours in vitro and then stained for maturation markers and intracellular TNF, as described in Materials and Methods. The TNF producers and non producers of the thymic and the splenic subsets were each classified into 4 subgroups based on their CD24 and Qa2 expression as shown namely Subgroup 1 (CD24^{hi} Qa2^{lo}) followed by Subgroup 2 (CD24$^{hi\text{-}int}$ Qa2^{lo}), Subgroup 3 (CD24^{lo} Qa2^{lo}) and finally Subgroup 4 (CD24^{lo} Qa2^{hi}). Panel C, shows the histogram comparison of the small population of TNF producing SP thymocytes (dotted line histograms), the majority of SP thymocytes that are TNF non-producers (gray histograms) and TNF producing splenic T cells (solid dark line histograms) and TNF non-producing splenic T cells (black histograms). The MFIs of each of the maturation markers in TNF producing and non-producing thymic and splenic T cells are indicated in the left hand side of the histograms respectively. Panel D, shows the maturation profile of the total CD8$^+$ P14 Tg SP thymocytes based on their CD24 and Qa2 expression. The proportion of cells capable of making TNF in the 4 subgroups is shown with respect to CD45RB expression.

Y. Adoptively transferred monoclonal transgenic SP thymocytes progressively gain the ability to produce TNF as function of time spent in the periphery.

The differences in TNF production between $CD8^+$ P14 Tg SP thymocytes and naïve $CD8^+$ P14 Tg splenic T cells upon TCR stimulation parallels the differences in the maturation status of T cells in these two compartments as shown in Fig 3.30. The functional maturation of developing T cells occurs progressively with time upon contact with secondary lymphoid organs after their exit from the thymus (3). Given this, I hypothesized that SP thymocytes migrating into the periphery will gradually acquire the capability to produce TNF efficiently upon TCR stimulation. To recapitulate thymic emigration, 20×10^6 Ly5.1 ($CD45.1^+$) $CD8^+$ P14 Tg SP thymocytes were adoptively transferred into uninfected Ly5.2 ($CD45.2^+$) B6 congenic mice. Spleens were harvested from recipient mice at the indicated time points (Fig 3.31: plots iii,iv,v,vi) and stained for donor Ly5.1 ($CD45.1^+$) $CD8^+$ P14 Tg SP thymocytes producing TNF upon *in vitro* TCR stimulation. The proportion of donor Ly5.1 ($CD45.1^+$) $CD8^+$ P14 Tg SP thymocytes producing TNF upon TCR stimulation increased over the time of the experiment (boxed quadrants in Fig 3.31: plots iii,iv,v,vi). The donor Ly5.1 ($CD45.1^+$) $CD8^+$ P14 Tg SP thymocytes capable of TNF production also exhibited an increasing maturation phenotype (down-regulation of CD24 and up-regulation of CD45RB, Qa2) that approached a level similar to that of splenic T cells by day 14 after transfer. While the recovery of donor cells diminished over time, as shown in Table I, I also observed increases in the mean fluorescence intensity (MFI) of the TNF signal in naïve ($CD44^{lo}$) donor Ly5.1 ($CD45.1^+$) $CD8^+$ P14 Tg SP thymocytes producing TNF from day 2 to day

14 after transfer (Table I). This increase in expression of TNF on a per cell basis by donor Ly5.1 ($CD45.1^+$) $CD8^+$ P14 Tg SP thymocytes was significant ($p<0.05$) and was consistent with the increasing maturation phenotype observed at these time points (Fig 3.31 and Table II). I next compared the changes in MFI of maturation markers in the TNF-producing and non-producing donor thymocytes at day 1 and 2 after transfer, as the $TNF^{negative}$ populations were very small at later time points (Table II). The TNF-producing cells were more mature, again suggesting that the changes in the maturation state of donor thymocytes correlated with increasing capability to produce TNF efficiently on a per cell basis. Stimulation of thymocytes ex vivo in the presence of Ly5.2 ($CD45.2^+$) B6 splenocytes in the co-culture did not affect their maturation status. Together, these results suggest that the progressive maturation of transferred Ly5.1 ($CD45.1^+$) $CD8^+$ P14 Tg SP thymocytes in the periphery positively influences their capability to competently produce TNF upon TCR stimulation.

Figure 3.31. Post-thymic maturation status of CD8+P14 TCR transgenic SP thymocytes in the periphery correlates with their TNF producing capability during stimulation.

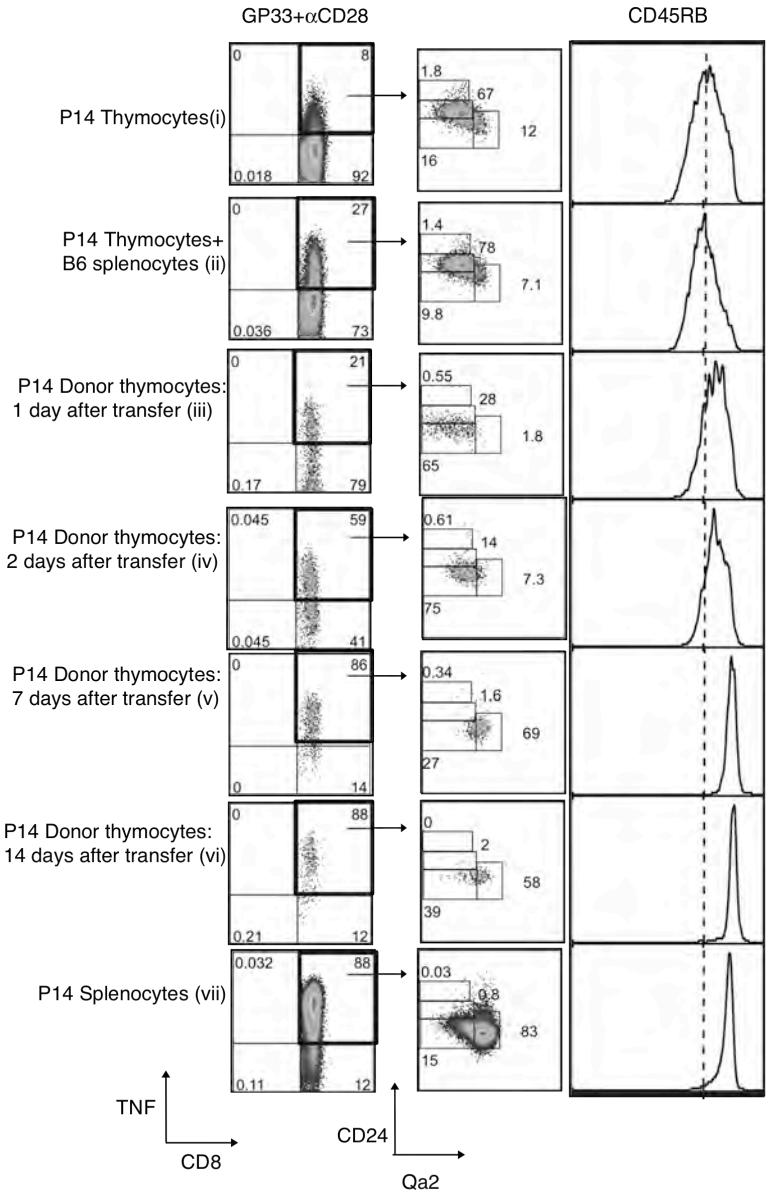

Figure 3.31. Post-thymic maturation status of naïve P14 transgenic T cells correlates with their TNF producing capability during stimulation.

Female Ly5.1 ($CD45.1^+$) $P14\text{-}CD8^+$ thymocytes were transferred into female Ly5.2 ($CD45.2^+$) B6 congenic mice. Host spleens were recovered after the indicated time periods and were stimulated in vitro for 4 hours with GP33+αCD28 and donor $CD45.1^+$ T cells were stained for intracellular TNF as described in Materials and Methods. Dead cells were excluded using Live Dead Aqua Dead cell stain for this experiment. For analysis, cells were gated on the live donor SP $P14\text{-}CD8^+$ T cells and the maturation profile of donor cells that are TNF^+ (indicated by arrows in the boxed quadrants in plots iii,iv,v,vi) were compared at all the time points shown (corresponding histograms). Additionally, some $CD45.1^+$ $P14\text{-}CD8^+$ thymocytes were stimulated before transfer in the context of $CD45.2^+$ B6 splenocytes in vitro for 4 hours with GP33+αCD28 and their maturation profile was compared to $CD45.1^+$ $P14\text{-}CD8^+$ thymocytes and splenocytes stimulated alone in vitro (plots i, ii and vii).

TABLE-I. *SP thymocytes acquire the ability to produce TNF as a function of time in the periphery*[a]

Group	Days post-transfer	Absolute number of Donor P14-CD8$^+$ T cells recovered in the spleen ($\times 10^4$)	TNF MFI of TNF$^+$CD44^{lo} donor T cells ($\times 10^2$)
1.	Day 1	48 ± 8	24 ± 4
2.	Day 2	36 ± 18	24 ± 2
3.	Day 7	14 ± 10[b]	47 ± 4[d,f]
4.	Day 14	5 ± 2[c]	64 ± 19[e,g,h]

[a] The recovery of the donor (CD44^{lo}) SP P14-CD8$^+$ thymocytes from recipient spleens and the MFI of TNF expression at the indicated time points post-transfer are shown. The average recovery and the MFI of TNF expression by donor thymocytes (n=6 per time point) were analysed using One-way ANOVA with a Tukey post-test as described in *Materials and Methods*. Error indicates SD.

[b] $p < 0.05$ vs Table 1, group1

[c] $p < 0.05$ vs Table 1, group 1

[d] $p < 0.05$ vs Table 1, group 1

[e] $p < 0.05$ vs Table 1, group 1

[f] $p < 0.05$ vs Table 1, group 2

[g] $p < 0.05$ vs Table 1, group 2

[h] $p < 0.05$ vs Table 1, group 3

N/A, Not Applicable

TABLE-II. *Maturation state of SP thymocytes reflects their TNF producing capability* [a]

Group	Days post-transfer	CD24 MFI of donor T cells (× 10^2)		CD45RB MFI of donor T cells (× 10^2)		Qa2 MFI of donor T cells (× 10^2)	
		TNF+	TNF-	TNF+	TNF-	TNF+	TNF-
1.	Day1	24 ± 6	34 ± 7[h]	239 ±15	137 ± 14[j]	1.4 ± 0.1	0.1± 0.1
2.	Day2	20 ± 3	31 ± 5[i]	305± 33[d]	244± 37	4.9± 2.2	2.8 ± 0.8
3.	Day7	15 ± 3[b]	N/A	588 ± 26[e]	N/A	7.4± 0.8	N/A
4.	Day14	13 ± 2[c]	N/A	629 ± 27[f]	N/A	11.5 ± 5.6[g]	N/A

[a] The average MFI of maturation markers CD24 (n=6), CD45RB (n=6) and Qa2 (n=3 for group1 and 2 and n=6 for for group 3 and 4) in TNF producing donor SP P14-$CD8^+$ are shown. The averages were analysed using One-way ANOVA with a Tukey post-test as described in *Materials and Methods*. Error indicates SD.

[b] $p < 0.05$ vs Table II, group1

[c] $p < 0.05$ vs Table II, group 1

[d] $p < 0.05$ vs Table II, group 1

[e] $p < 0.05$ vs Table II, group 1

[f] $p < 0.05$ vs Table II, group 1

[g] $p < 0.05$ vs Table II, group 1

[h] $p < 0.05$ vs Table II, group 1 TNF+

[i] $p < 0.05$ vs Table II, group 1 TNF+

[j] $p < 0.05$ vs Table II, group 1 TNF+

N/A, Not Applicable

Z. Adoptively transferred polyclonal thymocytes progressively gain the capability to produce TNF with time spent in the periphery without a requirement for any cell division.

Adoptive transfer of SP thymocytes is a model of forced emigration. However SP thymocytes have been shown to exhibit similar expression of molecules such as high expression of CD62L and α_E integrin and intermediate levels of $\alpha_E\beta_7$ integrin and CCR9 compared to their naturally emigrating thymic counterparts (46, 363). Additionally, both SP thymocytes and RTEs have also been showed have similar migratory potential (46, 363). Given that transgenic T cells acquire the capability to produce TNF with time spent in the periphery, I next wanted to determine if this was true with the polyclonal T cells as well. Also, I wanted to determine if thymocytes undergo any cell division to eventually gain the capability to produce TNF. In order to test this, I adoptively transferred CFSE labeled Ly5.1 ($CD45.1^+$) B6 thymocytes into Ly5.2 ($CD45.2^+$) congenic hosts for 6 and 12 hours and 1, 2, 4 and 8 days and then stimulated the recovered cells with anti-CD3. I had determined previously that *in vitro* pre-conditioning of thymocytes for 6 hours with splenocytes did not increase the percentage of TNF producers relative to thymocytes stimulated with splenocytes for 4 hours without any preconditioning (section M; Fig 3.15). Consistent with this finding, I observed that by 6 hours after adoptive transfer *in vivo*, 30% of the polyclonal thymocytes were TNF^+, and there was no CFSE dilution in these cells (Fig 3.32). At subsequent time points, no dilution of CFSE was detected in the thymocyte subsets. This was, however, accompanied by an increase in the proportion of TNF producing donor polyclonal thymocytes (Fig 3.32). Similar to transgenic SP

thymocytes in the previous section, the survival of the polyclonal thymocytes was also compromised at later time points, but the MFI of the TNF producers increased with time in the periphery (Table III). Together, these results suggest that, as with the transgenic T cells, polyclonal thymocytes also gain the ability to produce TNF with time in the periphery under conditions where they do not require any cell division.

Figure 3.32. Adoptively transferred polyclonal thymocytes gradually gain the ability to produce TNF with time spent in the periphery without any requirement for cell divison.

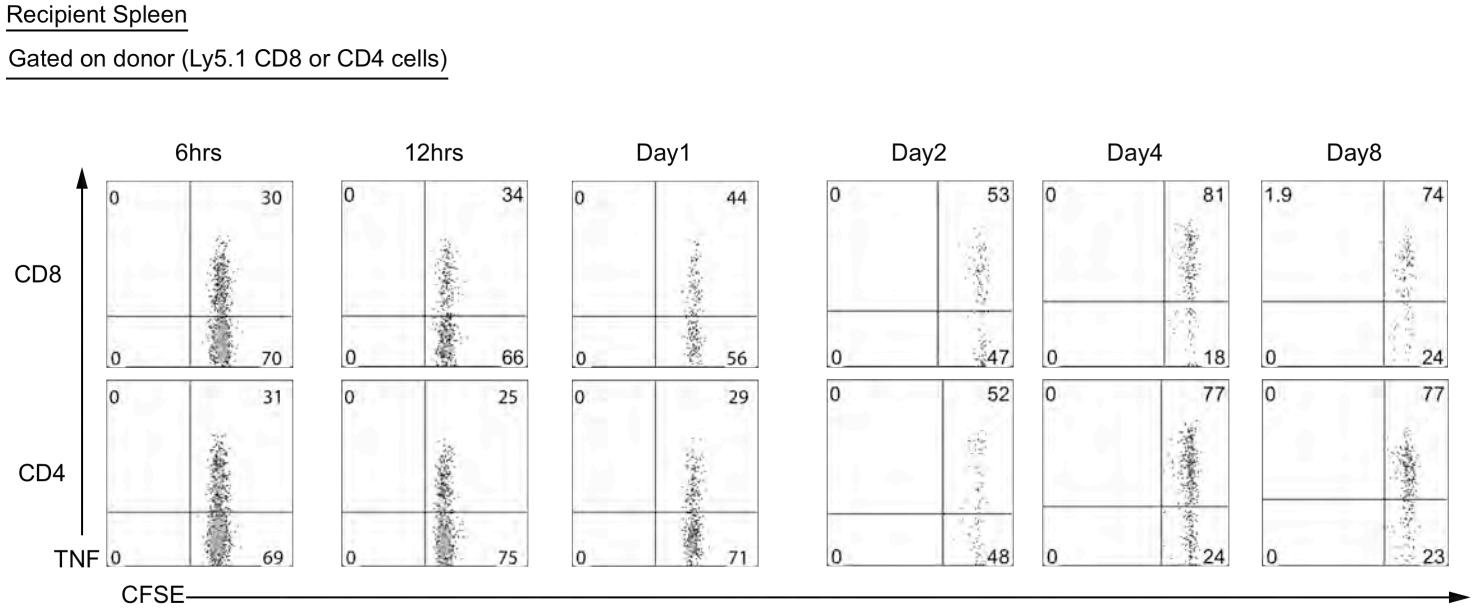

Figure 3.32. Adoptively transferred polyclonal SP thymocytes gain the ability to produce TNF with time spent in the periphery without the requirement of cell division.

Ly5.1 (CD45.1$^+$) thymocytes were labeled with 2μM of CFSE as described in Materials and Methods. 30 × 10^6 cells were transferred into Ly5.2 (CD45.2$^+$) congenic hosts for the indicated time periods. Host spleens were harvested after each time point and stimulated with αCD3 (250ng/ml) +αCD28 (2.5μg/ml) for 4 hours followed by intracellular staining for TNF. Shown are the percentages of TNF producing CD8$^+$ and CD4$^+$ thymocytes with respect to their CFSE staining.

TABLE-III. *Adoptively transferred polyclonal SP thymocytes acquire the ability to produce TNF as a function of time in the periphery*[a]

Group	Days post-transfer	Absolute number of Donor CD8$^+$ T cells recovered in the spleen ($\times 10^4$)	TNF MFI of CD8 CD44^{lo} donor T cells ($\times 10^2$)	Absolute number of Donor CD4$^+$ T cells recovered in the spleen ($\times 10^4$)	TNF MFI of CD4 CD44^{lo} donor T cells ($\times 10^2$)
1.	6 hours	14.1 ± 2.9	5.6 ± 0.3	39.0 ± 7.6	3.8 ± 0.6
2.	18 hours	16.3 ± 2.7	4.7 ± 0.4	38.5 ± 8.6	3.4 ± 0.2
3.	Day 1	15.1 ± 4.3	6.0 ± 1.5	42.8 ± 14.3	4.1 ± 0.6
4.	Day 2	3.8 ± 1.6[b]	9.3[d,f]	8.8 ± 3.5	7.6[h,j]
5.	Day 3	7.9 ± 1.7[c]	12.2 ± 0.4[e,g]	18.3 ± 3.5	9.0 ± 1.6[i,k]

[a] The recovery of the donor CD8$^+$ and CD4$^+$ thymocytes from recipient spleens and the MFI of TNF expression at the indicated time points post-transfer are shown. The average recovery and the MFI of TNF expression by donor thymocytes (n=3 per time point except day2 n=2) were analysed using One-way ANOVA with a Tukey post-test as described in *Materials and Methods*. Error indicates SD.

[b] $p < 0.05$ vs Table 1, group2

[c] $p < 0.05$ vs Table 1, group 2

[d] $p < 0.05$ vs Table 1, group 1 and [e] $p < 0.05$ vs Table 1, group 1

[f] $p < 0.05$ vs Table 1, group 2 and [g] $p < 0.05$ vs Table 1, group 2

[h] $p < 0.05$ vs Table 1, group 1 and [i] $p < 0.05$ vs Table 1, group 1

[j] $p < 0.05$ vs Table 1, group 2 and [j] $p < 0.05$ vs Table 1, group 2

N/A, Not Applicable

AA. Post-thymic maturation of naturally emigrating polyclonal SP thymocytes licenses them to produce TNF efficiently in the periphery.

I next wanted to directly test the ability of polyclonal RTEs that are naturally seeding into the periphery for their ability to produce TNF upon stimulation. For this, I used mice expressing GFP under the control of the Rag2 promoter (NG-BAC transgenic mice), which allow the study of unmanipulated RTEs. The level of GFP expression by T cells in the periphery of these mice can be used to identify T cells at different stages of post-thymic maturation. The GFP^{hi} T cells have resided in the periphery for 0-7 days, GFP^{lo} T cells have resided in the periphery for 7-14 days and GFP^{neg} T cells have joined the mature naïve (MN) T cell pool (> 14 days in the periphery) (41).

I compared TNF expression (mRNA and protein) in three T cell subsets: SP thymocytes (GFP^{hi}), RTEs (GFP^{hi+lo}) in the spleen, and MN T cells (GFP^{neg}) in the spleen (Fig.3.33A). Previously, I had determined in section H (Fig 3.8) that there were similar levels of TNF message expressed at resting steady state between polyclonal SP thymocytes and bulk splenic naïve ($CD44^{lo}$) T cells. To determine if there may be differences in TNF message levels between RTEs and MN T cells at resting state, I used GFP as an indicator to dissect the splenic subsets and examined the steady state levels of TNF message in unstimulated RTEs and MN T cells using semi-quantitative RTPCR. RTEs expressed similar steady state levels of TNF message as their mature naïve counterparts (Fig3.33B). The level of TNF mRNA appeared slightly lower in $CD8^{+}$RTEs

when compared to $CD8^+$ MN T cells. On the other hand, the levels of the TNF mRNA in $CD4^+$ RTEs seemed similar to that of $CD4^+$MN T cells (Fig3.33B).

A higher proportion of $CD8^+$ and $CD4^+$ RTEs produced TNF in response to αCD3 and αCD28 stimulation when compared to SP thymocytes (Fig.3.33C and D). However, the proportion of $CD8^+$ RTEs producing TNF was lower than MN $CD8^+$ T cell populations (Fig.3.33C). This hierarchical pattern of TNF production was also observed on a per cell basis in the three T cell subsets (Fig.3.33D). In contrast to the $CD8^+$ T cell compartment, a similar frequency of $CD4^+$ RTE and MN T cells produced TNF, but the MFI of the TNF signal was significantly higher in the $CD4^+$ MN T cells relative to both $CD4^+$ RTEs and SP $CD4^+$ thymocytes (Fig. 3.33 C and D). Together, these results suggest that differences in TNF production between RTEs and MN T cells may not be correlated to the differences in TNF message observed prior to stimulation. Collectively, these data support the adoptive transfer model indicating that post-thymic maturation confers the complete licensing of naïve T cells to rapidly produce TNF after TCR engagement.

Figure 3.33. Post-thymic maturation status of naïve polyclonal T cells determines their TNF producing capability

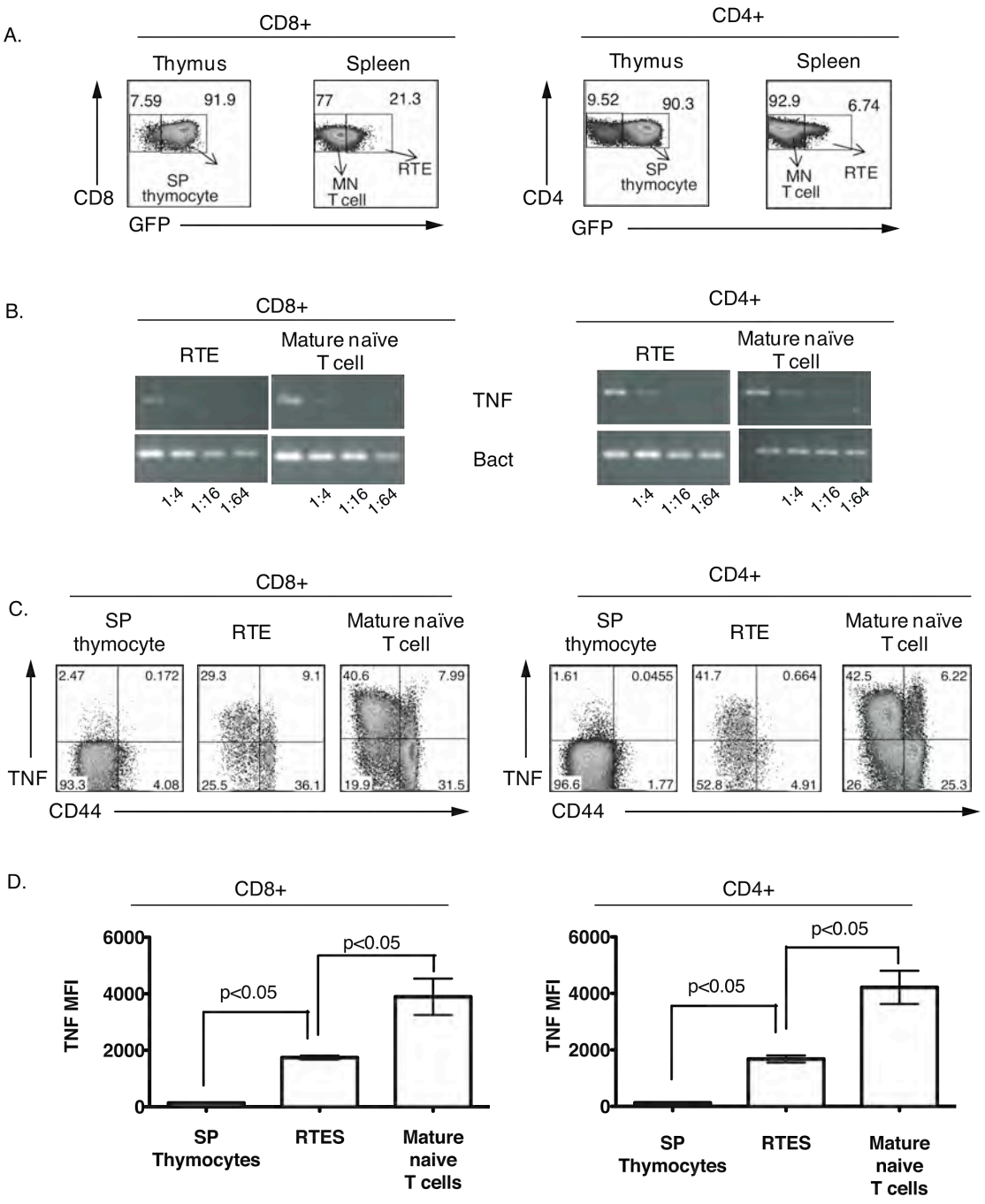

Figure 3.33. Post-thymic maturation status of naïve polyclonal T cells determines their TNF producing capability.

Panel A, shows the GFP profile of $CD8^+$ and $CD4^+$ T cells in the thymus and the spleen of NG-BAC mice. Panel B, RTEs (GFP hi and lo) and mature naïve T cells (GFP negative cells) were sorted (both $CD8^+$ and $CD4^+$ subsets) and the resting steady state levels of TNF mRNA were measured using semi-quantitative RTPCR as described in Materials and Methods. Panel C, Thymocytes and splenocytes from NG-BAC transgenic mice were stimulated with αCD3+αCD28 for 4 hours and then stained for maturation markers and intracellular TNF. The GFP profile of SP thymocytes, RTEs and MN T cells in the $CD8^+$ and $CD4^+$ compartments is shown. C and D, The percentages of $CD44^{lo}$ TNF producing cells in the 3 different T cell subsets and their respective average MFI for TNF expression are shown. The average MFIs of TNF expression were analyzed by one-way ANOVA with a Tukey post-test. The data are representative of 4 individual mice. The error bars indicate SD.

Chapter 3: Summary

1. T cell derived TNF plays an immunoregulatory role in limiting the magnitude of a virus-specific $CD8^+$ T cell response.
2. Naïve T cells in secondary lymphoid organs rapidly produce TNF upon activation of the antigen receptor.
3. In contrast, SP thymocytes show a very poor ability to produce TNF when compared to naïve T cells in the spleen.
    - *SP thymocytes share similar activation profile in terms of upregulation of CD25, CD69 and downregulation of CD62L relative to their splenic counterparts (in P14 Tg system).*
    - *SP thymocytes show impairment in one of the proximal TCR signaling events (pERK) relative to naïve splenic T cells.*
    - *SP thymocytes show reduced upregulation of TNF mRNA relative to splenic T cells upon activation.*
4. Despite their poor ability to produce TNF upon activation, SP thymocytes express mature TNF mRNA, suggesting a post-transcriptional regulation of TNF expression.
5. Antigen-presentation in the splenic environment does not enable SP thymocytes to optimally produce TNF during activation.
6. SP thymocytes gradually acquire full ability to produce TNF efficiently upon stimulation as a function of time spent in the periphery and without cell division.
7. Post-thymic maturation of the naïve T cells in secondary lymphoid organs completes the licensing for rapid TNF production during activation.

Chapter 3: Discussion

TNF is the earliest known cytokine produced by naïve T cells in secondary lymphoid organs after TCR stimulation (1). *In vitro* studies with effector T cells revealed that $CD8^+$ T cells undergo a transient and rapid burst of TNF production that is extinguished rapidly despite the continuous presence of the antigen whereas $CD4^+$ T cells show sustained production of TNF for up to 6 hours (355, 364). Our *in vitro* kinetic experiments with polyclonal T cells show that both $CD8^+$ and $CD4^+$ naïve splenic T cells transiently synthesize TNF, with its production peaking at 4-5 hours and diminishing by 7-8 hours despite continuous stimulation. This suggests that, similar to effector T cells, the regulation of TNF production is tightly regulated in naïve T cells as well.

TNF signaling via TNFRI and TNFRII has been shown to play a co-stimulatory role along with CD28 in augmenting early T cell responses, especially in increasing IL-2 production and by regulating the threshold of activation during priming (186-189, 365). Other studies have shown that the TNF plays an important role in down-regulating T cell responses during acute viral infections and against tumor cell growth (182, 190-192). These studies indicate that TNF may be playing distinct roles at different stages of an immune response. Our data suggest that absence of T cell-derived TNF also leads to accumulation of higher frequencies of antigen-specific T cells during a viral infection. The previous findings with TNF-deficient and TNFR-deficient mice also revealed that the mechanism behind the higher accumulation of TNF or TNFR-deficient T cells was due to their reduced apoptosis (191, 192). In contrast to these findings, however, adoptive

transfer of transgenic WT P14 and TNF- deficient P14 T cells into either WT or TNF deficient hosts indicated that there was no difference in the apoptotic status of TNF deficient P14 T cells relative to WT P14 cells during a viral infection, suggesting that reduced apoptosis may not be the mechanism for the accumulation of higher frequencies of antigen-specific T cells. Additionally, the differences between the previous reports and my results may perhaps be due to differences in the experimental systems used. In the adoptive transfer experiment of WT P14 and TNF-deficient P14 T cells into TNFR1/2 deficient hosts, I found that WT P14 T cells accumulated to similar levels as the TNF-deficient P14 T cells. This suggests that the accumulation of higher frequencies of TNF-deficient antigen-specific T cells may be due to the lack of signaling from host cells expressing the TNF receptors. Another signaling pathway that is disrupted in TNFR1/2 KO hosts involves LT (that exists as a homotrimer $LT\alpha_3$), another member of the TNF superfamily that exerts its effect through TNFR1 and 2. Both TNF and LT have been shown to play a role in the maintenance of the splenic microarchitecture (167). Anti-viral T cell responses are impaired in the absence of $LT\alpha$ owing to the abnormal lymphoid architecture and not due to intrinsic T cell defects (140). Absence of both TNF and LT signaling in the $TNFR1^{-/-}$ and $TNFR2^{-/-}$ hosts may therefore affect the overall T cell responses of donor P14 Tg T cells (both WT and TNF-deficient) compared to the WT hosts.

Given the immunoregulatory role of TNF and the ability of naïve T cells to produce this cytokine early during activation, I wanted to determine the developmental stage when naïve T cells become competent to produce TNF. I addressed this question in the

context of 2 modes of T cell activation, one is the non-specific αCD3+ αCD28 mediated cross-linking of the polyclonal TCR (B6) and the other is specific cognate peptide mediated stimulation of the transgenic TCR (P14 in this case). The major findings discussed in this chapter, showing differences in TNF production between SP thymocytes and splenic T cells and the ability of SP thymocytes to become competent to produce TNF in a post-thymic maturation-dependent manner, are consistent between the polyclonal and the transgenic TCR system. However, I found that there was absolute requirement of antigen presenting cells that facilitated αCD3+ αCD28 antibody mediated cross-linking for the differences in TNF production to become evident between polyclonal thymocytes and splenic T cells during activation. On the other hand, the differences in TNF production were evident between purified transgenic SP thymocytes and splenic T cells with mere peptide stimulation in the absence of antigen-presenting cells. The differences in the requirements of activation of T cells in the polyclonal versus transgenic T cells may reflect their different activation thresholds (366). *In vitro* studies using stimulation of Fyn deficient transgenic $CD4^+$ T cells (AD10 TCR transgenic that recognize pigeon cytochrome C peptide 88-104) with peptide pulsed APCs showed a robust proliferative and IL-2 response whereas αCD3 mediated stimulation led to a profound defect in proliferation. This defect was rescued when αCD3 was used to crosslink the TCR in the presence of αCD4 that initiated the Lck-mediated signaling (367). This study suggested that the mode of activation could result in the activation of different downstream signaling pathways from the TCR and thereby influence the outcome. Similar to this finding, the differences in αCD3+αCD28 mediated cross-linking

of the polyclonal T cells and peptide based stimulation of transgenic T cells may also reflect differences in the mode of stimulation and differences in the downstream signaling events.

Irrespective of the differences in activation of polyclonal thymic and splenic T cells, I show that the unique capability of naïve T cells (both polyclonal and transgenic) to produce TNF is only acquired after emigration into the periphery via a gradual licensing process that occurs progressively in the periphery. The thymus is a primary lymphoid organ, where developing thymocytes undergo positive and negative selection that ultimately determines thymic output and contributes to the establishment of the T cell repertoire in the periphery (368). Our data show that SP thymocytes are functionally less competent to produce TNF upon TCR stimulation relative to naïve T cells in the secondary lymphoid organs. This reduced capability for TNF production is also evident at the transcriptional level and correlates with lower levels of phosphorylated ERK in SP thymocytes relative to naïve splenic T cells during TCR stimulation. Despite this functional difference, SP thymocytes did not possess any apparent phenotypic defects when compared to naïve splenic T cells during activation (upregulation of CD25 and CD69 and down-regulation of CD62L). This suggests that the signaling pathway downstream of TCR activation that leads to the production of TNF is under a distinct and tightly regulated mechanism in developing SP thymocytes. The poor ability of SP thymocytes to produce TNF was not overcome upon receiving optimal signals from APCs of secondary lymphoid organs (spleen and lymph node) during TCR activation, suggesting that SP thymocytes possess an intrinsic defect in their ability to produce TNF

efficiently upon stimulation. SP thymocytes eventually gain full competence to produce TNF upon TCR stimulation as they undergo post-thymic maturation in the periphery and join the mature-naïve T cell pool in secondary lymphoid organs. This licensing for TNF production does not require homeostatic cell division.

Several studies have shown the expression and the physiological role of TNF within the thymus. For example, in situ hybridization studies revealed the localization of TNF mRNA to the cortical regions of the thymus during ontogeny and studies by Giroir et al showed that there was constitutive expression of TNF in thymic lymphocytes (369). *In vitro* functional studies showed that TNF induced CD25 expression in developing ($CD117^{+}CD25^{-}$) thymocytes *in vitro* (370). TNF has also been shown to induce apoptosis of $CD4^{-}$ $CD8^{-}$ double negative thymocytes that coexpressed both TNFR1 and TNFR2 at lower doses and proliferation at higher doses (371). Interestingly, TNFR1/2 double deficient mice exhibited thymic hypertrophy with an overall increase in total thymocytes but normal distribution of SP $CD4^{+}$ and SP $CD8^{+}$ T cell subsets due to absence of apoptosis in DN thymocytes (371). Collectively, the dual role of TNF in the thymus appears paradoxical and may depend on the location and the quantity of its production at various stages of development.

Alternatively, there is also evidence showing the dangerous effects of deregulated production of TNF in the thymus. For instance, mice that over-express human TNF within the thymus exhibit thymic atrophy, which is primarily associated with premature apoptosis of double negative (DN2) developing thymocytes and diminished numbers of

cortical thymic epithelial cells (cTECs) (372). Mice infected with *Trypanosoma cruzi* show severe thymocyte depletion of $CD4^+$ $CD8^+$ DP thymocytes due to an exacerbated inflammatory reaction mediated by TNF (373). Increased levels of TNF and IFN-γ message have been associated with increased thymocyte deletion and cortical depletion observed in the thymi of patients with Down-Syndrome (DS) (374, 375). It is proposed that this abnormality may be due to improper interactions between developing thymocytes and thymic stromal cells mediated by elevated levels of LFA-1 and ICAM-1 and an abnormal distribution of ICAM-1 in DS thymi that is then exacerbated by the expression of TNF and IFN-γ in DS thymi (376). These reports suggest that overproduction of TNF in the thymus may be detrimental to the T cell developmental process. I detected that resting unstimulated SP thymocytes expressed a small level of mature TNF message similar to their splenic counterparts. However, there was no spontaneous production of TNF protein detected in these cells. This suggests that despite having a similar basal level of TNF transcription, there is a lack of translation of the TNF protein under resting conditions in both these subsets. Therefore, the reduced ability of SP thymocytes to rapidly produce TNF during TCR engagement in the thymus under normal circumstances may be beneficial for the survival of SP thymocytes during T cell selection.

A previous report revealed that TNF production by T cells does not require de novo mRNA expression from the TNF locus, as primary $CD4^+$ T cells contain an immature TNF transcript which, following TCR engagement, is spliced to form a mature TNF message, that results in the synthesis of TNF protein in the absence of new transcription

(377). However, previous observations revealed that treatment of naïve $CD8^+$ T cells with the transcriptional inhibitor actinomycin-D and translational inhibitor cycloheximide completely abrogated the production of TNF, suggesting that new transcription and translation are vital TNF production by naïve $CD8^+$ T cells (1). These experiments were done with whole splenocyte populations. Here, I show that actinomycin-D and cycloheximide treatment of purified P14 TCR transgenic T cells abrogated TNF synthesis indicating that T cell intrinsic transcription and translation is required for early TNF production by naïve T cells. My results here show that there is a slight but significant upregulation of TNF message in the $CD8^+$ SP thymocytes upon TCR stimulation, but it is insufficient for the optimal protein production. Splenic T cells, however, show a dramatic upregulation in TNF message and protein upon activation. These findings suggest that there is distinct transcriptional and post-transcriptional control of TNF gene expression in SP thymocytes relative to splenic T cells. Work done in Jurkat T cells and macrophages has revealed that the 3'UTR of TNF mRNA is vital for TNF regulation. The AU rich regions of the 3'UTR serve as binding sites for translational repressor proteins such as heterogeneous nuclear ribonucleoprotein (hnRNP)A1. These repressors serve as substrates for MAP kinase signaling integrating kinases (Mnks) that are phosphorylated and activated by upstream kinases such as ERK1/2 during TCR stimulation. Once activated, Mnk1 phosphorylates hnRNPA1 that reduces the ability of hnRNPA1 to bind the 3'UTR of TNF mRNA, thereby allowing the translation of TNF message (229). My work supports this, as I observed reduced phosphorylation of ERK in SP thymocytes relative to naïve splenic T cells during the first hour of peptide stimulation. Therefore, the

poor transcription of TNF mRNA and reduced phosphorylation of ERK may together be associated with the limited ability of SP thymocytes to produce TNF. Additionally, another factor contributing to the difference could be differences in TNF mRNA stability. The TNF mRNA may be less stable in SP thymocytes than in naïve splenic T cells after stimulation, resulting in the net increase in TNF mRNA detected in naïve splenic T cells. Other RNA binding proteins (RBPs) such as Human antigen R (HuR) proteins have been shown to bind to the AU rich regions of TNF mRNA and induce its translational silencing (378, 379). Absence of HuR in SP thymocytes has been shown augment TNF biosynthesis in SP thymocytes (379). This suggests one mechanism by which TNF expression may be controlled in SP thymocytes.

Stimulation in the presence of splenocytes partially enabled SP thymocytes to produce TNF efficiently as there was only a partial increase in the proportion of cells producing the cytokine. This effect could be either due to better antigen presentation of exogenous peptides by splenocytes to SP thymocytes. For example, cells of the secondary lymphoid organs (spleen and lymph nodes) including B cells, APCs might offer additional accessory signals that enhance clustering of adhesion molecules during immunological synapse formation and leading the partial production of TNF (380, 381). Additionally, chemokine/ chemokine receptor interactions between stromal cells in the spleen and the T cells can also augment TNF responses (382). The alternative possibility is that there are more antigen presenting cells in the splenic environment that increase the strength of TCR-MHC interactions making SP thymocytes more sensitive to stimulation. Moreover, this effect occurs regardless of whether SP thymocytes are stimulated in the

presence of live or killed (γ-irradiated) splenocytes, suggesting that the peptide-MHC complexes and other potential molecules present on the surface of splenocytes are sufficient for this process. However, despite receiving optimal antigen presentation in the splenic environment, thymocytes are still incapable of producing producing TNF efficiently.

The differences in antigen presentation in the thymus versus the spleen may in turn be reflective of the major fundamental role of these tissues in the immune system. For instance, cells in the thymus are functionally equipped for T cell development and central tolerance while cells in the secondary lymphoid organs are equipped for the initiation of potent immune responses against pathogens in the periphery (383). The peripheral tissue micro-environment can regulate the production of cytokines such as IFN-γ and TNF in antigen-specific T cells as a mechanism to restrict local tissue damage and prevent immunopathology (384). I speculate that a similar mechanism of TNF control in naïve T cells may exist in the primary lymphoid organ (thymus) and secondary lymphoid organs (spleen and lymph node).

Contact with secondary lymphoid organs is vital for the completion of post-thymic maturation of developing SP thymocytes (3). RTEs that reach the periphery undergo phenotypic and functional maturation as they become resident in secondary lymphoid organs (41, 385). My findings indicate that the full competence for TNF production by naïve T cells in the peripheral T cell pool is acquired gradually in a post-thymic maturation dependent manner. One caveat of the adoptive transfer model is that the

recovery of thymocytes from the spleens of the recipient mice decreased over time. Therefore, I cannot exclude the possibility that the increase in the percentage of TNF producing donor CD45.1^{+} SP P14-CD8^{+} thymocytes with time in the periphery may be due to preferential survival of SP thymocytes that are capable of TNF production. Nevertheless, I have shown (using MFI of the TNF signal of transferred thymocytes and polyclonal RTEs) that the progressive gain in the TNF producing capability by naïve T cells occurs as they mature in the periphery.

In mice, developing thymocytes emigrate and populate the periphery at the rate of 1-2% of thymocytes per day throughout the lifespan (44, 47). Therefore, at any given time in an adult immune system, the naïve T cell pool is comprised of cells at various stages of post-thymic development, unlike neonates whose peripheral lymphoid organs are predominantly populated with RTEs (347, 385). The post-thymic maturation status of T cells is a component that has been recently shown to influence T cell fate decisions at the time of antigen encounter (347). This study showed that RTEs produced fewer memory-precursor effector cells (MPECs) and more short-lived effector cells (SLECS) during the immune response to LCMV. Our data show that RTEs produce less TNF relative to MN T cells. Given the immunoregulatory functions of TNF, I speculate that the differential ability of TNF production linked to the post-thymic maturation status of antigen-specific naïve T cells, may also contribute to influencing the fate of the responding T cells during the initial phase of activation. (Model in figure 3.34; Pg 215).

In conclusion, our findings indicate that the licensing of naïve T cells for rapid TNF production is determined by their developmental state. It is an intrinsic property of the developing T cells that is acquired gradually, where functional maturation in secondary lymphoid organs drives developing naïve T cells to eventually attain full competence to produce TNF efficiently during TCR stimulation.

Figure 3.34. Differential ability of TNF production confers functional heterogeneity in the naïve T cell pool

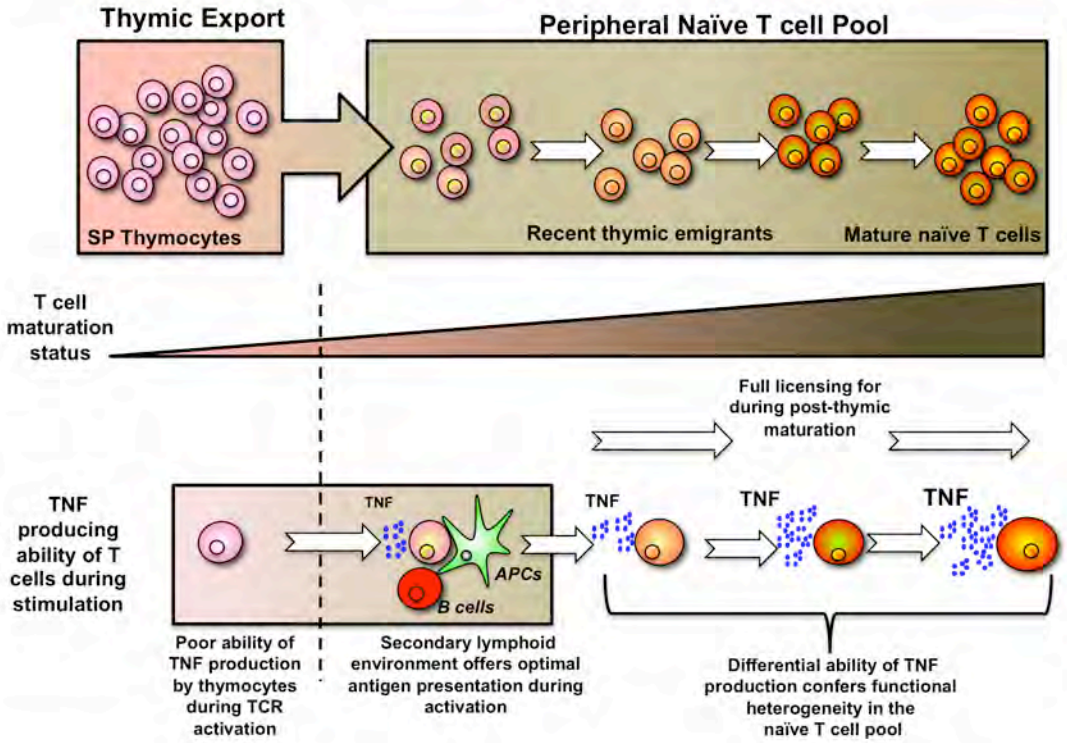

Chapter 4: Changes in the apoptotic signature of alloreactive T cells during TLR mediated abrogation of co-stimulation blockade induced tolerance.

Chapter 4: Abstract

T cell co-stimulatory blockade protocols have shown great promise as an alternative to chronic immunosuppressive drugs for the induction of transplantation tolerance. One such approach uses the administration of αCD154 mAb (αCD40L/MR1) and donor specific transfusion (DST) to induce allograft tolerance. This results in the deletion of host alloreactive T cells within 24 hrs after treatment. Activation via the TLRs at the time of co-stimulation blockade regimen, such as that found in opportunistic infections/inflammation during transplantation, rescues host alloreactive T cells from deletion and abrogates tolerance induction. To study the fate of alloreactive T cells and changes in their apoptotic molecular signature during co-stimulation blockade and during TLR4 administration, I used a syngeneic bone marrow chimeric mouse model, which contains a trace population of alloreactive KB5 Tg $CD8^+$ T cells that recognize $H2K^b$ as an alloantigen. I show here that activated KB5 Tg $CD8^+$ T cells begin to declined by 15 hours after co-stimulation blockade treatment that correlated with the increase in annexin-V positivity. In contrast, KB5-$CD8^+$ T cells from mice treated with LPS during co-stimulation blockade failed to become annexin-V positive. Further, the expression of FasL and BIM, two pro-apoptotic genes involved in apoptosis, was increased in KB5 $CD8^+$ T cells by 12 hrs after co-stimulation blockade, suggesting that both these molecules may be involved in the induction of alloreactive T cell death. During LPS treatment, however, the expression of FasL was inhibited but the expression of BIM was unaffected, suggesting that one mechanism by which TLR agonists may prevent the early apoptosis of alloreactive T cells during co-stimulation blockade is by suppressing the expression of FasL expression on alloreactive T cells. However, I found that despite the rescue from deletion in the presence of LPS, alloreactive T cells are sensitive to Fas-mediated apoptosis in vitro suggesting that there is an early window where alloreactive T cells can be deleted even in the presence of inflammatory agents.

Chapter 4: Introduction

The outcome of T cell activation is determined by the sum of positive and negative co-stimulatory signals that the T cell receives (72).The potential of targeting the co-stimulatory pathways in activated T cells that normally augment T cell responses has been recognized as a vital strategy to induce peripheral tolerance (72). The approach that is used in this chapter of my thesis to induce transplantation tolerance is a two-step combination therapy of donor specific transfusion (DST; donor splenocytes) along with anti-CD154 (αCD154) blocking antibody that leads to prolonged allograft survival (4). This strategy has been used to induce tolerance to allogeneic skin, islets and bone marrow (4, 5, 386). One mechanism by which co-stimulation blockade regimen induces tolerance is by the deletion of activated alloreactive T cells within 24 hours of treatment (4). Inflammation resulting from either the surgical procedure or viral infections at the time of transplantation jeopardizes the effects of co-stimulation blockade leading to graft rejection. The effects of inflammation during transplantation can be studied in an experimental setting by the use of TLR agonists at the time of co-stimulation blockade regimen. TLR activation during co-stimulation blockade has been shown to provoke a vigorous inflammatory reaction and prevent the deletion of alloreactive T cells. This has been shown to result in the abrogation of tolerance induction in a Type-I IFN dependent manner (5). Type 1 IFN provides survival signals to T cells and can act as a third signal for productive T cell activation (387). The induction of type-I IFN during co-stimulation blockade not only protects alloreactive T cells from deletion but also enhances the generation of effector cells (5). It is therefore possible that the lack of early deletion of

alloreactive T cells during TLR administration may be crucial in shifting the balance of effector T cells to T regulatory cells thereby leading to abrogation of tolerance induction (234).

There have been several transcriptional and proteome screening studies done to understand the molecular pathways/indicators that govern tolerance and rejection (388-390). However, the molecular mechanisms by which TLR-agonists protect alloreactive T cells from apoptosis during co-stimulation blockade is an area that has not been investigated. Understanding the changes in the molecular mechanisms functioning in early apoptosis versus survival of alloreactive T cells can be implicated in identifying potential molecular indicators of peripheral tolerance. Additionally, these indicators can also serve as potential targets while devising strategies to induce deletional tolerance in the presence of environmental perturbation as described previously. Therefore, I wanted to investigate the apoptotic signature of alloreactive T cells during co-stimulation blockade induced tolerance induction and in the presence of TLR activation. I hypothesized that TLRs prevent the deletion of alloreactive T cells by differentially regulating the apoptotic signature of alloreactive T cells.

To test this hypothesis, I performed transcriptional profiling of alloreactive T cells during co-stimulation blockade and in the presence or absence of the TLR4 agonist, LPS. To specifically track alloreactive T cells, I used a KB5 synchimeric (bone marrow chimeric) mouse model (described schematically in pg 221) that consists of a small, self-renewing population of alloreactive $CD8^+$ T cells, which recognize $H\text{-}2K^b$ as an

alloantigen and can be identified by the DES clonotypic antibody (338). Consistent with the early deletion of alloreactive T cells during co-stimulation blockade, one of pro-apoptotic molecules that showed a dramatic up-regulation in alloreactive T cells within 12 hours of treatment was FasL expression, a molecule involved in the activation induced cell death (AICD) of T cells. Concomitantly, there was also an early upregulation of BIM, a pro-apoptotic molecule involved in passive cell death (PCD), suggesting that both extrinsic and intrinsic apoptotic pathways may be involved in the early deletion of alloreactive T cells during co-stimulation blockade. Interestingly, absence of Fas or FasL (*lpr* and *gld*) did not abrogate co-stimulation blockade-induced tolerance, suggesting that Fas-FasL pathway may not be crucial for the induction alloreactive T cell death or that it may be playing a redundant role along with other pro-apoptotic molecules such as BIM in inducing alloreactive T cell death during co-stimulation blockade.

In the presence of LPS during co-stimulation blockade, the apoptotic profile of alloreactive T cells with respect to FasL was altered. The expression of FasL was diminished dramatically, while the expression of BIM was not affected in the presence of LPS. Moreover, the expression of Fas was upregulated in alloreactive T cells and non-transgenic $CD8^+$ and $CD4^+$ T cells in the presence of LPS. Given this, I hypothesized that alloreactive T cells emerging from a pro-inflammatory environment (LPS in this scenario) may still be sensitive to early deletion. Validating this hypothesis, I found that provision of exogenous Fas agonist *in vitro* rendered alloreactive T cells (isolated from mice treated with LPS during co-stimulation blockade) to undergo death *in vitro*. This suggests that alloreactive T cells are not completely refractory to the apoptotic signals

and intervention during this early time point can still be a potential strategy to bypass the anti-apoptotic effects of TLR agonists on alloreactive T cells.

Studying the fate of alloreactive CD8+ T cells using the KB5 synchimeric mouse model

A. Generation of KB5 synchimeric mouse model

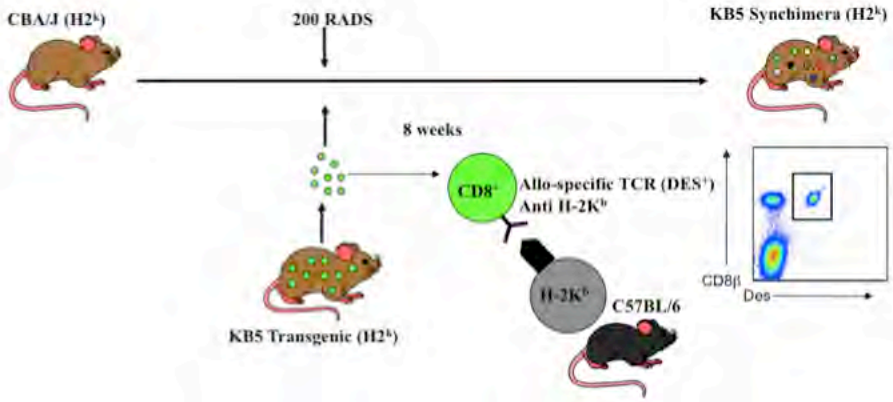

B. Tolerance induction regimen in KB5 synchimeric mouse model and the timing of TLR administration

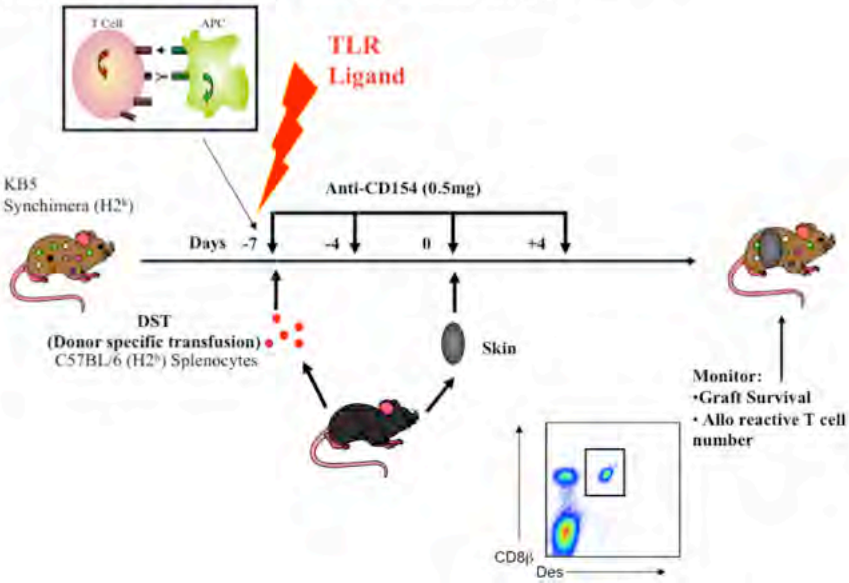

Chapter 4: Results

A. Early decline of alloreactive KB5 transgenic CD8$^+$ T cells correlates with increase in annexin-V positivity within 15 hours of co-stimulation blockade [DST+αCD154 (MR1)]

Previously Thornley and colleagues showed that alloreactive T cells undergo deletion by 24 hours after co-stimulation blockade (4). To determine the kinetics of the decline of alloreactive T cells prior to 24 hours, I first quantified the number of KB5 alloreactive T cells in the spleens of KB5 synchimeric mice treated with co-stimulation blockade regimen (DST+αCD154 also referred to as DST+ MR1) at 6, 11 and 15 hours. I observed that the percentage and the absolute number of alloreactive KB5 transgenic CD8$^+$ T cells (KB5 Tg CD8$^+$ T cells) decreased dramatically between 11 and 15 hours post-treatment (Fig 4.1A). The cells in untreated animals were not affected at all the time points tested (Fig 4.1A). To determine the apoptotic state of KB5 Tg CD8$^+$ T cells I performed annexin-V binding assay, which is a measure of early apoptosis. Briefly, spleens were recovered from mice that were either untreated or treated with DST+MR1 for 12 hours. The splenocytes were then incubated at 37℃ for 4 hours followed by annexin-V binding assay. Incubation of cells at 37℃ diminished the scavenging capacity of macrophages that phagocytose apoptotic cells thereby enhancing the detection of apoptotic cells. The decline of KB5 Tg CD8$^+$ T cells observed between 11 and 15 hours of co-stimulation blockade coincided with an increased frequency of annexin-V positive cells (Fig 4.1B). This was accompanied by the rapid down-regulation of CD127 (IL7Rα)

which indicates that T cells are activated (391)(Fig 4.1B). In addition to the increased frequency of annexin-V positive KB5 Tg $CD8^+$ T cells, there was increased annexin-V positivity on a per cell basis as indicated by the increase in annexin-V MFI after DST+MR1 treatment (Fig 4.1C). The endogenous non-transgenic $CD8^+$ T cells (Non-Transgenic; NTg) showed neither an increase in annexin-V positivity or a change in CD127 levels (Fig 4.1B).

In order to further confirm the apoptotic status of KB5 Tg $CD8^+$ T cells after co-stimulation blockade, the cells were evaluated for the expression of activated caspase3 and for the level of DNA fragmentation by TUNEL staining at 12 hours after DST+MR1 treatment. Caspase 3 is one the executioner caspases whose activation is an indicator of early-stage apoptosis. Briefly splenocytes were incubated for a total of 4 hours at 37℃ As a negative control, splenocytes were also incubated with the PAN caspase inhibitor Z-VAD during the this culture period. The cells were then stained using the FITC conjugated marker for caspase 3. Concurrent with the increase in annexin-V positivity, activated caspase3 was detected in the KB5 Tg $CD8^+$ T cells in mice treated with DST+MR1, but this was not observed with the endogenous non-transgenic $CD8^+$ T cells (Fig 4.2A). The presence of Z-VAD reduced the active caspase3 staining indicating that the stain was specific.

DNA fragmentation is another signature event of cells undergoing apoptosis, and TUNEL (dUTP—nick end labeling) staining can be used to determine the extent of DNA fragmentation. Similar to the increase in caspase 3 activity, there was an increase in

TUNEL positivity in KB5 Tg $CD8^+$ T cells from mice treated with DST+MR1 (Fig 4.2B). Non-transgenic $CD8^+$ T cells showed a higher level of background TUNEL staining, however the levels were similar between cells from untreated and DST+MR1 treated animals (Fig 4.2B). Together these results suggest that the decline of alloreactive KB5 transgenic $CD8^+$ T cells begins as early as 12 hours post-treatment.

Figure 4.1. Decrease in the number of alloreactive KB5 transgenic (Tg) CD8+ T cells by 15 hours post-costimulation blockade correlates with their apoptotic status (increase in annexin-V positivity).

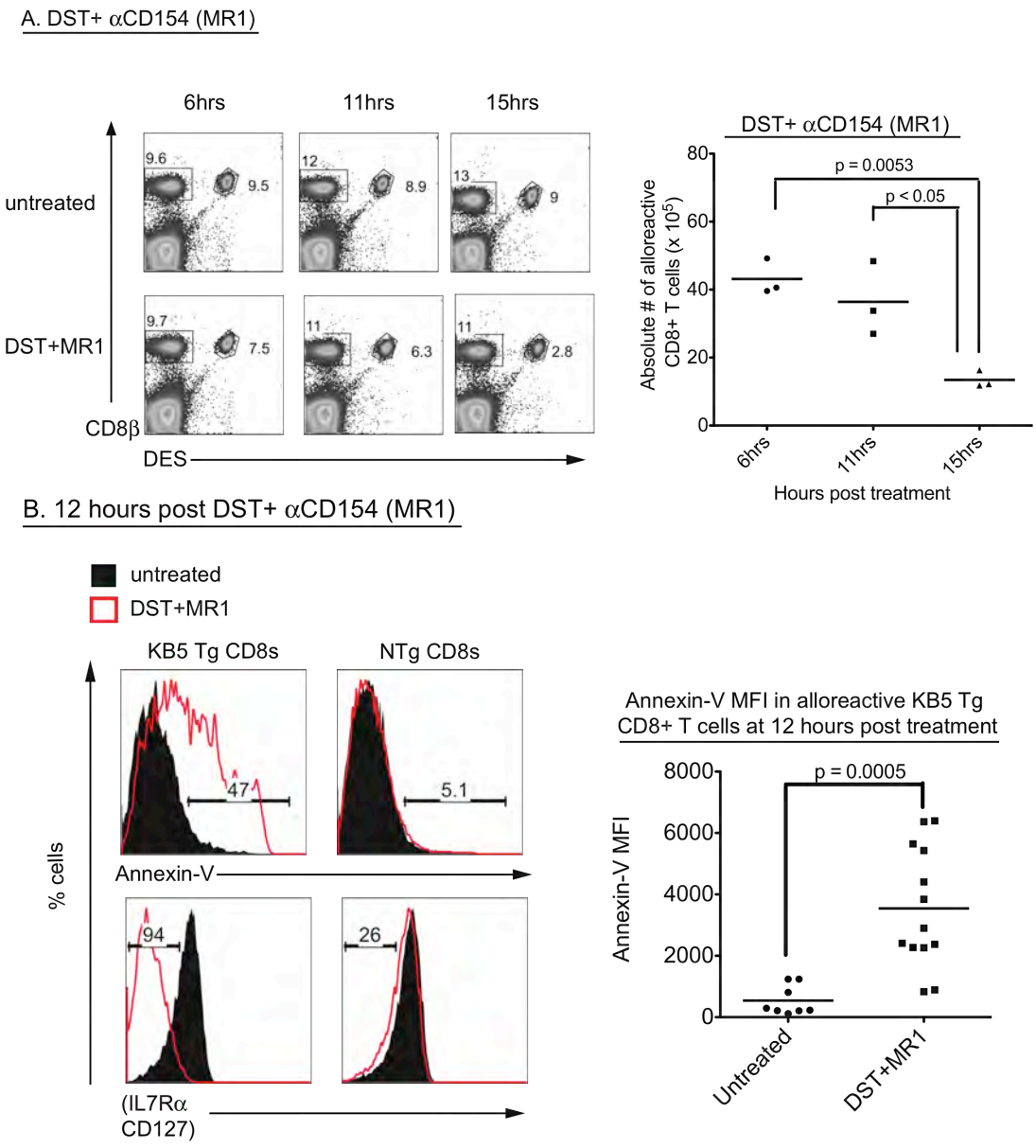

Figure 4.1. Decline of alloreactive KB5 transgenic CD8$^+$ T cell numbers by 15 hours post DST+αCD154 (MR1) correlates with their apoptotic status.

*KB5 CD8$^+$ synchimeric mice were given DST in the form of B6 splenocytes (10×10^6) i.v along with (200μg/mouse) αCD154 (MR1 antibody) i.p. At the indicated time points, recipient spleens were harvested and stained for transgenic alloreactive T cells using KB5-DES clonotypic antibody and CD8β. Panel A shows the percentages and the absolute numbers of KB5 Tg CD8$^+$ T cells at the indicated time points. The groups were compared using a one-way ANOVA analysis with Tukey-post test. P value =0.0053** and P <0.05*. At 12 hours post treatment, recipient spleens were isolated and incubated for 4 hours at 37℃ before annexin-V staining as described in Materials and Methods. Panel B shows the annexin-V profile of KB5 Tg CD8$^+$ T cells and the expression of IL7Rα (CD127) at 12 hours post treatment in both the transgenic and non-transgenic alloreactive CD8$^+$ T cells. The MFI of annexin-V in KB5 Tg CD8$^+$ T cells in untreated and DST+MR1 treated animals at 12 hours is also shown. The values were compared using one-way ANOVA analysis with Tukey post-test. P value = 0.0005***.*

Figure 4.2 Correlation of annexin-V positivity in alloreactive KB5 transgenic CD8+ T cells with activated caspase3 and TUNEL expression 12 hours post-costimulation blockade.

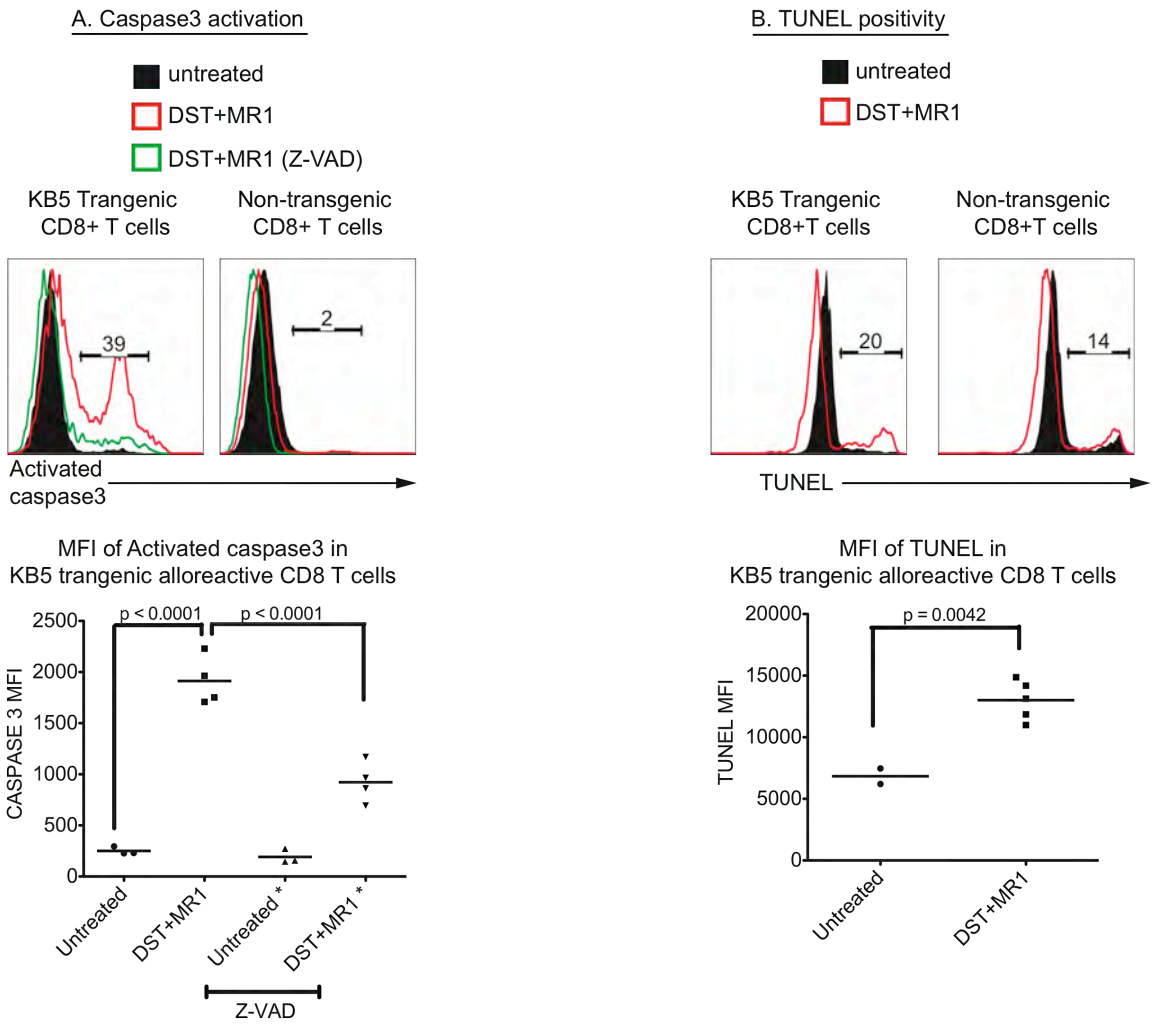

Figure 4.2. Correlation of annexin-V positivity in alloreactive KB5 Tg CD8$^+$ T cells during with activated caspase3 and TUNEL expression during co-stimulation blockade.

*KB5 CD8$^+$ synchimeric mice were given DST in the form of B6 splenocytes (10×10^6) i.v along with (200μg/mouse) αCD154 (MR1 antibody) i.p. At 12 hours post treatment, recipient spleens were isolated and incubated for 4 hours at 37℃ in absence of presence of the PAN caspase inhibitor Z-VAD (1μl/ml concentration). At the end of the 3rd hour, activated caspase 3 was added to all the wells and cells were incubated for another additional hour. Following incubation, cells were stained as per the manufacturers protocol as described in Materials and Methods. Panel A shows the percentages of cells positive for activated caspase3 and their respective activated caspase3 MFI in the indicated groups. The values were compared using one-way ANOVA analysis with Tukey post-test. The P value is <0.0001***. Panel B, splenocytes from the treated mice were incubated for 4 hours followed by TUNEL stain as described in Materials and methods. Briefly, cells were surface stained and cells were fixed with 90% ethanol at -20℃ overnight. This was followed by TUNEL staining and the percentages of TUNEL positive cells and their respective MFIs are shown. The values were compared using unpaired t-test and the p value was determined to be 0.0042***.*

B. Prevention of KB5 Tg CD8$^+$ T cell deletion by TLR4 activation during co-stimulation blockade correlates with inhibition of the early increase in annexin-V positivity.

To study the role of innate immunity in perturbing co-stimulation blockade induced peripheral tolerance, I used the TLR4 agonist LPS to activate the innate arm of the immune system. Exposure to TLR agonists at the time of co-stimulation blockade prevented the deletion of alloreactive KB5 Tg CD8$^+$ T cells and resulted in graft rejection (4). By 72 hours post-treatment, LPS protected alloreactive KB5 Tg CD8$^+$ T cells from undergoing apoptosis as determined by the reduction in the percentage of annexin-V$^+$ cells. To determine if LPS has a similar effect on the early (within the first 24 hours) annexin-V profile of alloreactive KB5 Tg CD8$^+$ T cells, splenocytes from mice treated with cells with DST, DST+MR1 and DST+MR1 and LPS for 9, 12 and 15 hours were incubated at 37℃ for 4 hours and then stained for annexin-V. Similar to the annexin-V profile at 72 hours shown previously by Thornely et al (4), I found a lower percentage of alloreactive KB5 Tg CD8$^+$ T cells that were annexin-V positive in the LPS treated group at all time points (Fig 4.3A). Additionally, the reduction in the percentage of annexin-V positive alloreactive KB5 Tg CD8$^+$ T cells correlated with their lower MFI for annexin-V during DST+MR1+LPS treatment (Fig 4.3B). Presence of DST alone resulted in a increase in annexin-V$^+$ cells and an increase in annexin-V MFI in KB5 Tg CD8$^+$ T cells similar to the cells in DST+MR1 group at these early time points tested. These results suggests that the similarity in annexin-V profile of KB5 Tg CD8$^+$ T cells between DST and DST+MR1 may also be due to early deletion of activated KB5 Tg CD8$^+$ T cells

during DST treatment. It is not clear why and how exactly DST treatment induces deletion of activated KB5 Tg $CD8^+$ T cells. I predict that in contrast to DST, the apoptotic pathways triggered during DST+MR1 may be different that may lead to a profound deletion of alloreactive T cells. The second possibility could be an existence of a threshold for the number of activated alloreactive T cells to mediate rejection. The extent of deletion may be more profound during DST+MR1 treatment bringing the number of alloreactive T cells below the threshold that cannot be recovered back. In contrast, although the apoptotic profile of alloreactive T cells after DST treatment may appear to be similar to DST+MR1 treatment, the number of alloreactive T cells during DST treatment may not be reduced below the threshold rendering them much easier to recover. Clearly, alloreactive T cells from the DST treated group recover and accumulate in numbers at later time points and mediate graft rejection. More importantly, these results show that LPS prevents the early increase in annexin-V positivity in alloreactive T cells that occurs during the first 12 hours of co-stimulation blockade treatment.

Figure 4.3. LPS administration at the time of costimulation blockade prevents the increase in annexin-V positivity in alloreactive KB5 transgenic CD8+ T cells.

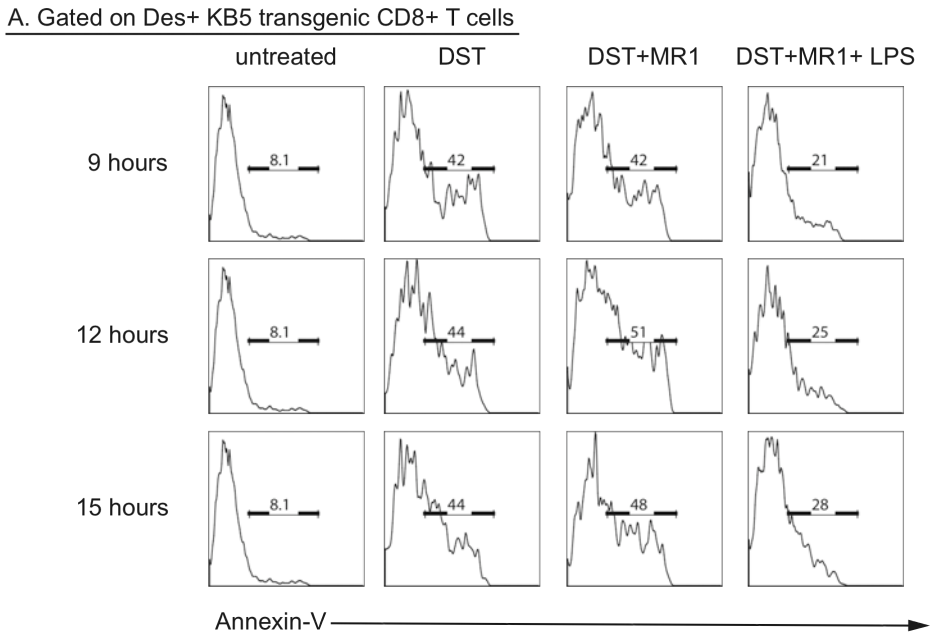

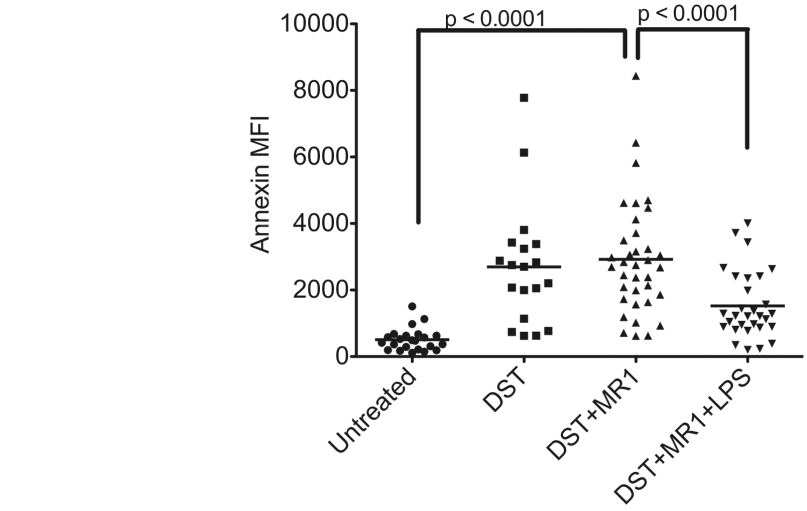

Figure 4.3. LPS treatment at the time of co-stimulation blockade prevents the increase in annexin-V positivity in alloreactive KB5 Tg CD8$^+$ T cells.

*Groups of KB5 synchimeric mice were either treated with DST, DST+MR1 or DST+MR1 along with LPS (100 μg/ mouse) i.p., as described in Materials and Methods. Splenocytes from mice were harvested at 3 time points and the annexin-V profile was determined in KB5 Tg CD8$^+$ T cells as described in Materials and Methods. Panel A, shows the percentages of annexin-V positive cell in three different treated groups (rows) at 3 time points (columns). Panel B shows the MFI of annexin-V of KB5 Tg CD8$^+$ T cells in 3 treated groups at 8-9 hours post treatment. Each dot indicates an individual mouse. The values were compared using one-way ANOVA analysis with Tukey post-test. P value is <0.0001***.*

C. LPS increases the expression of CD25 on alloreactive KB5 Tg CD8$^+$ T cells within 9 hours of co-stimulation blockade treatment.

Co-stimulation blockade does not prevent the activation and proliferation of alloreactive T cells in terms of up-regulation of CD44 and Ki67 staining (4). In order to determine if alloreactive T cells undergoing deletion have other defects in their activation profile, we examined changes in the expression of CD25, CD69, CD62L and CD127 in the KB5 Tg CD8$^+$ T cells, as these molecules are the earliest indicators for of T cell activation. Overall, alloreactive T cells from mice treated with co-stimulation blockade did not show any defects in activation as early as 9 hours post-treatment (Fig 4.4A and B). The percentage of CD44 positive cells and the MFI were similar among all the groups of mice. The percentage of cells that have down-regulated the CD62L and CD127 expression were also similar among DST, DST+MR1 and DST+MR1+LPS confirming that co-stimulation blockade does not prevent the early activation of alloreactive T cells and the effect is TCR dependent (Fig 4.4A). With regard to the up-regulation of CD69 and CD25, LPS resulted in the increased proportion of cells positive for these activation markers (Fig 4.4A). Additionally the expression of CD25 and CD69 was increased on a per cell basis (MFI) (Fig 4.4C and D). CD69 is also upregulated in the non-transgenic T cells upon LPS treatment (Fig 4.4B). It has been shown the type-I IFNs can upregulate CD69 independent of TCR-mediated activation (392). I also observed higher percentages of the cells positive for CD25 in the alloreactive KB5 CD8$^+$ Tg T cells in LPS treated groups. Fig 4.4 C and D show average increases in the percentages and MFI of the activation markers in mice treated with DST, DST+MR1 and DST+MR1+LPS. Together,

these results indicate that overall there is normal activation of alloreactive KB5 Tg $CD8^+$ T cells during co-stimulation blockade. Administration of LPS alters the activation profile of alloreactive T cells leading to enhanced upregulation of CD25 and CD69 compared to cells treated with DST or DST+MR1. This suggests that early differences in the activation profile of alloreactive T cells during DST+MR1 and during the presence of LPS may play a role in influencing the fate of alloreactive T cells at later time points.

Figure 4.4. Phenotypic characterization of alloreactive KB5 transgenic CD8+ T cells after 9 hours of treatment with DST, DST+MR1 and DST+MR1+LPS.

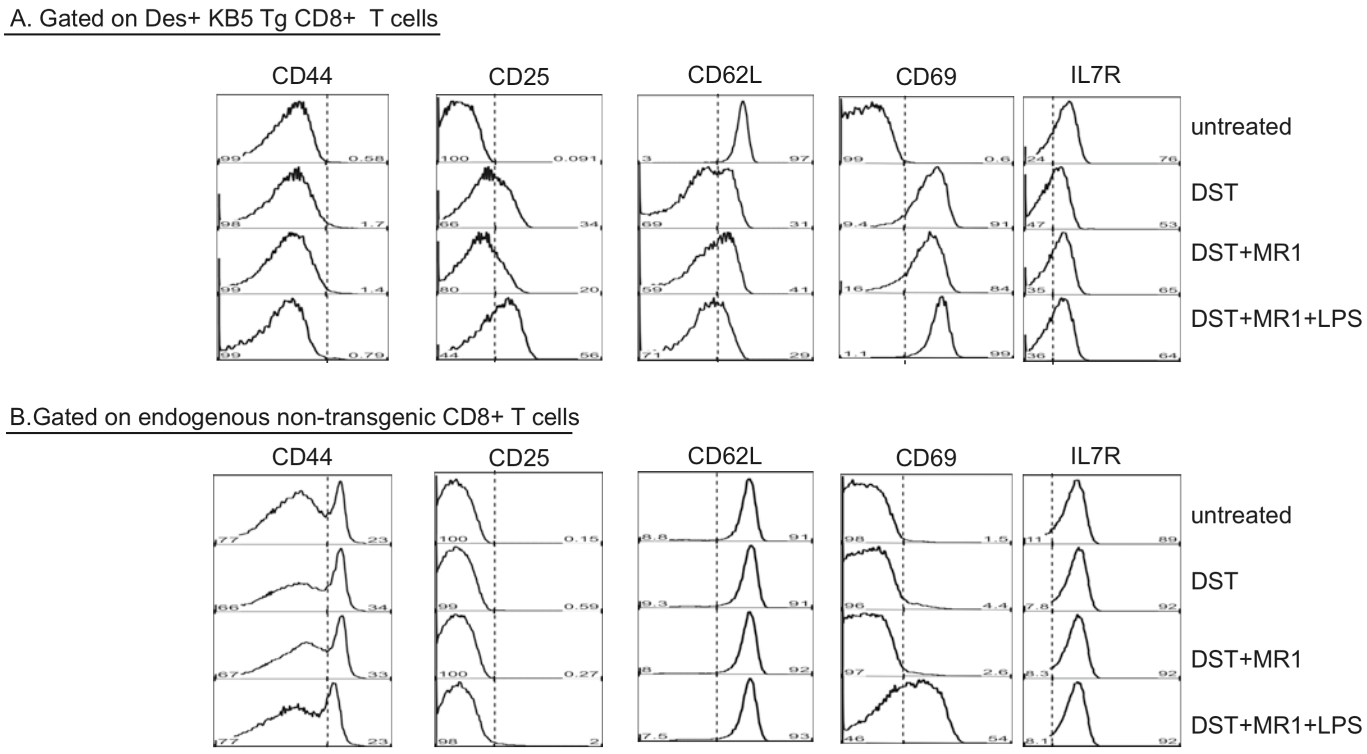

C. Gated on activated Des+ KB5 Tg CD8+T cells

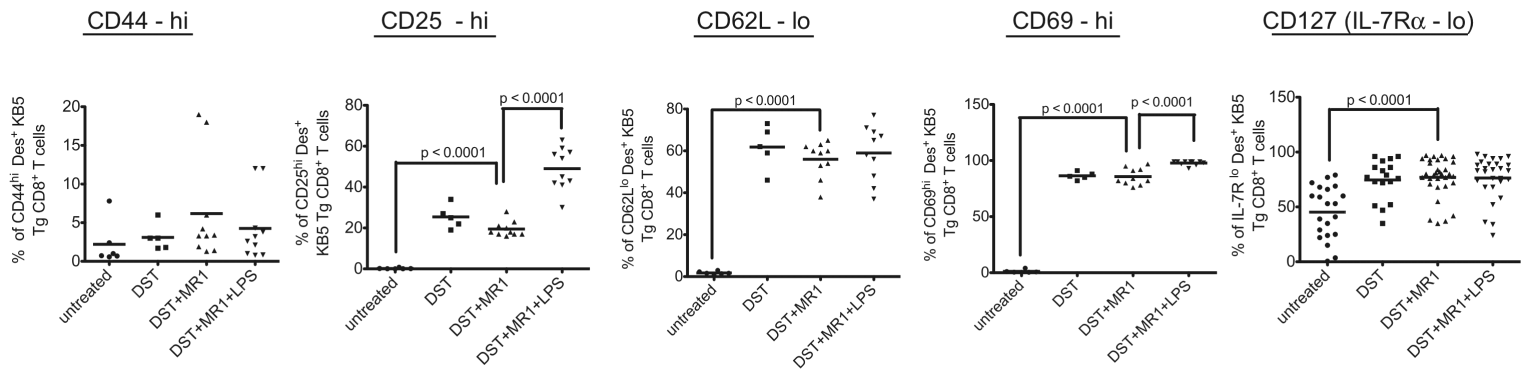

D. MFI of activation markers in total Des+ KB5 Tg CD8+ T cells

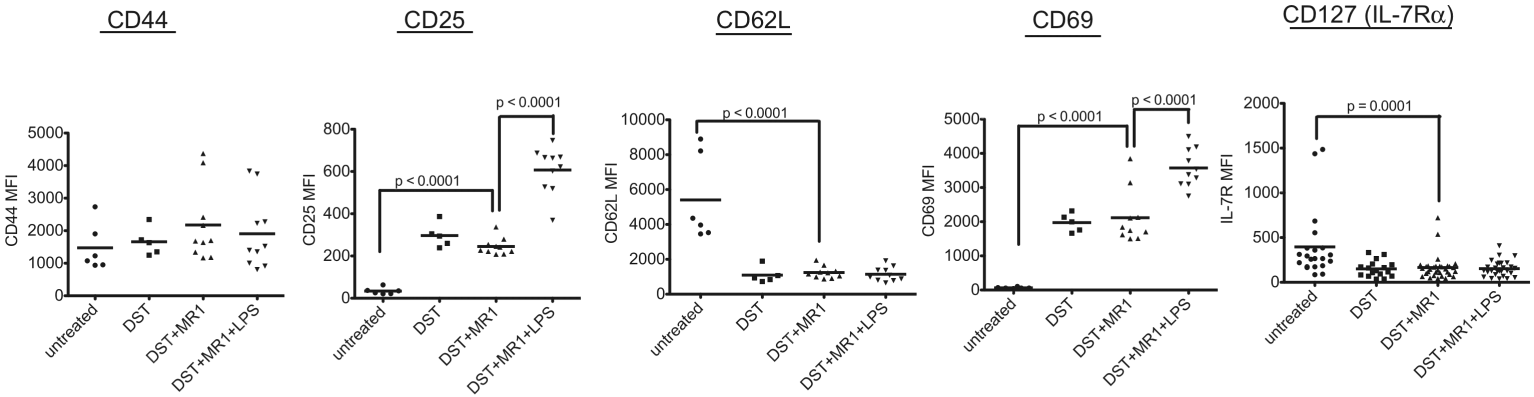

Figure 4.4. Co-stimulation blockade does not prevent the early activation of alloreactive KB5 Tg CD8$^+$ T cells.

Groups of KB5 synchimeric mice were either treated with DST, DST+MR1 or DST+MR1 along with LPS (100 μg/ mouse) i.p. as described in Materials and Methods. Panel A and B show the activation profile of the indicated markers during DST, DST+MR1 and DST+MR1+LPS treatment in KB5 Tg CD8$^+$ T cells and non-transgenic endogenous CD8$^+$ T cells. Panel C and D show the average percentages of activated alloreactive T cells with respect to each of the activation markers and their corresponding changes in the MFI intensities of each of the markers in KB5 Tg CD8$^+$ T cells.

D. LPS alters the apoptotic signature of alloreactive T cells that occurs during co-stimulation blockade.

Since the early changes in the annexin-V profile were detected between 9 and 15 hours in alloreactive T cells, I wanted to determine the apoptotic gene profile of alloreactive T cells during co-stimulation blockade and evaluate how the expression of these genes may be altered in the presence of LPS. To do this, I used an apoptotic gene array consisting of a focused set of genes involved in apoptosis and analyzed the transcriptional signatures of these apoptotic genes in alloreactive KB5 Tg $CD8^+$ T cells during DST, DST+MR1 and DST+MR1 and LPS at 12 hours post-treatment. Briefly, 4 groups (each consisting of 6-7 mice per group) were untreated, or treated with DST, DST+MR1 or DST+MR1+ LPS for 12 hours. KB5 Tg $CD8^+$ T cells were sorted to 99% purity, RNA was isolated from the recovered cells and cDNA was synthesized. The cDNA synthesized from the different groups was subjected to real-time PCR array to determine gene expression changes in 84 genes involved in apoptosis using difference in the Ct values. The fold induction values of various genes with respect to the untreated group are shown in Fig 4.5 A, B, C, D.

In the real time PCR array analysis, only genes possessing Ct (cycle threshold) values below 35 (set cut off) were included in the analysis. All the fold changes in gene expression were normalized to housekeeping genes and compared to the untreated group using the Superarray real time PCR array software. Fig 4.5 A–D shows the fold changes in expression of the genes with respect to the untreated groups and these fold regulation

values are an average of two experiments. Individual experimental analyses are documented in the appendix for further reference. Firstly, it was interesting to note that the apoptotic profile between DST and DST+MR1 was similar correlating with a similar annexin-V profile between the two groups observed previously. However, the DST+MR1 treated group showed a slightly higher level of expression of FasL compared to DST (Fig 4.5B and C and table IV). FasL and IL-10 were the most prominent and consistent of the genes that showed reciprocal expression in DST+MR1+LPS relative to DST+MR1 (Fig 4.5D). FasL mRNA was expressed at higher levels in alloreactive T cells from DST+MR1 group but was detected at low levels in the presence of LPS (E02 in Fig 4.5B and D). Concomitantly, IL-10 mRNA was absent during DST+MR1 treatment but was induced during LPS treated group (E04 in Fig 4.5C and D). Additionally, TNF was also found to be consistently upregulated during DST and DST+MR1 and is more dramatically increased in the presence of LPS. TNF was expressed at 8-10 fold higher in DST and DST+MR1 treated groups and was upregulated > 17fold in the LPS treated groups. In contrast to FasL that showed a dramatic change in its expression, Fas (receptor for FasL) on the other hand was dowregulated at least 3 fold in alloreactive T cells during DST and DST+ MR1 treatment with respect to the untreated group (E01 in Fig 4.5 B and C). Interestingly, the mRNA expression of Fas was not downregulated to the same extent upon LPS treatment resulting in 1.7 fold difference in its expression compared to DST+MR1 group (E01 in Fig 4.5D). The fold up/down-regulation of genes from different families with respect to the untreated group from two experiments is summarized in Table IV. In Table IV, the genes that are consistent between the

experiments are colored blue, and genes that showed a trend in at least one of the experiment are indicated by light orange. Together, these results indicate that the expression of FasL mRNA and IL-10 mRNA is significantly altered during the abrogation of tolerance by LPS treatment and may serve as molecular indicators of alloreactive T cell apoptotic status during co-stimulation blockade.

Figure 4.5. Apoptotic profiling of alloreactive KB5 Tg CD8$^+$ T cells 12 hours post DST, DST+MR1 and DST+MR1+LPS treatment

A. Heat map with log2 (Fold change in DST relative to untreated)

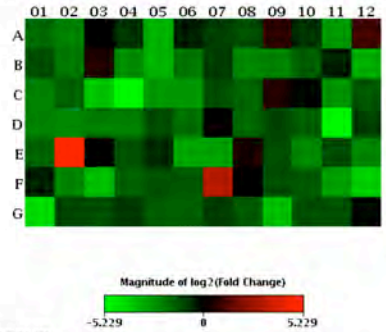

Fold regulation in DST relative to untreated group

Layout	01	02	03	04	05	06	07	08	09	10	11	12
A	Akt1 **-3.47**	Apaf1 **-4.74**	Api5 **-1.03**	Atf5 **-1.75**	Bad **-10.22**	Bag1 **-1.40**	Bag3 **-2.00**	Bak1 **-2.41**	Bax **1.55**	Bcl10 **-1.75**	Bcl2 **-6.75**	Bcl2l1 **1.86**
B	Bcl2l10 **-2.41**	Bcl2l2 **-4.17**	Bid **1.42**	Naip1 **-5.65**	Naip2 **-10.15**	Birc2 **-4.17**	Birc3 **-1.91**	Xiap **-5.17**	Birc5 **-4.96**	Bnip2 **-2.91**	Bnip3 **-1.42**	Bnip3l **-9.44**
C	Bok **-4.66**	Card10 **-3.13**	Nod1 **-14.06**	Card6 **-37.50**	Casp1 **-6.98**	Casp12 **-6.65**	Casp14 **-2.41**	Casp2 **-3.27**	Casp3 **1.44**	Casp4 **-1.17**	Casp6 **-6.21**	Casp7 **-2.81**
D	Casp8 **-4.82**	Casp9 **-5.42**	Cflar **-4.47**	Cidea **-4.62**	Cideb **-2.41**	Cradd **-3.85**	Dad1 **1.10**	Dapk1 **-3.35**	Dffa **-2.14**	Dffb **-3.05**	Tsc22d3 **-37.12**	Fadd **-2.03**
E	Fas **-3.21**	Fasl **32.58**	Hells **-1.02**	Il10 **-2.46**	Lhx4 **-1.62**	Ltbr **-8.54**	Mcl1 **-7.91**	Nfkb1 **1.29**	Nme5 **-2.39**	Nol3 **-5.31**	Pak7 **-2.41**	Pim2 **-5.18**
F	Polb **-1.42**	Prdx2 **-5.09**	Pycard **-12.29**	Ripk1 **-2.99**	Rnf7 **-2.51**	Sphk2 **-2.79**	Tnf **8.49**	Tnfrsf10b **-1.02**	Tnfrsf11b **-2.41**	Tnfrsf1a **-2.89**	Cd40 **-7.23**	Tnfsf10 **-16.10**
G	Tnfsf12 **-20.10**	Cd40lg **-2.23**	Cd70 **-2.41**	Traf1 **-1.86**	Traf2 **-2.85**	Traf3 **-2.94**	Trp53 **-1.92**	Trp53bp2 **-2.83**	Trp53inp1 **-12.29**	Trp63 **-2.41**	Trp73 **-2.41**	Zc3hc1 **-1.14**

B. Heat map with log2 (Fold change in DST+MR1 relative to untreated)

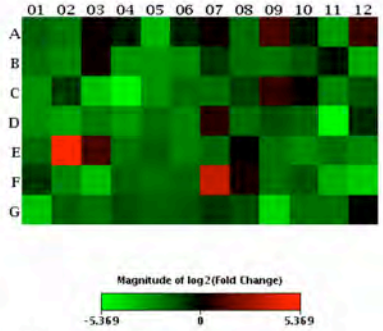

Fold regulation in DST+MR1 relative to untreated group

Layout	01	02	03	04	05	06	07	08	09	10	11	12
A	Akt1 **-3.15**	Apaf1 **-4.33**	Api5 **1.12**	Atf5 **-1.39**	Bad **-10.83**	Bag1 **-1.44**	Bag3 **1.16**	Bak1 **-3.59**	Bax **2.11**	Bcl10 **-1.27**	Bcl2 **-7.35**	Bcl2l1 **1.83**
B	Bcl2l10 **-3.92**	Bcl2l2 **-5.63**	Bid **1.19**	Naip1 **-6.86**	Naip2 **-6.86**	Birc2 **-5.42**	Birc3 **-1.87**	Xiap **-3.57**	Birc5 **-4.12**	Bnip2 **-2.59**	Bnip3 **-1.26**	Bnip3l **-9.56**
C	Bok **-6.08**	Card10 **-1.91**	Nod1 **-15.23**	Card6 **-34.35**	Casp1 **-6.74**	Casp12 **-3.69**	Casp14 **-3.92**	Casp2 **-2.10**	Casp3 **1.68**	Casp4 **1.12**	Casp6 **-5.21**	Casp7 **-2.65**
D	Casp8 **-6.12**	Casp9 **-8.90**	Cflar **-4.57**	Cidea **-7.53**	Cideb **-3.92**	Cradd **-5.04**	Dad1 **1.45**	Dapk1 **-3.72**	Dffa **-2.51**	Dffb **-3.34**	Tsc22d3 **-41.33**	Fadd **-1.64**
E	Fas **-3.45**	Fasl **31.44**	Hells **2.02**	Il10 **-4.01**	Lhx4 **-3.02**	Ltbr **-4.77**	Mcl1 **-3.35**	Nfkb1 **1.02**	Nme5 **-3.92**	Nol3 **-5.93**	Pak7 **-3.92**	Pim2 **-5.82**
F	Polb **-1.78**	Prdx2 **-5.47**	Pycard **-13.37**	Ripk1 **-3.14**	Rnf7 **-3.75**	Sphk2 **-3.11**	Tnf **10.87**	Tnfrsf10b **1.27**	Tnfrsf11b **-3.92**	Tnfrsf1a **-2.79**	Cd40 **-10.55**	Tnfsf10 **-16.82**
G	Tnfsf12 **-14.51**	Cd40lg **-3.02**	Cd70 **-3.92**	Traf1 **-2.50**	Traf2 **-3.03**	Traf3 **-2.71**	Trp53 **-1.78**	Trp53bp2 **-2.42**	Trp53inp1 **-18.93**	Trp63 **-3.92**	Trp73 **-3.92**	Zc3hc1 **-1.09**

C. Heat map with log2 (Fold change in DST+MR1+LPS relative to untreated)

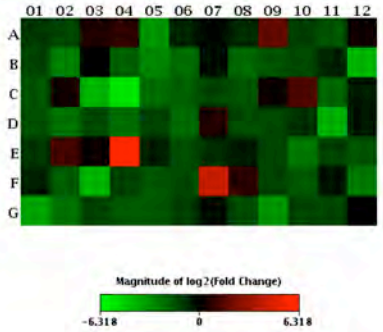

Fold regulation in DST+MR1+LPS relative to untreated group

Layout	01	02	03	04	05	06	07	08	09	10	11	12
A	Akt1 **-2.08**	Apaf1 **-2.60**	Api5 **1.43**	Atf5 **1.75**	Bad **-9.32**	Bag1 **-1.63**	Bag3 **-1.17**	Bak1 **-1.81**	Bax **3.31**	Bcl10 **-2.32**	Bcl2 **-3.14**	Bcl2l1 **1.28**
B	Bcl2l10 **-2.45**	Bcl2l2 **-6.29**	Bid **1.05**	Naip1 **-3.88**	Naip2 **-7.14**	Birc2 **-4.46**	Birc3 **-1.27**	Xiap **-4.38**	Birc5 **-3.07**	Bnip2 **-2.63**	Bnip3 **-1.63**	Bnip3l **-17.59**
C	Bok **-3.10**	Card10 **1.43**	Nod1 **-17.21**	Card6 **-44.89**	Casp1 **-4.93**	Casp12 **-3.64**	Casp14 **-2.45**	Casp2 **-3.25**	Casp3 **1.23**	Casp4 **2.58**	Casp6 **-4.09**	Casp7 **-1.45**
D	Casp8 **-3.05**	Casp9 **-5.16**	Cflar **-2.80**	Cidea **-4.71**	Cideb **-2.45**	Cradd **-4.44**	Dad1 **1.49**	Dapk1 **-2.93**	Dffa **-2.60**	Dffb **-1.92**	Tsc22d3 **-15.47**	Fadd **-1.44**
E	Fas **-2.00**	Fasl **2.17**	Hells **1.20**	Il10 **79.80**	Lhx4 **-1.55**	Ltbr **-2.92**	Mcl1 **-1.78**	Nfkb1 **-1.46**	Nme5 **-2.45**	Nol3 **-5.66**	Pak7 **-2.45**	Pim2 **-3.07**
F	Polb **-1.55**	Prdx2 **-3.54**	Pycard **-16.76**	Ripk1 **-2.38**	Rnf7 **-3.26**	Sphk2 **-2.66**	Tnf **17.67**	Tnfrsf10b **1.66**	Tnfrsf11b **-2.45**	Tnfrsf1a **-3.40**	Cd40 **-1.36**	Tnfsf10 **-5.82**
G	Tnfsf12 **-12.37**	Cd40lg **-5.16**	Cd70 **-2.45**	Traf1 **-3.41**	Traf2 **-3.41**	Traf3 **-2.29**	Trp53 **-1.28**	Trp53bp2 **-2.83**	Trp53inp1 **-9.22**	Trp63 **-2.45**	Trp73 **-2.45**	Zc3hc1 **1.00**

D. Heat map with log2 (Fold change in DST+MR1+LPS relative to DST+MR1)

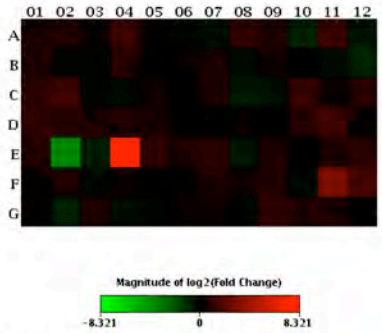

Fold regulation in DST+MR1+LPS relative to DST+MR1

Layout	01	02	03	04	05	06	07	08	09	10	11	12
A	Akt1 **1.52**	Apaf1 **1.67**	Api5 **1.28**	Atf5 **2.42**	Bad **1.16**	Bag1 **-1.13**	Bag3 **-1.36**	Bak1 **1.98**	Bax **1.57**	Bcl10 **-1.83**	Bcl2 **2.34**	Bcl2l1 **-1.43**
B	Bcl2l10 **1.60**	Bcl2l2 **-1.12**	Bid **-1.14**	Naip1 **1.77**	Naip2 **-1.04**	Birc2 **1.21**	Birc3 **1.47**	Xiap **-1.23**	Birc5 **1.34**	Bnip2 **-1.01**	Bnip3 **-1.29**	Bnip3l **-1.84**
C	Bok **1.96**	Card10 **2.75**	Nod1 **-1.13**	Card6 **-1.31**	Casp1 **1.37**	Casp12 **1.01**	Casp14 **1.60**	Casp2 **-1.55**	Casp3 **-1.37**	Casp4 **2.30**	Casp6 **1.28**	Casp7 **1.83**
D	Casp8 **2.01**	Casp9 **1.73**	Cflar **1.63**	Cidea **1.60**	Cideb **1.60**	Cradd **1.13**	Dad1 **1.03**	Dapk1 **1.27**	Dffa **-1.04**	Dffb **1.74**	Tsc22d3 **2.67**	Fadd **1.14**
E	Fas **1.72**	Fasl **-14.51**	Hells **-1.68**	Il10 **319.72**	Lhx4 **1.95**	Ltbr **1.63**	Mcl1 **1.88**	Nfkb1 **-1.50**	Nme5 **1.60**	Nol3 **1.05**	Pak7 **1.60**	Pim2 **1.89**
F	Polb **1.15**	Prdx2 **1.54**	Pycard **-1.25**	Ripk1 **1.32**	Rnf7 **1.15**	Sphk2 **1.17**	Tnf **1.63**	Tnfrsf10b **1.31**	Tnfrsf11b **1.60**	Tnfrsf1a **-1.22**	Cd40 **7.73**	Tnfsf10 **2.89**
G	Tnfsf12 **1.17**	Cd40lg **-1.71**	Cd70 **1.60**	Traf1 **-1.36**	Traf2 **-1.13**	Traf3 **1.18**	Trp53 **1.39**	Trp53bp2 **-1.17**	Trp53inp1 **2.05**	Trp63 **1.60**	Trp73 **1.60**	Zc3hc1 **1.10**

Table IV: Transcriptional differences in the expression of pro and anti-apoptotic genes in alloreactive KB5 Tg $CD8^+$ T cells during LPS-mediated abrogation of tolerance induction

Gene family		DST		DST+MR1 (DM)		DST+MR1+LPS (DML)	
Position	Gene symbol	Expt 1	Expt 2	Expt 1	Expt 2	Expt 1	Expt 2
Bcl-2 family							
A05	Bad	-14.14	-7.39	-9.77	-14.52	-9.65	-9.46
A09	Bax	1.78	1.36	3.04	1.39	4.61	2.31
A11	Bcl-2	-8.83	-5.16	-6.67	-9.32	-3.84	-2.19
A12	Bcl2l1	1.79	1.94	2.35	-1.03	1.39	-1.05
B03	Bid	1.56	1.3	1.35	1.09	1.17	-1.02
Card family							
C08	Casp2	-3.04	-3.52	-2.18	-2.62	-3.61	-3.54
C09	Casp3	2.20	-1.05	2.82	-1.49	1.57	-1.20
C10	Casp4	-1.09	-1.25	1.8	-2.53	3.03	1.70
C12	Casp7	-2.83	-2.78	-2.19	-3.56	-1.59	-1.11
D02	Casp9	-10.5	-2.80	-10.08	-14.93	-12.39	-1.92
Death effector domain family							
D01	Casp8	-6.37	-3.65	-7.88	-4.29	-4.03	-2.03
D12	Fadd	-2.97	-1.38	-1.65	-2.19	-2.21	1.22
TNF ligand family							
E02	FasL	41.87	25.53	30.00	31.56	1.83	2.77
F07	TNF	8.44	8.54	8.47	9.00	10.22	26.50
F12	TRAIL	-19.59	13.23	-20.94	-16.56	-7.14	-5.91
G02	CD40L	-4.09	-1.21	-4.46	-1.88	-6.35	-4.63
TNF receptor family							
E01	Fas	-3.32	-3.11	-2.91	-4.08	-1.85	-1.98
F11	CD40	-10.5	-4.98	-7.15	-25.81	-1.33	-1.62
Anti-apoptotic family							
E04	IL10	-2.32	-2.61	-3.41	-3.23	122.28	58.40

Positive values indicate the fold upregulation and negative values indicate fold down regulation of genes with respect to the untreated groups in two independent experiments

Figure 4.5. Apoptotic profiling of KB5 Tg CD8$^+$ T cells during DST, DST+MR1 and DST+MR1+LPS treatment.

Groups of KB5 synchimeric mice were either treated with DST, DST+MR1 or DST+MR1 along with LPS (100 μg/ mouse) i.p. as described in Materials and Methods. After 12 hours of treatment KB5 Tg CD8$^+$ T cells were sorted to > 97% purity from each of the groups. RNA was isolated and cDNA was synthesized and then amplified by apoptotic RT^2 Real time PCR array (PAMM-012) reagents as described in Materials and Methods. Raw Ct values obtained were uploaded into the Super array web based data analysis software and the ΔΔCt based fold-change calculations were generated with the software. Fold change comparisons were done between the indicated groups. Panel A, B and C show the comparison of apoptotic profile of KB5 alloreactive T cells in DST, DST+MR1 and DST+MR1+LPS treated groups relative to the untreated groups respectively. Panel D shows the comparison of apoptotic profile of KB5 Tg CD8$^+$ T cells in DST+MR1 +LPS relative to DST+MR1 group. The heat maps show magnitude of Log2 (Fold change) between the groups and the layout below show the fold regulation of genes. Genes marked blue showed consistent differences in both the experiments and genes marked in light orange showed desirable (key genes involved in apoptosis) differences in only one of the experiments. The positive values indicate the fold up-regulation (fold change>1) and negative values indicate fold down-regulation (which is negative inverse of the fold changes that < than 1). Table 4 summarizes the fold regulation values of the well-known genes involved in regulating apoptosis.

E. Validation of FasL expression at the mRNA and protein level in alloreactive T cells during co-stimulation blockade and LPS treatment.

Next I confirmed the dramatic increase in FasL mRNA expression in DST and DST+MR1 groups seen in the microarray studies by performing real time RT-PCR analysis using FasL specific primers purchased from two different companies, R&D and Superarray. I purified alloreactive KB5 Tg $CD8^+$ T cells and endogenous non-transgenic $CD8^+$ T cells from untreated and mice treated with DST for 12 hours. I isolated the RNA and synthesized cDNA followed by real time RT PCR. I found almost a 200 fold increase in the expression of FasL in DST treated group compared to the untreated group which was validated by running the sample on a 1% agarose gel (Fig 4.6A). Though there was a minor increase in non-transgenic $CD8^+$ T cells, the band intensities appeared similar on the gel, suggesting that the changes are very subtle in the non-transgenic $CD8^+$ T cells. I next confirmed the expression of FasL mRNA using R&D primers via RTPCR and found that FasL mRNA was detected in purified KB5 Tg $CD8^+$ T cells from DST treated group (Fig 4.6B). This result confirmed the microarray data that FasL mRNA was upregulated in KB5 Tg $CD8^+$ T cells upon DST and DST+MR1 treatment by 12 hours.

I then determined if the changes in the mRNA expression level of FasL correlated with its expression at the protein level. I hypothesized that FasL protein would be up-regulated in alloreactive KB5 Tg $CD8^+$ T cells as early as 9 hours after DST and DST+MR1 treatment as this was the earliest time-point I observed increases in the annexin-V profile of KB5 Tg $CD8^+$ T cells. There was, however, still the possibility the

changes in FasL may be occurring prior to 9 hours. KB5 synchimeric mice were treated with DST, DST+MR1 and DST+MR1+LPS for 9 hours and then stained for surface expression of FasL. The black histograms indicate samples stained with the isotype control and red histograms refer to samples stained with antibody specific to FasL for the indicated groups. There was a subtle increase in FasL in the percentage of cells positive for FasL in the KB5 Tg $CD8^+$ T cells during DST and DST+MR1 treatment (Red histograms) but this increase was not observed in the LPS-treated groups (Fig 4.7 A and B). Likewise there was an increase in the MFI of FasL in the KB5 alloreactive T cells in the DST and DST+MR1 treated groups. (Fig 4.7 B). This increased expression of FasL on the cell surface was not observed in the LPS treated groups (Fig 4.7A and B). These results therefore confirm our microarray data and suggest that FasL may be possibly involved in the early apoptosis of alloreactive T cells during co-stimulation blockade. These data also suggest that FasL may be one of the many pro-apoptotic genes that is differentially regulated in alloreactive T cells in the presence of LPS.

FasL binds its receptor Fas to induce apoptotic cell death. I therefore wanted to determine if there is a concomitant change in the expression of the Fas expression along with FasL on alloreactive T cells during co-stimulation blockade and during LPS administration. To determine this, I first tested the mRNA expression pattern of Fas in DST, DST+MR1 and LPS from the microarray analysis (Table IV). Unlike FasL, there was no dramatic upregulation but instead a 3-4 fold downregulation in the expression of Fas mRNA in DST and DST+MR1 group. With respect to the protein expression levels there was a considerable increase in the MFI of Fas expression during DST and

DST+MR1 treatment over the untreated groups (Fig 4.7 C and D). This discrepancy in the RNA and protein levels of Fas may be attributed to timing of the analysis. The Fas protein expression analysis was performed around 9 hours after treatment, whereas and the mRNA analysis of Fas in the microarray experiment was performed around 12 hours. Therefore it is possible that Fas mRNA detected around 12 hours after co-stimulation blockade may be in the process of degradation. LPS treatment, on the other hand, resulted only in a twofold downregulation of Fas mRNA with respect to DST+MR1 (Fig 4.5D and Table IV). Interestingly, LPS treatment during co-stimulation blockade induced an increase in the percentage and MFI of Fas+ cells in the KB5 Tg $CD8^+$ T cells and also in the endogenous non-transgenic $CD8^+$ T cells and $CD4^+$ T cells (Fig 4.7 C). Together, these results indicate that Fas and FasL may be differentially regulated in alloreactive T cells in the presence of LPS. This further suggests that the and absence sufficient FasL expression in alloreactive T cells despite the presence of Fas expression during LPS treatment may be a mechanism in preventing T cell suicide or fratricide that is initiated during co-stimulation blockade.

Figure 4.6. Confirmation of DST-induced FasL mRNA expression in alloreactive KB5 transgenic $CD8^+$ T cells.

A. Real time RT PCR using FasL specific gene primers (Super-array).

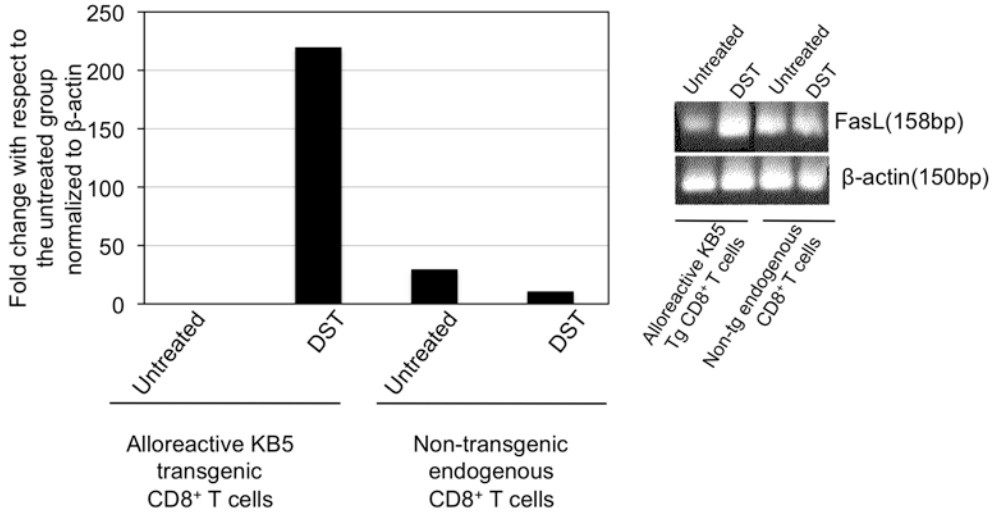

B. RT-PCR using FasL gene primers (R&D primers).

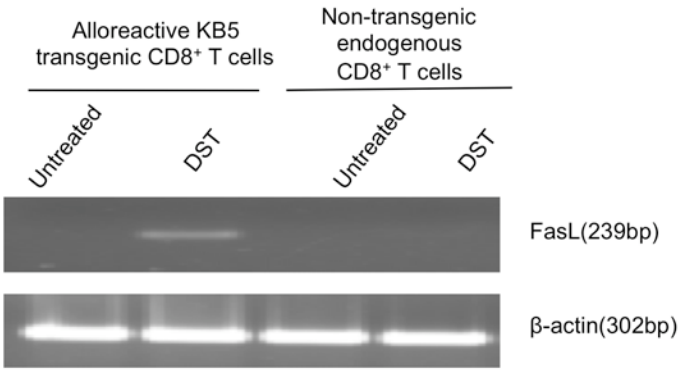

Figure 4.6. Confirmation of DST induced FasL mRNA expression in KB5 Tg CD8$^+$ T cells.

After 12 hours of treatment with DST, KB5 Tg CD8$^+$ T cells were sorted as described in Materials and Methods to 98% purity for samples from untreated mice (transgenic and non transgenic T cells) and 58 and 95% purity for DST treated animals (transgenic and non-transgenic T cells respectively). RNA was isolated and cDNA was synthesized. The cDNA was amplified by real time PCR using FasL specific primers purchased from Superarray. Concomitantly, the cDNA was also amplified by RTPCR using FasL specific primers purchased from R&D. Panel A shows the fold change of FasL mRNA detected with respect to the untreated control. Panel B shows the FasL mRNA detected in alloreactive T cells by RT-PCR.

Figure 4.7. Confirmation of Fas and FasL mRNA expression at the protein levels in alloreactive KB5 transgenic CD8+ T cells after DST, DST+MR1 and DST+MR1+LPS treatment.

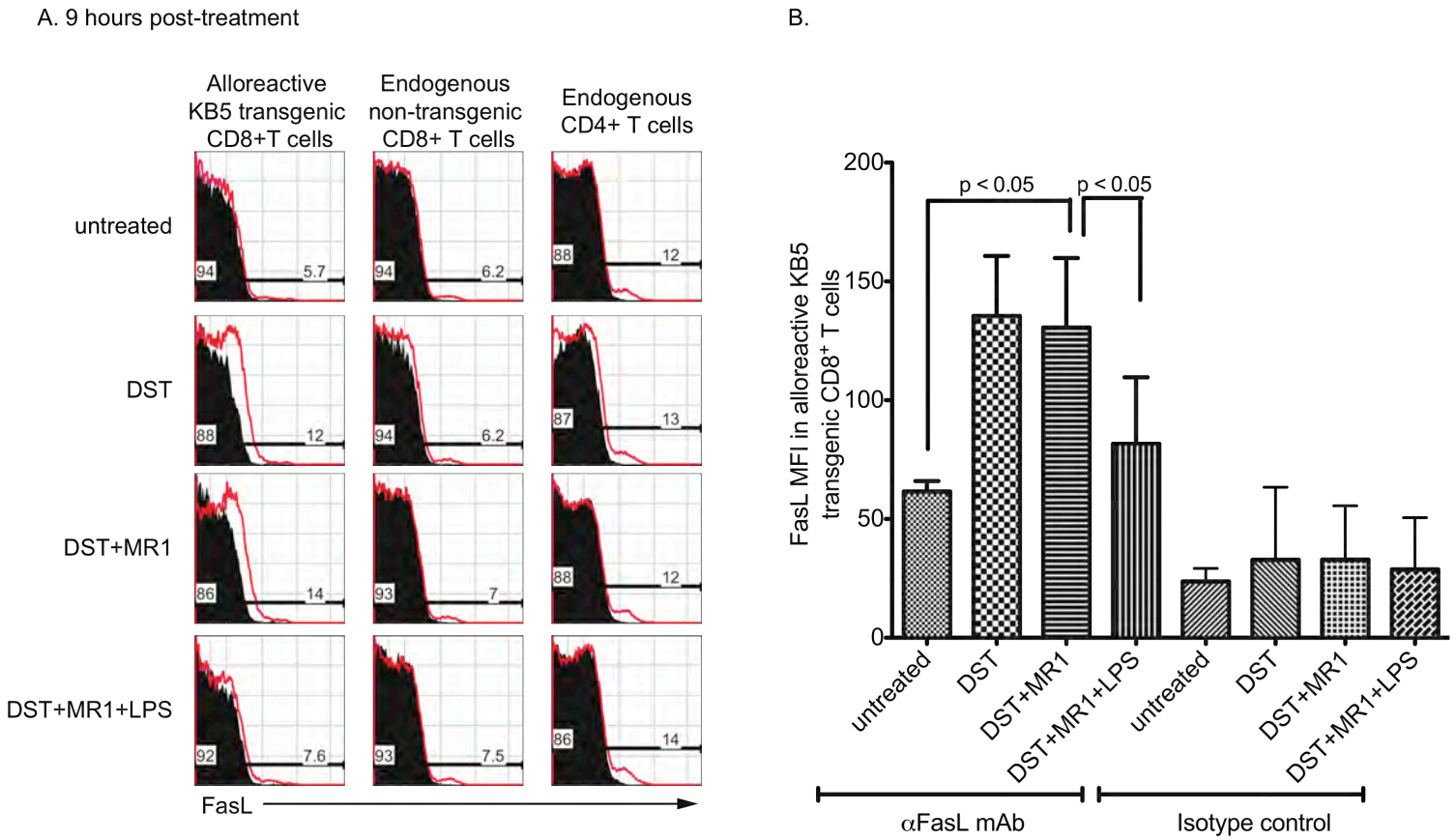

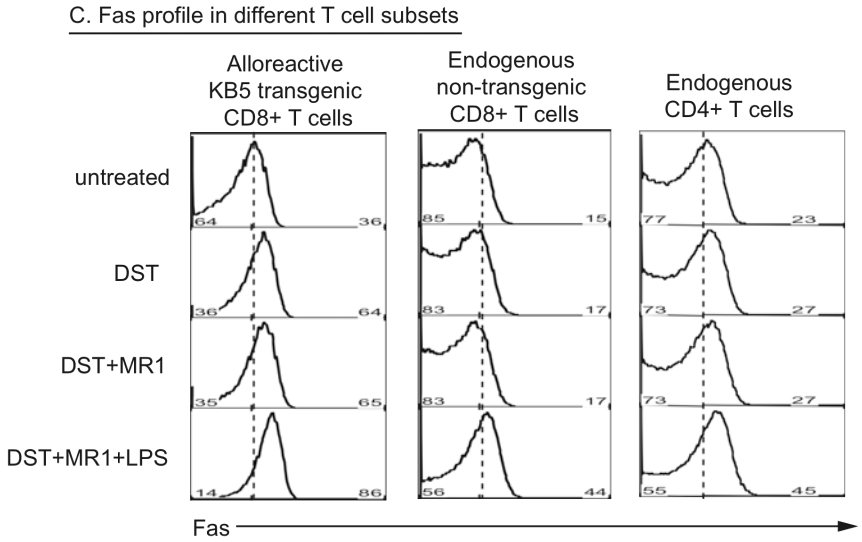
C. Fas profile in different T cell subsets
Alloreactive KB5 transgenic CD8+ T cells
Endogenous non-transgenic CD8+ T cells
Endogenous CD4+ T cells
untreated
DST
DST+MR1
DST+MR1+LPS
64
36
85
15
77
23
36
64
83
17
73
27
35
65
83
17
73
27
14
86
56
44
55
45
Fas

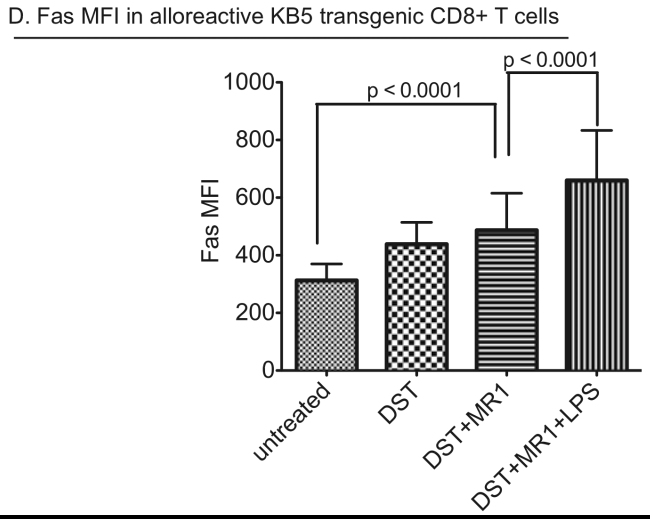
D. Fas MFI in alloreactive KB5 transgenic CD8+ T cells
p < 0.0001
p < 0.0001
Fas MFI
1000
800
600
400
200
0
untreated
DST
DST+MR1
DST+MR1+LPS

Figure 4.7. Correlation of Fas and FasL mRNA expression to the protein levels on the surface of KB5 Tg CD8$^+$ T cells during DST, DST+MR1 and DST+MR1+LPS treatment.

*Splenocytes of KB5 synchimeric mice treated with DST, DST+MR1 and DST+MR1+LPS for 9 hours were stained for surface FasL as described in Materials and Methods. Panel A shows the percentages of cells positive for FasL (Red histograms) in alloreactive KB5 CD8$^+$ transgenic T cells and the endogenous non transgenic CD8$^+$ T cells. The black histograms indicate the FasL isotype staining in each of the groups. Panel B is the comparison of averages of FasL MFI profile in KB5 Tg CD8$^+$ T cells from two experiments with p value < 0.05. Panel C and D show the percentages of cell positive for Fas receptor and their respective MFIs. The averages for the MFI were analyzed using one-way ANOVA analysis with Tukey post-test and the P value was <0.0001***.*

F. In vitro blocking of FasL does not prevent KB5 Tg CD8$^+$ T cell death during co-stimulation blockade

My data show that there is considerable up-regulation of Fas and FasL in KB5 Tg CD8$^+$ T cells undergoing apoptosis during co-stimulation blockade. I therefore hypothesized that blocking of the Fas-FasL pathway using anti-FasL antibodies would prevent the early apoptosis of alloreactive T cells. To test this *in vitro*, I incubated splenocytes isolated from KB5 synchimeric mice that were either untreated or treated with DST+MR1 (for 8 hours) with a FasL blocking antibody at (20 μg/ml) (342) for 4 hours. I then evaluated KB5 Tg CD8$^+$ T cells for apoptosis by annexin-V staining, activated caspase3 and TUNEL staining. I found that blocking FasL *in vitro* did not reduce the percentage of cells that were positive for annexin-V-binding, activated caspase3 and TUNEL as compared to control or isotype treated cells (Fig 4.8 A,B,C). FasL blocking also did not alter the MFI of annexin-V, activated caspase3 or TUNEL in alloreactive T cells from DST+MR1 treated groups (Fig 4.8 A, B and C). These results revealed that blocking Fas-FasL pathway after the initiation of programmed cell death in alloreactive T cells during co-stimulation blockade is not sufficient to inhibit apoptosis. Together, these results indicate that the Fas-FasL pathway is not important for the induction of apoptosis during co-stimulation blockade.

Figure 4.8. FasL blockade in vitro does not prevent costimulation blockade-induced alloreactive KB5 transgenic CD8+ T cell apoptosis.

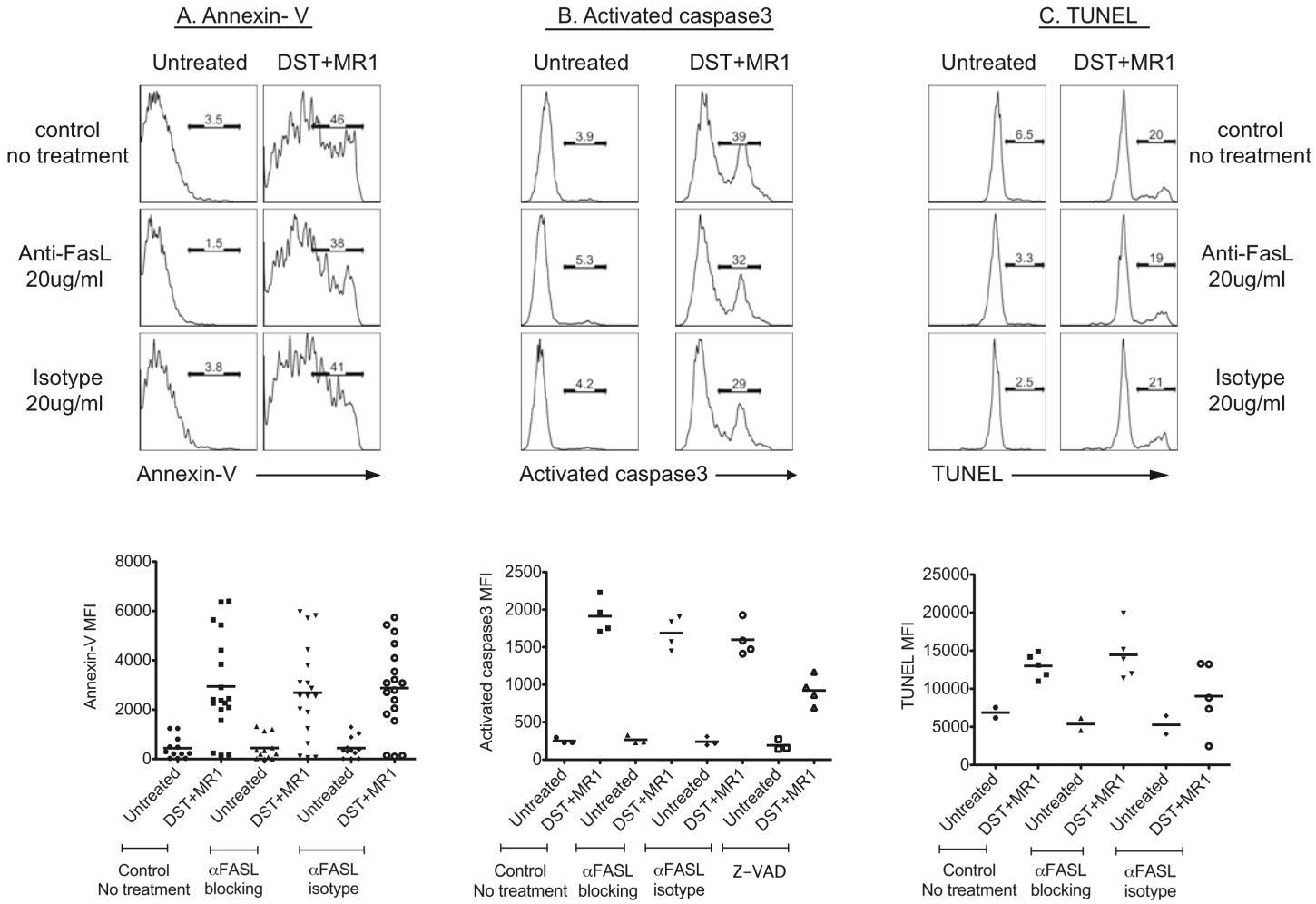

Figure 4.8. FasL blockade in vitro does not prevent co-stimulation blockade-induced alloreactive KB5 transgenic CD8$^+$ T cell apoptosis.

Splenocytes of KB5 synchimeric mice treated with DST, DST+MR1 and DST+MR1+LPS for 12 hours were incubated for 4 hours in the presence or absence of FasL blocking antibody and control isotype (20μg/ml). Cells were stained for annexin, activated caspse3 and TUNEL as described in Materials and Methods. Panel A shows the percentages of KB5 Tg CD8$^+$ T cells staining for annexin-V and the corresponding MFI of annexin in the samples. Panel B and Panel C show the percentages of KB5 Tg CD8$^+$ T cells staining for activated caspase3 and TUNEL and their corresponding MFIs respectively.

G. In vitro activation of Fas receptor can render alloreactive T cells from the LPS treated group susceptible to cell death

Although FasL expression was not increased on KB5 Tg $CD8^+$ T cells from mice treated with DST+MR1 and LPS, Fas was expressed on the surface of these cells. It was also shown that *in vivo* LPS administration increased FAS expression in microglial cells without causing apoptosis (Non $TUNEL^+$ cells) (393). Studies in vascular endothelial cells revealed that IFN-γ and LPS augmented Fas-antibody mediated apoptosis by increasing the expression of Fas receptor in these cells *in vitro* (394). Therefore I hypothesized that engagement of Fas receptors on the surface of alloreactive T cells from DST+MR1 and LPS treated mice would induce apoptosis *in vitro*. To determine this, spleens were recovered from KB5 synchimeric mice at 10 hours after treatment with DST, DST+MR1 and DST+MR1+LPS. The splenocytes were incubated with Fas agonistic or isotype antibody for 4 hours *in vitro* and then examined by annexin-V binding assay. The presence of Fas agonistic antibody increased the percentages of annexin-V positive cells and also increased the MFI of the annexin-V stain in the LPS treated groups, and this did not occur in the presence of control isotype antibody (Fig 4.9 A and B). Moreover, the endogenous non-transgenic $CD8^+$ and $CD4^+$ T cells did not show any changes in annexin-V profile in the presence of Fas agonistic antibody indicating that there is no non-specific effect of the antibody. Together, these results suggest that alloreactive T cells that are usually prevented from deletion in the presence of LPS are sensitive to Fas induced cell death.

Figure 4.9. Engagement of Fas in vitro selectively induces apoptosis of alloreactive KB5 trangenic (Tg) CD8+ T cells isolated from DST+ MR1+ LPS treated group.

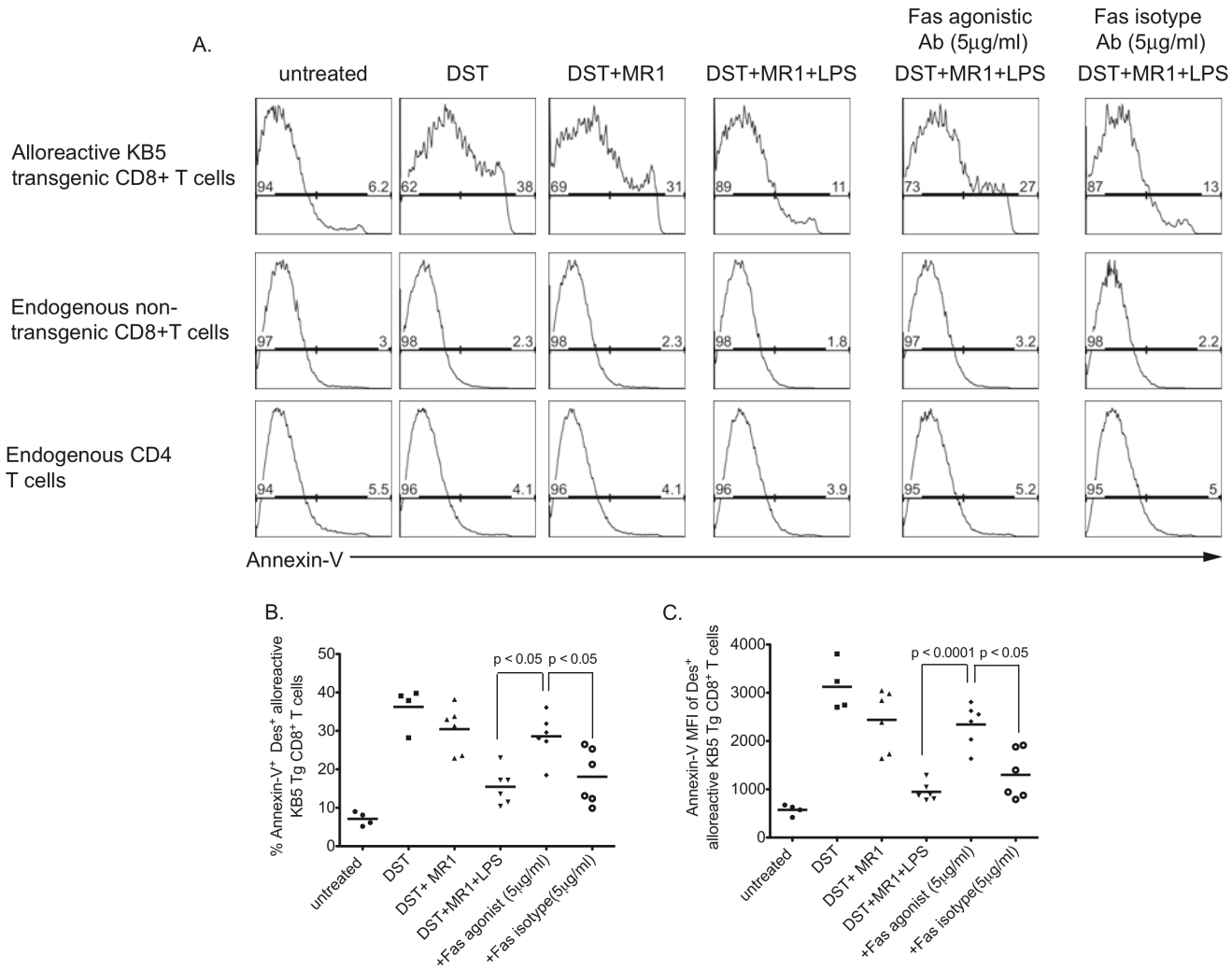

Figure 4.9. Engagement of Fas invitro selectively induces apoptosis in alloreactive KB5 Tg CD8$^+$ T cells from DST+MR1 and LPS treated group.

*Splenocytes of KB5 synchimeric mice treated with DST, DST+MR1 and DST+MR1+LPS for 9-10 hours were incubated for 4 hours before staining for annexin-V. Splenocytes from DST+MR1+LPS group were incubated in the presence of either Fas agonistic antibody or isotype (5μg/ml) during the 4hour incubation period followed by annexin-V staining. Panel A shows the representative percentages of cells that are annexin-V positive and Panel B shows the average percentages of annexin-V positive cells and the annexin-V MFI in the indicated groups. All the groups were compared by one-way ANOVA analysis with Tukey post-test. P value <0.0001***. Error bars indicate SD.*

H. The Fas-FasL pathway is not critical for co-stimulation blockade induced tolerance.

Deletion of alloreactive T cells by co-stimulation blockade is considered to be an important mechanism by which donor specific tolerance is induced (4). *In vitro* studies so far have suggested that the Fas-FasL death pathway may be mechanism by which the early deletion of alloreactive T cells occurs. Therefore, I hypothesized that *lpr* and *gld* mice would not be tolerized by co-stimulation blockade regimen. To test this hypothesis, I performed an *in vivo* cytotoxicity assay in NK-depleted *lpr* and *gld* mice (Fig 4.10 A and 4.11 A). This assay is a reliable indicator of activated alloreactive T cells, as it determines their ability to lyse allogeneic target cells. Since *lpr* and *gld* mice develop lymphoproliferative disorder with age, I used young mice that were age-matched (6 to 7 weeks) and weight matched with the WT control B6 mice. Very little to no killing of allogeneic target cells was detected in *lpr* or *gld* mice after co-stimulatory blockade regimen, suggesting that the Fas-FasL pathway may not be crucial in induction of tolerance (Fig 4.10B and C and Fig 4.11B and C). Both *lpr* and *gld* mice treated with DST were able to kill allogeneic target cells, indicating that these mice are able to generate alloreactive T cell responses. Additionally, this also indicates that that absence of killing of allogeneic target cells in *lpr* and *gld* mice after co-stimulation blockade was truly due to their tolerization and not due to the inability of alloreactive T cells to lyse target cells in the absence of Fas-FasL pathway. Together, these results indicate that Fas and FasL are not critical for co-stimulation blockade-induced tolerance induction.

Figure 4.10. Fas expression in the recipient is not necessary for costimulation blockade-induced tolerance

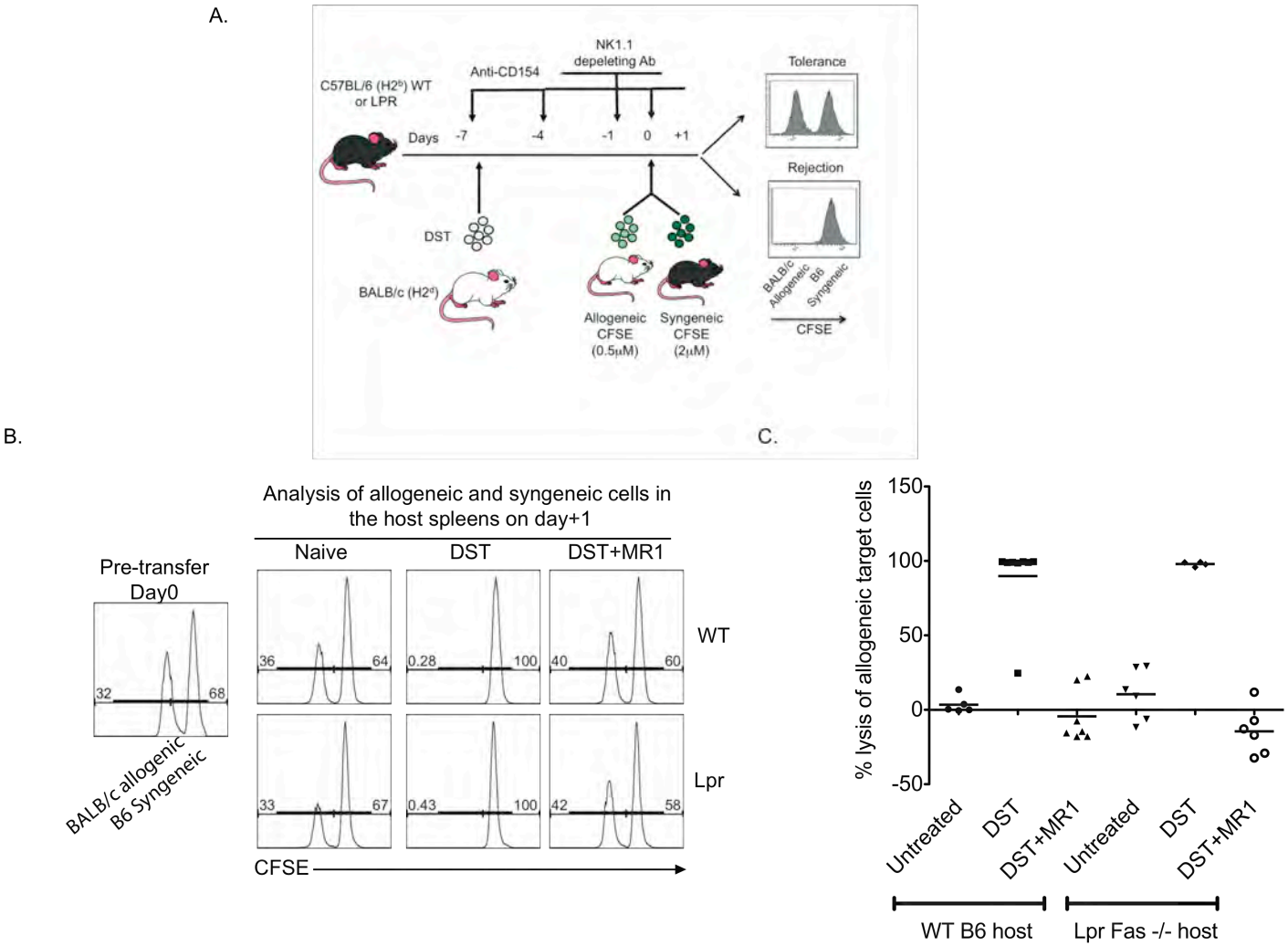

Figure 4.10. Fas expression in the recipient is not necessary for the induction of co-stimulation- blockade tolerance .

Panel A, WT B6 (H-2^b) and lpr (H-2^b) mice were subjected to co-stimulation blockade regimen in the form of allogeneic BALB/c splenocytes (H-2^d) as DST along with 3 injections of MR1 (αCD154)(Day-7, -4, 0). On day-1 mice were given NK1.1 depleting antibody followed by the transfer of 2 cell populations (both syngeneic and allogeneic) that were labeled with the indicated concentrations of CFSE as described in Materials and Methods. On day +1 recipient spleens (both WT and lpr) were harvested and the lysis of allogeneic target cells is determined as described in Materials and Methods. Panel B, shows the representative histograms of allogeneic (H-2^d) and syngeneic (H-2^b) target cells before transfer and after the indicated treatments. Panel C shows the % lysis of allogeneic target cells with respect to the syngeneic populations.

Figure 4.11. Expression of FasL on the recipient is not necessary for costimulation blockade-induced tolerance.

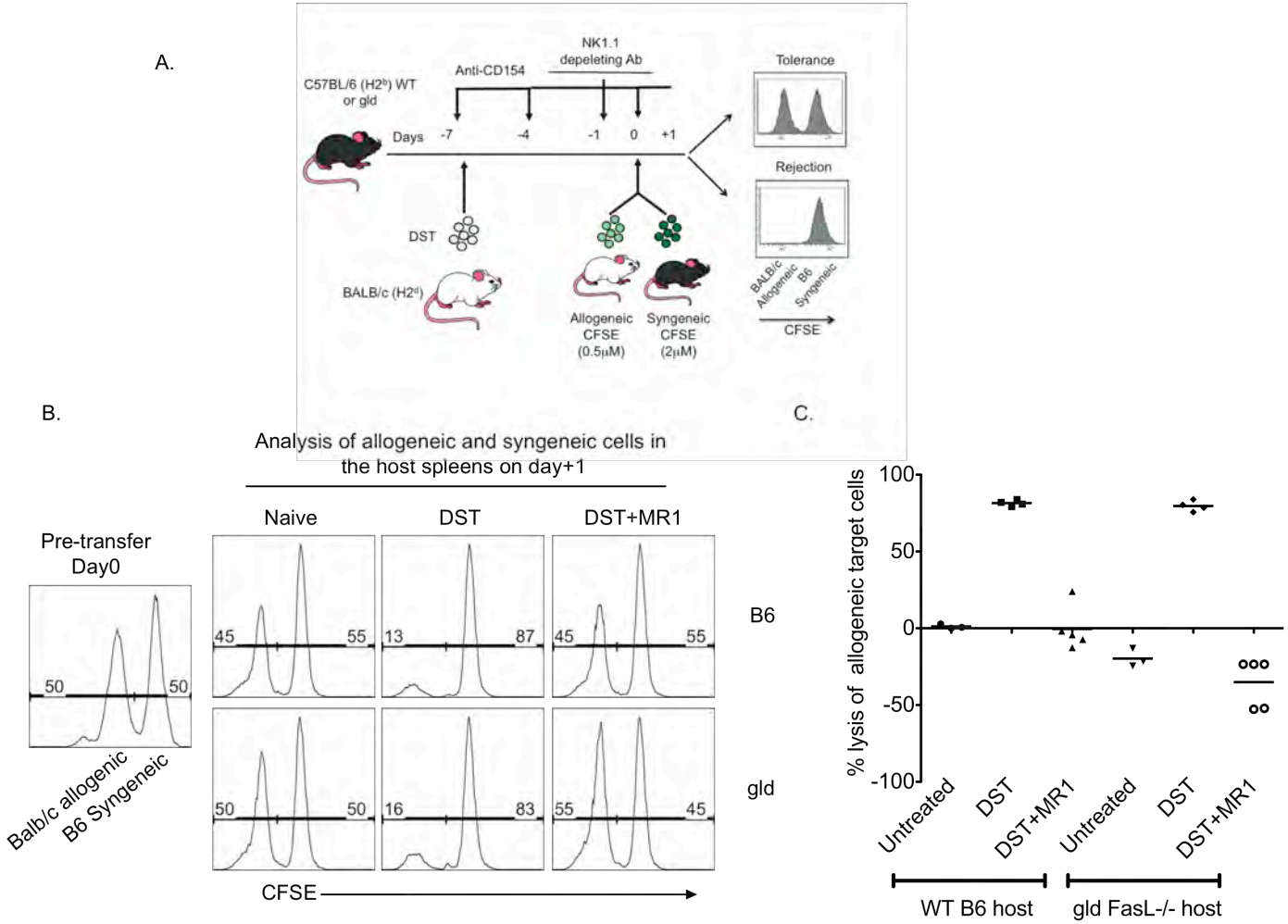

Figure 4.11. Expression of FasL on the recipient is not necessary for the co-stimulation blockade-induced tolerance.

Panel A, WT B6 (H-2^b) and gld (H-2^b) mice were subjected to co-stimulation blockade regimen in the form of allogeneic BALB/c splenocytes (H-2^d) as DST along with 3 injections of MR1 (αCD154) (Day-7, -4, 0). On day-1 mice were given NK1.1 depleting antibody followed by the transfer of 2 cell populations (both syngeneic and allogeneic) that were labeled with the indicated concentrations of CFSE as described in Materials and Methods. On day +1 recipient spleens (both WT and gld) were harvested and the lysis of allogeneic target cells is determined as described in Materials and Methods. Panel B, shows the representative histograms of allogeneic (H-2^d) and syngeneic (H-2^b) target cells before transfer and after the indicated treatments. Panel C shows the % lysis of allogeneic target cells with respect to the syngeneic populations.

I. Co-stimulation blockade-induced BIM expression is not prevented by LPS treatment.

Recently, studies using mice deficient of both Fas and BIM have indicated their complimentary roles in controlling T cell apoptosis (214). Since *lpr* and *gld* mice were tolerized by co-stimulation blockade, I hypothesized that BIM may be playing a compensatory role to induce apoptosis of alloreactive T cells in the absence of Fas or FasL. Unfortunately, the pro-apoptotic gene *bim* was not present in the apoptotic gene array. Instead of analyzing the mRNA expression of BIM, I directly tested the if expression BIM protein was upregulated during co-stimulation blockade and if its expression was affected during LPS treatment similar to FasL. BIM is found in 3 isoforms (BIM_S, BIM_L and BIM_{EL}; where S means short, L means large and EL means extralarge) due to alternate splicing. During apoptosis, BIM_S is known to be the most active. BIM_L and BIM_{EL} are believed to be released from the dynein motor complex as downstream events of JNK activation. The antibody used for staining is specific for total BIM. Briefly, splenocytes from KB5 synchimeric mice were treated as indicated and either stained for BIM directly ex vivo or stained after 4 hours of incubation *in vitro* (37℃). After 9 hours of DST+MR1 treatment BIM expression was higher in KB5 Tg $CD8^+$ T cells compared to the untreated group (both percentages and MFI, Fig 4.12 A and B). LPS treatment, on the other hand, did not affect BIM levels, although they were reduced in the percentages. The presence of higher levels of BIM in alloreactive T cells taken from mice treated with DST+MR1 and LPS suggest that it may contribute to the sensitivity of these cells to Fas-mediated apoptosis *in vitro*. Together, these results

suggest that BIM may be playing a role during co-stimulation blockade along with Fas to induce apoptosis of alloreactive T cells.

Figure 4.12. LPS does not prevent costimulation blockade-induced BIM expression on alloreactive KB5 transgenic CD8+ T cells.

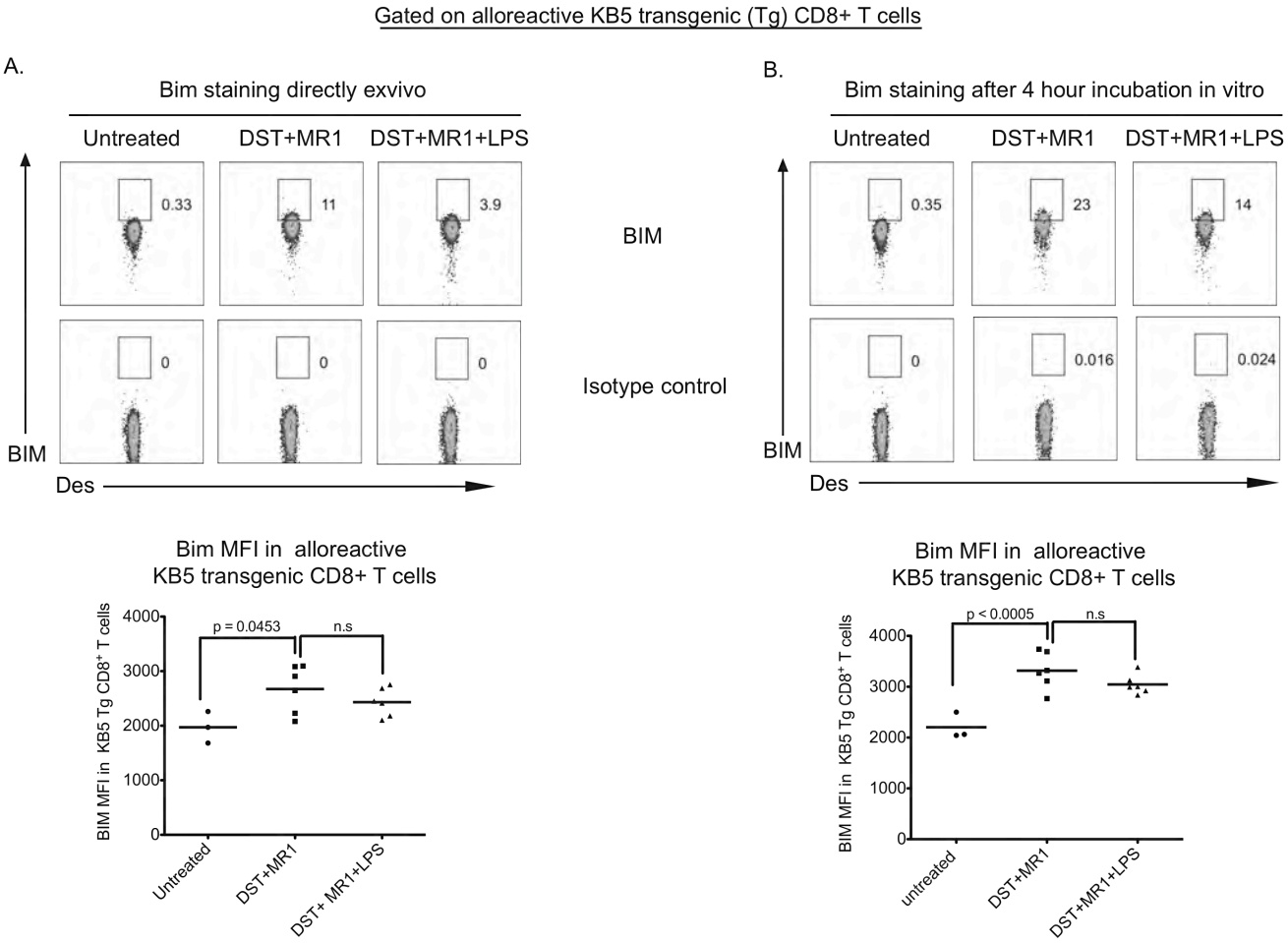

Figure 4.12. LPS does not prevent co-stimulation-blockade-induced BIM expression on KB5 Tg CD8$^+$ T cells.

Panel A and B, splenocytes of KB5 synchimeric mice treated with DST+MR1 and DST+MR1+LPS for 9 hours were stained for BIM directly ex vivo or after 4 hours of incubation at 37℃ as described in Materials and Methods. Panel A and B show the percentages of KB5 Tg CD8$^+$ T cells that are positive for BIM and the MFI of BIM. Additionally plots consisting of the staining with BIM isotype control antibody are also shown. Values were compared by one-way ANOVA analysis with Tukey post-test. P values for plots in panel A and B were 0.0453 and <0.0005*** respectively.*

J. Increased levels of inflammatory cytokines in the serum of mice treated with LPS during co-stimulation blockade.

TLR activation provokes the release of inflammatory cytokines that may be involved in preventing the deletion of alloreactive T cells thereby abrogating tolerance induction. Previously it was demonstrated that LPS-induced Type-I IFN impairs the deletion of alloreactive KB5 Tg $CD8^+$ T cells during co-stimulation blockade (5). To evaluate if other inflammatory cytokines are produced after LPS treatment that may abrogate tolerance, I first performed cytokine analysis on the serum of mice treated either with DST, DST+MR1 or DST+MR1 +LPS for 9 hours. Compared to DST and DST+MR1 treated groups, LPS induced significant quantities of the inflammatory cytokines namely, IL-6, IL-10, IL-12p40, TNF, IFNγ and MCP-1 (Fig 4.13). Importantly, the increase in TNF and IL-10 protein levels correlated with the microarray data where TNF mRNA was increased and IL-10 mRNA was detected at higher levels in alloreactive KB5 Tg $CD8^+$ T cells during LPS treatment. In section G (Fig 4.9), I had mentioned that studies in vascular endothelial cells revealed that IFN-γ and LPS augment Fas-antibody mediated apoptosis *in vitro* by increasing the expression of Fas receptor in these cells (394). Given the increase in IFN-γ in the serum of the LPS treated group and the previous observations (section G; Fig 4.9) made with regard to the increase in Fas receptor expression in alloreactive T cells and their susceptibility to Fas-mediated apoptosis *in vitro* reinforces the effect of LPS on Fas expression in activated alloreactive T cells as well. Together, these results indicate that the production of various inflammatory

cytokines within the first hours of LPS treatment affect the apoptotic signature of alloreactive T cells.

Figure 4.13. Detection of pro-inflammatory cytokines in the serum of KB5 synchimeric mice after 8 hours of treatment with DST+MR1+LPS.

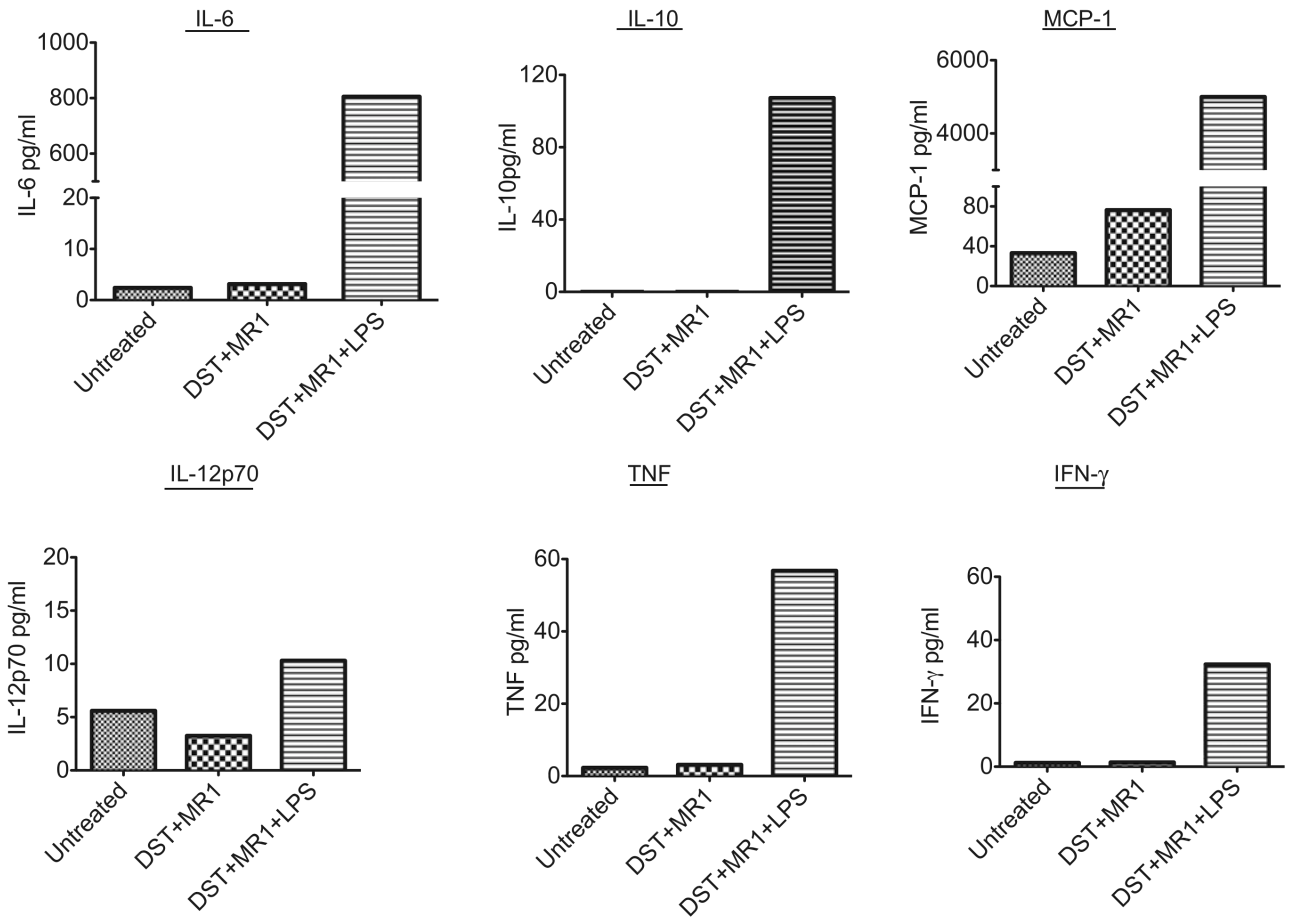

Figure 4.13. Detection of inflammatory cytokines in the serum of mice treated with DST+MR1+LPS.

Blood was isolated from KB5 synchimeric mice treated with DST+MR1 and DST+MR1+LPS for 8 hours. Serum isolated from blood was used for analysis for various cytokines using BD CBA inflammatory cytokine array as described in Materials and Methods. Shown are the amounts of various cytokines (pg/ml) detected in the serum in the treated groups (n=2).

K. IL-10 is not necessary for LPS mediated abrogation of tolerance induction

IL-10 is usually considered to be an anti-inflammatory cytokine that is produced by Tregs in response to LPS and suppresses $CD8^+$ T cell responses (232). Recently, IFN-α has been shown to modulate the balance of anti- and pro-inflammatory functions of IL-10 (395, 396). IFN-α priming of macrophage confers pro-inflammatory functions of IL-10 that result in the increase of STAT-1 activation and subsequent induction of STAT-1-dependent genes such as IRF-1 and chemokines CXCL-10 and CXCL-19 (395). LPS abrogates co-stimulation blockade-induced tolerance in a type-I IFN dependent manner (5). However it is not known if IL-10 is also required for LPS mediated abrogation of co-stimulation blockade (DST+MR1) mediated tolerance induction. Given this and the dramatic increase in IL-10 mRNA expression in T cells and protein levels in the serum of mice receiving LPS during co-stimulation blockade, I hypothesized that IL-10 may be mediating the pro-inflammatory effects of LPS leading to the abrogation of tolerance induction. I tested this hypothesis using IL-10-deficient mice with the *in vivo* cytotoxicity assay. I predicted that in the absence of IL-10, LPS would not be able to abrogate tolerance induction. IL-10 deficient mice treated with DST+MR1 and LPS rejected allogeneic target cells with nearly 98% percent lysis, suggesting that IL-10 is not required for LPS to abrogate tolerance induction (Fig 4.14 A, B and C). However, IL-10 may be playing a synergistic role with other pro-inflammatory cytokines in mediating the abrogation of tolerance in the presence of LPS.

Figure 4.14. IL-10 is not required for LPS mediated abrogation of costimulation blockade-induced tolerance

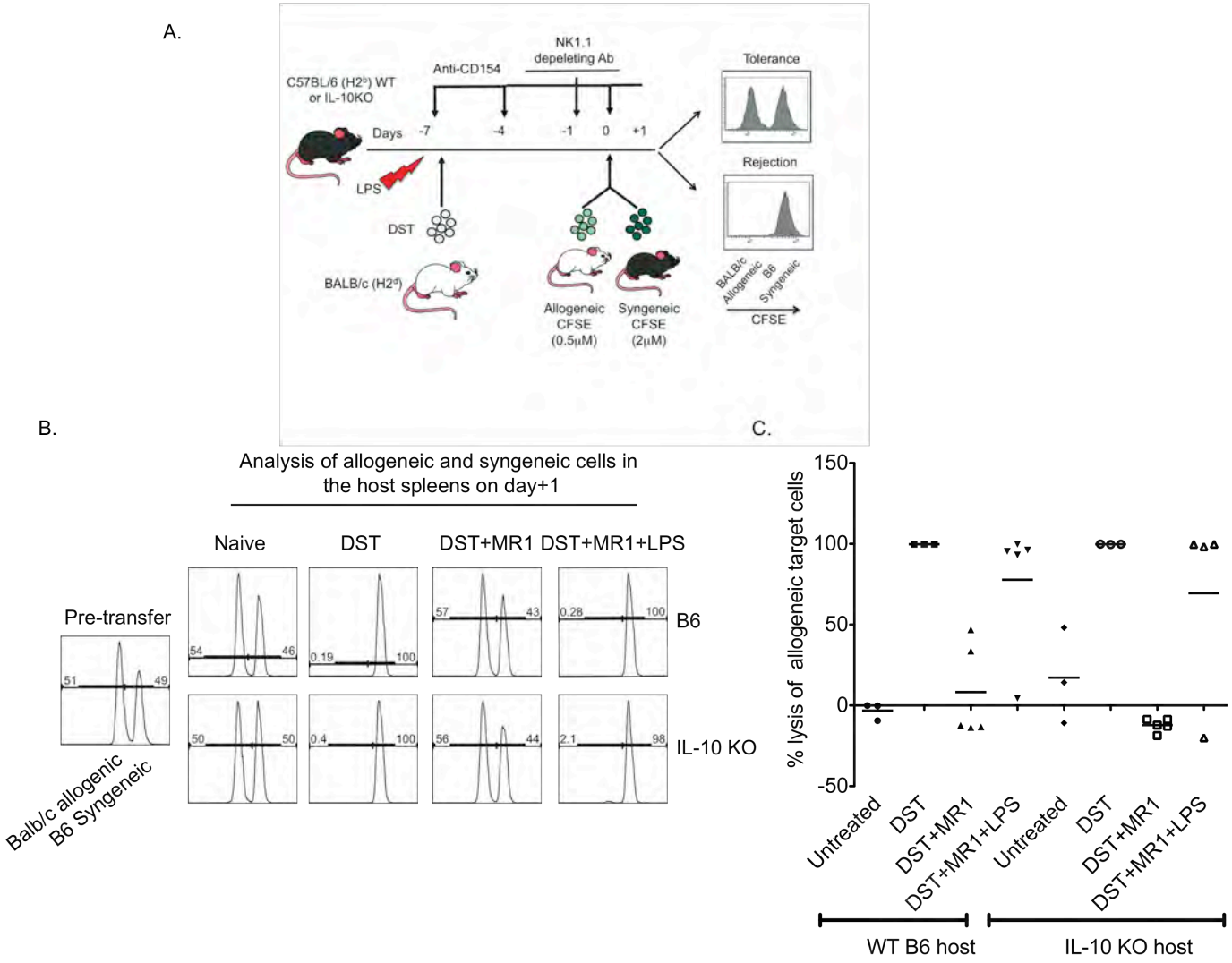

Figure 4.14. IL-10 is not necessary for LPS mediated abrogation of tolerance induction.

Panel A, WT B6 (H-2^b) and IL-10KO (H-2^b) mice were subjected to co-stimulation blockade regimen in the form of allogeneic BALB/c splenocytes (H-2^d) as DST along with 3 injections of MR1 (αCD154) (Day-7, -4, 0). Some mice also received a dose of LPS (100μg/mouse) on day-7. On day-1 mice were given NK1.1 depleting antibody followed by the transfer of 2 cell populations (both syngeneic and allogeneic) that were labeled with the indicated concentrations of CFSE as described in Materials and Methods. On day +1 recipient spleens (both WT and IL-10) were harvested and the lysis of allogeneic target cells is determined as described in Materials and Methods. Panel B, shows the representative histograms of allogeneic (H-2^d) and syngeneic (H-2^b) target cells before transfer and after the indicated treatments. Panel C shows the % lysis of allogeneic target cells with respect to the syngeneic populations.

Chapter 4: Summary

1. The two-step co-stimulation blockade (DST+MR1) protocol effectively induces donor-specific tolerance by causing an early deletion (by 15 hours) of donor-reactive $CD8^+$ T cells.
2. Co-stimulation blockade does not prevent the early activation (by 9 hours) of donor-reactive $CD8^+$ T cells that are deleted.
3. Co-stimulation blockade results in the upregulation of both FasL and BIM, two pro-apoptotic molecules that may be involved in the early deletion of activated donor-reactive $CD8^+$ T cells.
4. Exposure to LPS, a TLR4 agonist, at the time of co-stimulation blockade abrogates tolerance induction by preventing the deletion of donor-reactive $CD8^+$ T cells.
5. LPS prevents the deletion of donor-reactive $CD8^+$ T cells by suppressing the expression of other pro-apoptotic genes such as FasL, caspase 2, BID, BAX.
6. LPS treatment at the time of co-stimulation blockade also induces higher expression of CD25 in activated donor-reactive $CD8^+$ T cells.
7. Although LPS inhibits the expression of FasL, it induces non-specific upregulation of Fas expression in donor-reactive as well as endogenous $CD8^+$ T cells and $CD4^+$ T cells.
8. Donor-reactive $CD8^+$ T cells that are prevented from deletion in animals treated with LPS at the time of co-stimulation blockade are still sensitive to early Fas-mediated apoptosis *in vitro*.

Chapter 4: Discussion

The deletion of donor reactive T cells during the induction of peripheral transplantation tolerance is considered to be one of the important mechanisms that facilitates graft acceptance (234). The deletion of alloreactive T cells during co-stimulation blockade was shown to occur by 24 hours post-treatment (4), and exposure to TLRs during tolerance induction prevents this early deletion via a Type-I IFN dependent manner (4, 5). Here, I examined the expression of apoptosis-related genes by alloreactive $CD8^+$ T cells undergoing deletion after treatment with co-stimulation blockade. I observed alterations in the expression of 2 pro-apoptotic molecules, FasL (involved in the extrinsic apoptotic pathway) and BIM (involved in the intrinsic apoptotic pathway) in alloreactive $CD8^+$ T cells by 12 hours of treatment with co-stimulation blockade. In particular, FasL was upregulated by alloreactive T cells at both the mRNA and protein levels as early as 12 hours after co-stimulation blockade. Interestingly, TLR4 (LPS) treatment during co-stimulation blockade, which prevents the early deletion of alloreactive T cells, inhibited the up-regulation of FasL (mRNA and protein), suggesting a potential role for the Fas-FasL pathway in the deletion process. However, blocking of FasL *in vitro* did not rescue alloreactive T cells from undergoing apoptosis after co-stimulation blockade. This finding correlated with the ability of co-stimulation blockade to induce tolerance in *lpr* and *gld* mice that are deficient in Fas-FasL pathway. These data suggest that either Fas-FasL apoptotic pathway is not directly involved in deletion of alloreactive cells during the induction of tolerance or that there is a compensatory mechanism involved in the deletion of alloreactive T cells in absence of Fas-FasL

signaling. I found that alloreactive T cells undergoing deletion had increased BIM expression, supporting the possibility that BIM and Fas may have redundant roles in controlling alloreactive T cell death during co-stimulation blockade. Importantly, although FasL expression by alloreactive T cells was inhibited in mice treated with DST+MR1 and LPS, these cells were still susceptible to Fas-mediated apoptosis *in vitro*. This suggests that alloreactive T cells emerging from an inflammatory environment and that are known to survive and expand after 24 hours are still sensitive to apoptosis within 24 hours after treatment.

Although the Fas-FasL pathway plays a vital role in mediating the process of AICD, *lpr* and *gld* mice that are deficient of Fas-FasL signaling accept allografts (265, 397, 398) suggesting that Fas-FasL may be just one component of the apoptotic pathway and other compensatory apoptotic mechanisms may be involved in the elimination of activated alloreactive T cells during co-stimulation blockade. Studies on immune privileged sites such as the cornea have revealed the involvement of FasL and TRAIL in mediating tolerance (399, 400). These studies suggest that death receptor pathways other than Fas-FasL may mediate the death of activated alloreactive T cells in *gld* mice during tolerance induction. Concomitantly, I also observed a modest increase in BIM expression in alloreactive T cells during co-stimulation blockade. Recently, both Fas and BIM have been shown to have a synergistic role in maintaining homeostasis, as defects in both the molecules led to a rapid onset of autoimmune diseases in mice than single molecule deficient counterparts (131, 401, 402). Given this, I predict that the induction of tolerance

in the absence of Fas and FasL may be compensated by BIM-mediated pro-apoptotic pathway.

My *in vivo* cytotoxicity experiments with *lpr* and *gld* mice revealed that these mice are tolerized during DST+MR1 treatment. It is noteworthy to mention that the *lpr* mutation is leaky, and mice with *lpr* mutation have higher FasL mRNA expression $CD4^{-}CD8^{-}$ T cells that are specifically cytotoxic to Fas expressing cells (209, 403). Given this, the induction of tolerance in *lpr* mice by co-stimulation blockade may be attributed to the leaky expression of Fas and the over-expression of FasL in this system. In contrast to this, CTLA-4 Ig+MR1 therapy (at the time of skin transplantation and post-operatively) in *lpr* mice resulted in skin graft rejection (397). Graft rejection observed in *lpr* mice may be attributed to negative co-stimulatory role of Fas. A recent study showed that activation of Fas inhibited the activation and proliferation of human alloantigen-specific T cells (212). Alternatively, the differences observed between the previous studies and mine may be just attributed to the differences in nature of the co-stimulation-blockade regimens and the timing of the regimens.

Gld mice given CTLA-4Ig and MR1 therapy (at the time of skin transplantation and post-operatively) showed significant skin graft survival relative to their WT counterparts (397). Although there was significant extension of skin graft survival in *gld* mice compared to WT recipients, these studies showed that the grafts failed in approximately 50% of the recipients in these studies. In addition to inducing death signals, FasL has also been shown to play a co-stimulatory role and augment the

proliferation of T cells via retrograde (reverse signaling into T cells) signaling early during T cell activation (211, 404, 405). One alternative explanation for the ability of the *gld* mice to be tolerized is that the absence of Fas/FasL signaling during co-stimulation blockade may result in reduced proliferation of alloreactive T cells that in turn may limit the magnitude of alloreactive T cells below the required threshold for graft rejection thereby leading to tolerance induction (397). Together, these results suggest that sensitivity of activated T cells to apoptosis mediated by Fas and FasL during tolerance induction may vary with the time of alloantigen exposure as these molecules may exhibit other co-stimulatory roles in addition to being involved in apoptosis.

Although LPS inhibited the expression of FasL by alloreactive T cells, it non-specifically led to a modest up-regulation of Fas protein on the surface of all cells (non-transgenic $CD8^+$ T cell and $CD4^+$ T cells). Studies in other systems have shown differential effects of LPS on Fas and FasL mRNA and protein expression. LPS has been shown to stimulate Fas protein expression by vascular endothelial cells via the activation of p38 MAPK pathway thereby this increasing the susceptibility of these cells to Fas agonistic antibody killing (394). Administration of LPS in mice has been known to lead to the increase in FasL protein expression in blood leukocytes (394). In humans, administration of LPS induces up-regulation of Fas mRNA by 4 hours and expression of protein on neutrophils after 24 hours of treatment (406). LPS was, however, not shown to affect FasL mRNA in leukocytes, though there was an increase in soluble FasL in the plasma (406). My data with alloreactive T cells show that, *in vitro* Fas agonistic antibody treatment caused selective apoptosis of alloreactive T cells from DST+MR1+ LPS treated

animals suggesting that alloreactive T cells in this scenario are still susceptible to Fas-mediated apoptosis. In light of this observation, I speculate that targeting the Fas-FasL death pathway may result in alloreactive T cell death during the early period after LPS and co-stimulation blockade administration and possibly contribute to the induction of tolerance.

My data show that mice injected with LPS during co-stimulation blockade produce several pro-inflammatory cytokines within 8 hours of treatment. This inflammatory environment may have an important role in abrogating tolerance. However, identifying roles for individual cytokines has proven challenging. Previous studies with TNFR2 and IL-12R deficient mice revealed that IL-12 and TNF signaling are not required for LPS (TLR4) mediated abrogation of tolerance (4). CpG (TLR9) was recently shown to abrogate tolerance induced by αCD154 and rapamycin therapy in an IL-6 independent manner (316). This study showed that CpG instead promoted Th1 effector differentiation from naïve alloreactive T cells, and this mechanism was suggested to mediate graft rejection (316). My data show that IL-10 secreted during LPS treatment does not contribute to the abrogation of tolerance by co-stimulation blockade. The above studies and my results together suggest that the effect of inflammatory cytokines during tolerance abrogation may be synergistic. In line with this, a recent study in a skin allograft model (CTLA4-Ig and αCD154) showed that mice deficient in IL-6 and TNF had prolonged skin graft survival compared to their respective single deficient counterparts, suggesting a synergistic role of these cytokines in mediating allograft

rejection (407). IL-6 and TNF were shown to abrogate tolerance by inhibiting Treg function to suppress effector T cell proliferation (407).

TLR signaling abrogates co-stimulation blockade induced tolerance by a Type-1 IFN dependent pathway (5). This study showed that LPS and Poly I:C do not abrogate tolerance in Type-I IFNRI-deficient mice as compared to WT mice (5). In this scenario, the Type-I IFN dependent mechanism that prevents the deletion of alloreactive T cells may occur either directly or indirectly. Direct signaling through the Type-I IFNRI on T cells is known to be vital for $CD8^+$ T cell survival and proliferation during viral infection (105, 408). Alternatively, Type-I IFN induces the production of survival cytokines such as IL-15 by dendritic cells that can in turn act on T cells (109, 409). Given these findings, I speculate that the effect of Type-I IFNs in rescuing alloreactive T cells from apoptosis during LPS mediated abrogation of co-stimulation blockade induced tolerance, may be occurring either by a direct inhibition of FasL expression by alloreactive T cells or it may be an indirect effect of Type-1 IFNs in inducing survival cytokines such as (IL-15)(109).

One observation that requires attention is that it is not very clear why the apoptotic profile of KB5 Tg $CD8^+$ T cells between DST and DST+MR1 is very similar (Section B; Fig 4.3). This may be due to early deletion of activated KB5 Tg $CD8^+$ T cells during DST treatment. If DST treatment alone can cause apoptosis, then two questions arise. First, what then is the effect of MR1 during co-stimulation blockade? Secondly, is early deletion of alloreactive T cells necessary for tolerance induction? We know that alloreactive T cells in DST treated mice eventually become primed to become effector

cells after 7 days and mediate graft rejection. In section B, I had predicted 2 possibilities. One possibility could be that the apoptotic pathways triggered during DST may be different from that triggered during DST+MR1 treatment. The second possibility could be that the extent of deletion may be more profound during DST+MR1 treatment than DST treatment, resulting in the number of alloreactive cells to be reduced below a certain threshold that cannot be recovered back. The molecular profiling of alloreactive T cells during DST and DST+MR1 treatment reveal that the apoptotic signaling pathways may be similar between the two groups. However, I cannot rule out the possibility of subtle gene expression differences that may result in two different biological outcomes during DST and DST+MR1 treatment. As far as the importance of early deletion of alloreactive T cells during co-stimulation blockade induced tolerance is concerned, this remains to be investigated further.

Collectively, in this chapter of my thesis I investigated the early apoptotic signature of alloreactive $CD8^+$ T cells during co-stimulation blockade and how this signature is altered in the presence of LPS (TLR4). I identified FasL as a reliable molecular indicator of early alloreactive T cell death during co-stimulation blockade that is inhibited in the presence of LPS. However its role in the induction of tolerance is also under investigation. (Model in figure 4.15; pg 285).

Figure 4.15. LPS inhibits the expression of FasL in alloreactive T cells during costimulation blockade yet makes them sensitive to early Fas mediated apoptosis

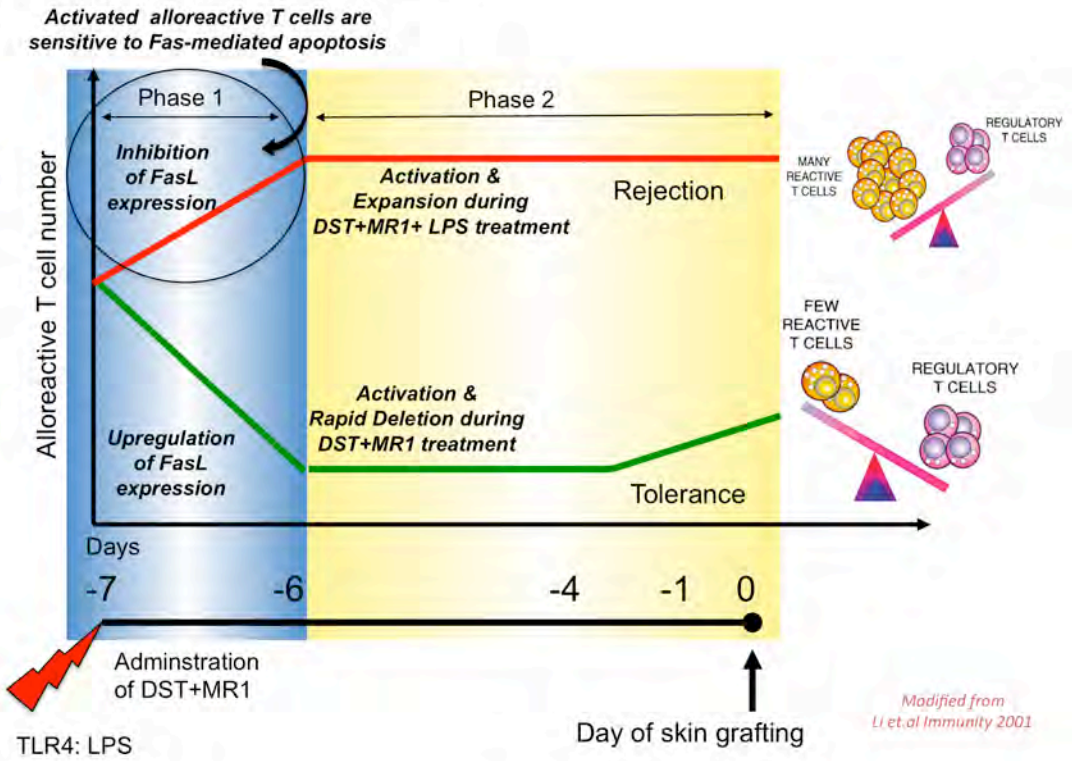

Chapter 5: Discussion

In this thesis, I examined the importance of two prototypic members of the TNF superfamily, namely TNF and FasL in the regulation of early events in naïve T cell activation. In Chapter 3 of this thesis, I investigated the immunoregulatory role of T cell-derived TNF and its ability to limit antigen-specific T cell responses during the acute phase of an infection. Subsequently, I determined that naïve developing T cells in the thymus embark on a journey of post-thymic maturation in secondary lymphoid tissues, during which they gain the capability to produce TNF in a hierarchical manner. This creates a population of cells possessing varying capabilities to produce TNF resulting in functional heterogeneity of the naïve T cell pool similar to what is found in effector and memory T cell populations (136). In Chapter 4 of this thesis, I examined the importance of the Fas-FasL pathway in the early apoptosis of activated alloantigen-specific T cells during co-stimulation blockade. The dramatic up-regulation of FasL on activated alloreactive T cells suggests that the process of apoptosis of these T cells may be occurring either by alloreactive T cell suicide or fratricide. One possible mechanism by which inflammation (TLR activation) leads to the rescue of alloantigen-specific T cells from early apoptosis in this scenario may be by inhibition of Fas-FasL pathway. Interestingly, I determined that despite this rescue from apoptosis, alloantigen-specific T cells are sensitive to Fas-mediated apoptosis within 24 hours of treatment. This finding suggests that during inflammation-mediated abrogation of co-stimulation blockade tolerance, there may still be an early window where alloantigen-specific T cells can be

targeted to undergo deletion that may in turn facilitate allograft acceptance despite early exposure to inflammatory agents.

Studies in the first part of chapter 3 revealed a suppressive role of T cell-derived TNF that required a yet unknown signal acting in a localized fashion, provided by the surrounding cells that my study did not investigate. Questions such as whether this signal is cell-contact-mediated or due a soluble mediator produced by APCs in response to T cell-derived TNF or whether the suppressive signal is delivered directly back to T cells or if it occur indirectly via an intermediary cell type are future avenues that can be explored. One hint comes from studies showing expression of TNFR2 on $CD4^+CD25^+Foxp3^+$ mouse Treg cells (410, 411). Recently, a study showed that TNF modulates the human Treg cell function by the induction of several NFκB induced genes (412). Previous work from our laboratory and my work here suggest that TNF produced by recently activated naïve T cells can exist in soluble and membrane-bound forms (1). These studies suggest that the suppressive effect of T cell-derived TNF on $CD8^+$ T cells may be mediated in localized manner by membrane-bound TNF via interactions with TNFR2 expressed on $CD4^+$ T regulatory T cells. On the other hand, recent studies have also shown that TNF is secreted in a multidirectional manner, away from the immunological synapse and hence serves to create chemokine gradients to recruit several target cells (413). Therefore, the suppressive effect of T cell derived TNF that occurs in a localized manner can also be mediated through its soluble form. Additionally, a T cell-intrinsic role for T cell-derived TNF may also be playing role in this scenario. A recent study with human T cells showed that increased production of TNF correlates with the loss of CD28 expression and leads

cells to a non-proliferative end-stage replicative senescence that is correlated to higher expression of caspase 3 (414). Increases in caspase3 are correlated to susceptibility to AICD in effector T cells (415). I did not see any marked differences in CD28 expression in TNF-deficient and WT T cells in my study. However, as caspase 3 is one of the downstream caspases in the TNF signaling pathway, I speculate that the absence of intrinsic TNF signaling in $CD8^+$ T cells may result in less caspase 3 activation and therefore reduced cell death during the effector phase. This prediction is consistent with previous reports suggesting that the absence of TNF signaling in TNF-deficient and TNFR-deficient mice led to reduced apoptosis (reduced annexin-V binding) of tetramer positive effector T cells on day 8 post LCMV infection (191, 192). In contrast to this study, however, our adoptive transfer experiments using P14 TCR transgenic TNF deficient and WT T cells did not show any apoptotic differences by annexin-V binding studies. The differences may be attributed to the differences transgenic versus endogenous T cells used in the experiments.

The next part of chapter 3 investigated the question of how naïve T cells become licensed to produce TNF. I determined that this licensing occurs in a maturation dependent manner after cells leave the thymus. SP thymocytes showed a poor ability to produce TNF upon TCR stimulation despite expressing mature TNF message at resting steady state. One of the questions that I did not dwell on here is the physiological role of low levels of TNF detected in SP thymocytes during TCR stimulation. There is a possibility that these low levels of TNF detected in the SP thymocytes may be sufficient for its effect in the thymus. It has been shown that some RTEs also require TCR-

mediated signals for a proliferative burst immediately, before emigration (416-418). New evidence suggests that thymic Treg cells also express TNFR2 (410). Given this, I speculate that it may be beneficial for SP thymocytes to produce little or no TNF so that they can be resistant to suppression by thymic Treg cells and undergo proliferation before emigration. Additionally, as developing SP thymocytes are dependent upon TCR interactions during positive and negative selection, the poor ability of developing T cells to produce TNF upon TCR activation may reflect a location-dependent regulation of TNF expression owing to its pro-inflammatory nature that may be detrimental to selection process (discussed in chapter 3 in detail).

In the periphery, naïve T cells exhibit a maturation-status dependent ability to produce TNF, with the young immature RTEs producing less TNF compared to their older mature naïve counterparts. As cells functionally mature, they begin to change their phenotypic profile as they downregulate the expression of markers such a CD24 and upregulate CD45RB and Qa2. In addition to serving as maturation markers, these molecules also have been shown to have a secondary role in T cell activation (419-422). For example, although CD24 is downregulated as T cells mature in the periphery, it is upregulated upon activation and has been shown to play a co-stimulatory role and involved in homeostatic proliferation of T cells (420). The intracellular domain of CD45 contains a tyrosine protein phosphatase required for the activation of proteins Lck and Fyn during T cell activation (423) and studies using antibodies to Qa2 (directed against α-3 region of Qa2 that is near the membrane) have been shown to augment T cell proliferation during stimulation (421). Therefore, the subtle changes in the maturation

markers may contribute to the differences in the activation status of different naïve T cell subsets (RTEs versus MN T cells). Although I did not perform an exact quantification of TNF message in RTEs versus MN T cells, analysis of TNF message in RTEs and mature naïve T cells at resting steady state by semi-quantitative RT-PCR suggests that the differences are not major. However, further quantification studies may reveal subtle differences in TNF mRNA expression between RTEs and MN T cells and if these differences contribute to the difference in their TNF producing capabilities.

Another limitation of my study is that I did not specifically determine the mechanism by which T cells at different stages of development in the periphery produced TNF upon activation and if there was specific molecule in the secondary lymphoid organs that was required for optimal production of TNF by T cells. Nonetheless, my study highlights the functional heterogeneity of the naïve T cell pool that may be beneficial for an optimal T cell response during infection. The discovery that naive T cells produce TNF before any other effector cytokines such as IFN-γ upon activation was applied in the field of transplantation tolerance. Our laboratory used the unique profile of naïve T cells to produce TNF but not IFN-γ to determine the precursor frequency of alloreactive T cells during co-stimulation blockade regimen graft rejection (345).

In chapter 4 of my thesis I examined the apoptotic signature of alloreactive T cells during co-stimulation blockade induced transplantation tolerance. This study identified that FasL expression is differentially regulated during LPS mediated abrogation of co-stimulation blockade induced tolerance. However, experiments in chapter 4 suggest that

Fas may be acting in concert with other molecules such as BIM or other pro-apoptotic molecules to induce tolerance. Delineating the downstream mechanisms of apoptosis in alloreactive T cells induced by co-stimulation blockade treatment and identifying the key players is relevant as novel strategies to induce peripheral deletion and tolerance are being developed. Understanding these apoptotic molecular pathways is important as co-stimulation blockade regimens using αCD154 therapy have shown great promise, but recent studies have revealed a major side effect of the use of this antibody in humans (424-426). It was determined that platelets express CD40 and hence the administration of αCD154 (αCD40L) leads to platelet aggregation, resulting in thromboembolism. In this chapter I speculated that targeting the Fas-FasL death pathway may result in alloreactive T cell death during the early period after LPS and co-stimulation blockade treatment that can possibly facilitate tolerance induction despite inflammation.

One of the challenges of using Fas agonistic antibodies *in vivo* is that it results in fulminant hepatitis in mouse models (427). Therefore, to exploit the full potential of FasL to induce tolerance, several strategies have been developed (165). For example, syngeneic myoblasts engineered to express FasL that were co-transplanted with islet grafts protected islets from rejection (428). The use of CTLA-4Ig fused with FasL has been shown to induce corneal allograft survival by causing deletion of $CD4^+$ T cells infiltrating the corneal transplants (429). Recently, cardiac allograft survival was achieved in rat models using DST engineered to display chimeric SA-FasL that is non-cleavable (430). Graft survival correlated with the deletion of alloreactive T cells and the expansion of Tregs (430). These studies suggest that targeting Fas-FasL pathway in a

localized manner (as in the above strategies) can maximize its apoptotic effects during tolerance induction and may potentially overcome the effects of TLR activation on co-stimulation blockade.

My studies revealed that co-stimulation blockade regimen resulted in the early upregulation of various activation markers including CD25. The presence of LPS resulted in further upregulation of this marker on alloreactive T cells. Studies have shown that co-stimulation via CD80 leads to higher levels of CD25 on $CD8^+$ T cells (431). As mentioned previously, although IL-2 is a cytokine involved in the induction of AICD in activated T cells, it is also involved in the proliferation of activated T cells. Studies using αCD25 mAb (Simulect) (that blocks IL-2 and IL-2Rα interactions) has showed reduced lymphocyte numbers (CD25+ T cells) after 24 hours of treatment in the peripheral blood of kidney transplant patients (432, 433). Studies have shown that αCD25 mAb (Simulect) has many advantages. Firstly, It is an antibody that has undergone phase-I and phase-II clinical trials. These studies revealed that it has a half-life of 1-2 weeks and is well tolerated by transplant patients (432). Secondly, Simulect binds only activated T cells and macrophages and inhibits their proliferation and does not mediate complement-mediated cytotoxicity (432). CD25 is also expressed on Treg cells that require IL-2 signaling for their maintenance (278, 434). Since Treg cells are important for transplantation tolerance, one of the concerns is the effect of αCD25 mAb (Simulect) mediated blockade on Treg populations. A recent study showed that CD25 blockade was not required for the maintenance of human T regulatory cells *in vivo* as it did not lead to *in vivo* depletion of T regulatory cells (278). Given these findings, and the enhanced ability of CD25 in

alloreactive T cells during after LPS and co-stimulation blockade treatment, CD25 may be another potential target that can be used to induce early apoptosis in alloreactive T cells after treatment when they are still sensitive to apoptosis.

Previous studies from our laboratory discovered that TLRs abrogated co-stimulation blockade induced tolerance by preventing the deletion of alloreactive T cells through a Type-I IFN manner. One of the limitations of my study in chapter 4 was that I could not identify the mechanisms linking LPS induced Type I IFNs to the inhibition of FasL expression in alloreactive T cells was not deduced. One potential candidate that could link Type-I IFN and FasL expression may be IL-15, another member of γc cytokines. LPS is known to stimulate the rapid expression of IL-15 on the cell surface of activated monocytes (435). Type-I IFN also stimulates the production of IL-15 (109). Moreover, IL-15 has been shown to inhibit Fas-FasL induced apoptosis of human effector memory $CD4^+$ and $CD8^+$ T cells and enhance their survival (436, 437). Studies in NK cells have shown that IL-15 mediates their survival through maintenance of myeloid-leukemia cell differentiation protein-1 (Mcl-1) expression (438) and that IL-15 withdrawal induces BIM and NOXA that inhibit Mcl-1(438). Additionally, IL-15-IgG2b fusion protein has been shown to inhibit anti-Fas (clone-Jo2) mediated apoptosis *in vitro* and *in vivo* in mice (439). Studies using an antagonist IL-15/Fc protein blocked $CD8^+$ T cell dominant rejection by inhibiting the proliferation of $CD8^+$ T cells during co-stimulation blockade treatment (CTLA-4Ig) (440). Altogether, these findings lead me to predict that Type-I IFN induced IL-15 may be mediating FasL inhibition and promoting alloreactive T cell survival during LPS treatment. This is another possibility that can be

tested and if proven true could potentially serve as another early target to induce tolerance induction during LPS treatment.

Although TNF and FasL are two of well-known TNF family members involved in apoptosis, studies indicate that they are both dispensable under some circumstance. *Gld* mice treated with neutralizing anti-TNF antibody did not abrogate alloreactive T cell death during co-stimulation blockade (CTLA-4Ig) suggesting that alloreactive T cell deletion is not mediated by FasL and TNF for cardiac allograft tolerance (398). Another study revealed that TNFR1 and FasL signaling are not required for P14 TCR transgenic T cell deletion after LCMV infection (124). However, in non-transgenic mice deficient of TNFR1 and FasL showed defects in peptide-induced deletion of T cells suggesting their unique role in T cell apoptosis depending upon the nature of antigen-challenge.

Overall my thesis sheds light into the role of TNF and FasL, two prototypic members of the TNF superfamily and their respective roles in some of the earliest events of T cell activation. The immunoregulatory role of TNF in the altering T cell responses has recently been appreciated. 1) Studies in mice reveal that the absence of TNF leads to enhanced activation of T cells and immunopathology (441). Studies in collagen-induced arthritis on the other hand demonstrated that anti-TNF therapy enhances expansion of Th-1 and Th-17 cell populations that can be pathogenic in rheumatoid arthritis models (195). 2) Studies using low-dose TNF or TNFR2 agonist treatments have been shown to play a therapeutic role in specifically inducing autoreactive T cell death in certain autoimmune diseases such as type-1 diabetes (442). Alternatively, in the context for vaccine design

strategy, TNF blockade may in fact be beneficial in boosting the effector T cell response and possibly a better memory T cell response. On the basis of the diverse effects of TNF in immunity towards bacterial and viral infections and self-tolerance, this suggests that the role of TNF may differ depending on nature of the antigenic challenge and time. Therefore, caution should be taken while evaluating the efficacy of TNF blockade therapeutic strategies. Understanding the potential of inducing early apoptosis in alloreactive T cells exposed to inflammatory agents may have a practical implication in designing specific strategies that can induce multiple apoptotic pathways simultaneously in activated alloreactive T cells despite the presence of inflammation.

References:

1. Brehm, M. A., K. A. Daniels, and R. M. Welsh. 2005. Rapid production of TNF-alpha following TCR engagement of naive CD8 T cells. *J Immunol* 175:5043-5049.
2. Singh, A., and M. Suresh. 2007. A role for TNF in limiting the duration of CTL effector phase and magnitude of CD8 T cell memory. *J Leukoc Biol* 82:1201-1211.
3. Houston, E. G., R. Nechanitzky, and P. J. Fink. 2008. Cutting edge: Contact with secondary lymphoid organs drives postthymic T cell maturation. *J Immunol* 181:5213-5217.
4. Thornley, T. B., M. A. Brehm, T. G. Markees, L. D. Shultz, J. P. Mordes, R. M. Welsh, A. A. Rossini, and D. L. Greiner. 2006. TLR agonists abrogate costimulation blockade-induced prolongation of skin allografts. *J Immunol* 176:1561-1570.
5. Thornley, T. B., N. E. Phillips, B. C. Beaudette-Zlatanova, T. G. Markees, K. Bahl, M. A. Brehm, L. D. Shultz, E. A. Kurt-Jones, J. P. Mordes, R. M. Welsh, A. A. Rossini, and D. L. Greiner. 2007. Type 1 IFN mediates cross-talk between innate and adaptive immunity that abrogates transplantation tolerance. *J Immunol* 179:6620-6629.
6. Takahama, Y., E. W. Shores, and A. Singer. 1992. Negative selection of precursor thymocytes before their differentiation into CD4+CD8+ cells. *Science* 258:653-656.
7. Godfrey, D. I., J. Kennedy, T. Suda, and A. Zlotnik. 1993. A developmental pathway involving four phenotypically and functionally distinct subsets of CD3-CD4-CD8- triple-negative adult mouse thymocytes defined by CD44 and CD25 expression. *J Immunol* 150:4244-4252.
8. Murga, C., and D. F. Barber. 2002. Molecular mechanisms of pre-T cell receptor-induced survival. *J Biol Chem* 277:39156-39162.
9. von Boehmer, H., and F. Melchers. 2010. Checkpoints in lymphocyte development and autoimmune disease. *Nat Immunol* 11:14-20.
10. Bassing, C. H., W. Swat, and F. W. Alt. 2002. The mechanism and regulation of chromosomal V(D)J recombination. *Cell* 109 Suppl:S45-55.
11. Krangel, M. S. 2009. Mechanics of T cell receptor gene rearrangement. *Curr Opin Immunol* 21:133-139.
12. Passoni, L., E. S. Hoffman, S. Kim, T. Crompton, W. Pao, M. Q. Dong, M. J. Owen, and A. C. Hayday. 1997. Intrathymic delta selection events in gammadelta cell development. *Immunity* 7:83-95.
13. Kang, J., M. Coles, D. Cado, and D. H. Raulet. 1998. The developmental fate of T cells is critically influenced by TCRgammadelta expression. *Immunity* 8:427-438.
14. von Boehmer, H., I. Aifantis, F. Gounari, O. Azogui, L. Haughn, I. Apostolou, E. Jaeckel, F. Grassi, and L. Klein. 2003. Thymic selection revisited: how essential is it? *Immunol Rev* 191:62-78.

15. Michie, A. M., and J. C. Zúñiga-Pflücker. 2002. Regulation of thymocyte differentiation: pre-TCR signals and beta-selection. *Semin Immunol* 14:311-323.
16. Lauritsen, J. P. H., M. C. Haks, J. M. Lefebvre, D. J. Kappes, and D. L. Wiest. 2006. Recent insights into the signals that control alphabeta/gammadelta-lineage fate. *Immunol Rev* 209:176-190.
17. Borgulya, P., H. Kishi, Y. Uematsu, and H. von Boehmer. 1992. Exclusion and inclusion of alpha and beta T cell receptor alleles. *Cell* 69:529-537.
18. Germain, R. N. 2002. T-cell development and the CD4-CD8 lineage decision. *Nat Rev Immunol* 2:309-322.
19. Swat, W., L. Ignatowicz, H. von Boehmer, and P. Kisielow. 1991. Clonal deletion of immature CD4+8+ thymocytes in suspension culture by extrathymic antigen-presenting cells. *Nature* 351:150-153.
20. Yasutomo, K., C. Doyle, L. Miele, C. Fuchs, and R. N. Germain. 2000. The duration of antigen receptor signalling determines CD4+ versus CD8+ T-cell lineage fate. *Nature* 404:506-510.
21. Brugnera, E., A. Bhandoola, R. Cibotti, Q. Yu, T. I. Guinter, Y. Yamashita, S. O. Sharrow, and A. Singer. 2000. Coreceptor reversal in the thymus: signaled CD4+8+ thymocytes initially terminate CD8 transcription even when differentiating into CD8+ T cells. *Immunity* 13:59-71.
22. Alarcón, B., and H. M. van Santen. 2010. Two receptors, two kinases, and T cell lineage determination. *Science signaling* 3:pe11.
23. Sleckman, B. P., B. Khor, R. Monroe, and F. W. Alt. 1998. Assembly of productive T cell receptor delta variable region genes exhibits allelic inclusion. *J Exp Med* 188:1465-1471.
24. Haks, M. C., J. M. Lefebvre, J. P. H. Lauritsen, M. Carleton, M. Rhodes, T. Miyazaki, D. J. Kappes, and D. L. Wiest. 2005. Attenuation of gammadeltaTCR signaling efficiently diverts thymocytes to the alphabeta lineage. *Immunity* 22:595-606.
25. Hayes, S. M., L. Li, and P. E. Love. 2005. TCR signal strength influences alphabeta/gammadelta lineage fate. *Immunity* 22:583-593.
26. Fontenot, J. D., and A. Y. Rudensky. 2005. A well adapted regulatory contrivance: regulatory T cell development and the forkhead family transcription factor Foxp3. *Nat Immunol* 6:331-337.
27. Cabarrocas, J., C. Cassan, F. Magnusson, E. Piaggio, L. Mars, J. Derbinski, B. Kyewski, D.-A. Gross, B. L. Salomon, K. Khazaie, A. Saoudi, and R. S. Liblau. 2006. Foxp3+ CD25+ regulatory T cells specific for a neo-self-antigen develop at the double-positive thymic stage. *Proc Natl Acad Sci USA* 103:8453-8458.
28. Berg, L. J. 2007. Signalling through TEC kinases regulates conventional versus innate CD8(+) T-cell development. *Nat Rev Immunol* 7:479-485.
29. Urdahl, K. B., J. C. Sun, and M. J. Bevan. 2002. Positive selection of MHC class Ib-restricted CD8(+) T cells on hematopoietic cells. *Nat Immunol* 3:772-779.
30. Sullivan, B. A., P. Kraj, D. A. Weber, L. Ignatowicz, and P. E. Jensen. 2002. Positive selection of a Qa-1-restricted T cell receptor with specificity for insulin. *Immunity* 17:95-105.

31. Treiner, E., L. Duban, S. Bahram, M. Radosavljevic, V. Wanner, F. Tilloy, P. Affaticati, S. Gilfillan, and O. Lantz. 2003. Selection of evolutionarily conserved mucosal-associated invariant T cells by MR1. *Nature* 422:164-169.
32. Bix, M., M. Coles, and D. Raulet. 1993. Positive selection of V beta 8+ CD4-8- thymocytes by class I molecules expressed by hematopoietic cells. *J Exp Med* 178:901-908.
33. Ohteki, T., and H. R. MacDonald. 1994. Major histocompatibility complex class I related molecules control the development of CD4+8- and CD4-8- subsets of natural killer 1.1+ T cell receptor-alpha/beta+ cells in the liver of mice. *J Exp Med* 180:699-704.
34. Bendelac, A. 1995. Positive selection of mouse NK1+ T cells by CD1-expressing cortical thymocytes. *J Exp Med* 182:2091-2096.
35. Egerton, M., R. Scollay, and K. Shortman. 1990. Kinetics of mature T-cell development in the thymus. *Proc Natl Acad Sci USA* 87:2579-2582.
36. Scollay, R., and D. I. Godfrey. 1995. Thymic emigration: conveyor belts or lucky dips? *Immunol Today* 16:268-273; discussion 273-264.
37. Derbinski, J., A. Schulte, B. Kyewski, and L. Klein. 2001. Promiscuous gene expression in medullary thymic epithelial cells mirrors the peripheral self. *Nat Immunol* 2:1032-1039.
38. Chen, W. 2004. The late stage of T cell development within mouse thymus. *Cell Mol Immunol* 1:3-11.
39. Ramsdell, F., M. Jenkins, Q. Dinh, and B. J. Fowlkes. 1991. The majority of CD4+8- thymocytes are functionally immature. *J Immunol* 147:1779-1785.
40. Gabor, M. J., D. I. Godfrey, and R. Scollay. 1997. Recent thymic emigrants are distinct from most medullary thymocytes. *Eur J Immunol* 27:2010-2015.
41. Boursalian, T. E., J. Golob, D. M. Soper, C. J. Cooper, and P. J. Fink. 2004. Continued maturation of thymic emigrants in the periphery. *Nat Immunol* 5:418-425.
42. Kelly, K. A., and R. Scollay. 1990. Analysis of recent thymic emigrants with subset- and maturity-related markers. *International immunology* 2:419-425.
43. McCaughtry, T. M., M. S. Wilken, and K. A. Hogquist. 2007. Thymic emigration revisited. *J Exp Med* 204:2513-2520.
44. Berzins, S., D. Godfrey, and J. Miller. 1999. A central role for thymic emigrants in peripheral T cell homeostasis. *Proc Natl Acad Sci USA* 96:9787-9791.
45. Stutman, O. 1978. Intrathymic and extrathymic T cell maturation. *Immunol Rev* 42:138-184.
46. Staton, T. L., A. Habtezion, M. M. Winslow, T. Sato, P. E. Love, and E. C. Butcher. 2006. CD8+ recent thymic emigrants home to and efficiently repopulate the small intestine epithelium. *Nat Immunol* 7:482-488.
47. Berzins, S. P., A. P. Uldrich, J. S. Sutherland, J. Gill, J. F. A. P. Miller, D. I. Godfrey, and R. L. Boyd. 2002. Thymic regeneration: teaching an old immune system new tricks. *Trends Mol Med* 8:469-476.
48. Weiss, A., and D. R. Littman. 1994. Signal transduction by lymphocyte antigen receptors. *Cell* 76:263-274.

49. Garboczi, D. N., P. Ghosh, U. Utz, Q. R. Fan, W. E. Biddison, and D. C. Wiley. 1996. Structure of the complex between human T-cell receptor, viral peptide and HLA-A2. *Nature* 384:134-141.
50. Zinkernagel, R. M., and P. C. Doherty. 1974. Immunological surveillance against altered self components by sensitised T lymphocytes in lymphocytic choriomeningitis. *Nature* 251:547-548.
51. Zinkernagel, R. M., and P. C. Doherty. 1974. Restriction of in vitro T cell-mediated cytotoxicity in lymphocytic choriomeningitis within a syngeneic or semiallogeneic system. *Nature* 248:701-702.
52. Davis, M. M., Y. H. Chien, N. R. Gascoigne, and S. M. Hedrick. 1984. A murine T cell receptor gene complex: isolation, structure and rearrangement. *Immunol Rev* 81:235-258.
53. Braciale, T. J., V. L. Braciale, M. Winkler, I. Stroynowski, L. Hood, J. Sambrook, and M. J. Gething. 1987. On the role of the transmembrane anchor sequence of influenza hemagglutinin in target cell recognition by class I MHC-restricted, hemagglutinin-specific cytolytic T lymphocytes. *J Exp Med* 166:678-692.
54. Townsend, A. R., J. Bastin, K. Gould, and G. G. Brownlee. 1986. Cytotoxic T lymphocytes recognize influenza haemagglutinin that lacks a signal sequence. *Nature* 324:575-577.
55. Townsend, A. R., F. M. Gotch, and J. Davey. 1985. Cytotoxic T cells recognize fragments of the influenza nucleoprotein. *Cell* 42:457-467.
56. Townsend, A. R., J. Rothbard, F. M. Gotch, G. Bahadur, D. Wraith, and A. J. McMichael. 1986. The epitopes of influenza nucleoprotein recognized by cytotoxic T lymphocytes can be defined with short synthetic peptides. *Cell* 44:959-968.
57. Bjorkman, P. J., M. A. Saper, B. Samraoui, W. S. Bennett, J. L. Strominger, and D. C. Wiley. 1987. Structure of the human class I histocompatibility antigen, HLA-A2. *Nature* 329:506-512.
58. Bjorkman, P. J., M. A. Saper, B. Samraoui, W. S. Bennett, J. L. Strominger, and D. C. Wiley. 1987. The foreign antigen binding site and T cell recognition regions of class I histocompatibility antigens. *Nature* 329:512-518.
59. Ada, G. 1994. Twenty years into the saga of MHC-restriction. *Immunol Cell Biol* 72:447-454.
60. Davis, M. M., J. J. Boniface, Z. Reich, D. Lyons, J. Hampl, B. Arden, and Y. Chien. 1998. Ligand recognition by alpha beta T cell receptors. *Annu Rev Immunol* 16:523-544.
61. Nel, A. E. 2002. T-cell activation through the antigen receptor. Part 1: signaling components, signaling pathways, and signal integration at the T-cell antigen receptor synapse. *J Allergy Clin Immunol* 109:758-770.
62. Iwashima, M., B. A. Irving, N. S. van Oers, A. C. Chan, and A. Weiss. 1994. Sequential interactions of the TCR with two distinct cytoplasmic tyrosine kinases. *Science* 263:1136-1139.
63. Pelosi, M., V. Di Bartolo, V. Mounier, D. Mège, J. M. Pascussi, E. Dufour, A. Blondel, and O. Acuto. 1999. Tyrosine 319 in the interdomain B of ZAP-70 is a

binding site for the Src homology 2 domain of Lck. *J Biol Chem* 274:14229-14237.

64. Sloan-Lancaster, J., A. S. Shaw, J. B. Rothbard, and P. M. Allen. 1994. Partial T cell signaling: altered phospho-zeta and lack of zap70 recruitment in APL-induced T cell anergy. *Cell* 79:913-922.
65. Madrenas, J., R. L. Wange, J. L. Wang, N. Isakov, L. E. Samelson, and R. N. Germain. 1995. Zeta phosphorylation without ZAP-70 activation induced by TCR antagonists or partial agonists. *Science* 267:515-518.
66. Love, P. E., and E. W. Shores. 2000. ITAM multiplicity and thymocyte selection: how low can you go? *Immunity* 12:591-597.
67. Li, L., and V. A. Boussiotis. 2006. Physiologic regulation of central and peripheral T cell tolerance: lessons for therapeutic applications. *J Mol Med* 84:887-899.
68. Crabtree, G. R., and E. N. Olson. 2002. NFAT signaling: choreographing the social lives of cells. *Cell* 109 Suppl:S67-79.
69. Alessi, D. R., and P. Cohen. 1998. Mechanism of activation and function of protein kinase B. *Curr Opin Genet Dev* 8:55-62.
70. Schwartz, R. H. 1990. A cell culture model for T lymphocyte clonal anergy. *Science* 248:1349-1356.
71. Jenkins, M. K., P. S. Taylor, S. D. Norton, and K. B. Urdahl. 1991. CD28 delivers a costimulatory signal involved in antigen-specific IL-2 production by human T cells. *J Immunol* 147:2461-2466.
72. Clarkson, M. R., and M. H. Sayegh. 2005. T-cell costimulatory pathways in allograft rejection and tolerance. *Transplantation* 80:555-563.
73. Linsley, P. S., W. Brady, M. Urnes, L. S. Grosmaire, N. K. Damle, and J. A. Ledbetter. 1991. CTLA-4 is a second receptor for the B cell activation antigen B7. *J Exp Med* 174:561-569.
74. Coyle, A. J., S. Lehar, C. Lloyd, J. Tian, T. Delaney, S. Manning, T. Nguyen, T. Burwell, H. Schneider, J. A. Gonzalo, M. Gosselin, L. R. Owen, C. E. Rudd, and J. C. Gutierrez-Ramos. 2000. The CD28-related molecule ICOS is required for effective T cell-dependent immune responses. *Immunity* 13:95-105.
75. Sharpe, A. H., and G. J. Freeman. 2002. The B7-CD28 superfamily. *Nat Rev Immunol* 2:116-126.
76. Freeman, G. J., A. J. Long, Y. Iwai, K. Bourque, T. Chernova, H. Nishimura, L. J. Fitz, N. Malenkovich, T. Okazaki, M. C. Byrne, H. F. Horton, L. Fouser, L. Carter, V. Ling, M. R. Bowman, B. M. Carreno, M. Collins, C. R. Wood, and T. Honjo. 2000. Engagement of the PD-1 immunoinhibitory receptor by a novel B7 family member leads to negative regulation of lymphocyte activation. *J Exp Med* 192:1027-1034.
77. Rothstein, D. M., and M. H. Sayegh. 2003. T-cell costimulatory pathways in allograft rejection and tolerance. *Immunol Rev* 196:85-108.
78. Latchman, Y., C. R. Wood, T. Chernova, D. Chaudhary, M. Borde, I. Chernova, Y. Iwai, A. J. Long, J. A. Brown, R. Nunes, E. A. Greenfield, K. Bourque, V. A. Boussiotis, L. L. Carter, B. M. Carreno, N. Malenkovich, H. Nishimura, T.

Okazaki, T. Honjo, A. H. Sharpe, and G. J. Freeman. 2001. PD-L2 is a second ligand for PD-1 and inhibits T cell activation. *Nat Immunol* 2:261-268.

79. Nishimura, H., N. Minato, T. Nakano, and T. Honjo. 1998. Immunological studies on PD-1 deficient mice: implication of PD-1 as a negative regulator for B cell responses. *International immunology* 10:1563-1572.
80. Viola, A., S. Schroeder, Y. Sakakibara, and A. Lanzavecchia. 1999. T lymphocyte costimulation mediated by reorganization of membrane microdomains. *Science* 283:680-682.
81. Klasen, S., F. Pages, J. F. Peyron, D. A. Cantrell, and D. Olive. 1998. Two distinct regions of the CD28 intracytoplasmic domain are involved in the tyrosine phosphorylation of Vav and GTPase activating protein-associated p62 protein. *International immunology* 10:481-489.
82. Sadra, A., T. Cinek, J. L. Arellano, J. Shi, K. E. Truitt, and J. B. Imboden. 1999. Identification of tyrosine phosphorylation sites in the CD28 cytoplasmic domain and their role in the costimulation of Jurkat T cells. *J Immunol* 162:1966-1973.
83. Khoshnan, A., D. Bae, C. A. Tindell, and A. E. Nel. 2000. The physical association of protein kinase C theta with a lipid raft-associated inhibitor of kappa B factor kinase (IKK) complex plays a role in the activation of the NF-kappa B cascade by TCR and CD28. *J Immunol* 165:6933-6940.
84. Khoshnan, A., C. Tindell, I. Laux, D. Bae, B. Bennett, and A. E. Nel. 2000. The NF-kappa B cascade is important in Bcl-xL expression and for the anti-apoptotic effects of the CD28 receptor in primary human CD4+ lymphocytes. *J Immunol* 165:1743-1754.
85. Boise, L. H., A. J. Minn, P. J. Noel, C. H. June, M. A. Accavitti, T. Lindsten, and C. B. Thompson. 1995. CD28 costimulation can promote T cell survival by enhancing the expression of Bcl-XL. *Immunity* 3:87-98.
86. Croft, M. 2003. Co-stimulatory members of the TNFR family: keys to effective T-cell immunity? *Nat Rev Immunol* 3:609-620.
87. Larsen, C. P., and T. C. Pearson. 1997. The CD40 pathway in allograft rejection, acceptance, and tolerance. *Curr Opin Immunol* 9:641-647.
88. Borst, J., C. Sluyser, E. De Vries, H. Klein, C. J. Melief, and R. A. Van Lier. 1989. Alternative molecular form of human T cell-specific antigen CD27 expressed upon T cell activation. *Eur J Immunol* 19:357-364.
89. Morel, Y., J. M. Schiano de Colella, J. Harrop, K. C. Deen, S. D. Holmes, T. A. Wattam, S. S. Khandekar, A. Truneh, R. W. Sweet, J. A. Gastaut, D. Olive, and R. T. Costello. 2000. Reciprocal expression of the TNF family receptor herpes virus entry mediator and its ligand LIGHT on activated T cells: LIGHT down-regulates its own receptor. *J Immunol* 165:4397-4404.
90. de Jong, R., W. A. Loenen, M. Brouwer, L. van Emmerik, E. F. de Vries, J. Borst, and R. A. Van Lier. 1991. Regulation of expression of CD27, a T cell-specific member of a novel family of membrane receptors. *J Immunol* 146:2488-2494.
91. Harty, J. T., and V. P. Badovinac. 2008. Shaping and reshaping CD8+ T-cell memory. *Nat Rev Immunol* 8:107-119.

92. Bennett, S. R., F. R. Carbone, F. Karamalis, R. A. Flavell, J. F. Miller, and W. R. Heath. 1998. Help for cytotoxic-T-cell responses is mediated by CD40 signalling. *Nature* 393:478-480.
93. Janssen, E. M., N. M. Droin, E. E. Lemmens, M. J. Pinkoski, S. J. Bensinger, B. D. Ehst, T. S. Griffith, D. R. Green, and S. P. Schoenberger. 2005. CD4+ T-cell help controls CD8+ T-cell memory via TRAIL-mediated activation-induced cell death. *Nature* 434:88-93.
94. Bevan, M. J. 2004. Helping the CD8(+) T-cell response. *Nat Rev Immunol* 4:595-602.
95. Ridge, J. P., F. Di Rosa, and P. Matzinger. 1998. A conditioned dendritic cell can be a temporal bridge between a CD4+ T-helper and a T-killer cell. *Nature* 393:474-478.
96. Schoenberger, S. P., R. E. Toes, E. I. van der Voort, R. Offringa, and C. J. Melief. 1998. T-cell help for cytotoxic T lymphocytes is mediated by CD40-CD40L interactions. *Nature* 393:480-483.
97. D'Souza, W. N., and L. Lefrançois. 2003. IL-2 is not required for the initiation of CD8 T cell cycling but sustains expansion. *J Immunol* 171:5727-5735.
98. Williams, M. A., A. J. Tyznik, and M. J. Bevan. 2006. Interleukin-2 signals during priming are required for secondary expansion of CD8+ memory T cells. *Nature* 441:890-893.
99. Boyman, O., M. Kovar, M. P. Rubinstein, C. D. Surh, and J. Sprent. 2006. Selective stimulation of T cell subsets with antibody-cytokine immune complexes. *Science* 311:1924-1927.
100. Curtsinger, J. M., C. S. Schmidt, A. Mondino, D. C. Lins, R. M. Kedl, M. K. Jenkins, and M. F. Mescher. 1999. Inflammatory cytokines provide a third signal for activation of naive CD4+ and CD8+ T cells. *J Immunol* 162:3256-3262.
101. Schmidt, C. S., and M. F. Mescher. 1999. Adjuvant effect of IL-12: conversion of peptide antigen administration from tolerizing to immunizing for CD8+ T cells in vivo. *J Immunol* 163:2561-2567.
102. Curtsinger, J. M., J. O. Valenzuela, P. Agarwal, D. Lins, and M. F. Mescher. 2005. Type I IFNs provide a third signal to CD8 T cells to stimulate clonal expansion and differentiation. *J Immunol* 174:4465-4469.
103. Hochrein, H., K. Shortman, D. Vremec, B. Scott, P. Hertzog, and M. O'Keeffe. 2001. Differential production of IL-12, IFN-alpha, and IFN-gamma by mouse dendritic cell subsets. *J Immunol* 166:5448-5455.
104. Mescher, M. F., J. M. Curtsinger, P. Agarwal, K. A. Casey, M. Gerner, C. D. Hammerbeck, F. Popescu, and Z. Xiao. 2006. Signals required for programming effector and memory development by CD8+ T cells. *Immunol Rev* 211:81-92.
105. Aichele, P., H. Unsoeld, M. Koschella, O. Schweier, U. Kalinke, and S. Vucikuja. 2006. CD8 T cells specific for lymphocytic choriomeningitis virus require type I IFN receptor for clonal expansion. *J Immunol* 176:4525-4529.
106. Curtsinger, J. M., C. M. Johnson, and M. F. Mescher. 2003. CD8 T cell clonal expansion and development of effector function require prolonged exposure to antigen, costimulation, and signal 3 cytokine. *J Immunol* 171:5165-5171.

107. Kolumam, G. A., S. Thomas, L. J. Thompson, J. Sprent, and K. Murali-Krishna. 2005. Type I interferons act directly on CD8 T cells to allow clonal expansion and memory formation in response to viral infection. *J Exp Med* 202:637-650.
108. Mitchell, T. C., D. Hildeman, R. M. Kedl, T. K. Teague, B. C. Schaefer, J. White, Y. Zhu, J. Kappler, and P. Marrack. 2001. Immunological adjuvants promote activated T cell survival via induction of Bcl-3. *Nat Immunol* 2:397-402.
109. Mattei, F., G. Schiavoni, F. Belardelli, and D. F. Tough. 2001. IL-15 is expressed by dendritic cells in response to type I IFN, double-stranded RNA, or lipopolysaccharide and promotes dendritic cell activation. *J Immunol* 167:1179-1187.
110. Schluns, K. S., and L. Lefrançois. 2003. Cytokine control of memory T-cell development and survival. *Nat Rev Immunol* 3:269-279.
111. Kaech, S. M., E. J. Wherry, and R. Ahmed. 2002. Effector and memory T-cell differentiation: implications for vaccine development. *Nat Rev Immunol* 2:251-262.
112. Shahinian, A., K. Pfeffer, K. P. Lee, T. M. Kündig, K. Kishihara, A. Wakeham, K. Kawai, P. S. Ohashi, C. B. Thompson, and T. W. Mak. 1993. Differential T cell costimulatory requirements in CD28-deficient mice. *Science* 261:609-612.
113. Tan, J. T., J. K. Whitmire, R. Ahmed, T. C. Pearson, and C. P. Larsen. 1999. 4-1BB ligand, a member of the TNF family, is important for the generation of antiviral CD8 T cell responses. *J Immunol* 163:4859-4868.
114. Iezzi, G., K. Karjalainen, and A. Lanzavecchia. 1998. The duration of antigenic stimulation determines the fate of naive and effector T cells. *Immunity* 8:89-95.
115. Jelley-Gibbs, D. M., N. M. Lepak, M. Yen, and S. L. Swain. 2000. Two distinct stages in the transition from naive CD4 T cells to effectors, early antigen-dependent and late cytokine-driven expansion and differentiation. *J Immunol* 165:5017-5026.
116. Gett, A. V., and P. D. Hodgkin. 2000. A cellular calculus for signal integration by T cells. *Nat Immunol* 1:239-244.
117. Kaech, S. M., and R. Ahmed. 2001. Memory CD8+ T cell differentiation: initial antigen encounter triggers a developmental program in naïve cells. *Nat Immunol* 2:415-422.
118. Mempel, T. R., S. E. Henrickson, and U. H. von Andrian. 2004. T-cell priming by dendritic cells in lymph nodes occurs in three distinct phases. *Nature* 427:154-159.
119. Wherry, E. J., and R. Ahmed. 2004. Memory CD8 T-cell differentiation during viral infection. *J Virol* 78:5535-5545.
120. Kaech, S. M., J. T. Tan, E. J. Wherry, B. T. Konieczny, C. D. Surh, and R. Ahmed. 2003. Selective expression of the interleukin 7 receptor identifies effector CD8 T cells that give rise to long-lived memory cells. *Nat Immunol* 4:1191-1198.
121. Joshi, N. S., W. Cui, A. Chandele, H. K. Lee, D. R. Urso, J. Hagman, L. Gapin, and S. M. Kaech. 2007. Inflammation directs memory precursor and short-lived effector CD8(+) T cell fates via the graded expression of T-bet transcription factor. *Immunity* 27:281-295.

122. Huster, K. M., V. Busch, M. Schiemann, K. Linkemann, K. M. Kerksiek, H. Wagner, and D. H. Busch. 2004. Selective expression of IL-7 receptor on memory T cells identifies early CD40L-dependent generation of distinct CD8+ memory T cell subsets. *Proc Natl Acad Sci USA* 101:5610-5615.
123. Badovinac, V. P., B. B. Porter, and J. T. Harty. 2002. Programmed contraction of CD8(+) T cells after infection. *Nat Immunol* 3:619-626.
124. Nguyen, L. T., K. McKall-Faienza, A. Zakarian, D. E. Speiser, T. W. Mak, and P. S. Ohashi. 2000. TNF receptor 1 (TNFR1) and CD95 are not required for T cell deletion after virus infection but contribute to peptide-induced deletion under limited conditions. *Eur J Immunol* 30:683-688.
125. Razvi, E. S., Z. Jiang, B. A. Woda, and R. M. Welsh. 1995. Lymphocyte apoptosis during the silencing of the immune response to acute viral infections in normal, lpr, and Bcl-2-transgenic mice. *Am J Pathol* 147:79-91.
126. Hildeman, D. A., Y. Zhu, T. C. Mitchell, P. Bouillet, A. Strasser, J. Kappler, and P. Marrack. 2002. Activated T cell death in vivo mediated by proapoptotic bcl-2 family member bim. *Immunity* 16:759-767.
127. Pellegrini, M., G. Belz, P. Bouillet, and A. Strasser. 2003. Shutdown of an acute T cell immune response to viral infection is mediated by the proapoptotic Bcl-2 homology 3-only protein Bim. *Proc Natl Acad Sci USA* 100:14175-14180.
128. Wojciechowski, S., M. B. Jordan, Y. Zhu, J. White, A. J. Zajac, and D. A. Hildeman. 2006. Bim mediates apoptosis of CD127(lo) effector T cells and limits T cell memory. *Eur J Immunol* 36:1694-1706.
129. Wojciechowski, S., P. Tripathi, T. Bourdeau, L. Acero, H. L. Grimes, J. D. Katz, F. D. Finkelman, and D. A. Hildeman. 2007. Bim/Bcl-2 balance is critical for maintaining naive and memory T cell homeostasis. *J Exp Med* 204:1665-1675.
130. Grayson, J. M., A. E. Weant, B. C. Holbrook, and D. Hildeman. 2006. Role of Bim in regulating CD8+ T-cell responses during chronic viral infection. *J Virol* 80:8627-8638.
131. Weant, A. E., R. D. Michalek, I. U. Khan, B. C. Holbrook, M. C. Willingham, and J. M. Grayson. 2008. Apoptosis regulators Bim and Fas function concurrently to control autoimmunity and CD8+ T cell contraction. *Immunity* 28:218-230.
132. Sallusto, F., D. Lenig, R. Förster, M. Lipp, and A. Lanzavecchia. 1999. Two subsets of memory T lymphocytes with distinct homing potentials and effector functions. *Nature* 401:708-712.
133. Intlekofer, A. M., N. Takemoto, C. Kao, A. Banerjee, F. Schambach, J. K. Northrop, H. Shen, E. J. Wherry, and S. L. Reiner. 2007. Requirement for T-bet in the aberrant differentiation of unhelped memory CD8+ T cells. *J Exp Med* 204:2015-2021.
134. Pearce, E. L., and H. Shen. 2007. Generation of CD8 T cell memory is regulated by IL-12. *J Immunol* 179:2074-2081.
135. Freitas, A. A., and B. Rocha. 2000. Population biology of lymphocytes: the flight for survival. *Annu Rev Immunol* 18:83-111.

136. Kaech, S. M., and E. J. Wherry. 2007. Heterogeneity and cell-fate decisions in effector and memory CD8+ T cell differentiation during viral infection. *Immunity* 27:393-405.
137. Chang, J. T., V. R. Palanivel, I. Kinjyo, F. Schambach, A. M. Intlekofer, A. Banerjee, S. A. Longworth, K. E. Vinup, P. Mrass, J. Oliaro, N. Killeen, J. S. Orange, S. M. Russell, W. Weninger, and S. L. Reiner. 2007. Asymmetric T lymphocyte division in the initiation of adaptive immune responses. *Science* 315:1687-1691.
138. Stemberger, C., K. M. Huster, M. Koffler, F. Anderl, M. Schiemann, H. Wagner, and D. H. Busch. 2007. A single naive CD8+ T cell precursor can develop into diverse effector and memory subsets. *Immunity* 27:985-997.
139. Gerlach, C., J. W. J. van Heijst, E. Swart, D. Sie, N. Armstrong, R. M. Kerkhoven, D. Zehn, M. J. Bevan, K. Schepers, and T. N. M. Schumacher. 2010. One naive T cell, multiple fates in CD8+ T cell differentiation. *J Exp Med* 207:1235-1246.
140. Suresh, M., G. Lanier, M. K. Large, J. K. Whitmire, J. D. Altman, N. H. Ruddle, and R. Ahmed. 2002. Role of lymphotoxin alpha in T-cell responses during an acute viral infection. *J Virol* 76:3943-3951.
141. Aggarwal, B. B. 2003. Signalling pathways of the TNF superfamily: a double-edged sword. *Nat Rev Immunol* 3:745-756.
142. Coley, W. B. 1891. II. Contribution to the Knowledge of Sarcoma. *Ann Surg* 14:199-220.
143. Berendt, M., R. North, and D. Kirstein. 1978. The immunological basis of endotoxin-induced tumor regression. Requirement for a pre-existing state of concomitant anti-tumor immunity. *The Journal of Experimental Medicine* 148:1560-1569.
144. O'Malley, W. E., B. Achinstein, and M. J. Shear. 1988. Journal of the National Cancer Institute, Vol. 29, 1962: Action of bacterial polysaccharide on tumors. II. Damage of sarcoma 37 by serum of mice treated with Serratia marcescens polysaccharide, and induced tolerance. *Nutr Rev* 46:389-391.
145. Carswell, E. A., L. J. Old, R. L. Kassel, S. Green, N. Fiore, and B. Williamson. 1975. An endotoxin-induced serum factor that causes necrosis of tumors. *Proc Natl Acad Sci USA* 72:3666-3670.
146. Williamson, B. D., E. A. Carswell, B. Y. Rubin, J. S. Prendergast, and L. J. Old. 1983. Human tumor necrosis factor produced by human B-cell lines: synergistic cytotoxic interaction with human interferon. *Proc Natl Acad Sci USA* 80:5397-5401.
147. Williams, T. W., and G. A. Granger. 1968. Lymphocyte in vitro cytotoxicity: lymphotoxins of several mammalian species. *Nature* 219:1076-1077.
148. Ruddle, N. H., and B. H. Waksman. 1968. Cytotoxicity mediated by soluble antigen and lymphocytes in delayed hypersensitivity. I. Characterization of the phenomenon. *J Exp Med* 128:1237-1254.

149. Ruddle, N. H., and B. H. Waksman. 1968. Cytotoxicity mediated by soluble antigen and lymphocytes in delayed hypersensitivity. II. Correlation of the in vitro response with skin reactivity. *J Exp Med* 128:1255-1265.
150. Ruddle, N. H., and B. H. Waksman. 1968. Cytotoxicity mediated by soluble antigen and lymphocytes in delayed hypersensitivity. 3. Analysis of mechanism. *J Exp Med* 128:1267-1279.
151. Aggarwal, B. B., W. J. Henzel, B. Moffat, W. J. Kohr, and R. N. Harkins. 1985. Primary structure of human lymphotoxin derived from 1788 lymphoblastoid cell line. *J Biol Chem* 260:2334-2344.
152. Aggarwal, B. B., W. J. Kohr, P. E. Hass, B. Moffat, S. A. Spencer, W. J. Henzel, T. S. Bringman, G. E. Nedwin, D. V. Goeddel, and R. N. Harkins. 1985. Human tumor necrosis factor. Production, purification, and characterization. *J Biol Chem* 260:2345-2354.
153. Aggarwal, B. B., T. E. Eessalu, and P. E. Hass. 1985. Characterization of receptors for human tumour necrosis factor and their regulation by gamma-interferon. *Nature* 318:665-667.
154. Beutler, B., D. Greenwald, J. D. Hulmes, M. Chang, Y. C. Pan, J. Mathison, R. Ulevitch, and A. Cerami. 1985. Identity of tumour necrosis factor and the macrophage-secreted factor cachectin. *Nature* 316:552-554.
155. Takeda, K., S. Iwamoto, H. Sugimoto, T. Takuma, N. Kawatani, M. Noda, A. Masaki, H. Morise, H. Arimura, and K. Konno. 1986. Identity of differentiation inducing factor and tumour necrosis factor. *Nature* 323:338-340.
156. Hehlgans, T., and D. N. Männel. 2002. The TNF-TNF receptor system. *Biol Chem* 383:1581-1585.
157. Hehlgans, T., and K. Pfeffer. 2005. The intriguing biology of the tumour necrosis factor/tumour necrosis factor receptor superfamily: players, rules and the games. *Immunology* 115:1-20.
158. Chan, F. K., H. J. Chun, L. Zheng, R. M. Siegel, K. L. Bui, and M. J. Lenardo. 2000. A domain in TNF receptors that mediates ligand-independent receptor assembly and signaling. *Science* 288:2351-2354.
159. Smyth, M. J., and R. W. Johnstone. 2000. Role of TNF in lymphocyte-mediated cytotoxicity. *Microsc Res Tech* 50:196-208.
160. MacEwan, D. J. 2002. TNF receptor subtype signalling: differences and cellular consequences. *Cell Signal* 14:477-492.
161. Vandenabeele, P., W. Declercq, F. Van Herreweghe, and T. Vanden Berghe. 2010. The role of the kinases RIP1 and RIP3 in TNF-induced necrosis. *Science signaling* 3:re4.
162. Dempsey, P. W., S. E. Doyle, J. Q. He, and G. Cheng. 2003. The signaling adaptors and pathways activated by TNF superfamily. *Cytokine Growth Factor Rev* 14:193-209.
163. Faustman, D., and M. Davis. 2010. TNF receptor 2 pathway: drug target for autoimmune diseases. *Nat Rev Drug Discov* 9:482-493.
164. Li, X., Y. Yang, and J. D. Ashwell. 2002. TNF-RII and c-IAP1 mediate ubiquitination and degradation of TRAF2. *Nature* 416:345-347.

165. Askenasy, N., E. S. Yolcu, I. Yaniv, and H. Shirwan. 2005. Induction of tolerance using Fas ligand: a double-edged immunomodulator. *Blood* 105:1396-1404.
166. Strasser, A., P. J. Jost, and S. Nagata. 2009. The many roles of FAS receptor signaling in the immune system. *Immunity* 30:180-192.
167. Kuprash, D. V., M. B. Alimzhanov, A. V. Tumanov, S. I. Grivennikov, A. N. Shakhov, L. N. Drutskaya, M. W. Marino, R. L. Turetskaya, A. O. Anderson, K. Rajewsky, K. Pfeffer, and S. A. Nedospasov. 2002. Redundancy in tumor necrosis factor (TNF) and lymphotoxin (LT) signaling in vivo: mice with inactivation of the entire TNF/LT locus versus single-knockout mice. *Molecular and Cellular Biology* 22:8626-8634.
168. Wajant, H., K. Pfizenmaier, and P. Scheurich. 2003. Tumor necrosis factor signaling. *Cell Death Differ* 10:45-65.
169. Zheng, Y., P. Saftig, D. Hartmann, and C. Blobel. 2004. Evaluation of the contribution of different ADAMs to tumor necrosis factor alpha (TNFalpha) shedding and of the function of the TNFalpha ectodomain in ensuring selective stimulated shedding by the TNFalpha convertase (TACE/ADAM17). *J Biol Chem* 279:42898-42906.
170. Kollias, G., E. Douni, and G. Kassiotis. 1999. The function of tumour necrosis factor and receptors in models of multi-organ inflammation, rheumatoid arthritis,multiple sclerosis and inflammatory bowel disease. *British Medical Journal* 58:i32-i39.
171. Locksley, R. M., N. Killeen, and M. J. Lenardo. 2001. The TNF and TNF receptor superfamilies: integrating mammalian biology. *Cell* 104:487-501.
172. Ware, C. F., P. D. Crowe, M. H. Grayson, M. J. Androlewicz, and J. L. Browning. 1992. Expression of surface lymphotoxin and tumor necrosis factor on activated T, B, and natural killer cells. *J Immunol* 149:3881-3888.
173. Mebius, R. E., P. Rennert, and I. L. Weissman. 1997. Developing lymph nodes collect CD4+CD3- LTbeta+ cells that can differentiate to APC, NK cells, and follicular cells but not T or B cells. *Immunity* 7:493-504.
174. Crowe, P. D., T. L. VanArsdale, B. N. Walter, C. F. Ware, C. Hession, B. Ehrenfels, J. L. Browning, W. S. Din, R. G. Goodwin, and C. A. Smith. 1994. A lymphotoxin-beta-specific receptor. *Science* 264:707-710.
175. Grivennikov, S. I., A. V. Tumanov, D. J. Liepinsh, A. A. Kruglov, B. I. Marakusha, A. N. Shakhov, T. Murakami, L. N. Drutskaya, I. Förster, B. E. Clausen, L. Tessarollo, B. Ryffel, D. V. Kuprash, and S. A. Nedospasov. 2005. Distinct and nonredundant in vivo functions of TNF produced by t cells and macrophages/neutrophils: protective and deleterious effects. *Immunity* 22:93-104.
176. Pasparakis, M., L. Alexopoulou, V. Episkopou, and G. Kollias. 1996. Immune and inflammatory responses in TNF alpha-deficient mice: a critical requirement for TNF alpha in the formation of primary B cell follicles, follicular dendritic cell networks and germinal centers, and in the maturation of the humoral immune response. *J Exp Med* 184:1397-1411.
177. Alimzhanov, M. B., D. V. Kuprash, M. H. Kosco-Vilbois, A. Luz, R. L. Turetskaya, A. Tarakhovsky, K. Rajewsky, S. A. Nedospasov, and K. Pfeffer.

1997. Abnormal development of secondary lymphoid tissues in lymphotoxin beta-deficient mice. *Proc Natl Acad Sci USA* 94:9302-9307.

178. Banks, T. A., B. T. Rouse, M. K. Kerley, P. J. Blair, V. L. Godfrey, N. A. Kuklin, D. M. Bouley, J. Thomas, S. Kanangat, and M. L. Mucenski. 1995. Lymphotoxin-alpha-deficient mice. Effects on secondary lymphoid organ development and humoral immune responsiveness. *J Immunol* 155:1685-1693.
179. De Togni, P., J. Goellner, N. H. Ruddle, P. R. Streeter, A. Fick, S. Mariathasan, S. C. Smith, R. Carlson, L. P. Shornick, and J. Strauss-Schoenberger. 1994. Abnormal development of peripheral lymphoid organs in mice deficient in lymphotoxin. *Science* 264:703-707.
180. Fütterer, A., K. Mink, A. Luz, M. H. Kosco-Vilbois, and K. Pfeffer. 1998. The lymphotoxin beta receptor controls organogenesis and affinity maturation in peripheral lymphoid tissues. *Immunity* 9:59-70.
181. Koni, P. A., R. Sacca, P. Lawton, J. L. Browning, N. H. Ruddle, and R. A. Flavell. 1997. Distinct roles in lymphoid organogenesis for lymphotoxins alpha and beta revealed in lymphotoxin beta-deficient mice. *Immunity* 6:491-500.
182. Calzascia, T., M. Pellegrini, H. Hall, L. Sabbagh, N. Ono, A. R. Elford, T. W. Mak, and P. S. Ohashi. 2007. TNF-alpha is critical for antitumor but not antiviral T cell immunity in mice. *J Clin Invest* 117:3833-3845.
183. Kasahara, S., K. Ando, K. Saito, K. Sekikawa, H. Ito, T. Ishikawa, H. Ohnishi, M. Seishima, S. Kakumu, and H. Moriwaki. 2003. Lack of tumor necrosis factor alpha induces impaired proliferation of hepatitis B virus-specific cytotoxic T lymphocytes. *J Virol* 77:2469-2476.
184. Elkon, K. B., C. C. Liu, J. G. Gall, J. Trevejo, M. W. Marino, K. A. Abrahamsen, X. Song, J. L. Zhou, L. J. Old, R. G. Crystal, and E. Falck-Pedersen. 1997. Tumor necrosis factor alpha plays a central role in immune-mediated clearance of adenoviral vectors. *Proc Natl Acad Sci USA* 94:9814-9819.
185. Trevejo, J. M., M. W. Marino, N. Philpott, R. Josien, E. C. Richards, K. B. Elkon, and E. Falck-Pedersen. 2001. TNF-alpha -dependent maturation of local dendritic cells is critical for activating the adaptive immune response to virus infection. *Proc Natl Acad Sci USA* 98:12162-12167.
186. Kim, E. Y., and H.-S. Teh. 2004. Critical role of TNF receptor type-2 (p75) as a costimulator for IL-2 induction and T cell survival: a functional link to CD28. *J Immunol* 173:4500-4509.
187. Kim, E. Y., J. J. Priatel, S.-J. Teh, and H.-S. Teh. 2006. TNF receptor type 2 (p75) functions as a costimulator for antigen-driven T cell responses in vivo. *J Immunol* 176:1026-1035.
188. McKarns, S. C., and R. H. Schwartz. 2008. Biphasic regulation of Il2 transcription in CD4+ T cells: roles for TNF-alpha receptor signaling and chromatin structure. *J Immunol* 181:1272-1281.
189. Evangelidou, M., V. Tseveleki, S.-S. Vamvakas, and L. Probert. 2010. TNFRI is a positive T-cell costimulatory molecule important for the timing of cytokine responses. *Immunol Cell Biol* 88:586-595.

190. Kim, E. Y., S.-J. Teh, J. Yang, M. T. Chow, and H.-S. Teh. 2009. TNFR2-deficient memory CD8 T cells provide superior protection against tumor cell growth. *J Immunol* 183:6051-6057.
191. Suresh, M., A. Singh, and C. Fischer. 2005. Role of tumor necrosis factor receptors in regulating CD8 T-cell responses during acute lymphocytic choriomeningitis virus infection. *J Virol* 79:202-213.
192. Singh, A., M. Wuthrich, B. Klein, and M. Suresh. 2007. Indirect regulation of CD4 T-cell responses by tumor necrosis factor receptors in an acute viral infection. *J Virol* 81:6502-6512.
193. Pang, L., L. Wang, T. Suo, H. Hao, X. Fang, J. Jia, F. Huang, and J. Tang. 2008. Tumor necrosis factor-alpha blockade leads to decreased peripheral T cell reactivity and increased dendritic cell number in peripheral blood of patients with ankylosing spondylitis. *J Rheumatol* 35:2220-2228.
194. Gunnlaugsdottir, B., I. Skaftadottir, and B. R. Ludviksson. 2008. Naive human T-cells become non-responsive towards anti-TNFalpha (infliximab) treatment in vitro if co-stimulated through CD28. *Scand J Immunol* 68:624-634.
195. Notley, C. A., J. J. Inglis, S. Alzabin, F. E. McCann, K. E. McNamee, and R. O. Williams. 2008. Blockade of tumor necrosis factor in collagen-induced arthritis reveals a novel immunoregulatory pathway for Th1 and Th17 cells. *J Exp Med* 205:2491-2497.
196. Tracey, D., L. Klareskog, E. H. Sasso, J. G. Salfeld, and P. P. Tak. 2008. Tumor necrosis factor antagonist mechanisms of action: a comprehensive review. *Pharmacol Ther* 117:244-279.
197. Bruns, H., C. Meinken, P. Schauenberg, G. Härter, P. Kern, R. L. Modlin, C. Antoni, and S. Stenger. 2009. Anti-TNF immunotherapy reduces CD8+ T cell-mediated antimicrobial activity against Mycobacterium tuberculosis in humans. *J Clin Invest* 119:1167-1177.
198. Eggermont, A. M. M., J. H. W. de Wilt, and T. L. M. ten Hagen. 2003. Current uses of isolated limb perfusion in the clinic and a model system for new strategies. *Lancet Oncol* 4:429-437.
199. Lans, T. E., D. L. Bartlett, S. K. Libutti, M. F. Gnant, D. J. Liewehr, D. J. Venzon, E. M. Turner, and H. R. Alexander. 2001. Role of tumor necrosis factor on toxicity and cytokine production after isolated hepatic perfusion. *Clin Cancer Res* 7:784-790.
200. O' Reilly, L. A., L. Tai, L. Lee, E. A. Kruse, S. Grabow, W. D. Fairlie, N. M. Haynes, D. M. Tarlinton, J.-G. Zhang, G. T. Belz, M. J. Smyth, P. Bouillet, L. Robb, and A. Strasser. 2009. Membrane-bound Fas ligand only is essential for Fas-induced apoptosis. *Nature* 461:659-663.
201. Green, D. R., and T. A. Ferguson. 2001. The role of Fas ligand in immune privilege. *Nat Rev Mol Cell Biol* 2:917-924.
202. Watanabe-Fukunaga, R., C. I. Brannan, N. G. Copeland, N. A. Jenkins, and S. Nagata. 1992. Lymphoproliferation disorder in mice explained by defects in Fas antigen that mediates apoptosis. *Nature* 356:314-317.

203. Takahashi, T., M. Tanaka, C. I. Brannan, N. A. Jenkins, N. G. Copeland, T. Suda, and S. Nagata. 1994. Generalized lymphoproliferative disease in mice, caused by a point mutation in the Fas ligand. *Cell* 76:969-976.
204. Fisher, G. H., F. J. Rosenberg, S. E. Straus, J. K. Dale, L. A. Middleton, A. Y. Lin, W. Strober, M. J. Lenardo, and J. M. Puck. 1995. Dominant interfering Fas gene mutations impair apoptosis in a human autoimmune lymphoproliferative syndrome. *Cell* 81:935-946.
205. Rieux-Laucat, F., F. Le Deist, C. Hivroz, I. A. Roberts, K. M. Debatin, A. Fischer, and J. P. de Villartay. 1995. Mutations in Fas associated with human lymphoproliferative syndrome and autoimmunity. *Science* 268:1347-1349.
206. Hao, Z., G. S. Duncan, J. Seagal, Y.-W. Su, C. Hong, J. Haight, N.-J. Chen, A. Elia, A. Wakeham, W. Y. Li, J. Liepa, G. A. Wood, S. Casola, K. Rajewsky, and T. W. Mak. 2008. Fas receptor expression in germinal-center B cells is essential for T and B lymphocyte homeostasis. *Immunity* 29:615-627.
207. Shlomchik, M. J., M. P. Madaio, D. Ni, M. Trounstein, and D. Huszar. 1994. The role of B cells in lpr/lpr-induced autoimmunity. *J Exp Med* 180:1295-1306.
208. Fukuyama, H., M. Adachi, S. Suematsu, K. Miwa, T. Suda, N. Yoshida, and S. Nagata. 2002. Requirement of Fas expression in B cells for tolerance induction. *Eur J Immunol* 32:223-230.
209. Nagata, S., and T. Suda. 1995. Fas and Fas ligand: lpr and gld mutations. *Immunol Today* 16:39-43.
210. Singer, G. G., and A. K. Abbas. 1994. The fas antigen is involved in peripheral but not thymic deletion of T lymphocytes in T cell receptor transgenic mice. *Immunity* 1:365-371.
211. Suzuki, I., S. Martin, T. E. Boursalian, C. Beers, and P. J. Fink. 2000. Fas ligand costimulates the in vivo proliferation of CD8+ T cells. *J Immunol* 165:5537-5543.
212. Strauss, G., J. A. Lindquist, N. Arhel, E. Felder, S. Karl, T. L. Haas, S. Fulda, H. Walczak, F. Kirchhoff, and K.-M. Debatin. 2009. CD95 co-stimulation blocks activation of naive T cells by inhibiting T cell receptor signaling. *J Exp Med* 206:1379-1393.
213. Elmore, S. 2007. Apoptosis: a review of programmed cell death. *Toxicol Pathol* 35:495-516.
214. Bouillet, P., and L. A. O'reilly. 2009. CD95, BIM and T cell homeostasis. *Nat Rev Immunol* 9:514-519.
215. Bouillet, P., D. Metcalf, D. C. Huang, D. M. Tarlinton, T. W. Kay, F. Köntgen, J. M. Adams, and A. Strasser. 1999. Proapoptotic Bcl-2 relative Bim required for certain apoptotic responses, leukocyte homeostasis, and to preclude autoimmunity. *Science* 286:1735-1738.
216. Bouillet, P., J. F. Purton, D. I. Godfrey, L.-C. Zhang, L. Coultas, H. Puthalakath, M. Pellegrini, S. Cory, J. M. Adams, and A. Strasser. 2002. BH3-only Bcl-2 family member Bim is required for apoptosis of autoreactive thymocytes. *Nature* 415:922-926.

217. Hu, Q., A. Sader, J. C. Parkman, and T. A. Baldwin. 2009. Bim-mediated apoptosis is not necessary for thymic negative selection to ubiquitous self-antigens. *J Immunol* 183:7761-7767.
218. Redmond, W. L., and L. A. Sherman. 2005. Peripheral tolerance of CD8 T lymphocytes. *Immunity* 22:275-284.
219. Anderson, M. S., E. S. Venanzi, L. Klein, Z. Chen, S. P. Berzins, S. J. Turley, H. von Boehmer, R. Bronson, A. Dierich, C. Benoist, and D. Mathis. 2002. Projection of an immunological self shadow within the thymus by the aire protein. *Science* 298:1395-1401.
220. Gardner, J. M., A. L. Fletcher, M. S. Anderson, and S. J. Turley. 2009. AIRE in the thymus and beyond. *Curr Opin Immunol* 21:582-589.
221. Mathis, D., and C. Benoist. 2010. Levees of immunological tolerance. *Nat Immunol* 11:3-6.
222. Rocha, B., A. Grandien, and A. A. Freitas. 1995. Anergy and exhaustion are independent mechanisms of peripheral T cell tolerance. *J Exp Med* 181:993-1003.
223. Tivol, E. A., F. Borriello, A. N. Schweitzer, W. P. Lynch, J. A. Bluestone, and A. H. Sharpe. 1995. Loss of CTLA-4 leads to massive lymphoproliferation and fatal multiorgan tissue destruction, revealing a critical negative regulatory role of CTLA-4. *Immunity* 3:541-547.
224. Waterhouse, P., J. M. Penninger, E. Timms, A. Wakeham, A. Shahinian, K. P. Lee, C. B. Thompson, H. Griesser, and T. W. Mak. 1995. Lymphoproliferative disorders with early lethality in mice deficient in Ctla-4. *Science* 270:985-988.
225. Friedline, R. H., D. S. Brown, H. Nguyen, H. Kornfeld, J. Lee, Y. Zhang, M. Appleby, S. D. Der, J. Kang, and C. A. Chambers. 2009. CD4+ regulatory T cells require CTLA-4 for the maintenance of systemic tolerance. *J Exp Med* 206:421-434.
226. Jain, N., H. Nguyen, C. Chambers, and J. Kang. 2010. Dual function of CTLA-4 in regulatory T cells and conventional T cells to prevent multiorgan autoimmunity. *Proc Natl Acad Sci USA* 107:1524-1528.
227. Nishimura, H., M. Nose, H. Hiai, N. Minato, and T. Honjo. 1999. Development of lupus-like autoimmune diseases by disruption of the PD-1 gene encoding an ITIM motif-carrying immunoreceptor. *Immunity* 11:141-151.
228. Khoury, S. J., and M. H. Sayegh. 2004. The roles of the new negative T cell costimulatory pathways in regulating autoimmunity. *Immunity* 20:529-538.
229. Buxadé, M., J. Parra, S. Rousseau, and N. Shpiro. 2005. The Mnks are novel components in the control of TNFα biosynthesis and phosphorylate and regulate hnRNP A1. *Immunity* 23:177-189.
230. Jordan, M. S., A. Boesteanu, A. J. Reed, A. L. Petrone, A. E. Holenbeck, M. A. Lerman, A. Naji, and A. J. Caton. 2001. Thymic selection of CD4+CD25+ regulatory T cells induced by an agonist self-peptide. *Nat Immunol* 2:301-306.
231. Wildin, R. S., and A. Freitas. 2005. IPEX and FOXP3: clinical and research perspectives. *Journal of Autoimmunity* 25 Suppl:56-62.

232. den Haan, J. M. M., G. Kraal, and M. J. Bevan. 2007. Cutting edge: Lipopolysaccharide induces IL-10-producing regulatory CD4+ T cells that suppress the CD8+ T cell response. *J Immunol* 178:5429-5433.
233. Mueller, D. L. 2010. Mechanisms maintaining peripheral tolerance. *Nat Immunol* 11:21-27.
234. Li, X. C., T. B. Strom, L. A. Turka, and A. D. Wells. 2001. T cell death and transplantation tolerance. *Immunity* 14:407-416.
235. Ildstad, S. T., and D. H. Sachs. 1984. Reconstitution with syngeneic plus allogeneic or xenogeneic bone marrow leads to specific acceptance of allografts or xenografts. *Nature* 307:168-170.
236. Adler, S. H., and L. A. Turka. 2002. Immunotherapy as a means to induce transplantation tolerance. *Curr Opin Immunol* 14:660-665.
237. Posselt, A. M., C. F. Barker, J. E. Tomaszewski, J. F. Markmann, M. A. Choti, and A. Naji. 1990. Induction of donor-specific unresponsiveness by intrathymic islet transplantation. *Science* 249:1293-1295.
238. Odorico, J. S., A. M. Posselt, A. Naji, J. F. Markmann, and C. F. Barker. 1993. Promotion of rat cardiac allograft survival by intrathymic inoculation of donor splenocytes. *Transplantation* 55:1104-1107.
239. Jones, N. D., N. C. Fluck, A. L. Mellor, P. J. Morris, and K. J. Wood. 1998. The induction of transplantation tolerance by intrathymic (i.t.) delivery of alloantigen: a critical relationship between i.t. deletion, thymic export of new T cells and the timing of transplantation. *International immunology* 10:1637-1646.
240. Lechler, R. I., O. A. Garden, and L. A. Turka. 2003. The complementary roles of deletion and regulation in transplantation tolerance. *Nat Rev Immunol* 3:147-158.
241. Newell, K. A., C. P. Larsen, and A. D. Kirk. 2006. Transplant tolerance: converging on a moving target. *Transplantation* 81:1-6.
242. Lakkis, F. G., A. Arakelov, B. T. Konieczny, and Y. Inoue. 2000. Immunologic 'ignorance' of vascularized organ transplants in the absence of secondary lymphoid tissue. *Nat Med* 6:686-688.
243. Kreisel, D., A. S. Krupnick, A. E. Gelman, F. H. Engels, S. H. Popma, A. M. Krasinskas, K. R. Balsara, W. Y. Szeto, L. A. Turka, and B. R. Rosengard. 2002. Non-hematopoietic allograft cells directly activate CD8+ T cells and trigger acute rejection: an alternative mechanism of allorecognition. *Nat Med* 8:233-239.
244. Chalasani, G., Z. Dai, B. T. Konieczny, F. K. Baddoura, and F. G. Lakkis. 2002. Recall and propagation of allospecific memory T cells independent of secondary lymphoid organs. *Proc Natl Acad Sci USA* 99:6175-6180.
245. Bushell, A., and K. Wood. 2004. Permanent survival of organ transplants without immunosuppression: Experimental approaches and possibilities for tolerance induction in clinical transplantation. *Expert Reviews in Molecular Medicine*:1-31.
246. Saleem, S., B. T. Konieczny, R. P. Lowry, F. K. Baddoura, and F. G. Lakkis. 1996. Acute rejection of vascularized heart allografts in the absence of IFNgamma. *Transplantation* 62:1908-1911.

247. Nickerson, P., X. X. Zheng, J. Steiger, A. W. Steele, W. Steurer, P. Roy-Chaudhury, W. Müller, and T. B. Strom. 1996. Prolonged islet allograft acceptance in the absence of interleukin 4 expression. *Transpl Immunol* 4:81-85.
248. Lakkis, F. G., B. T. Konieczny, S. Saleem, F. K. Baddoura, P. S. Linsley, D. Z. Alexander, R. P. Lowry, T. C. Pearson, and C. P. Larsen. 1997. Blocking the CD28-B7 T cell costimulation pathway induces long term cardiac allograft acceptance in the absence of IL-4. *J Immunol* 158:2443-2448.
249. Feng, G., K. J. Wood, and A. Bushell. 2008. Interferon-gamma conditioning ex vivo generates CD25+CD62L+Foxp3+ regulatory T cells that prevent allograft rejection: potential avenues for cellular therapy. *Transplantation* 86:578-589.
250. Thebault, P., T. Condamine, M. Heslan, M. Hill, I. Bernard, A. Saoudi, R. Josien, I. Anegon, M. C. Cuturi, and E. Chiffoleau. 2007. Role of IFNgamma in allograft tolerance mediated by CD4+CD25+ regulatory T cells by induction of IDO in endothelial cells. *Am J Transplant* 7:2472-2482.
251. Xu, X. Y., K. Honjo, D. Devore-Carter, and R. P. Bucy. 1997. Immunosuppression by inhibition of cellular adhesion mediated by leukocyte function-associated antigen-1/intercellular adhesion molecule-1 in murine cardiac transplantation. *Transplantation* 63:876-885.
252. Mottram, P. L., W. R. Han, L. J. Purcell, I. F. McKenzie, and W. W. Hancock. 1995. Increased expression of IL-4 and IL-10 and decreased expression of IL-2 and interferon-gamma in long-surviving mouse heart allografts after brief CD4-monoclonal antibody therapy. *Transplantation* 59:559-565.
253. LaRosa, D. F., A. H. Rahman, and L. A. Turka. 2007. The innate immune system in allograft rejection and tolerance. *J Immunol* 178:7503-7509.
254. Boussiotis, V. A., G. J. Freeman, A. Berezovskaya, D. L. Barber, and L. M. Nadler. 1997. Maintenance of human T cell anergy: blocking of IL-2 gene transcription by activated Rap1. *Science* 278:124-128.
255. Jones, L. A., L. T. Chin, G. R. Merriam, L. M. Nelson, and A. M. Kruisbeck. 1990. Failure of clonal deletion in neonatally thymectomized mice: tolerance is preserved through clonal anergy. *J Exp Med* 172:1277-1285.
256. Dallman, M. J., O. Shiho, T. H. Page, K. J. Wood, and P. J. Morris. 1991. Peripheral tolerance to alloantigen results from altered regulation of the interleukin 2 pathway. *J Exp Med* 173:79-87.
257. Vendetti, S., J. G. Chai, J. Dyson, E. Simpson, G. Lombardi, and R. Lechler. 2000. Anergic T cells inhibit the antigen-presenting function of dendritic cells. *J Immunol* 165:1175-1181.
258. Boussiotis, V. A., D. L. Barber, T. Nakarai, G. J. Freeman, J. G. Gribben, G. M. Bernstein, A. D. D'Andrea, J. Ritz, and L. M. Nadler. 1994. Prevention of T cell anergy by signaling through the gamma c chain of the IL-2 receptor. *Science* 266:1039-1042.
259. Suchin, E. J., P. B. Langmuir, E. Palmer, M. H. Sayegh, A. D. Wells, and L. A. Turka. 2001. Quantifying the frequency of alloreactive T cells in vivo: new answers to an old question. *J Immunol* 166:973-981.

260. Wells, A. D., X. C. Li, Y. Li, M. C. Walsh, X. X. Zheng, Z. Wu, G. Nuñez, A. Tang, M. Sayegh, W. W. Hancock, T. B. Strom, and L. A. Turka. 1999. Requirement for T-cell apoptosis in the induction of peripheral transplantation tolerance. *Nat Med* 5:1303-1307.
261. Dai, Z., B. T. Konieczny, F. K. Baddoura, and F. G. Lakkis. 1998. Impaired alloantigen-mediated T cell apoptosis and failure to induce long-term allograft survival in IL-2-deficient mice. *J Immunol* 161:1659-1663.
262. Refaeli, Y., L. Van Parijs, C. A. London, J. Tschopp, and A. K. Abbas. 1998. Biochemical mechanisms of IL-2-regulated Fas-mediated T cell apoptosis. *Immunity* 8:615-623.
263. Strasser, A., A. W. Harris, and S. Cory. 1991. bcl-2 transgene inhibits T cell death and perturbs thymic self-censorship. *Cell* 67:889-899.
264. Lehnert, A. M., L. Murray-Segal, P. J. Cowan, A. J. d'Apice, and P. J. O'Connell. 2007. Blockade of the passive cell death pathway does not prevent tolerance induction to islet grafts. *Transplantation* 83:653-655.
265. Li, X. C., A. D. Wells, T. B. Strom, and L. A. Turka. 2000. The role of T cell apoptosis in transplantation tolerance. *Curr Opin Immunol* 12:522-527.
266. Wekerle, T., J. Kurtz, M. Sayegh, H. Ito, A. Wells, S. Bensinger, J. Shaffer, L. Turka, and M. Sykes. 2001. Peripheral deletion after bone marrow transplantation with costimulatory blockade has features of both activation-induced cell death and passive cell death. *J Immunol* 166:2311-2316.
267. Taylor, P. A., R. J. Noelle, and B. R. Blazar. 2001. CD4(+)CD25(+) immune regulatory cells are required for induction of tolerance to alloantigen via costimulatory blockade. *J Exp Med* 193:1311-1318.
268. Gregori, S., M. Casorati, S. Amuchastegui, S. Smiroldo, A. M. Davalli, and L. Adorini. 2001. Regulatory T cells induced by 1 alpha,25-dihydroxyvitamin D3 and mycophenolate mofetil treatment mediate transplantation tolerance. *J Immunol* 167:1945-1953.
269. Wise, M. P., F. Bemelman, S. P. Cobbold, and H. Waldmann. 1998. Linked suppression of skin graft rejection can operate through indirect recognition. *J Immunol* 161:5813-5816.
270. Niimi, M., N. Shirasugi, Y. Ikeda, and K. J. Wood. 2001. Oral antigen induces allograft survival by linked suppression via the indirect pathway. *Transplant Proc* 33:81.
271. Qin, S., S. P. Cobbold, H. Pope, J. Elliott, D. Kioussis, J. Davies, and H. Waldmann. 1993. "Infectious" transplantation tolerance. *Science* 259:974-977.
272. Jonuleit, H., E. Schmitt, H. Kakirman, M. Stassen, J. Knop, and A. H. Enk. 2002. Infectious tolerance: human CD25(+) regulatory T cells convey suppressor activity to conventional CD4(+) T helper cells. *J Exp Med* 196:255-260.
273. Murray, J. E. 1992. Human organ transplantation: background and consequences. *Science* 256:1411-1416.
274. Starzl, T. E., and R. M. Zinkernagel. 2001. Transplantation tolerance from a historical perspective. *Nat Rev Immunol* 1:233-239.

275. Shreffler, D. C. 1988. Seventy-five years of immunology: the view from the MHC. *J Immunol* 141:1791-1798.
276. Welsh, R. M. 2000. Lymphocytic Choriomeningitis Virus as a Model for the Study of Cellular Immunology. *Effects of Microbes on the Immune System*.
277. Suthanthiran, M., and T. B. Strom. 1997. Immunoregulatory drugs: mechanistic basis for use in organ transplantation. *Pediatr Nephrol* 11:651-657.
278. de Goër de Herve, M.-G., E. Gonzales, H. Hendel-Chavez, J.-L. Décline, O. Mourier, K. Abbed, E. Jacquemin, and Y. Taoufik. 2010. CD25 Appears Non Essential for Human Peripheral T(reg) Maintenance In Vivo. *PLoS ONE* 5:e11784.
279. Sayegh, M. H., E. Akalin, W. W. Hancock, M. E. Russell, C. B. Carpenter, P. S. Linsley, and L. A. Turka. 1995. CD28-B7 blockade after alloantigenic challenge in vivo inhibits Th1 cytokines but spares Th2. *J Exp Med* 181:1869-1874.
280. Turka, L. A., P. S. Linsley, H. Lin, W. Brady, J. M. Leiden, R. Q. Wei, M. L. Gibson, X. G. Zheng, S. Myrdal, and D. Gordon. 1992. T-cell activation by the CD28 ligand B7 is required for cardiac allograft rejection in vivo. *Proc Natl Acad Sci USA* 89:11102-11105.
281. Lin, H., S. F. Bolling, P. S. Linsley, R. Q. Wei, D. Gordon, C. B. Thompson, and L. A. Turka. 1993. Long-term acceptance of major histocompatibility complex mismatched cardiac allografts induced by CTLA4Ig plus donor-specific transfusion. *J Exp Med* 178:1801-1806.
282. Sayegh, M. H., X. G. Zheng, C. Magee, W. W. Hancock, and L. A. Turka. 1997. Donor antigen is necessary for the prevention of chronic rejection in CTLA4Ig-treated murine cardiac allograft recipients. *Transplantation* 64:1646-1650.
283. Yamada, A., K. Kishimoto, V. M. Dong, M. Sho, A. D. Salama, N. G. Anosova, G. Benichou, D. A. Mandelbrot, A. H. Sharpe, L. A. Turka, H. Auchincloss, and M. H. Sayegh. 2001. CD28-independent costimulation of T cells in alloimmune responses. *J Immunol* 167:140-146.
284. Larsen, C. P., E. T. Elwood, D. Z. Alexander, S. C. Ritchie, R. Hendrix, C. Tucker-Burden, H. R. Cho, A. Aruffo, D. Hollenbaugh, P. S. Linsley, K. J. Winn, and T. C. Pearson. 1996. Long-term acceptance of skin and cardiac allografts after blocking CD40 and CD28 pathways. *Nature* 381:434-438.
285. Hancock, W. W., M. H. Sayegh, X. G. Zheng, R. Peach, P. S. Linsley, and L. A. Turka. 1996. Costimulatory function and expression of CD40 ligand, CD80, and CD86 in vascularized murine cardiac allograft rejection. *Proc Natl Acad Sci U S A* 93:13967-13972.
286. Shimizu, K., U. Schönbeck, F. Mach, P. Libby, and R. N. Mitchell. 2000. Host CD40 ligand deficiency induces long-term allograft survival and donor-specific tolerance in mouse cardiac transplantation but does not prevent graft arteriosclerosis. *J Immunol* 165:3506-3518.
287. Kirk, A. D., D. M. Harlan, N. N. Armstrong, T. A. Davis, Y. Dong, G. S. Gray, X. Hong, D. Thomas, J. H. Fechner, and S. J. Knechtle. 1997. CTLA4-Ig and anti-CD40 ligand prevent renal allograft rejection in primates. *Proc Natl Acad Sci USA* 94:8789-8794.

288. Kirk, A. D., L. C. Burkly, D. S. Batty, R. E. Baumgartner, J. D. Berning, K. Buchanan, J. H. Fechner, R. L. Germond, R. L. Kampen, N. B. Patterson, S. J. Swanson, D. K. Tadaki, C. N. TenHoor, L. White, S. J. Knechtle, and D. M. Harlan. 1999. Treatment with humanized monoclonal antibody against CD154 prevents acute renal allograft rejection in nonhuman primates. *Nat Med* 5:686-693.

289. Kenyon, N. S., M. Chatzipetrou, M. Masetti, A. Ranuncoli, M. Oliveira, J. L. Wagner, A. D. Kirk, D. M. Harlan, L. C. Burkly, and C. Ricordi. 1999. Long-term survival and function of intrahepatic islet allografts in rhesus monkeys treated with humanized anti-CD154. *Proc Natl Acad Sci USA* 96:8132-8137.

290. Kenyon, N. S., L. A. Fernandez, R. Lehmann, M. Masetti, A. Ranuncoli, M. Chatzipetrou, G. Iaria, D. Han, J. L. Wagner, P. Ruiz, M. Berho, L. Inverardi, R. Alejandro, D. H. Mintz, A. D. Kirk, D. M. Harlan, L. C. Burkly, and C. Ricordi. 1999. Long-term survival and function of intrahepatic islet allografts in baboons treated with humanized anti-CD154. *Diabetes* 48:1473-1481.

291. Kosuge, H., J.-I. Suzuki, R. Gotoh, N. Koga, H. Ito, M. Isobe, M. Inobe, and T. Uede. 2003. Induction of immunologic tolerance to cardiac allograft by simultaneous blockade of inducible co-stimulator and cytotoxic T-lymphocyte antigen 4 pathway. *Transplantation* 75:1374-1379.

292. Sandner, S. E., M. R. Clarkson, A. D. Salama, A. Sanchez-Fueyo, H. Yagita, L. A. Turka, and M. H. Sayegh. 2005. Mechanisms of tolerance induced by donor-specific transfusion and ICOS-B7h blockade in a model of CD4+ T-cell-mediated allograft rejection. *Am J Transplant* 5:31-39.

293. Ito, T., T. Ueno, M. R. Clarkson, X. Yuan, M. M. Jurewicz, H. Yagita, M. Azuma, A. H. Sharpe, H. Auchincloss, M. H. Sayegh, and N. Najafian. 2005. Analysis of the role of negative T cell costimulatory pathways in CD4 and CD8 T cell-mediated alloimmune responses in vivo. *J Immunol* 174:6648-6656.

294. Womer, K. L., M. H. Sayegh, and H. Auchincloss. 2001. Involvement of the direct and indirect pathways of allorecognition in tolerance induction. *Philos Trans R Soc Lond, B, Biol Sci* 356:639-647.

295. Spadafora-Ferreira, M., C. Caldas, K. C. Faé, I. Marrero, S. M. Monteiro, H. T. Lin-Wang, A. Socorro-Silva, S. G. Fonseca, J. A. Fonseca, J. Kalil, and V. Coelho. 2007. CD4+CD25+Foxp3+ indirect alloreactive T cells from renal transplant patients suppress both the direct and indirect pathways of allorecognition. *Scand J Immunol* 66:352-361.

296. Ochando, J. C., N. R. Krieger, and J. S. Bromberg. 2006. Direct versus indirect allorecognition: Visualization of dendritic cell distribution and interactions during rejection and tolerization. *Am J Transplant* 6:2488-2496.

297. Pietra, B. A., A. Wiseman, A. Bolwerk, M. Rizeq, and R. G. Gill. 2000. CD4 T cell-mediated cardiac allograft rejection requires donor but not host MHC class II. *J Clin Invest* 106:1003-1010.

298. van Maurik, A., B. Fazekas de St Groth, K. J. Wood, and N. D. Jones. 2004. Dependency of direct pathway CD4+ T cells on CD40-CD154 costimulation is

determined by nature and microenvironment of primary contact with alloantigen. *J Immunol* 172:2163-2170.

299. Choi, S., and P. Reddy. 2010. Graft-versus-host disease. *Panminerva Med* 52:111-124.
300. Land, W., H. Schneeberger, S. Schleibner, W. D. Illner, D. Abendroth, G. Rutili, K. E. Arfors, and K. Messmer. 1994. The beneficial effect of human recombinant superoxide dismutase on acute and chronic rejection events in recipients of cadaveric renal transplants. *Transplantation* 57:211-217.
301. He, H., J. R. Stone, and D. L. Perkins. 2003. Analysis of differential immune responses induced by innate and adaptive immunity following transplantation. *Immunology* 109:185-196.
302. He, H., J. R. Stone, and D. L. Perkins. 2002. Analysis of robust innate immune response after transplantation in the absence of adaptive immunity. *Transplantation* 73:853-861.
303. Rahman, A. H., D. K. Taylor, and L. A. Turka. 2009. The contribution of direct TLR signaling to T cell responses. *Immunol Res* 45:25-36.
304. Kawai, T., and S. Akira. 2010. The role of pattern-recognition receptors in innate immunity: update on Toll-like receptors. *Nat Immunol* 11:373-384.
305. Janeway, C. A. 1992. The immune system evolved to discriminate infectious nonself from noninfectious self. *Immunol Today* 13:11-16.
306. Matzinger, P. 1994. Tolerance, danger, and the extended family. *Annu Rev Immunol* 12:991-1045.
307. Akira, S., and K. Takeda. 2004. Toll-like receptor signalling. *Nat Rev Immunol* 4:499-511.
308. Gao, B., and M.-F. Tsan. 2003. Endotoxin contamination in recombinant human heat shock protein 70 (Hsp70) preparation is responsible for the induction of tumor necrosis factor alpha release by murine macrophages. *J Biol Chem* 278:174-179.
309. Scheibner, K. A., M. A. Lutz, S. Boodoo, M. J. Fenton, J. D. Powell, and M. R. Horton. 2006. Hyaluronan fragments act as an endogenous danger signal by engaging TLR2. *J Immunol* 177:1272-1281.
310. Schaefer, L., A. Babelova, E. Kiss, H.-J. Hausser, M. Baliova, M. Krzyzankova, G. Marsche, M. F. Young, D. Mihalik, M. Götte, E. Malle, R. M. Schaefer, and H.-J. Gröne. 2005. The matrix component biglycan is proinflammatory and signals through Toll-like receptors 4 and 2 in macrophages. *J Clin Invest* 115:2223-2233.
311. Goldstein, D. R., B. M. Tesar, S. Akira, and F. G. Lakkis. 2003. Critical role of the Toll-like receptor signal adaptor protein MyD88 in acute allograft rejection. *J Clin Invest* 111:1571-1578.
312. Tesar, B. M., J. Zhang, Q. Li, and D. R. Goldstein. 2004. TH1 immune responses to fully MHC mismatched allografts are diminished in the absence of MyD88, a toll-like receptor signal adaptor protein. *Am J Transplant* 4:1429-1439.

313. Walker, W. E., I. W. Nasr, G. Camirand, B. M. Tesar, C. J. Booth, and D. R. Goldstein. 2006. Absence of innate MyD88 signaling promotes inducible allograft acceptance. *J Immunol* 177:5307-5316.
314. Chen, L., T. Wang, P. Zhou, L. Ma, D. Yin, J. Shen, L. Molinero, T. Nozaki, T. Phillips, S. Uematsu, S. Akira, C.-R. Wang, R. L. Fairchild, M.-L. Alegre, and A. Chong. 2006. TLR engagement prevents transplantation tolerance. *Am J Transplant* 6:2282-2291.
315. Pasare, C., and R. Medzhitov. 2003. Toll pathway-dependent blockade of CD4+CD25+ T cell-mediated suppression by dendritic cells. *Science* 299:1033-1036.
316. Porrett, P. M., X. Yuan, D. F. LaRosa, P. T. Walsh, J. Yang, W. Gao, P. Li, J. Zhang, J. M. Ansari, W. W. Hancock, M. H. Sayegh, M. Koulmanda, T. B. Strom, and L. A. Turka. 2008. Mechanisms underlying blockade of allograft acceptance by TLR ligands. *J Immunol* 181:1692-1699.
317. Wu, Z., S. J. Bensinger, J. Zhang, C. Chen, X. Yuan, X. Huang, J. F. Markmann, A. Kassaee, B. R. Rosengard, W. W. Hancock, M. H. Sayegh, and L. A. Turka. 2004. Homeostatic proliferation is a barrier to transplantation tolerance. *Nat Med* 10:87-92.
318. Newell, K. A., and C. P. Larsen. 2007. Transplantation tolerance. *Semin Nephrol* 27:487-497.
319. Yang, J., M. O. Brook, M. Carvalho-Gaspar, J. Zhang, H. E. Ramon, M. H. Sayegh, K. J. Wood, L. A. Turka, and N. D. Jones. 2007. Allograft rejection mediated by memory T cells is resistant to regulation. *Proc Natl Acad Sci USA* 104:19954-19959.
320. Selin, L. K., and M. A. Brehm. 2007. Frontiers in nephrology: heterologous immunity, T cell cross-reactivity, and alloreactivity. *J Am Soc Nephrol* 18:2268-2277.
321. Brehm, M. A., K. A. Daniels, B. Priyadharshini, T. B. Thornley, D. L. Greiner, A. A. Rossini, and R. M. Welsh. 2010. Allografts stimulate cross-reactive virus-specific memory CD8 T cells with private specificity. *Am J Transplant* 10:1738-1748.
322. Lin, M. Y., and R. M. Welsh. 1998. Stability and diversity of T cell receptor repertoire usage during lymphocytic choriomeningitis virus infection of mice. *J Exp Med* 188:1993-2005.
323. Brehm, M. A., T. G. Markees, K. A. Daniels, D. L. Greiner, A. A. Rossini, and R. M. Welsh. 2003. Direct visualization of cross-reactive effector and memory allo-specific CD8 T cells generated in response to viral infections. *J Immunol* 170:4077-4086.
324. Welsh, R. M., T. G. Markees, B. A. Woda, K. A. Daniels, M. A. Brehm, J. P. Mordes, D. L. Greiner, and A. A. Rossini. 2000. Virus-induced abrogation of transplantation tolerance induced by donor-specific transfusion and anti-CD154 antibody. *J Virol* 74:2210-2218.
325. Adams, A. B., M. A. Williams, T. R. Jones, N. Shirasugi, M. M. Durham, S. M. Kaech, E. J. Wherry, T. Onami, J. G. Lanier, K. E. Kokko, T. C. Pearson, R.

Ahmed, and C. P. Larsen. 2003. Heterologous immunity provides a potent barrier to transplantation tolerance. *J Clin Invest* 111:1887-1895.

326. Williams, M. A., T. M. Onami, A. B. Adams, M. M. Durham, T. C. Pearson, R. Ahmed, and C. P. Larsen. 2002. Cutting edge: persistent viral infection prevents tolerance induction and escapes immune control following CD28/CD40 blockade-based regimen. *J Immunol* 169:5387-5391.
327. Williams, M. A., J. T. Tan, A. B. Adams, M. M. Durham, N. Shirasugi, J. K. Whitmire, L. E. Harrington, R. Ahmed, T. C. Pearson, and C. P. Larsen. 2001. Characterization of virus-mediated inhibition of mixed chimerism and allospecific tolerance. *J Immunol* 167:4987-4995.
328. Turgeon, N., N. Iwakoshi, W. Meyers, R. Welsh, D. Greiner, J. Mordes, and A. Rossini. 2000. Virus infection abrogates cd8(+) t cell deletion induced by donor-specific transfusion and anti-cd154 monoclonal antibody. *Curr Surg* 57:505-506.
329. Pircher, H., K. Bürki, R. Lang, H. Hengartner, and R. M. Zinkernagel. 1989. Tolerance induction in double specific T-cell receptor transgenic mice varies with antigen. *Nature* 342:559-561.
330. Oxenius, A., M. F. Bachmann, R. M. Zinkernagel, and H. Hengartner. 1998. Virus-specific MHC-class II-restricted TCR-transgenic mice: effects on humoral and cellular immune responses after viral infection. *Eur J Immunol* 28:390-400.
331. Santori, F. R., S. M. Brown, Y. Lu, T. A. Neubert, and S. Vukmanovic. 2001. Cutting edge: positive selection induced by a self-peptide with TCR antagonist activity. *J Immunol* 167:6092-6095.
332. Markiewicz, M. A., C. Girao, J. T. Opferman, J. Sun, Q. Hu, A. A. Agulnik, C. E. Bishop, C. B. Thompson, and P. G. Ashton-Rickardt. 1998. Long-term T cell memory requires the surface expression of self-peptide/major histocompatibility complex molecules. *Proc Natl Acad Sci USA* 95:3065-3070.
333. Hogquist, K. A., S. C. Jameson, W. R. Heath, J. L. Howard, M. J. Bevan, and F. R. Carbone. 1994. T cell receptor antagonist peptides induce positive selection. *Cell* 76:17-27.
334. Robertson, J., P. Jensen, and B. Evavold. 2000. DO11. 10 and OT-II T cells recognize a C-terminal ovalbumin 323-339 epitope. *The Journal of Immunology* 164:4706-4712.
335. Yu, W., H. Nagaoka, M. Jankovic, Z. Misulovin, H. Suh, A. Rolink, F. Melchers, E. Meffre, and M. C. Nussenzweig. 1999. Continued RAG expression in late stages of B cell development and no apparent re-induction after immunization. *Nature* 400:682-687.
336. Schönrich, G., U. Kalinke, F. Momburg, M. Malissen, A. M. Schmitt-Verhulst, B. Malissen, G. J. Hämmerling, and B. Arnold. 1991. Down-regulation of T cell receptors on self-reactive T cells as a novel mechanism for extrathymic tolerance induction. *Cell* 65:293-304.
337. Tafuri, A., J. Alferink, P. Möller, G. J. Hämmerling, and B. Arnold. 1995. T cell awareness of paternal alloantigens during pregnancy. *Science* 270:630-633.
338. Iwakoshi, N. N., T. G. Markees, N. Turgeon, T. Thornley, A. Cuthbert, J. Leif, N. E. Phillips, J. P. Mordes, D. L. Greiner, and A. A. Rossini. 2001. Skin allograft

maintenance in a new synchimeric model system of tolerance. *J Immunol* 167:6623-6630.

339. Hahn, K., D. Jewell, I. Wilson, and M. Oldstone. 1995. CTL Escape Viral Variants I. Generation and Molecular Characterization. *Virology* 210:29-40.
340. Valckx, D., B. Decallonne, R. Bouillon, and C. Mathieu. 2001. An overview of real-time quantitative PCR: applications to quantify cytokine gene expression. *Methods* 25:386-401.
341. Liu, F., and J. L. Whitton. 2005. Cutting edge: re-evaluating the in vivo cytokine responses of CD8+ T cells during primary and secondary viral infections. *J Immunol* 174:5936-5940.
342. Krzyzowska, M., M. Polanczyk, M. Bas, J. Cymerys, A. Schollenberger, F. Chiodi, and M. Niemialtowski. 2005. Mousepox conjunctivitis: the role of Fas/FasL-mediated apoptosis of epithelial cells in virus dissemination. *J Gen Virol* 86:2007-2018.
343. Ogasawara, J., T. Suda, and S. Nagata. 1995. Selective apoptosis of CD4+CD8+ thymocytes by the anti-Fas antibody. *J Exp Med* 181:485-491.
344. Oehen, S., K. Brduscha-Riem, A. Oxenius, and B. Odermatt. 1997. A simple method for evaluating the rejection of grafted spleen cells by flow cytometry and tracing adoptively transferred cells by light microscopy. *J Immunol Methods* 207:33-42.
345. Brehm, M. A., J. Mangada, T. G. Markees, T. Pearson, K. A. Daniels, T. B. Thornley, R. M. Welsh, A. A. Rossini, and D. L. Greiner. 2007. Rapid quantification of naive alloreactive T cells by TNF-alpha production and correlation with allograft rejection in mice. *Blood* 109:819-826.
346. Barber, D. L., E. J. Wherry, and R. Ahmed. 2003. Cutting edge: rapid in vivo killing by memory CD8 T cells. *J Immunol* 171:27-31.
347. Makaroff, L. E., D. W. Hendricks, R. E. Niec, and P. J. Fink. 2009. Postthymic maturation influences the CD8 T cell response to antigen. *Proc Natl Acad Sci USA* 106:4799-4804.
348. Mercado, R., S. Vijh, S. E. Allen, K. Kerksiek, I. M. Pilip, and E. G. Pamer. 2000. Early programming of T cell populations responding to bacterial infection. *J Immunol* 165:6833-6839.
349. Wong, P., and E. G. Pamer. 2001. Cutting edge: antigen-independent CD8 T cell proliferation. *J Immunol* 166:5864-5868.
350. van Stipdonk, M. J., E. E. Lemmens, and S. P. Schoenberger. 2001. Naïve CTLs require a single brief period of antigenic stimulation for clonal expansion and differentiation. *Nat Immunol* 2:423-429.
351. Tuma, R. A., and E. G. Pamer. 2002. Homeostasis of naïve, effector and memory CD8 T cells. *Curr Opin Immunol* 14:348-353.
352. van Stipdonk, M. J. B., G. Hardenberg, M. S. Bijker, E. E. Lemmens, N. M. Droin, D. R. Green, and S. P. Schoenberger. 2003. Dynamic programming of CD8+ T lymphocyte responses. *Nat Immunol* 4:361-365.
353. Badovinac, V. P., and J. T. Harty. 2006. Programming, demarcating, and manipulating CD8+ T-cell memory. *Immunol Rev* 211:67-80.

354. Pham, N.-L. L., V. P. Badovinac, and J. T. Harty. 2009. A default pathway of memory CD8 T cell differentiation after dendritic cell immunization is deflected by encounter with inflammatory cytokines during antigen-driven proliferation. *J Immunol* 183:2337-2348.
355. Corbin, G. A., and J. T. Harty. 2005. T cells undergo rapid ON/OFF but not ON/OFF/ON cycling of cytokine production in response to antigen. *J Immunol* 174:718-726.
356. Surh, C. D., and J. Sprent. 2000. Homeostatic T cell proliferation: how far can T cells be activated to self-ligands? *J Exp Med* 192:F9-F14.
357. Schodin, B. A., T. J. Tsomides, and D. M. Kranz. 1996. Correlation between the number of T cell receptors required for T cell activation and TCR-ligand affinity. *Immunity* 5:137-146.
358. Ashton-Rickardt, P. G., A. Bandeira, J. R. Delaney, L. Van Kaer, H. P. Pircher, R. M. Zinkernagel, and S. Tonegawa. 1994. Evidence for a differential avidity model of T cell selection in the thymus. *Cell* 76:651-663.
359. Schott, E., N. Bertho, Q. Ge, M. M. Maurice, and H. L. Ploegh. 2002. Class I negative CD8 T cells reveal the confounding role of peptide-transfer onto CD8 T cells stimulated with soluble H2-Kb molecules. *Proc Natl Acad Sci USA* 99:13735-13740.
360. Crispe, I. N., and M. J. Bevan. 1987. Expression and functional significance of the J11d marker on mouse thymocytes. *J Immunol* 138:2013-2018.
361. Vernachio, J., M. Li, A. D. Donnenberg, and M. J. Soloski. 1989. Qa-2 expression in the adult murine thymus. A unique marker for a mature thymic subset. *J Immunol* 142:48-56.
362. Uldrich, A. P., S. P. Berzins, M. A. Malin, P. Bouillet, A. Strasser, M. J. Smyth, R. L. Boyd, and D. I. Godfrey. 2006. Antigen challenge inhibits thymic emigration. *J Immunol* 176:4553-4561.
363. Clise-Dwyer, K., G. E. Huston, A. L. Buck, D. K. Duso, and S. L. Swain. 2007. Environmental and intrinsic factors lead to antigen unresponsiveness in CD4(+) recent thymic emigrants from aged mice. *J Immunol* 178:1321-1331.
364. Badovinac, V. P., G. A. Corbin, and J. T. Harty. 2000. Cutting edge: OFF cycling of TNF production by antigen-specific CD8+ T cells is antigen independent. *J Immunol* 165:5387-5391.
365. Aspalter, R. M., M. M. Eibl, and H. M. Wolf. 2003. Regulation of TCR-mediated T cell activation by TNF-RII. *J Leukoc Biol* 74:572-582.
366. Cawthon, A. G., H. Lu, and M. A. Alexander-Miller. 2001. Peptide requirement for CTL activation reflects the sensitivity to CD3 engagement: correlation with CD8alphabeta versus CD8alphaalpha expression. *J Immunol* 167:2577-2584.
367. Sugie, K., M.-S. Jeon, and H. M. Grey. 2004. Activation of naïve CD4 T cells by anti-CD3 reveals an important role for Fyn in Lck-mediated signaling. *Proc Natl Acad Sci USA* 101:14859-14864.
368. Rocha, B., and H. von Boehmer. 1991. Peripheral selection of the T cell repertoire. *Science* 251:1225-1228.

369. Deman, J., M. T. Martin, P. Delvenne, C. Humblet, J. Boniver, and M. P. Defresne. 1992. Analysis by in situ hybridization of cells expressing mRNA for tumor-necrosis factor in the developing thymus of mice. *Developmental Immunology* 2:103-109.
370. Zúñiga-Pflücker, J. C., D. Jiang, and M. J. Lenardo. 1995. Requirement for TNF-alpha and IL-1 alpha in fetal thymocyte commitment and differentiation. *Science* 268:1906-1909.
371. Baseta, J. G., and O. Stutman. 2000. TNF regulates thymocyte production by apoptosis and proliferation of the triple negative (CD3-CD4-CD8-) subset. *J Immunol* 165:5621-5630.
372. Liepinsh, D. J., A. A. Kruglov, A. R. Galimov, A. N. Shakhov, Y. V. Shebzukhov, A. A. Kuchmiy, S. I. Grivennikov, A. V. Tumanov, M. S. Drutskaya, L. Feigenbaum, D. V. Kuprash, and S. A. Nedospasov. 2009. Accelerated thymic atrophy as a result of elevated homeostatic expression of the genes encoded by the TNF/lymphotoxin cytokine locus. *Eur J Immunol* 39:2906-2915.
373. Pérez, A. R., E. Roggero, A. Nicora, J. Palazzi, H. O. Besedovsky, A. Del Rey, and O. A. Bottasso. 2007. Thymus atrophy during Trypanosoma cruzi infection is caused by an immuno-endocrine imbalance. *Brain Behav Immun* 21:890-900.
374. Murphy, M., and L. B. Epstein. 1992. Down syndrome (DS) peripheral blood contains phenotypically mature CD3+TCR alpha, beta+ cells but abnormal proportions of TCR alpha, beta+, TCR gamma, delta+, and CD4+ CD45RA+ cells: evidence for an inefficient release of mature T cells by the DS thymus. *Clin Immunol Immunopathol* 62:245-251.
375. Murphy, M., D. S. Friend, L. Pike-Nobile, and L. B. Epstein. 1992. Tumor necrosis factor-alpha and IFN-gamma expression in human thymus. Localization and overexpression in Down syndrome (trisomy 21). *J Immunol* 149:2506-2512.
376. Murphy, M., R. M. Insoft, L. Pike-Nobile, K. S. Derbin, and L. B. Epstein. 1993. Overexpression of LFA-1 and ICAM-1 in Down syndrome thymus. Implications for abnormal thymocyte maturation. *J Immunol* 150:5696-5703.
377. Chang, J., J. Parnes, and C. Garrison Fathman. 1998. T Cell Receptor (TCR) engagement leads to activation-induced splicing of tumor necrosis factor (TNF) nuclear pre-mRNA. *Journal of Experimental Medicine* 188:247-254.
378. Katsanou, V., O. Papadaki, S. Milatos, P. J. Blackshear, P. Anderson, G. Kollias, and D. L. Kontoyiannis. 2005. HuR as a negative posttranscriptional modulator in inflammation. *Mol Cell* 19:777-789.
379. Papadaki, O., S. Milatos, S. Grammenoudi, N. Mukherjee, J. D. Keene, and D. L. Kontoyiannis. 2009. Control of thymic T cell maturation, deletion and egress by the RNA-binding protein HuR. *J Immunol* 182:6779-6788.
380. Sims, T. N., and M. L. Dustin. 2002. The immunological synapse: integrins take the stage. *Immunol Rev* 186:100-117.
381. Inaba, K., M. Pack, M. Inaba, H. Sakuta, F. Isdell, and R. M. Steinman. 1997. High levels of a major histocompatibility complex II-self peptide complex on dendritic cells from the T cell areas of lymph nodes. *J Exp Med* 186:665-672.

382. Bromley, S. K., and M. L. Dustin. 2002. Stimulation of naive T-cell adhesion and immunological synapse formation by chemokine-dependent and -independent mechanisms. *Immunology* 106:289-298.
383. Proietto, A. I., M. H. Lahoud, and L. Wu. 2008. Distinct functional capacities of mouse thymic and splenic dendritic cell populations. *Immunol Cell Biol* 86:700-708.
384. Fulton, R. B., M. R. Olson, and S. M. Varga. 2008. Regulation of cytokine production by virus-specific CD8 T cells in the lungs. *J Virol* 82:7799-7811.
385. Opiela, S. J., T. Koru-Sengul, and B. Adkins. 2009. Murine neonatal recent thymic emigrants are phenotypically and functionally distinct from adult recent thymic emigrants. *Blood* 113:5635-5643.
386. Miller, D. M., T. B. Thornley, T. Pearson, A. J. Kruger, M. Yamazaki, L. D. Shultz, R. M. Welsh, M. A. Brehm, A. A. Rossini, and D. L. Greiner. 2009. TLR agonists prevent the establishment of allogeneic hematopoietic chimerism in mice treated with costimulation blockade. *J Immunol* 182:5547-5559.
387. Marrack, P., J. Kappler, and T. Mitchell. 1999. Type I Interferons Keep Activated T Cells Alive. *Journal of Experimental Medicine*.
388. Parish, I. A., S. Rao, G. K. Smyth, T. Juelich, G. S. Denyer, G. M. Davey, A. Strasser, and W. R. Heath. 2009. The molecular signature of CD8+ T cells undergoing deletional tolerance. *Blood* 113:4575-4585.
389. El Essawy, B., H. H. Otu, B. Choy, X. X. Zheng, T. A. Libermann, and T. B. Strom. 2006. Proteomic analysis of the allograft response. *Transplantation* 82:267-274.
390. Perco, P., P. Blaha, A. Kainz, B. Mayer, P. Hauser, T. Wekerle, and R. Oberbauer. 2006. Molecular signature of mice T lymphocytes following tolerance induction by allogeneic BMT and CD40-CD40L costimulation blockade. *Transpl Int* 19:146-157.
391. Bradley, L. M., L. Haynes, and S. L. Swain. 2005. IL-7: maintaining T-cell memory and achieving homeostasis. *Trends Immunol* 26:172-176.
392. Sun, S., X. Zhang, D. F. Tough, and J. Sprent. 1998. Type I interferon-mediated stimulation of T cells by CpG DNA. *J Exp Med* 188:2335-2342.
393. Terrazzino, S., A. Bauleo, A. Baldan, and A. Leon. 2002. Peripheral LPS administrations up-regulate Fas and FasL on brain microglial cells: a brain protective or pathogenic event? *J Neuroimmunol* 124:45-53.
394. Koide, N., A. Morikawa, G. Tumurkhuu, J. Dagvadorj, F. Hassan, S. Islam, Y. Naiki, I. Mori, T. Yoshida, and T. Yokochi. 2007. Lipopolysaccharide and interferon-γ enhance Fas-mediated cell death in mouse vascular endothelial cells via augmentation of Fas expression. *Clinical & Experimental Immunology* 150:553-560.
395. Sharif, M. N., I. Tassiulas, Y. Hu, I. Mecklenbräuker, A. Tarakhovsky, and L. B. Ivashkiv. 2004. IFN-alpha priming results in a gain of proinflammatory function by IL-10: implications for systemic lupus erythematosus pathogenesis. *J Immunol* 172:6476-6481.

396. Lauw, F. N., D. Pajkrt, C. E. Hack, M. Kurimoto, S. J. van Deventer, and T. van der Poll. 2000. Proinflammatory effects of IL-10 during human endotoxemia. *J Immunol* 165:2783-2789.
397. Trambley, J., A. Lin, E. Elwood, A. W. Bingaman, F. Lakkis, M. Corbascio, T. C. Pearson, and C. P. Larsen. 2001. FasL is important in costimulation blockade-resistant skin graft rejection. *Transplantation* 71:537-543.
398. Wagener, M. E., B. T. Konieczny, Z. Dai, G. H. Ring, and F. G. Lakkis. 2000. Alloantigen-driven T cell death mediated by Fas ligand and tumor necrosis factor-alpha is not essential for the induction of allograft acceptance. *Transplantation* 69:2428-2432.
399. Xie, L., W. Shi, and P. Guo. 2003. Roles of tumor necrosis factor-related apoptosis-inducing ligand in corneal transplantation. *Transplantation* 76:1556-1559.
400. Ferguson, T. A., and T. S. Griffith. 2007. The role of Fas ligand and TNF-related apoptosis-inducing ligand (TRAIL) in the ocular immune response. *Chem Immunol Allergy* 92:140-154.
401. Hutcheson, J., J. C. Scatizzi, A. M. Siddiqui, G. K. Haines, T. Wu, Q.-Z. Li, L. S. Davis, C. Mohan, and H. Perlman. 2008. Combined deficiency of proapoptotic regulators Bim and Fas results in the early onset of systemic autoimmunity. *Immunity* 28:206-217.
402. Hughes, P. D., G. T. Belz, K. A. Fortner, R. C. Budd, A. Strasser, and P. Bouillet. 2008. Apoptosis regulators Fas and Bim cooperate in shutdown of chronic immune responses and prevention of autoimmunity. *Immunity* 28:197-205.
403. Watanabe, D., T. Suda, H. Hashimoto, and S. Nagata. 1995. Constitutive activation of the Fas ligand gene in mouse lymphoproliferative disorders. *EMBO J* 14:12-18.
404. Suzuki, I., and P. J. Fink. 2000. The dual functions of fas ligand in the regulation of peripheral CD8+ and CD4+ T cells. *Proc Natl Acad Sci USA* 97:1707-1712.
405. Suzuki, I., and P. J. Fink. 1998. Maximal proliferation of cytotoxic T lymphocytes requires reverse signaling through Fas ligand. *J Exp Med* 187:123-128.
406. Marsik, C., T. Halama, F. Cardona, W. Wlassits, F. Mayr, J. Pleiner, and B. Jilma. 2003. Regulation of Fas (APO-1, CD95) and Fas ligand expression in leukocytes during systemic inflammation in humans. *Shock* 20:493-496.
407. Shen, H., and D. R. Goldstein. 2009. IL-6 and TNF-alpha synergistically inhibit allograft acceptance. *J Am Soc Nephrol* 20:1032-1040.
408. Le Bon, A., V. Durand, E. Kamphuis, C. Thompson, S. Bulfone-Paus, C. Rossmann, U. Kalinke, and D. F. Tough. 2006. Direct stimulation of T cells by type I IFN enhances the CD8+ T cell response during cross-priming. *J Immunol* 176:4682-4689.
409. Berard, M., K. Brandt, S. Bulfone-Paus, and D. F. Tough. 2003. IL-15 promotes the survival of naive and memory phenotype CD8+ T cells. *J Immunol* 170:5018-5026.
410. Chen, X., J. J. Subleski, H. Kopf, O. M. Z. Howard, D. N. Männel, and J. J. Oppenheim. 2008. Cutting edge: expression of TNFR2 defines a maximally

suppressive subset of mouse CD4+CD25+FoxP3+ T regulatory cells: applicability to tumor-infiltrating T regulatory cells. *J Immunol* 180:6467-6471.

411. Chen, X., R. Hamano, J. J. Subleski, A. A. Hurwitz, O. M. Z. Howard, and J. J. Oppenheim. 2010. Expression of costimulatory TNFR2 induces resistance of CD4(+)FoxP3(-) conventional T cells to suppression by CD4(+)FoxP3(+) regulatory T Cells. *J Immunol* 185:174-182.
412. Nagar, M., J. Jacob-Hirsch, H. Vernitsky, Y. Berkun, S. Ben-Horin, N. Amariglio, I. Bank, Y. Kloog, G. Rechavi, and I. Goldstein. 2010. TNF activates a NF-kappaB-regulated cellular program in human CD45RA- regulatory T cells that modulates their suppressive function. *J Immunol* 184:3570-3581.
413. Huse, M., B. F. Lillemeier, M. Kuhns, D. Chen, and M. Davis. 2006. T cells use two directionally distinct pathways for cytokine secretion. *Nat Immunol* 7:247-255.
414. Parish, S. T., J. E. Wu, and R. B. Effros. 2009. Modulation of T lymphocyte replicative senescence via TNF-{alpha} inhibition: role of caspase-3. *J Immunol* 182:4237-4243.
415. Sabbagh, L., S. M. Kaech, M. Bourbonnière, M. Woo, L. Y. Cohen, E. K. Haddad, N. Labrecque, R. Ahmed, and R.-P. Sékaly. 2004. The selective increase in caspase-3 expression in effector but not memory T cells allows susceptibility to apoptosis. *J Immunol* 173:5425-5433.
416. Pénit, C., and F. Vasseur. 1997. Expansion of mature thymocyte subsets before emigration to the periphery. *J Immunol* 159:4848-4856.
417. Le Campion, A., B. Lucas, N. Dautigny, S. Léaument, F. Vasseur, and C. Pénit. 2002. Quantitative and qualitative adjustment of thymic T cell production by clonal expansion of premigrant thymocytes. *J Immunol* 168:1664-1671.
418. Le Campion, A., F. Vasseur, and C. Pénit. 2000. Regulation and kinetics of premigrant thymocyte expansion. *Eur J Immunol* 30:738-746.
419. Ten Hove, T., F. The Olle, M. Berkhout, J. P. Bruggeman, F. A. Vyth-Dreese, J. F. M. Slors, S. J. H. Van Deventer, and A. A. Te Velde. 2004. Expression of CD45RB functionally distinguishes intestinal T lymphocytes in inflammatory bowel disease. *J Leukoc Biol* 75:1010-1015.
420. Li, O., P. Zheng, and Y. Liu. 2004. CD24 expression on T cells is required for optimal T cell proliferation in lymphopenic host. *J Exp Med* 200:1083-1089.
421. Hahn, A. B., and M. J. Soloski. 1989. Anti-Qa-2-induced T cell activation. The parameters of activation, the definition of mitogenic and nonmitogenic antibodies, and the differential effects on CD4+ vs CD8+ T cells. *J Immunol* 143:407-413.
422. Saini, M., C. Sinclair, D. Marshall, M. Tolaini, S. Sakaguchi, and B. Seddon. 2010. Regulation of Zap70 expression during thymocyte development enables temporal separation of CD4 and CD8 repertoire selection at different signaling thresholds. *Science signaling* 3:ra23.
423. Mustelin, T., T. Pessa-Morikawa, M. Autero, M. Gassmann, L. C. Andersson, C. G. Gahmberg, and P. Burn. 1992. Regulation of the p59fyn protein tyrosine kinase by the CD45 phosphotyrosine phosphatase. *Eur J Immunol* 22:1173-1178.

424. Karnovsky, M. J., M. E. Russell, W. Hancock, M. H. Sayegh, and D. H. Adams. 1994. Chronic rejection in experimental cardiac transplantation in a rat model. *Clin Transplant* 8:308-312.
425. Kawai, T., D. Andrews, R. Colvin, D. Sachs, and A. Cosimi. 2000. Thromboembolic complications after treatment with monoclonal antibody against CD40 ligand. *Nat Med* 6:114.
426. Robles-Carrillo, L., T. Meyer, M. Hatfield, H. Desai, M. Dávila, F. Langer, M. Amaya, E. Garber, J. L. Francis, Y.-M. Hsu, and A. Amirkhosravi. 2010. Anti-CD40L Immune Complexes Potently Activate Platelets In Vitro and Cause Thrombosis in FCGR2A Transgenic Mice. *J Immunol* 185:1577-1583.
427. Kondo, T., T. Suda, H. Fukuyama, M. Adachi, and S. Nagata. 1997. Essential roles of the Fas ligand in the development of hepatitis. *Nat Med* 3:409-413.
428. Lau, H. T., M. Yu, A. Fontana, and C. J. Stoeckert. 1996. Prevention of islet allograft rejection with engineered myoblasts expressing FasL in mice. *Science* 273:109-112.
429. Shi, W., M. Chen, and L. Xie. 2007. Prolongation of corneal allograft survival by CTLA4-FasL in a murine model. *Graefes Arch Clin Exp Ophthalmol* 245:1691-1697.
430. Yolcu, E. S., X. Gu, C. Lacelle, H. Zhao, L. Bandura-Morgan, N. Askenasy, and H. Shirwan. 2008. Induction of tolerance to cardiac allografts using donor splenocytes engineered to display on their surface an exogenous fas ligand protein. *J Immunol* 181:931-939.
431. Pejawar-Gaddy, S., and M. A. Alexander-Miller. 2006. Ligation of CD80 is critical for high-level CD25 expression on CD8+ T lymphocytes. *J Immunol* 177:4495-4502.
432. Bingyi, S., C. Ming, Q. Yeyong, M. Chunbai, and Z. Wenqiang. 2003. The effect of anti-CD25 monoclonal antibody (Simulect) to the lymphocytes in the peripheral blood of the recipients of kidney transplantation. *Transplant Proc* 35:243-245.
433. Tan, J., S. Yang, and W. Wu. 2005. Basiliximab (Simulect) reduces acute rejection among sensitized kidney allograft recipients. *Transplant Proc* 37:903-905.
434. Rochman, Y., R. Spolski, and W. J. Leonard. 2009. New insights into the regulation of T cells by gamma(c) family cytokines. *Nat Rev Immunol* 9:480-490.
435. Neely, G. G., S. M. Robbins, E. K. Amankwah, S. Epelman, H. Wong, J. C. Spurrell, K. K. Jandu, W. Zhu, D. K. Fogg, C. B. Brown, and C. H. Mody. 2001. Lipopolysaccharide-stimulated or granulocyte-macrophage colony-stimulating factor-stimulated monocytes rapidly express biologically active IL-15 on their cell surface independent of new protein synthesis. *J Immunol* 167:5011-5017.
436. Mueller, Y. M., P. M. Bojczuk, E. S. Halstead, A. H. J. Kim, J. Witek, J. D. Altman, and P. D. Katsikis. 2003. IL-15 enhances survival and function of HIV-specific CD8+ T cells. *Blood* 101:1024-1029.

437. Mueller, Y. M., V. Makar, P. M. Bojczuk, J. Witek, and P. D. Katsikis. 2003. IL-15 enhances the function and inhibits CD95/Fas-induced apoptosis of human CD4+ and CD8+ effector-memory T cells. *International immunology* 15:49-58.
438. Huntington, N. D., H. Puthalakath, P. Gunn, E. Naik, E. M. Michalak, M. J. Smyth, H. Tabarias, M. A. Degli-Esposti, G. Dewson, S. N. Willis, N. Motoyama, D. C. S. Huang, S. L. Nutt, D. M. Tarlinton, and A. Strasser. 2007. Interleukin 15-mediated survival of natural killer cells is determined by interactions among Bim, Noxa and Mcl-1. *Nat Immunol* 8:856-863.
439. Bulfone-Paus, S., D. Ungureanu, T. Pohl, G. Lindner, R. Paus, R. Rückert, H. Krause, and U. Kunzendorf. 1997. Interleukin-15 protects from lethal apoptosis in vivo. *Nat Med* 3:1124-1128.
440. Ferrari-Lacraz, S., X. X. Zheng, Y. S. Kim, Y. Li, W. Maslinski, X. C. Li, and T. B. Strom. 2001. An antagonist IL-15/Fc protein prevents costimulation blockade-resistant rejection. *J Immunol* 167:3478-3485.
441. Zganiacz, A., M. Santosuosso, J. Wang, T. Yang, L. Chen, M. Anzulovic, S. Alexander, B. Gicquel, Y. Wan, J. Bramson, M. Inman, and Z. Xing. 2004. TNF-alpha is a critical negative regulator of type 1 immune activation during intracellular bacterial infection. *J Clin Invest* 113:401-413.
442. Ban, L., J. Zhang, L. Wang, W. Kuhtreiber, D. Burger, and D. L. Faustman. 2008. Selective death of autoreactive T cells in human diabetes by TNF or TNF receptor 2 agonism. *Proc Natl Acad Sci USA* 105:13644-13649.